SLAMMING OF A SHIP STRUCUTRAL MODEL

by

REDMOND L. CLEVENGER, LIEUTENANT, UNITED STATES NAVY
B.S., U. S. Naval Academy
(1957)

LEROY C. MELBERG, JR., LIEUTENANT, UNITED STATES COAST GUARD
B.S., U. S. Coast Guard Academy
(1956)

SUBMITTED IN PARTIAL FULFILLMENT OF THE REQUIREMENTS
FOR THE DEGREE OF NAVAL ENGINEER
AND THE DEGREE OF
MASTER OF SCIENCE IN NAVAL ARCHITECTURE
AND MARINE ENGINEERING
at the
MASSACHUSETTS INSTITUTE OF TECHNOLOGY

May 1963

SLAMMING OF A SHIP STRUCTURAL MODEL

by

REDMOND L. CLEVENGER, LIEUTENANT, UNITED STATES NAVY
B.S., U. S. Naval Academy
(1957)

LEROY C. MELBERG, JR., LIEUTENANT, UNITED STATES COAST GUARD
B.S., U. S. Coast Guard Academy
(1956)

SUBMITTED IN PARTIAL FULFILLMENT OF THE REQUIREMENTS

FOR THE DEGREE OF NAVAL ENGINEER

AND THE DEGREE OF

MASTER OF SCIENCE IN NAVAL ARCHITECTURE

AND MARINE ENGINEERING

at the
MASSACHUSETTS INSTITUTE OF TECHNOLOGY
May 1963

SLAMMING OF A SHIP STRUCTURAL MODEL

by Redmond L. Clevenger, U.S.N, and LeRoy C. Melberg, Jr., U.S.C.G.

Submitted to the Department of Naval Architecture and Marine Engineering on 17 May 1963 in partial fulfillment of the requirements for the Master of Science degree in Naval Architecture and Marine Engineering and the professional degree, Naval Engineer.

ABSTRACT

A four ton 1/4 scale elastic model was designed, built and tested to determine the nature of pressures encountered by a slamming ship on its bottom structure and point out ways to a more efficient bow and forefoot design. Extensive experimental results are included which are considered to be excellent data.

The model was tested by free-fall drops in tracks onto a water surface and instrumented in the center panels for pressures, deflections, strains, velocities and acceleration.

The records were compared to the simple two-dimensional theory of wedge shape drops developed by Wagner and Von Karman and the forms of blast and shock waves. They show that the peak pressure signatures are like shock waves and their shape is not predicted by the theory. After the model has immersed beyond the gage in question, the theory predicts the mean pressure for elastic response of the model well.

Damage to the model is conclusively linked to the peak shock or pressure by superposition of deflection, pressure and strain histories. Design criteria are recommended for the plates and the framing of ships structures.

Motion of the bottom relative to the overall section motion is shown to be a major factor in divergence of theoretical results and helps to explain the shock waves developed on impact.

ACKNOWLEDGEMENTS

The authors wish to express their appreciation to Professor J. Harvey Evans, Department of Naval Architecture and Marine Engineering, Massachusetts Institute of Technology, for his guidance and continuing interest in this work, to Dr. Alfred H. Keil, Technical Director, David Taylor Model Basin; Dr. Heinrich M. Schauer, Head, Underwater Explosions Research Division, David Taylor Model Basin; Mr. James W. Church, Head, Seaworthiness Branch, David Taylor Model Basin, for their advice and encouragement, and to Mr. Elso Elsarelli, Engineering and Test Section, Underwater Explosions Research Division, David Taylor Model Basin, for his outstanding liaison during the testing.

The theoretical calculations in this work were done on the IBM 7090 Digital Computor at the Computation Center at the Massachusetts Institute of Technology, Cambridge, Massachusetts.

The models, carriage and track were built at the Norfolk Naval Shipyard. The testing under the direction of the authors was conducted by the Underwater Explosions Research Division of the David Taylor Model Basin at Norfolk Naval Shipyard. This project was funded by the Structure Mechanics Laboratory, David Taylor Model Basin.

Permission has been granted to David Taylor Model Basin to reproduce or copy, wholly or in part, any of this thesis by the Department of Naval Architecture and Marine Engineering, Massachusetts Institute of Technology.

TABLE OF CONTENTS

TABLE OF CONTENTS (continued)

LIST OF FIGURES

NOTATION

A = Shape coefficient = $\frac{64}{45}\left(\frac{a}{b} + \frac{b}{a}\right)$

A_1 = Slope = H/B

A^1 = Coefficient of $\frac{c}{B}$

a, b = Width and length of panel

B = Half beam

c = Half breadth at piled up water

c_1 = Speed of sound in water = 4800 ft/sec

D = Draft at test waterline

E = Modulus of elasticity

F_b = Buoyant force

F_d = Drage force

F_s = Section force from shear

F_u = Unsteady hydrodynamic force

g = Acceleration due to gravity

H = Design draft

h = Drop height

h_o = Plate thickness (sometimes defined by "h")

I = Moment of inertia

k = Stiffness ratio = $\frac{I}{\ell}$

ℓ = Length of beam

ℓ_1 = Half width of the keel

M = Mass of model and carriage per unit length

M_o = Total mass of model and carriage

m = Added apparent mass

p = Pressure

T = Natural period of vibration

t = Time

t_o = Rise time of modified shock wave

t_1 = Effective time of positive pressure

$u(c) = \frac{V}{dc/dt} = \frac{dz\ (c)}{dc}$

V = Velocity

V_o = Velocity at impact

V_η = Velocity around plate

V_∞ = Undisturbed velocity

W = Half breadth at test waterline

$W_\square$ = Plastic deformation energy

WL = Waterline

y = Variable half breadth

z = Variable immersion

$z(c)$ = Immersion corresponding to instantaneous WL

$z(y)$ = Immersion corresponding to y

$\dot{z}_o$ = Impact velocity

α = Nondimensional circular frequency

γ = Weight density

δ_c = Deformation of the center of a panel

ζ = Mapping transform

$\eta(y)$ = Free surface

μ = Ratio of $\frac{m}{M}$

$\mu(c)$ = Added mass corresponding to c

ν = Poisson's ratio

ρ = Mass density

σ_y = Yield strength

Φ = Complex velocity potential

ω_n = Natural circular frequency

I. INTRODUCTION

Whenever a ship is trying to maintain its speed in heavy weather the hull, especially the forefoot, is likely to experience a violent hydrodynamic impact. This phenomenon, associated in the minds of seamen with severe hull vibrations of significant duration and often damage, is commonly called pounding or slamming. Pounding is a general description of large heaving and pitching due to decreased periods of encounter with larger wave systems by the ship, which periods are close to the ships periods of heave and pitch. Slamming is the specific event of hull-shaking impact due to re-entry of the forefoot or entry of a highly flared bow.

On most ships, the damage is restricted to the bottom plating of the fore part of the ship. Severe impacts put some ships into a longitudinal whipping mode of vibration increasing stresses in the main structure away from the impact area over and above the wave bending stress. These stresses have resulted in damage to superstructures and main decks on some ships.

Major work in this area began in the 1920's when due to design improvements the power to drive ships became sufficient to maintain speed in heavier weather and thus assure motions favorable to slamming. Earlier works concerned themselves with rigid body, hydrodynamics, wedge impact studies such as Von Karman's work [4].* Contemporary work now considers or has considered the complicated process of ships motions relative to the sea [18, 9], the effects of hull form [8], weight

---

* Numbers in brackets refer to bibliography.

distribution [19] and structure response [27]. Several works [12] [37] have formulated theories to explain what happens at the instant of impact.

This work will investigate experimentally the nature of impact and the mechanism of plate and local structure damage. To examine the impact and damage phenomenon a 1/4 scale model of a section of a new Coast Guard ship was extensively instrumented and dropped from various heights to get desired steps of terminal velocity. On each drop, thirty channels of information provided pressere, deflection, strain, velocity, and acceleration histories.

The models were constructed of HTS and MS steel plate and had the following dimensions: length--90 inches, beam--80 inches, and displacement--8910 pounds. These dimensions correspond to 1/10 the length of the ship, 1/2 the beam, and 1/10 the displacement (full load). The model is wedge shaped with a 10-degree deadrise angle and represents the ship's section in the area of .25 - .35L.

The aim of this work was to provide experimental evidence upon which conclusions or trends could be made with respect to the following:

1) the exact nature of the pressures, whether the shock wave is present and its effect on the structure and the effect of steady dynamic pressures;

2) the interaction of plate motion and pressure;

3) a quantative comparison of plate motion, pressure and strain at the same location;

4) the effect of repeated drops from a predetermined drop height, i.e., terminal velocity;

5) the difference in response of the plate and pressures if the model acts elastically or plastically; and

6) the trends in model limitations to determine modification to the testing schedule.

To compare and evaluate some of the experimental data, theoretical data was generated using a simple two-dimensional slamming theory developed by Wagner and programmed for the M. I. T. 7090 computer by Howard [34]. Experimental data was also compared with plastic work theories of Dr. Kiel [20] and calculated vibratory motions [32].

II. PROCEDURE

A. Experimental

1. Models

To carry out the objectives of the experimental work, models of 10° deadrise have been selected over 0° or greater angles as more representative of present designs and the best approach to evidence to support a general theory. The choice of 1/4 scale results from scaling law considerations and test facilities available to handle large models. Scaling considerations were the effect of panel and model dimensions in relation to ease of construction and the speed of sound in water. For this first series it was felt a changing plate size and stiffener arrangement would not be as valuable as studying the effects of plate response under different drop heights. The models are 10° dead rise sections typical of .25 to .35 L of the prototype, a new Coast Guard class of medium rescue vessels. The model represents 1/10th the length, 1/2 the beam and has a displacement corresponding to 1/10th of the full load displacement. (See Figure I.) This choice of weight is an adjustment over the actual scale weight to account for the force due to bow section and the buoyant effect aft of it. Studies of ships motions show that the after quarter point is the pivot point [18]. For this prototype, maximum slamming pressures will occur at 0.30 L as shown in studies of Dutch destroyers [36].

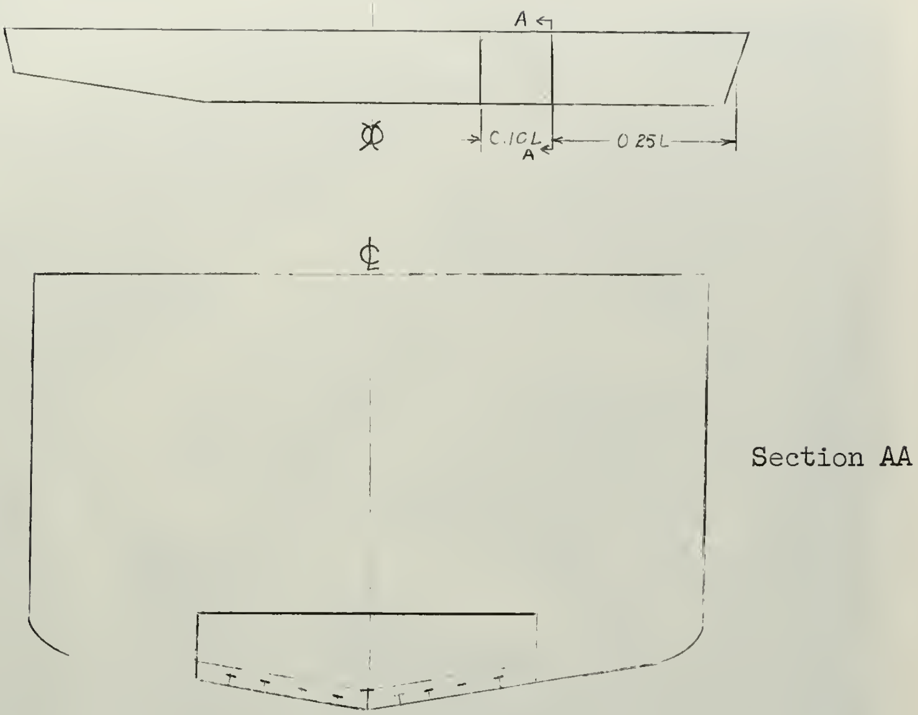

Figure I--Model Geometry

Figures II, III and IV show the detail paid to construction; and Plate 1, the construction plan, gives the exact dimensions and specifications. Bottom plating and stringers were made of HTS plate.* Other material was M.S. Particular attention was made to insure near fixed end conditions for the sides and ends of the model which represent continuation of the ship. Connection of the CVK to the end bulkheads was one of the stiffness connections checked and designed. Using moment distribution stiffness factors ($k = I/\ell$), it was found in way of the CVK and end bulkheads the distribution was .95 to .05. Factors at the

---

* Models were constructed at the U. S. Naval Shipyard, Norfolk, Virginia of HTS plate of WW II vintage. Yield tests conducted after construction found Y.S. varied from 31,200 PSI to 67,800 PSI. Fortunate choice of plates lead to use of high yield HTS in the stringers and webs and lower yield in the bottom plating.

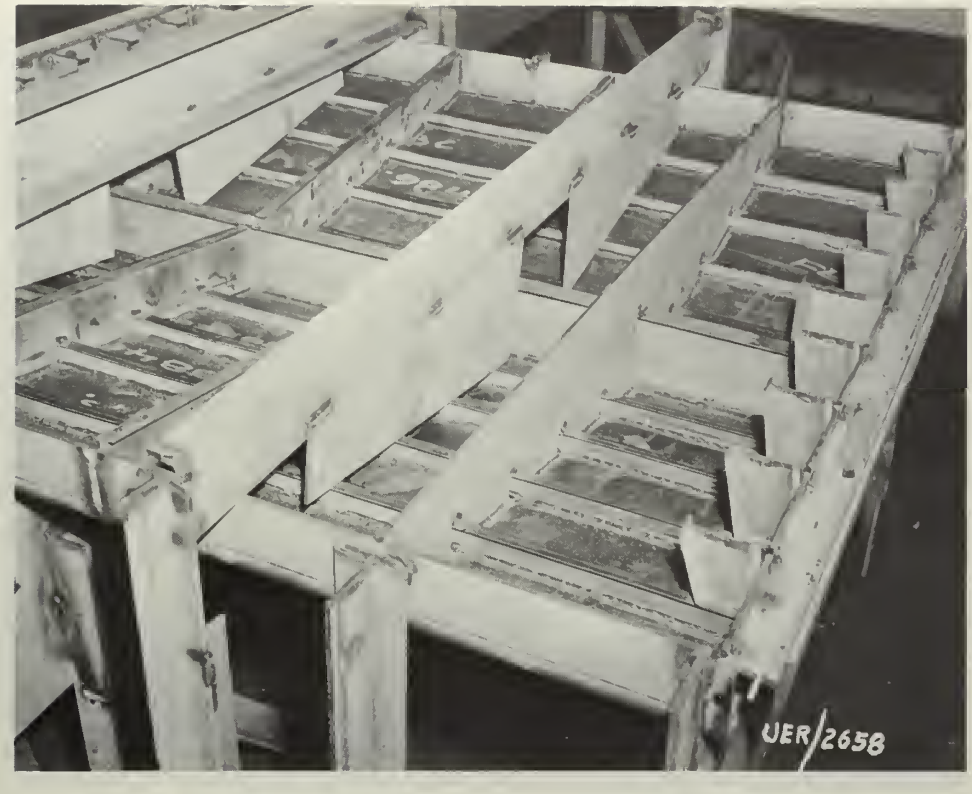

Figure II
Model Construction

Figure III
Completed Model--Side View

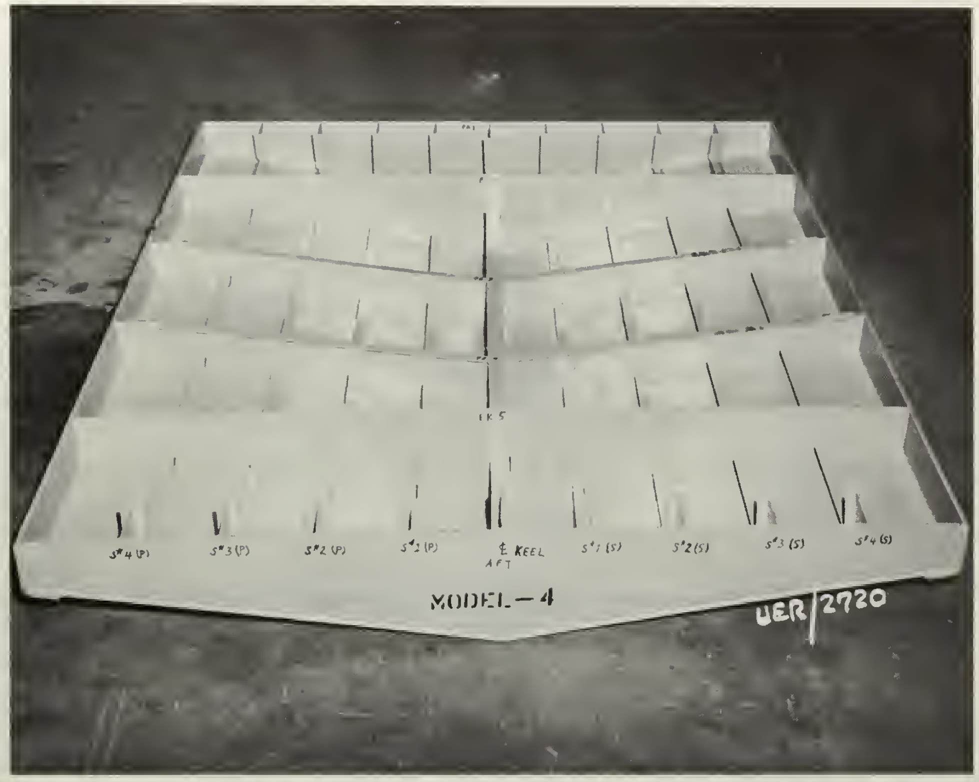

Figure IV
Completed Model

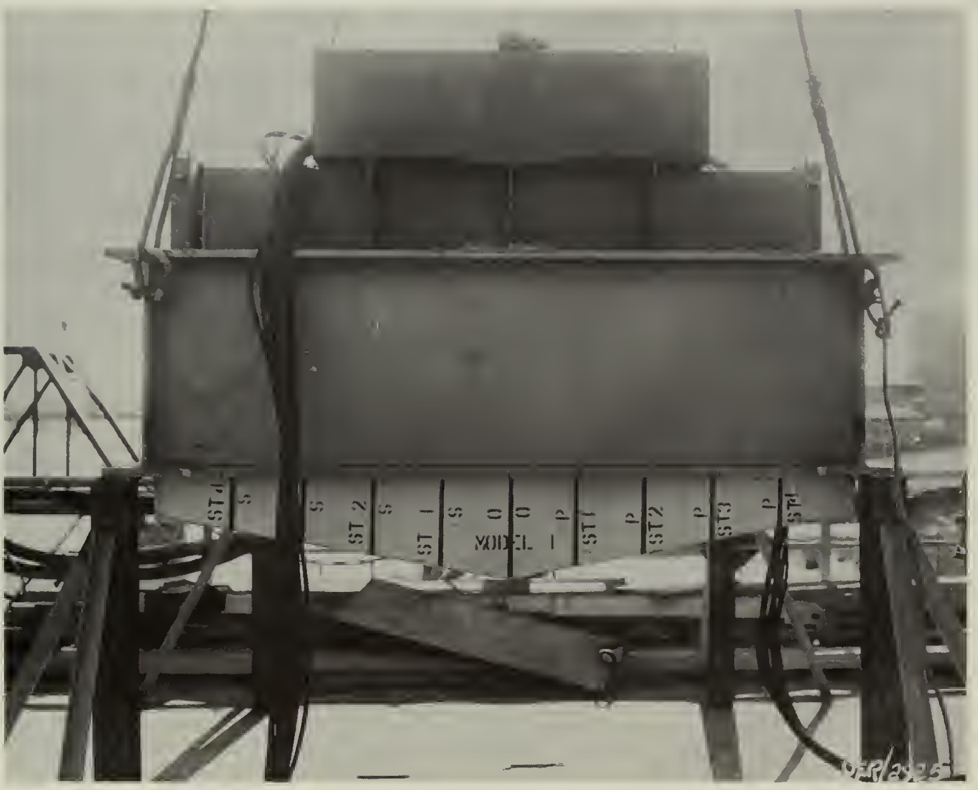

Figure V
Carriage and Model Assembled

[illegible]

[illegible]

side and stringers (continuous) were calculated to be .95 to .05 also. The weight of the model is 760 pounds and the rest of the section weight of 8910 pounds is provided by the carriage and large steel blocks. See Figure V and Plate 2 for complete carriage and model assembly.

To obtain the data, the model was dropped in a slide track, see Figures VI and VII, from various heights.* The carriage was suspended and released with a Dupont explosive bolt which was fired remotely and acted as a trigger for instrumentation. The original test schedule for four models is shown in Appendix A and revisions as testing progressed are noted.

The schedule followed is an attempt to obtain as much information as possible with a limited number of expensive models. Test 1 consisted of drops in the elastic range where lower limits on pressure and damage were found. Test 2 was a drop from the maximum distance to observe the worst condition. Tests 3 and 4 were drops from the same height to determine the effect of repeated impact in the plastic deformation range. Test 5 will be drops used to determine the effects of plate backing and decreased model weight. These will be done later as a part of a continuing study and extension of this work.

---

* The models, carriage and track were constructed by the Norfolk Naval Shipyard under the guidance of the Engineering and Test Section, Underwater Explosions Research Division, David Taylor Model Basin according to specifications drawn up by the authors. The tracks were mounted on the UEB-1, a research barge.

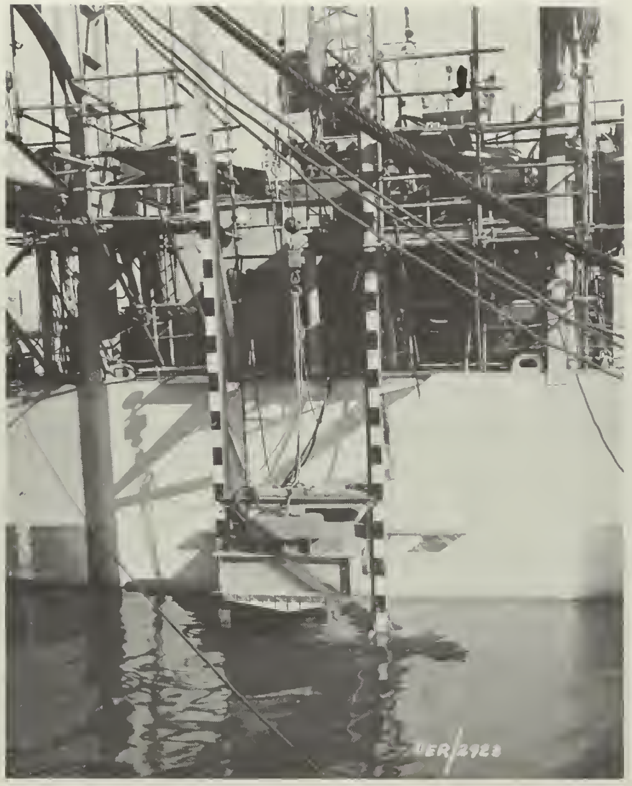

Figure VI
Dropping Rig

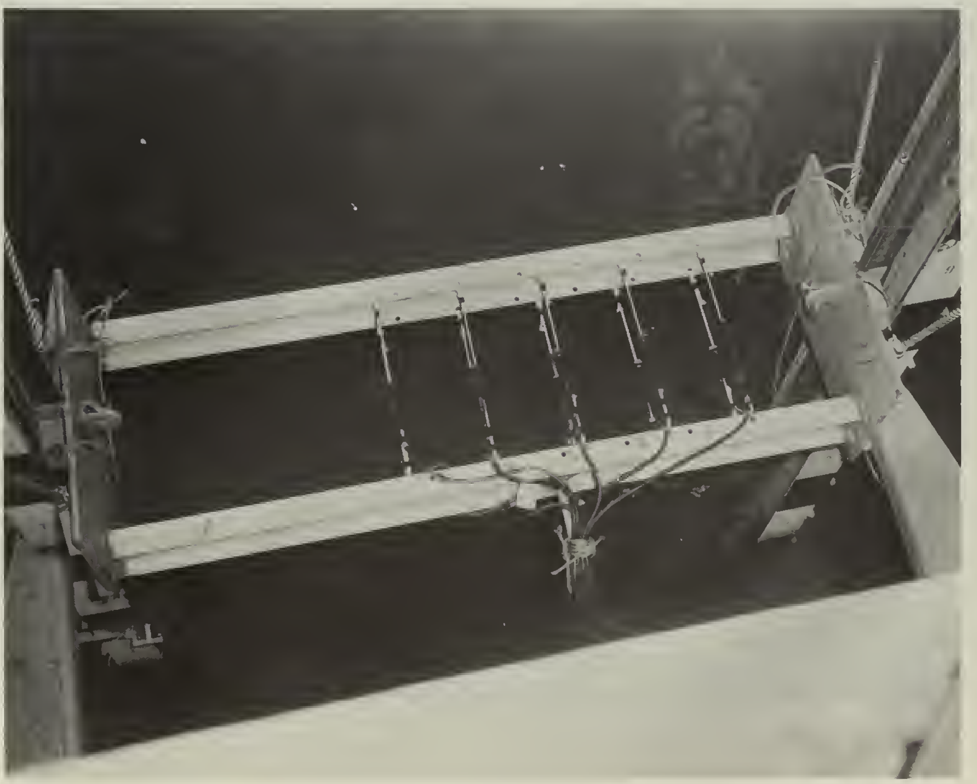

Figure VII
Piezo Electric Gages--Out of Water

2. Instrumentation

a) General

The center girthwise panels were instrumented in order to get as close to two-dimensional results as possible. Checks on symmetry were offered by high-speed photography and gages along the length. See Figures VII, VIII, IX and X for photographs and number locations.

b) Pressure

Pressure gages were piezo electric and were located in the test area on the keel, stringer, plate centers and in the water on the side. Depending on the recording system, a response of 10 kc or 50 kc was available. Calculations show the impact of a 4" keel (from c_1/ℓ_1) requires a response of 60 kc to pick up the spikes. Pressure gages are referred to as PE's with a number for location.

c) Strain

SR-4 strain gages were mounted in some of the same locations as pressure gages and by symmetry with deflection gages.

d) Velocity, Deflections and Accelerations

Deflection and velocity gages were mounted on the other side of the test section, on the keel, stringers and panel centers. The velocity gages are magnetic gages designed at UERD. The deflection gages are light weight, accurate response magnetic gages [24]. Acceleration of the model was measured by mounting one accelerometer on the CVK.

e) Recording Instruments

Recording apparatus installed on the UEB-1 was used. See

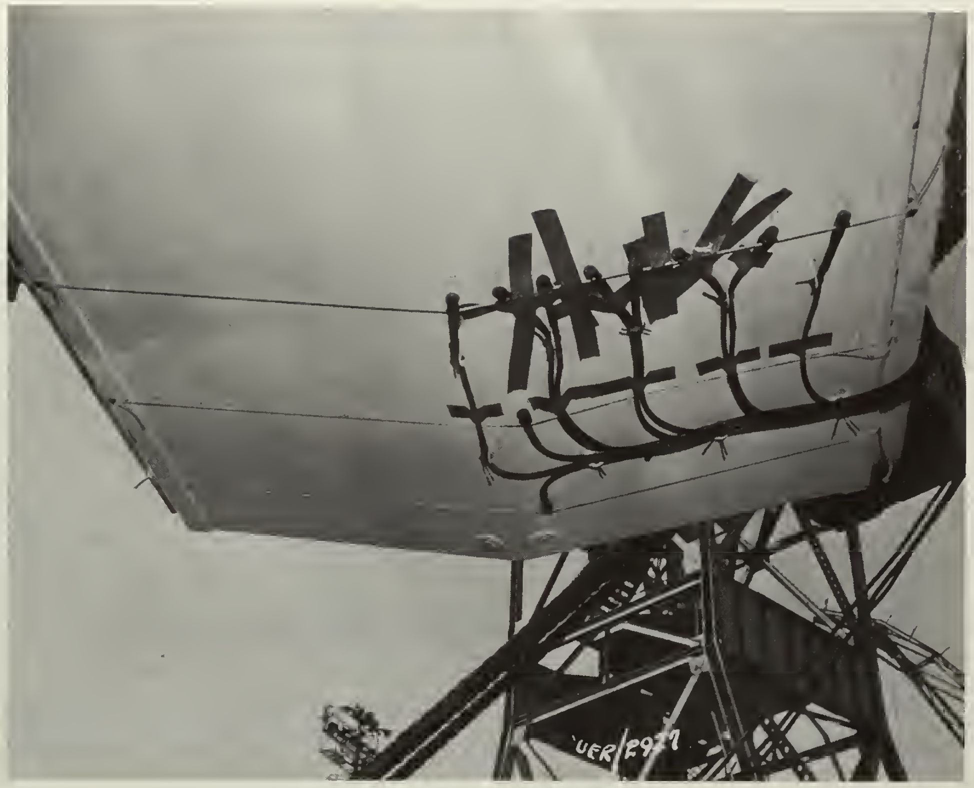

Figure VIII
Piezo Electric Gages Mounted On Bottom

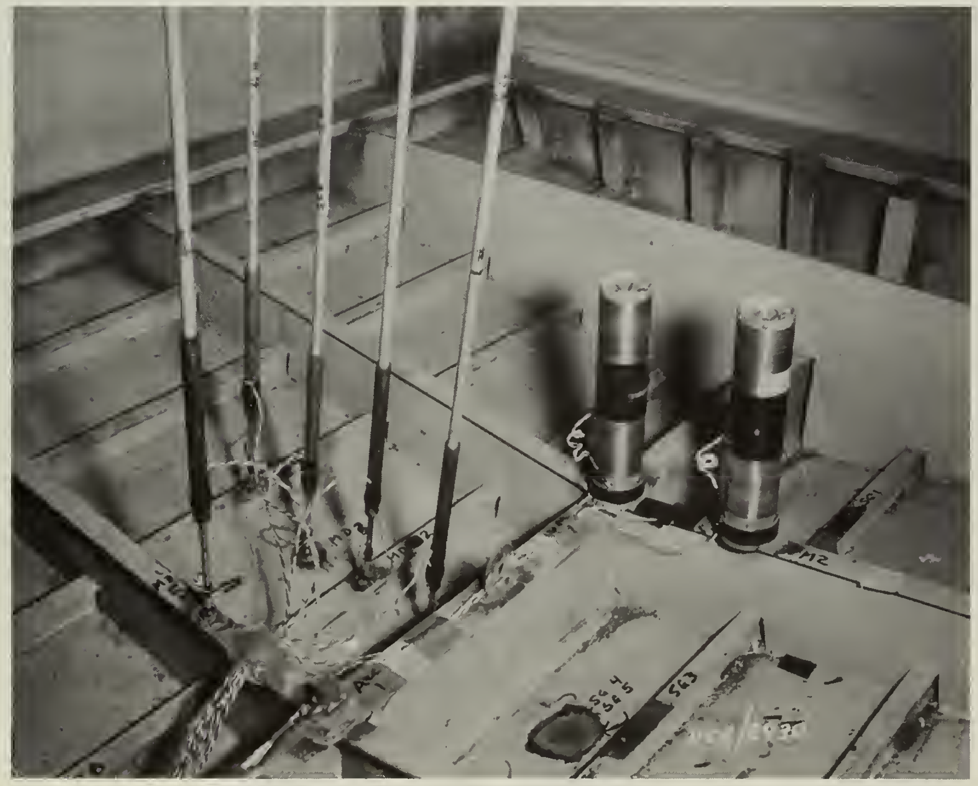

Figure IX
Various Instruments Mounted Inside the Model

[illegible]

[illegible]

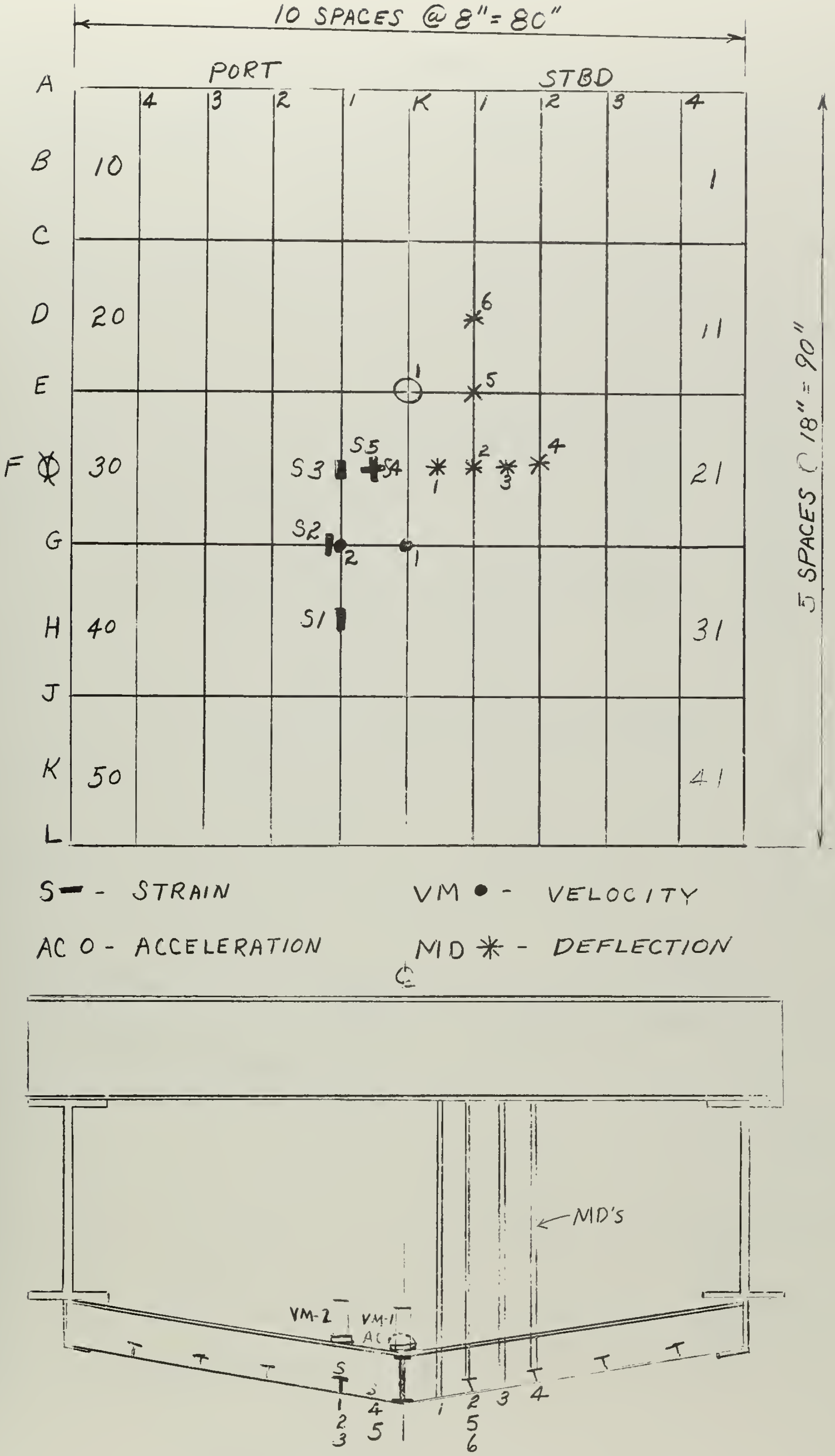

Figure X-1--Gage Locations

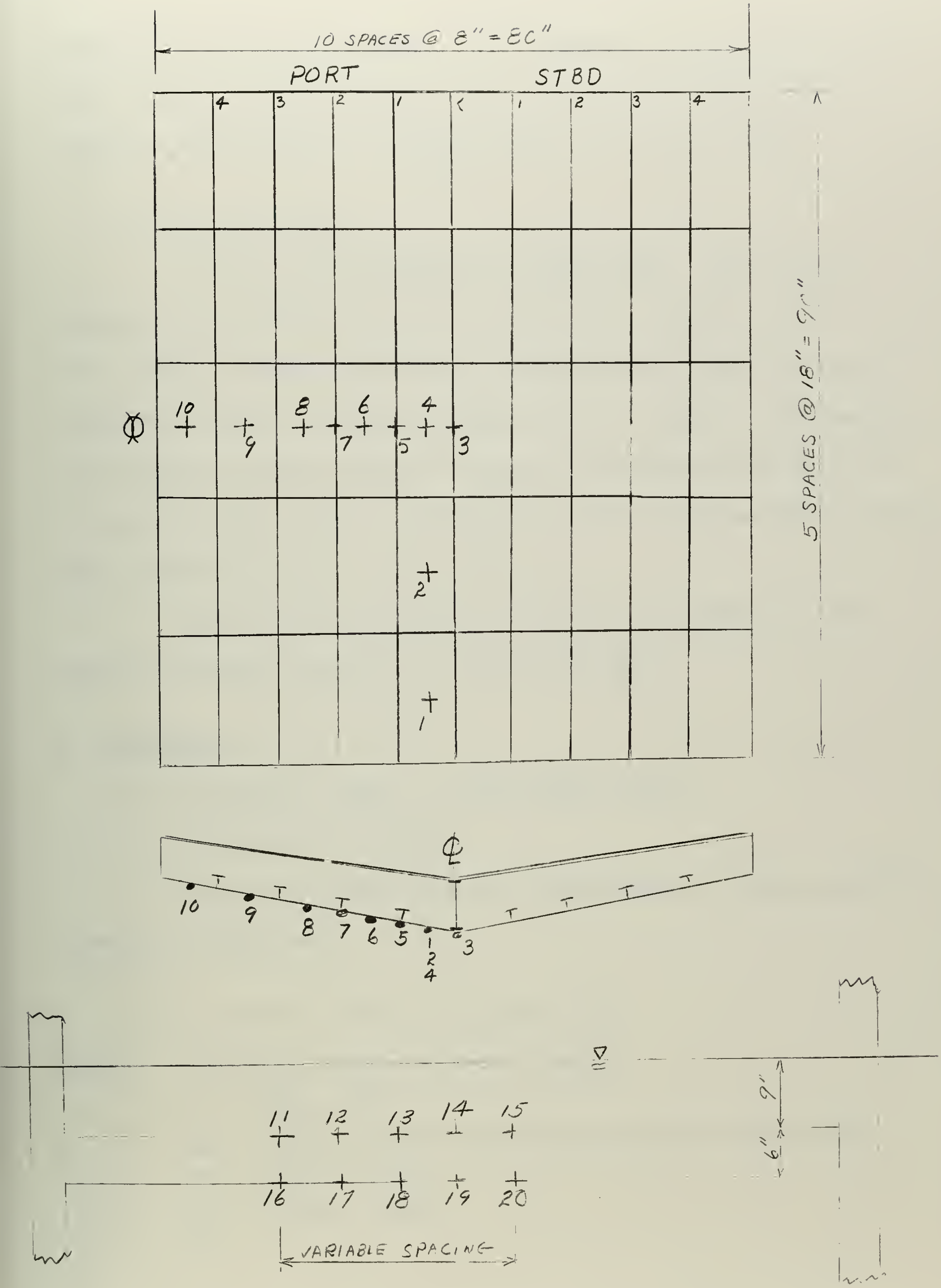

Figure X-2--Locations of Piezo-Electric Gages

Appendix B for block diagram. This equipment was selected for its high response and reliability to wake measurements of underwater explosion tests and gave excellent results on the drop tests.

3. Test Procedure

The models were dropped in a track guide. There was no measurable pitch angle and roll was limited to a maximum of 1/2° by the track. Dropping from two to twenty-five feet the velocity of impact varies from 11.3 fps to 40 fps; i.e., $V = (2gh)^{\frac{1}{2}}$. Instruments were triggered by the explosive bolt and a contact when the keel was 6" above the water. Most records cover a period of 40 ms which is full model immersion of 12".

High speed photography also recorded the impacts of most drops and confirmed that the roll angle was small.

B. Theoretical

1. Hydrodynamic impact of wedge-shaped bodies.

a) Equation of motion

At any time after impact the equilibrium of forces gives the equation of motion as:

$$(M + m)\ddot{z} + \dot{m}\dot{z} + F_d + F_b - gM_o = F_s \tag{1}$$

where: M = hull section mass/unit length

m = added mass

F_d = damping forces resulting from drag and wave making

F_b = buoyant forces

gM_o = weight of wedge

$(M + m)\ddot{z} + \dot{m}\dot{z}$ = inertia forces found by differentiating the momentum

z = vertical immersion of keel to undisturbed water line.

$$\dot{z} = \frac{dz}{dt} \quad ; \quad \ddot{z} = \frac{d^2z}{dt^2}$$

g = acceleration due to gravity

F_s = vertical forces with which remainder of hull acts on section.

In the first phases of contact and immersion, the buoyant force, F_b, and the drag forces, F_d, are small in comparison to other forces [5]; so (1) becomes

$$F_s = (M + m)\ddot{z} + \dot{m}\dot{z} - gM_o \tag{2}$$

Now the unsteady hydrodynamic force, F_u, is

$$F_u = F_s - M_o\ddot{z} \tag{3}$$

which upon substitution

$$F_u = m\ddot{z} + \dot{m}\dot{z} - gM \tag{3a}$$

For a wedge in free fall $F_s = 0$, so (2) becomes:

$$(M + m)\ddot{z} + \dot{m}\dot{z} = gM \tag{4}$$

and with the notation $\mu = \frac{m}{M}$ is:

$$(1 + \mu)\ddot{z} + \dot{\mu}\dot{z} = g \tag{4a}$$

b) Apparent Mass

In this study the elementary Von Karman [4] apparent mass relation as modified by Wagner [10] is used. This relation provides that the apparent mass per unit length be taken to that of a semi-cyclinder of water equal to the wetted area. References [4] and [10] give

$$m = \frac{\pi \rho c^2}{2}$$

where c is the wetted half bredth for a given immersion z.

c) Model Geometry and Notation

Since the model is a wedge, its surface is described by $z = A_1 y$

where z = immersion

y = half bredth

A_1 = slope $= \frac{H}{B}$

and non-dimensionally

$$\frac{z}{H} = A \frac{y}{B} \quad \text{and} \quad A = 1 \tag{5}$$

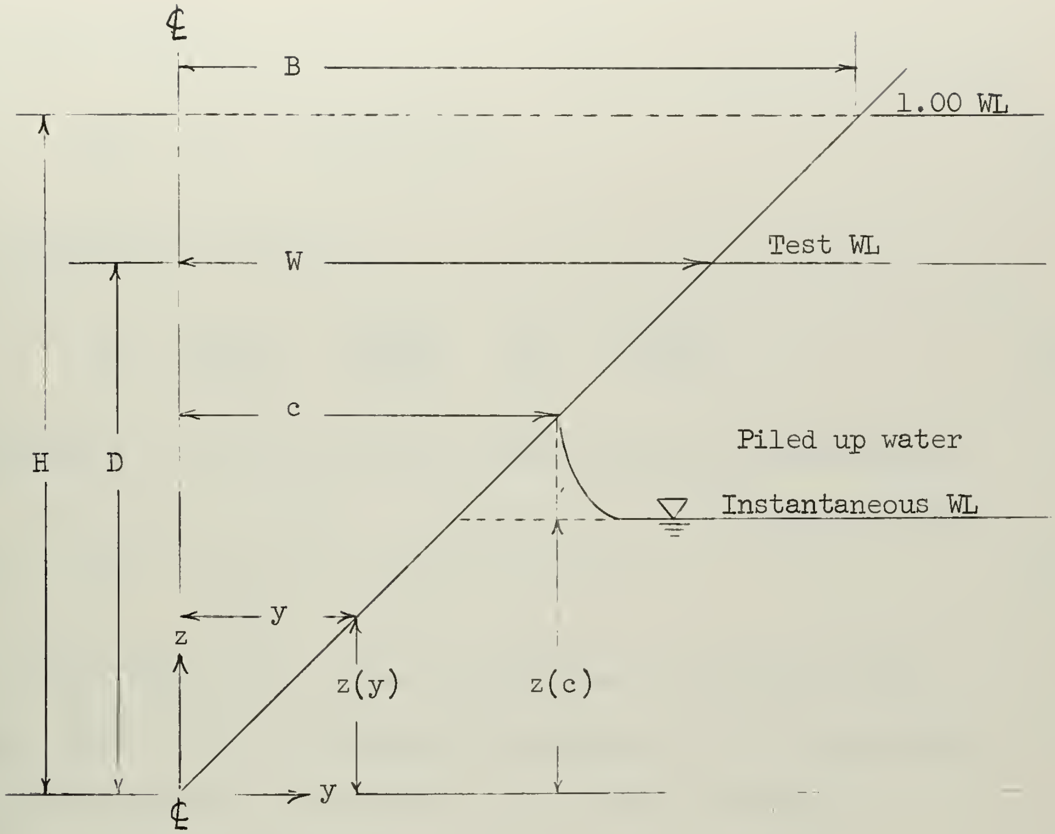

Figure XI--Hull and Flow Nomenclature

d) Flow about the model

If the free water surface is defined as a zero potential surface [2], the free surface may be defined by:

$$\eta\,(y) = \int_0^t V_\eta\, dt \tag{6}$$

where V_η is the velocity of the surface water particles relative to the plate and is a function of y. The normal velocity distribution of flow past a flat plate is given by [35] as:

$$V_\eta = V\left(1 - \frac{c^2}{y^2}\right)^{-\frac{1}{2}} \qquad \text{for } y > c \tag{7}$$

Substituting in (6):

$$\eta(y) = \int_{o}^{t} V\left(1 - \frac{c^2}{y^2}\right)^{-\frac{1}{2}} dt \tag{8}$$

and for convenience later let:

$$u(c) = \frac{V}{dc/dt} = \frac{dz/dt}{dc/dt} = \frac{dz}{dc} = \frac{dz(c)}{dc} \tag{9}$$

Substituting this into (8), the free water surface is described as:

$$\eta(y) = \int_{o}^{c < y} \left(1 - \frac{c^2}{y^2}\right)^{-\frac{1}{2}} u(c)\, dc \tag{10}$$

From Figure XII it may be seen that at the hull-water interface $\eta(y) = z(y)$. Therefore, the equation of the wetted hull surface, accounting for the piled up water effect, becomes:

$$z(y) = \int_{o}^{c = y} \left(1 - \frac{c^2}{y^2}\right)^{-\frac{1}{2}} u(c)\, dc \tag{11}$$

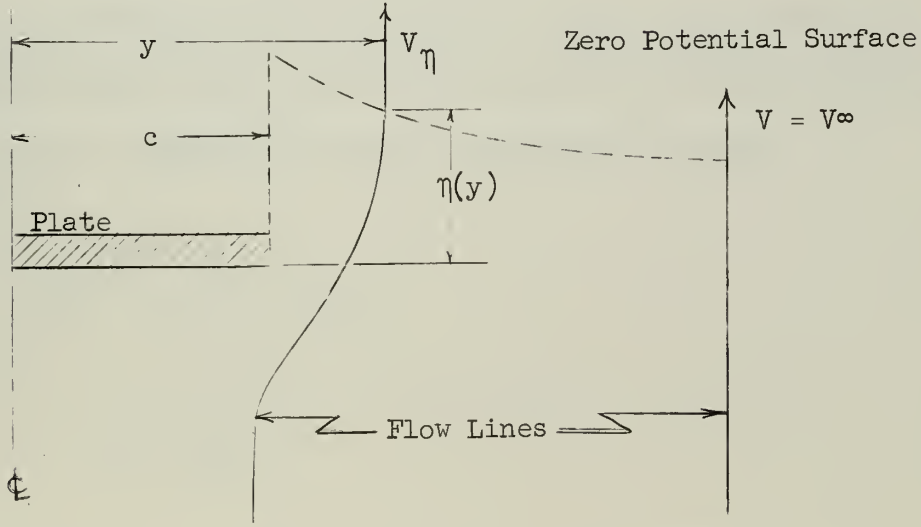

Figure XII--Potential Flow About a Flat Plate
(Velocities are relative to plate)

Now the expression for z(y), Equation (5), may be substituted in to the left side of Equation (11). If u(c) is described by the form

$$\frac{u(c)}{H} = A' \left(\frac{c}{B}\right) \tag{12}$$

Equation (11) may be integrated and like powers of y equated to yield:

$$\frac{u(c)}{H} = \frac{2}{B\pi} A \tag{13}$$

Using Equation (9), which defines u(c), z(c) the distance from the keel to the instantaneous waterline may be obtained:

$$z(c) = \int_0^c u(c)\, dc = \frac{H}{B}\int_0^c \frac{2A}{\pi}\, dc \tag{14}$$

or

$$\frac{z(c)}{H} = \frac{c}{B}\,\frac{2A}{\pi} \tag{14a}$$

e) Velocity, Acceleration and Time

Now having equations for z(y), z(c) and m, the equation of motion, Equation (4a), may be solved for velocity and acceleration given values of c and t. Equation (4a) may be integrated to yield z, reference [5]:

$$\int_0^t \ddot{z} dt = \int_0^t \frac{g - \dot{\mu} \dot{z}}{1 + \mu}\, dt$$

$$\dot{z} = \frac{g + \dot{z}_o}{1 + \mu} \tag{15}$$

where $\dot{z}_o$ = the velocity at the instant of impact (+ downward).

$$\mu = \mu(c) = \frac{\pi \rho c^2}{2M}$$

After some substitution, the equation of motion may be used directly to solve for $\ddot{z}(c, t)$. Equation (4a) is then rewritten as:

$$\ddot{z} = \frac{g}{1 + \mu} - \frac{\dot{\mu}\dot{z}}{1 + \mu} = \frac{g}{1 + \mu} - \frac{\dot{z}}{1 + \mu} \frac{d\mu}{dc} \cdot \frac{dc}{dt}$$

and $$\dot{c} = \frac{dc}{dt} = \frac{\dot{z}}{u(c)}$$

substituting:

$$\ddot{z} = \frac{g}{1 + \mu} - \frac{\dot{z}^2}{(1 + \mu)\, u(c)} \frac{d\mu}{dt}$$

or

$$\ddot{z} = \frac{g}{1 + \mu} - \frac{\dot{z}^2}{(1 + \mu)\, u(c)} \cdot \frac{\pi \rho c}{M} \tag{16}$$

Finally to relate c and t, combining Equations (9) and (15):

$$u(c) = \frac{1}{\dot{c}} \frac{\dot{z}_o + gt}{1 + \mu} \tag{17}$$

which when integrated is:

$$\int_o^c u(c)\,(1 + \mu)dc = \dot{z}_o t + \frac{1}{2} gt^2 \tag{18}$$

Using the equations developed $z(c)$, $u(c)$, μ, t, $\dot{z}$, and $\ddot{z}$ may be evaluated for any given value of c, $\dot{z}_o$ and g.

f) Pressure Distribution

Again using the flat plate approximation for the hull, the pressure distribution on the hull may be developed from the Bernoulli equation. From [35], the complex velocity potential for irrotational flow about a flat plate is found to be:

$$\Phi = V(\zeta e^{-i\alpha} + \zeta^{-1} e^{i\alpha}) \tag{19}$$

where: $\zeta = \frac{1}{2}(y + \sqrt{y^2 + c^2})$ is a mapping transform; and

$\alpha = \pi/2$

is the angle of incidence between the plate and the incident flow velocity V. Substituting for ζ in (19), one obtains:

$$\Phi = -iV\sqrt{y^2 - c^2} = -V\sqrt{c^2 - y^2}$$

The Bernoulli equation for unsteady, irrotational potential flow may be used to obtain a relationship between the pressure and the various flow variables. For two-dimensional, incompressible flow (neglecting the gravity effect on pressure), the Bernoulli equation has the form:

$$\frac{\partial \Phi}{\partial t} = \frac{V^2}{2} + \frac{p}{\rho} = 0 \tag{21}$$

where Φ = the velocity potential (20) and $V = \frac{\partial \Phi}{\partial y}$

Equation (21) is valid throughout the region of irrotational flow, relating the pressure to the flow velocity and body position irrespective of stream line location. Substitution of (20) in (21):

$$-V_c(c^2 - y^2)^{-\frac{1}{2}} \frac{dc}{dt} - (c^2 - y^2)^{\frac{1}{2}} \frac{dV}{t} + \frac{1}{2} \frac{y^2V^2}{c^2 - y^2} + \frac{p}{\rho} = 0 \qquad (22)$$

Finally, substituting for $\frac{dc}{dt}$ from Equation (10),

$$\frac{dc}{dt} = \frac{V}{u(c)},$$

Equation (22) takes the form:

$$\frac{p}{\rho} = \frac{V^2c}{u(c) \quad c^2 - y^2} + \dot{V} \quad c^2 - y^2 - \frac{y^2V^2}{2(c^2 - y^2)} \qquad (23)$$

g) Calculations

One is now in a position to solve for the pressure given any actual semi breadth c. For the same c, the keel immersion z(c), the time t, the hull velocity $\dot{z}$, the hull acceleration $\ddot{z}$, the added mass m must be found before calculating p. These calculations were programmed by J. L. Howard for the IBM 709 Digital Computor. With a few modifications to Howard's program, the calculations were then done on the IBM 7090 Digital Computor at the M. I. T. Computation Center and are presented in the results.

2. Plastic Deformation Energy

The energy absorbed by a rectangular plate when it is plastically deformed can be expressed as [20]:

$$W_{\square} = A\sigma_y h_{\square} \delta_c^2 \qquad (24)$$

This formulation has been shown to represent underwater explosion phenomenon if modified by an empirical numerical constant. The plastic deformation energy was calculated for the bottom of the model for different drop heights. These are presented as a percent of potential energy available.

3. Response to Shock Pressure Waves

It has been shown that the shape which a dynamically loaded panel assumes is markedly different from the shape assumed by the same panel under a static load which yields the same maximum deflection, δ_c, [21]. The dynamically loaded circular diaphragm takes a conical shape; whereas, the statically loaded one assumes a spherical shape. This difference has been observed to hold for rectangular plates as well. However, in order to gain some useful design criteria, the dynamic load factor concept will be employed to derive a design load for given impact velocities. Franklin [31] has calculated the dynamic load factor for the blast pulse (shockwave). See Figure XIII.

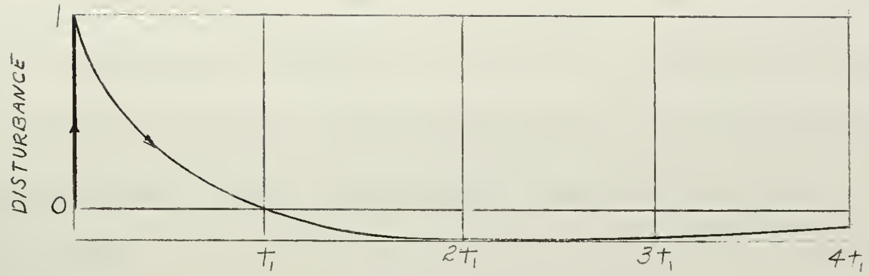

Figure XIII--Shock Pulse

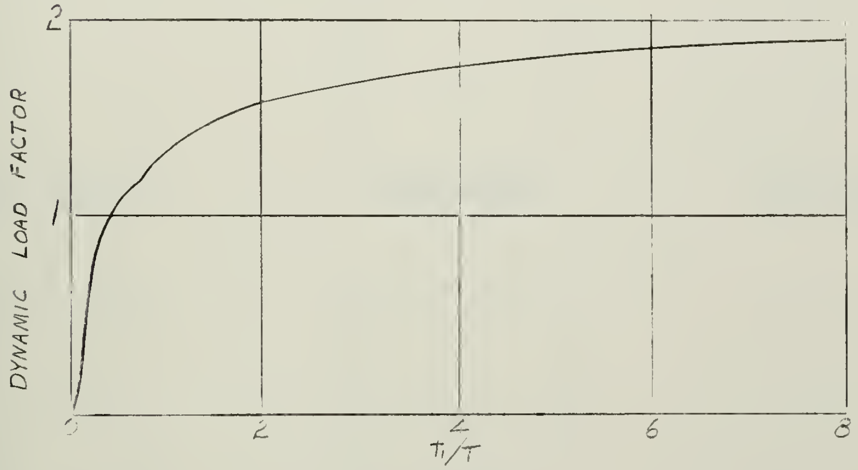

Figure XIV--Dynamic Load Factor for Shock Pulse

His results are presented in Figure XIV. As can be seen, the dynamic load factor depends on the ratio of the effective positive loading time, t_1, and the natural period of system, T. There are several systems to be considered in the bottom structure of the model; however, these systems are fairly simple if they are considered separately and under different end conditions. Hearmon [32] has calculated the natural periods of rectangular isotropic plates for all possible end conditions and aspect ratios. Using Hearmon's results, the natural period of a 1/8" x 6" x 18" panel is 1.27 msec; 1/8" x 8" x 18" panel is 2.2 msec if both are assumed to be completely clamped and undamped. Other possible panel elements are the overall bottom, 80" x [illegible]0" x equivalent thickness of

0.236 inch, and the panel bounded by the keel, side and bulkheads, 40" x 54" x equivalent thickness of 0.175 inch. These have natural periods for the first mode of 82.3 msec and 33 msec respectively. The natural period of the overall bottom for the third mode is 27.3 msec, Figure XV.

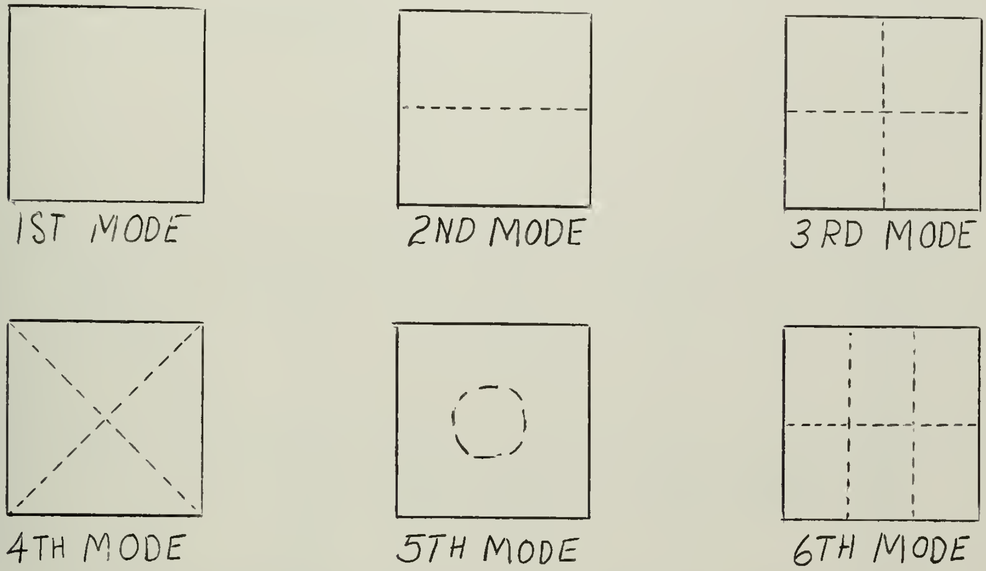

Figure XV--Nodal Lines of a Fully-Clamped Square Plate

Other possible systems are the beam mechanisms [33], such as the keel which with associated bottom plating of 1/8" x 60h, has a natural period, T, of 5.6 msec. For the web frames with fixed ends and 18" of stringers with single ends, the natural periods are 0.9 msec for both. After calculating a few of these natural periods, it is very clear that for them to be meaningful, the end conditions and the loading must be known. Also, the mode in which the element vibrates must be known. These natural periods are found by proper interpretation of the time histories of the strain gages and deflection gages. No attempt was made to predict the damping effect of the water and air environment or of the

non-linear modulus of elasticity resulting from entering the plastic range of the material, both of which increase the natural periods.

Another type of loading considered in an impact study is best described as a modified blast loading (Figure XVI). This type of shock wave has a finite rise time, t_o, instead of the instantaneous rise observed for the blast pulse.

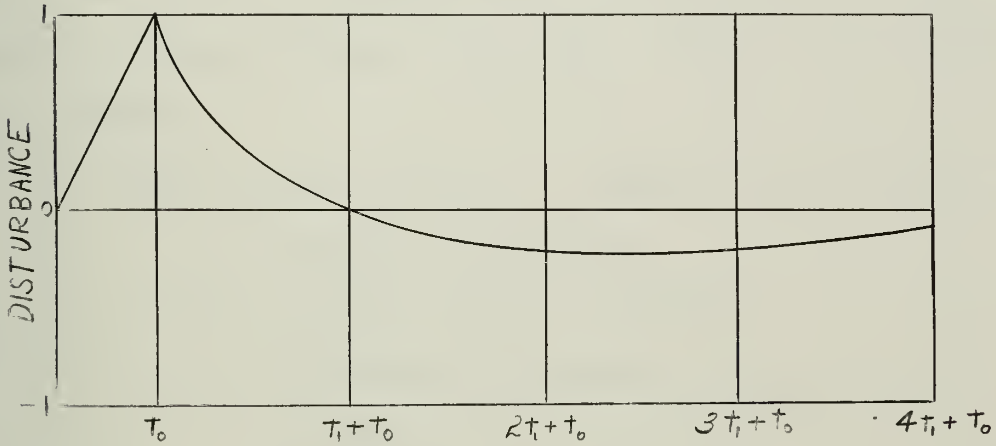

Figure XVI--Modified Shock Wave

For the modified blast pulse, the dynamic load factor is = 1 if $t_o/T > 1$. If $t_o/T < 1$, the dynamic load factor approaches 2 as $\frac{t_o}{T}$ approaches 0 provided $\frac{t_1}{T} > 10$. If $\frac{t_1}{T} < 10$, the dynamic load factor must be decreased in proportion to the dynamic load factor given for the blast pulse, Figure XIII.

III. RESULTS

The experimental and theoretical data are presented in groups of figures, each figure relating to the shot number and the drop height. The major parts of the discussion and conclusions are based on shots 5532(6-foot drop), 5533(8-foot drop), 5534(25-foot drop), 5549(12-foot A drop), 5550(12-foot B drop), 5551(12-foot C drop), 5553(12-foot D drop), and the velocity data for the above drops. Data supplementary to these results is included in Appendix C under shots 5530(2-foot drop), 5531(4-foot drop), 5545(2nd 4-foot drop), 5546(2nd 6-foot drop) and damage offsets.

Each shot, hence Figure, is organized in the following sequence:

1. pressure time histories
2. girthwise pressure histories
3. deflection time histories
4. girthwise deflection histories
5. strain time histories; and
6. superimposed time histories.

Where theoretical pressures were calculated, they are shown as dashed lines on each particular gage history.

Zero time for all drops is an electric trigger set off as the keel passes a point six inches above the water surface. Time for theoretical pressures are adjusted to this time scale or are written from impact time which is zero time for the computed data. Impact time is used as zero time for the velocity data.

Photographs of the structural damage of the two models tested

are shown as Figures XXIV through XXX. Figures XXIV through XXVI are the results of the 25-foot drop which corresponds to an impact velcoity of 40 feet per second. Figures XXVII through XXX are the results of repeated impacts from a height of 12 feet and an impact velocity of 27.8 feet per second.

High speed photographs of most of the drops are available at David Taylor Model Basin and in the Plans File Section, Department of Naval Architecture and Marine Engineering, Massachusetts Institute of Technology. These photographs correlate the impact velocities calculated and show the spray and water surface conditions as well. The attitude of each model as it impacted is also shown and confirms that no roll angle greater than 1/2 degree occurred. Water condition at the time of each drop was calm.

Inspection of the various records from each drop reveals the following predominant periods of vibrations: 25, 6, 3 and 1.4 msec.

Using data from Figures XXXVI and XXXVII of Appendix C, the deformation energy computed as a percent of the total potential energy of the models is as follows:

	12-foot drops	25-foot drops
panels	2.6%	8.2%
total	3.8%	19.5%

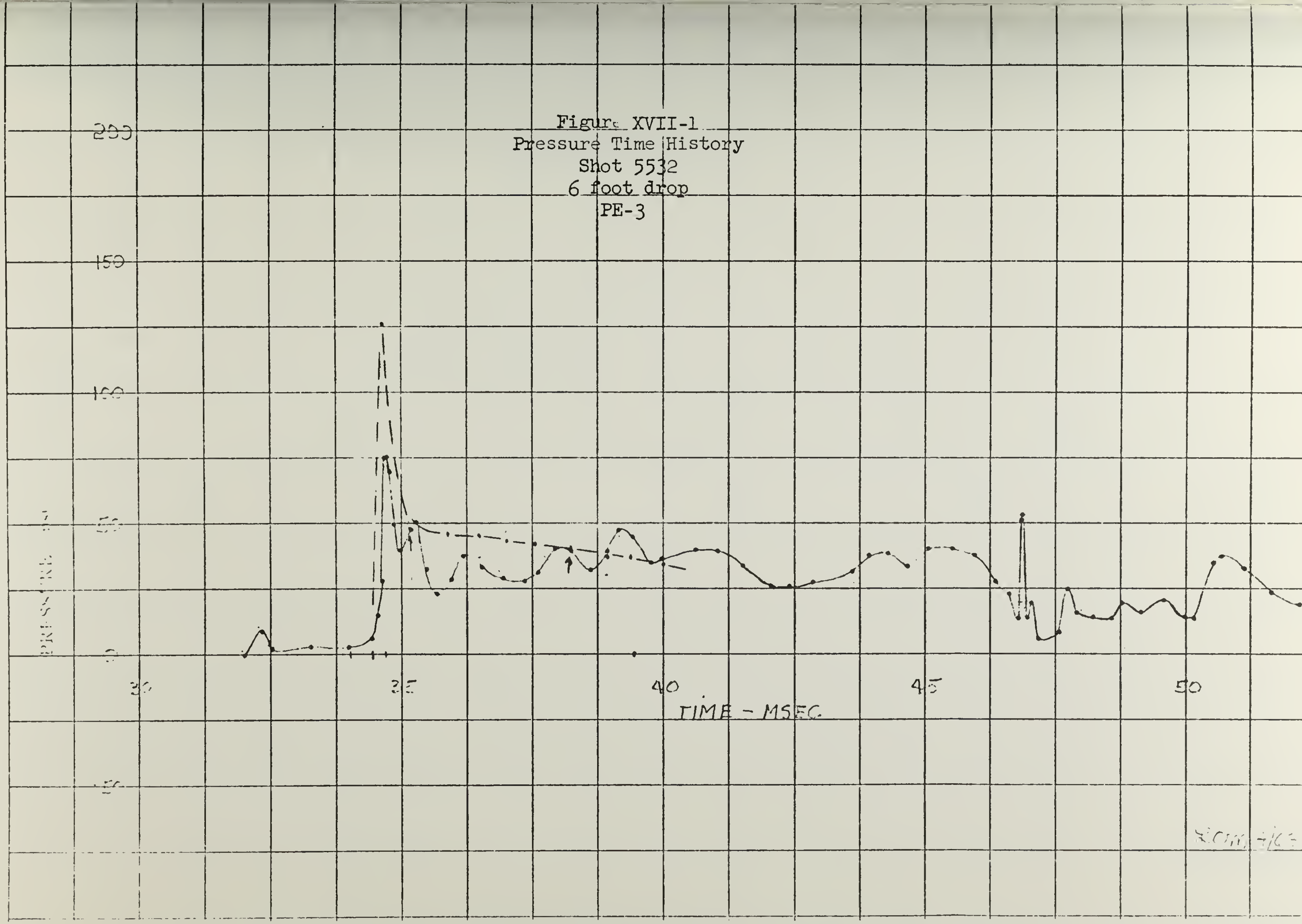

Figure XVII-1
Pressure Time History
Shot 5532
6 foot drop
PE-3

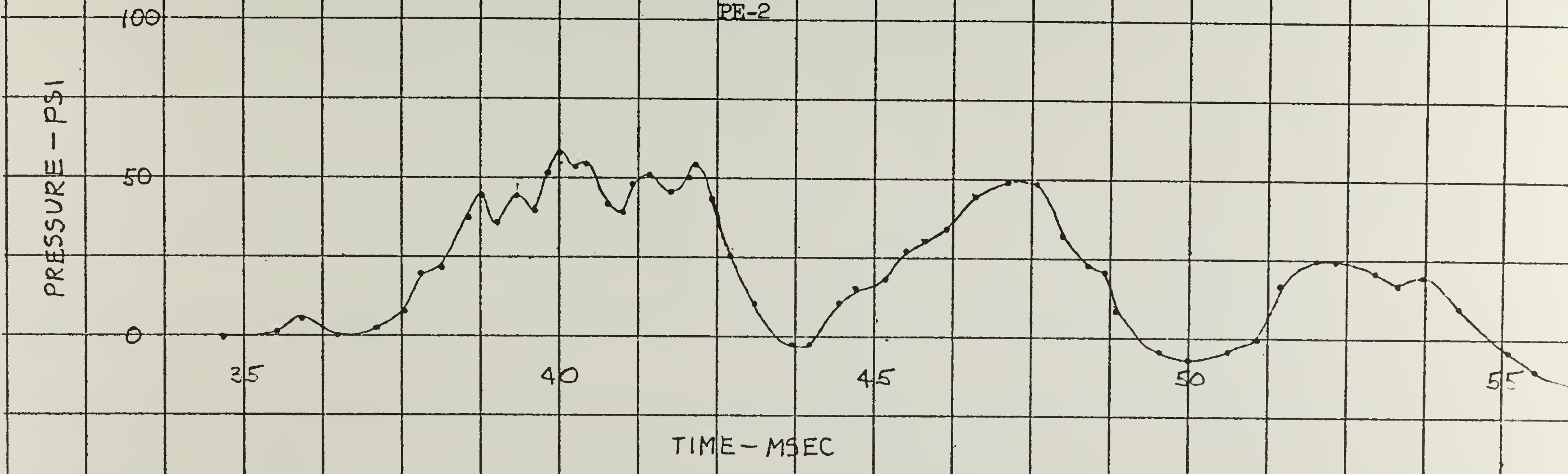

Figure XVII-2
Pressure Time History
Shot 5532--6 foot drop
PE-2

LCM 4/63

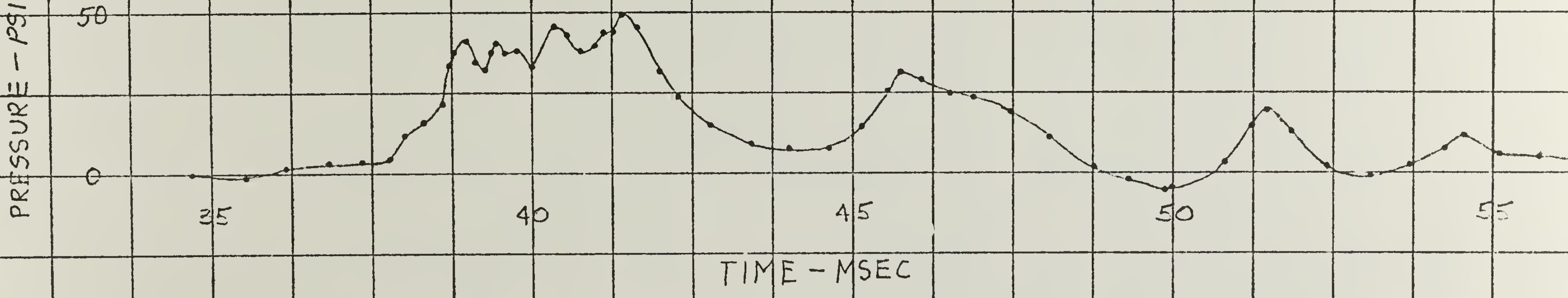

Figure XVII-3
Pressure Time History
Shot 5532--6 foot drop
PE-1

LCM 4/63

Figure XVII-4
Pressure Time History
Shot 5532--6 foot drop
PE-4

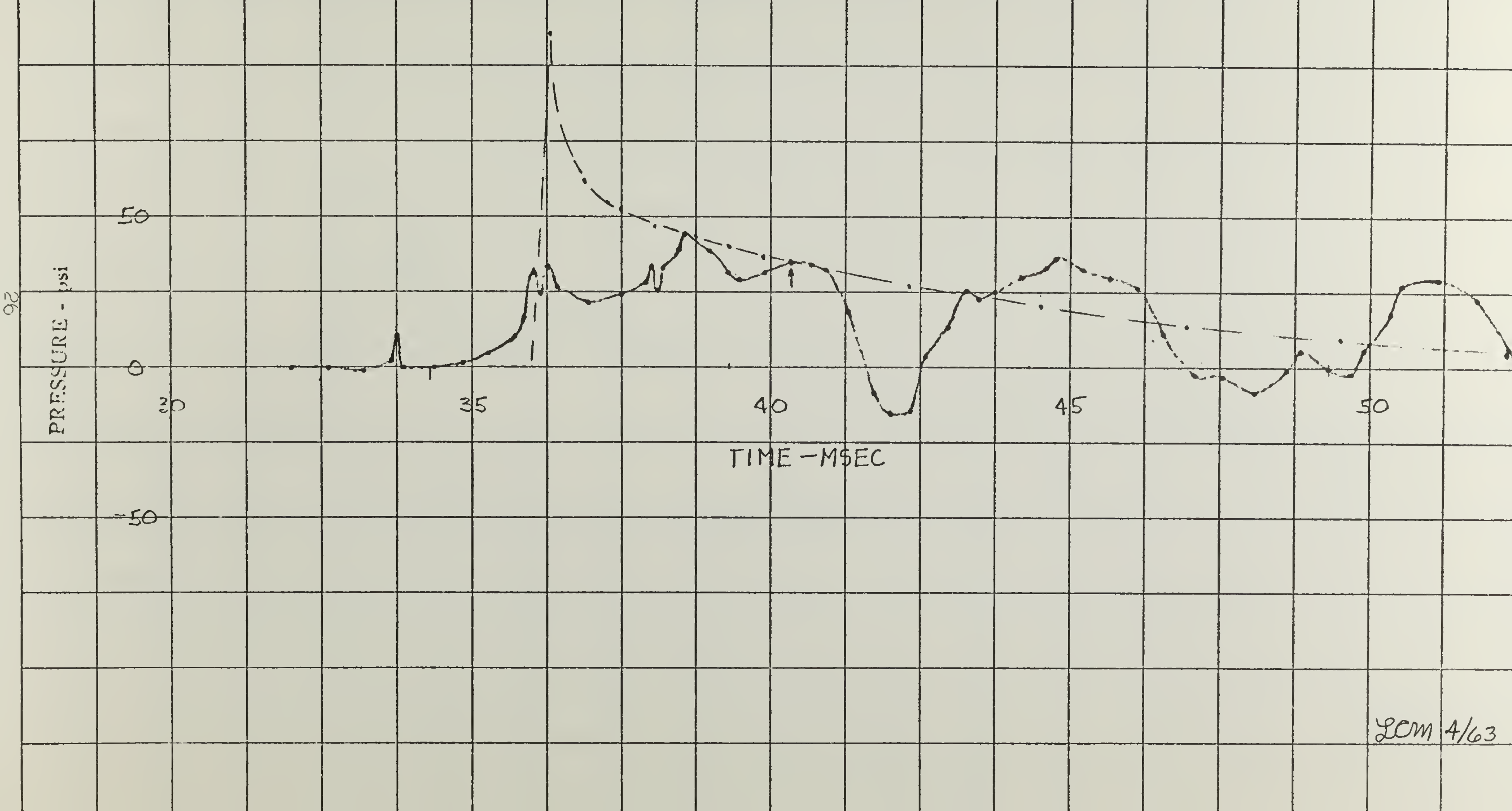

LCM 4/63

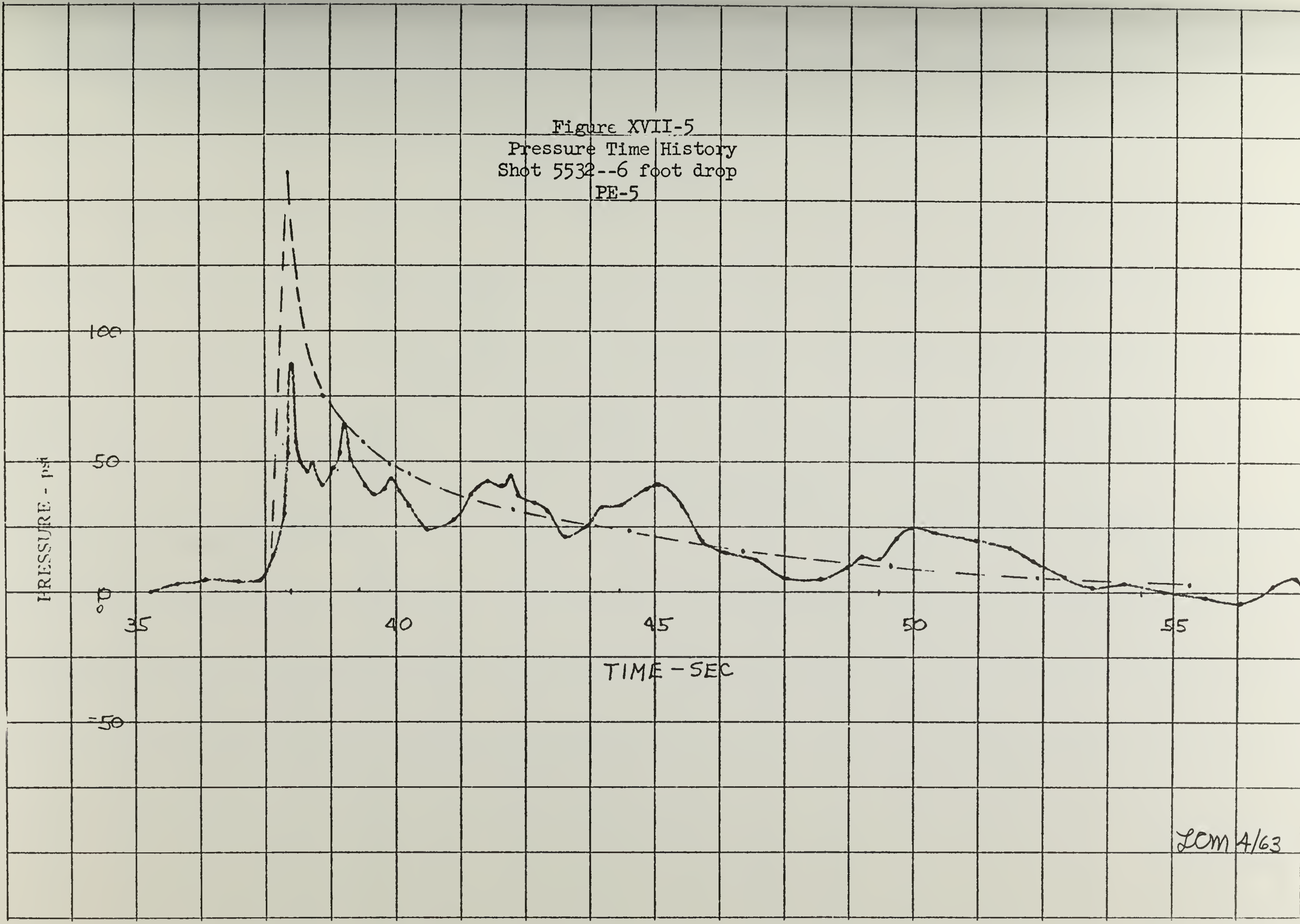

Figure XVII-5
Pressure Time History
Shot 5532--6 foot drop
PE-5

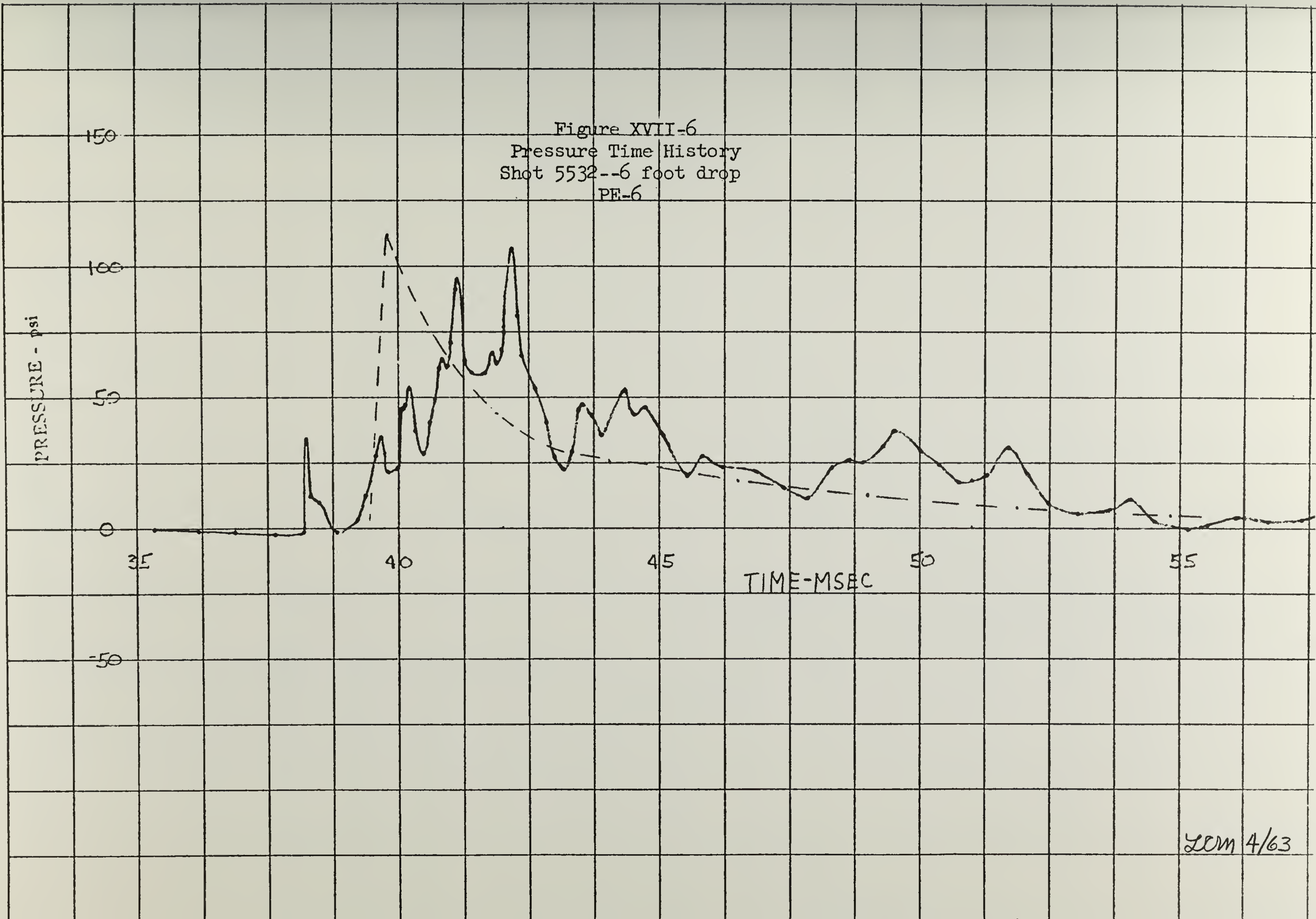

Figure XVII-6
Pressure Time History
Shot 5532--6 foot drop
PE-6

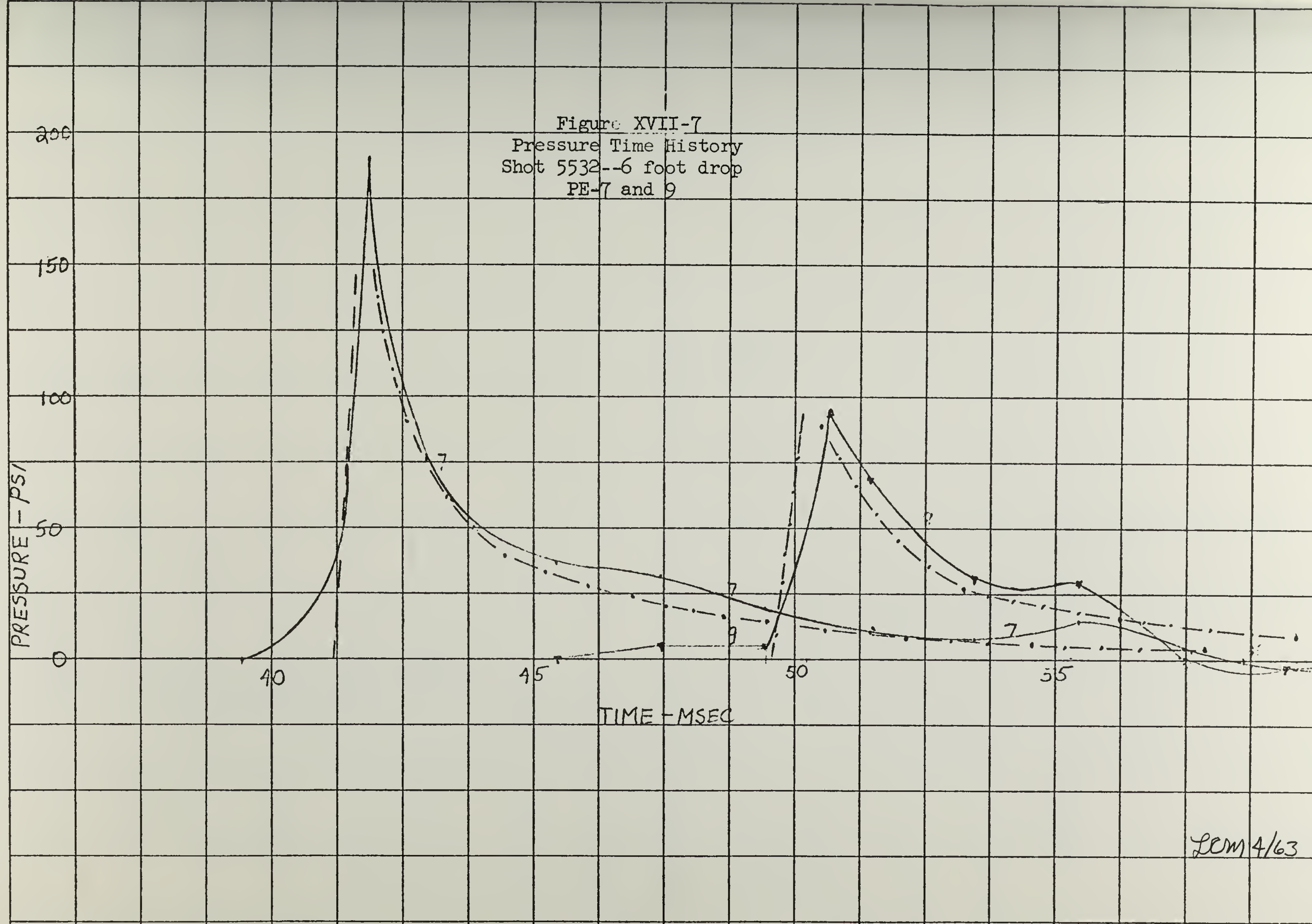

Figure XVII-7
Pressure Time History
Shot 5532--6 foot drop
PE-7 and 9

LCM 4/63

Figure XVII-8
Experimental Girthwise Pressure Distribution
Shot 5532--6 foot drop
At discrete times

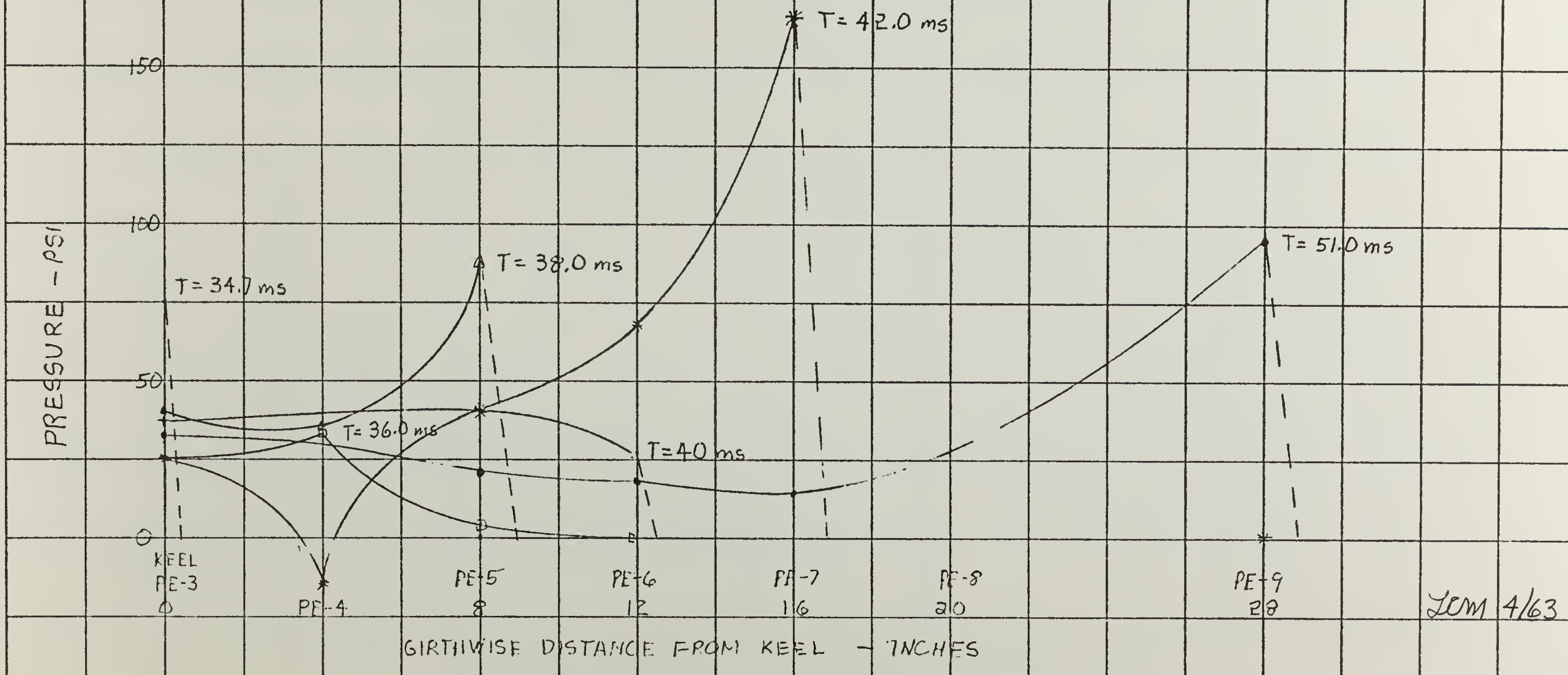

Figure XVII-9
Theoretical Girthwise Pressure Distribution
Shot 5532-6 foot drop
At discrete times

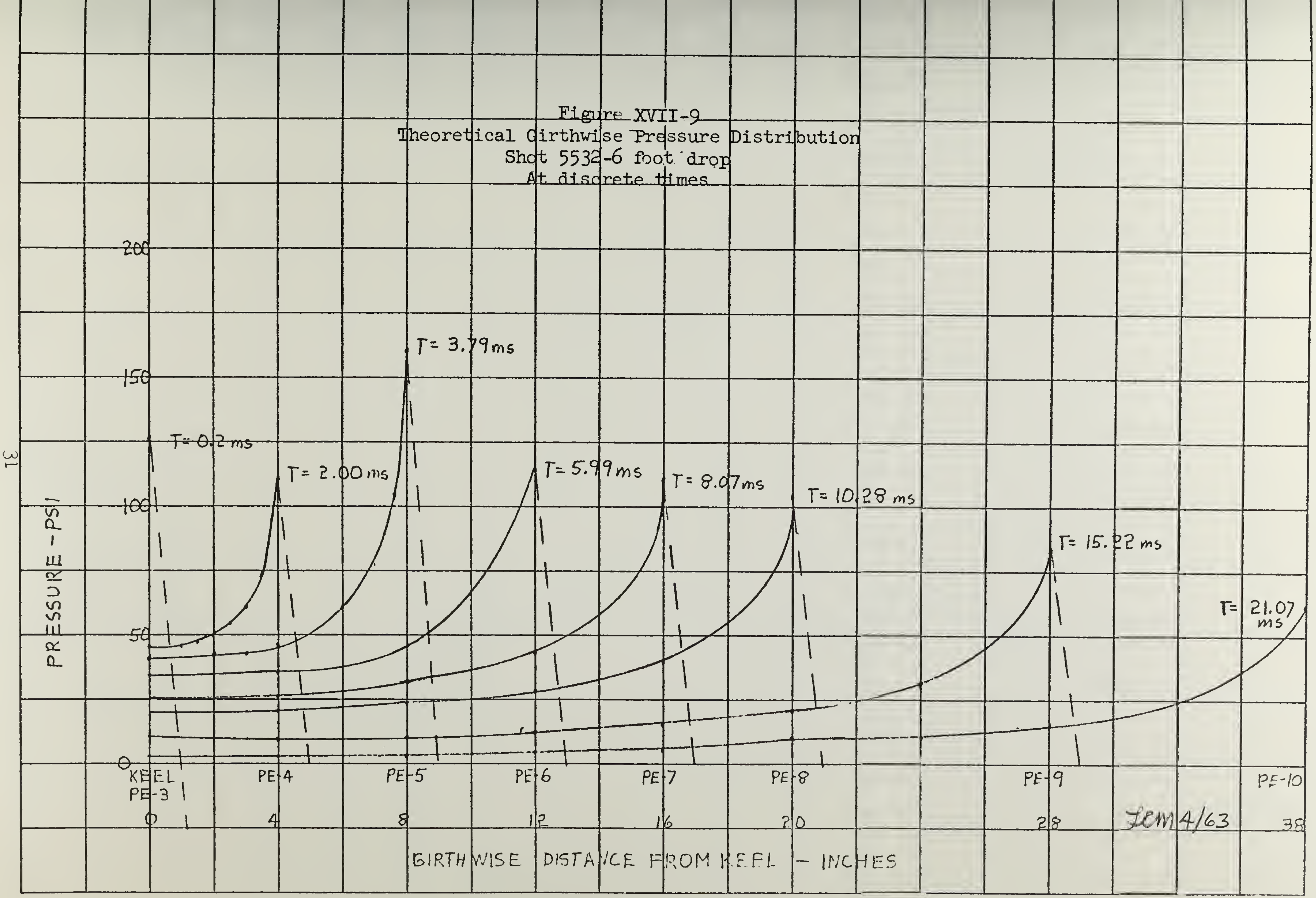

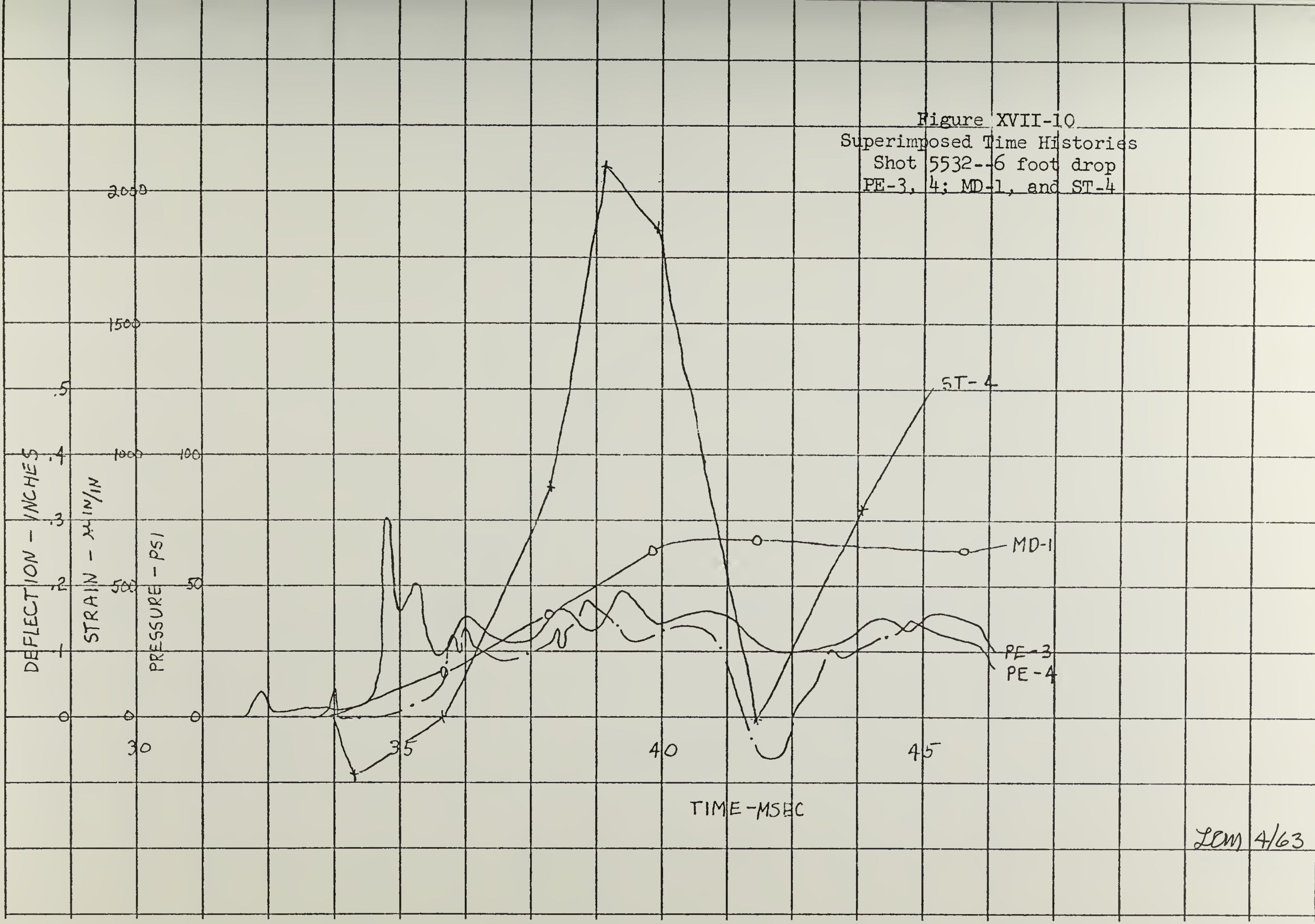

Figure XVII-10
Superimposed Time Histories
Shot 5532--6 foot drop
PE-3, 4; MD-1, and ST-4

LCM 4/63

Figure XVII-11
Superimposed Time Histories
Shot 5532--6 foot drop
MD-3 and PE-6

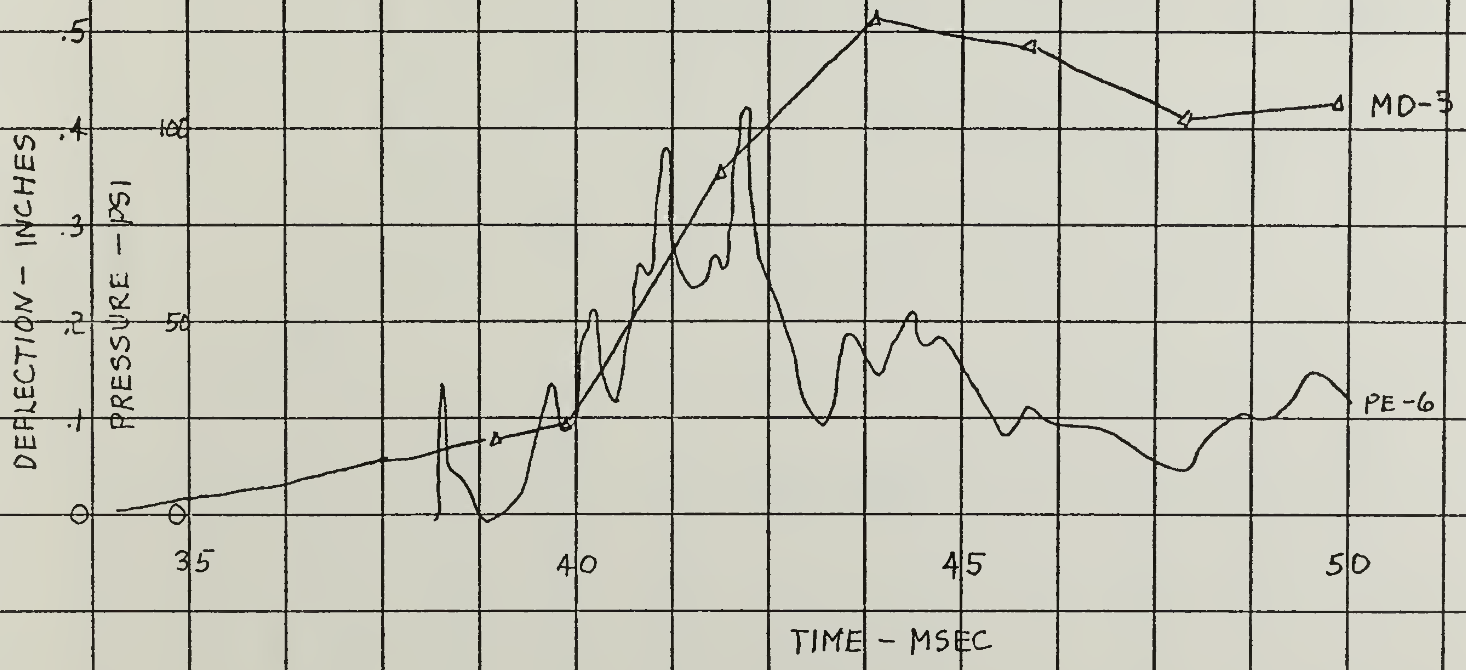

JCM 4/63

Figure XVII-12
Superimposed Time Histories
Shot 5532--6 foot drop
ST-3, MD-2 and PE-5

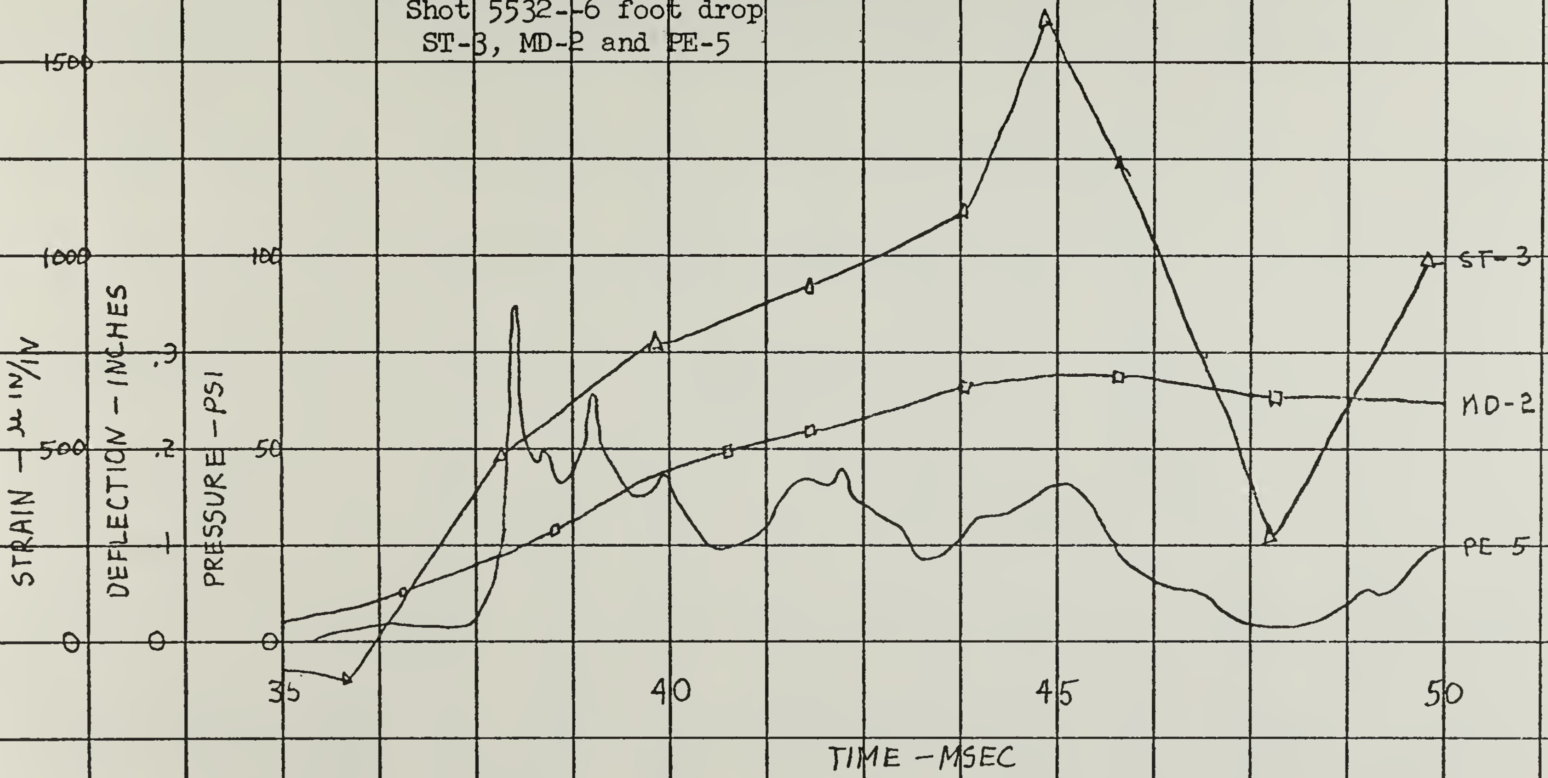

Lcm 4/63

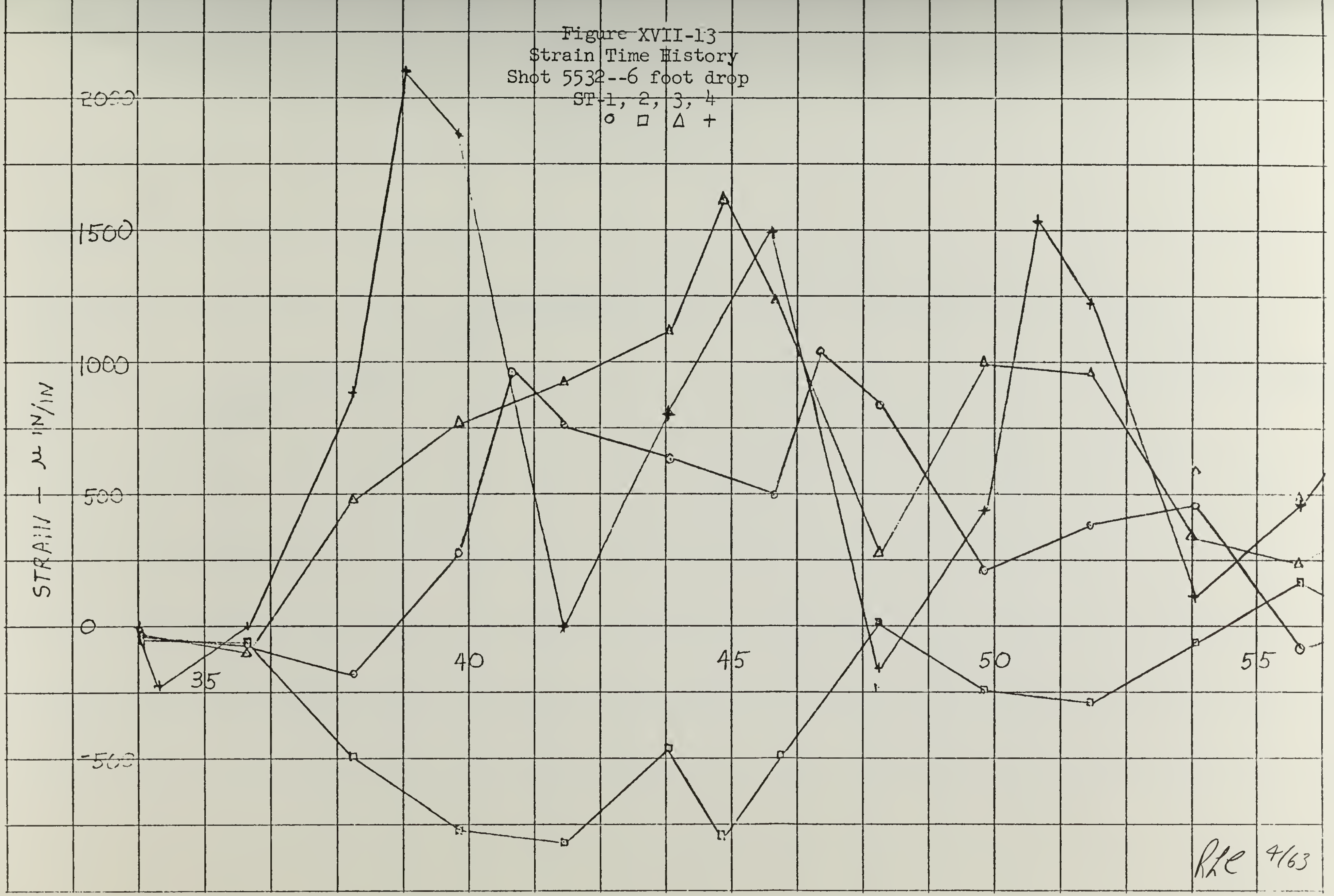

Figure XVII-13
Strain Time History
Shot 5532--6 foot drop
ST-1, 2, 3, 4
o □ Δ +

RLC 4/63

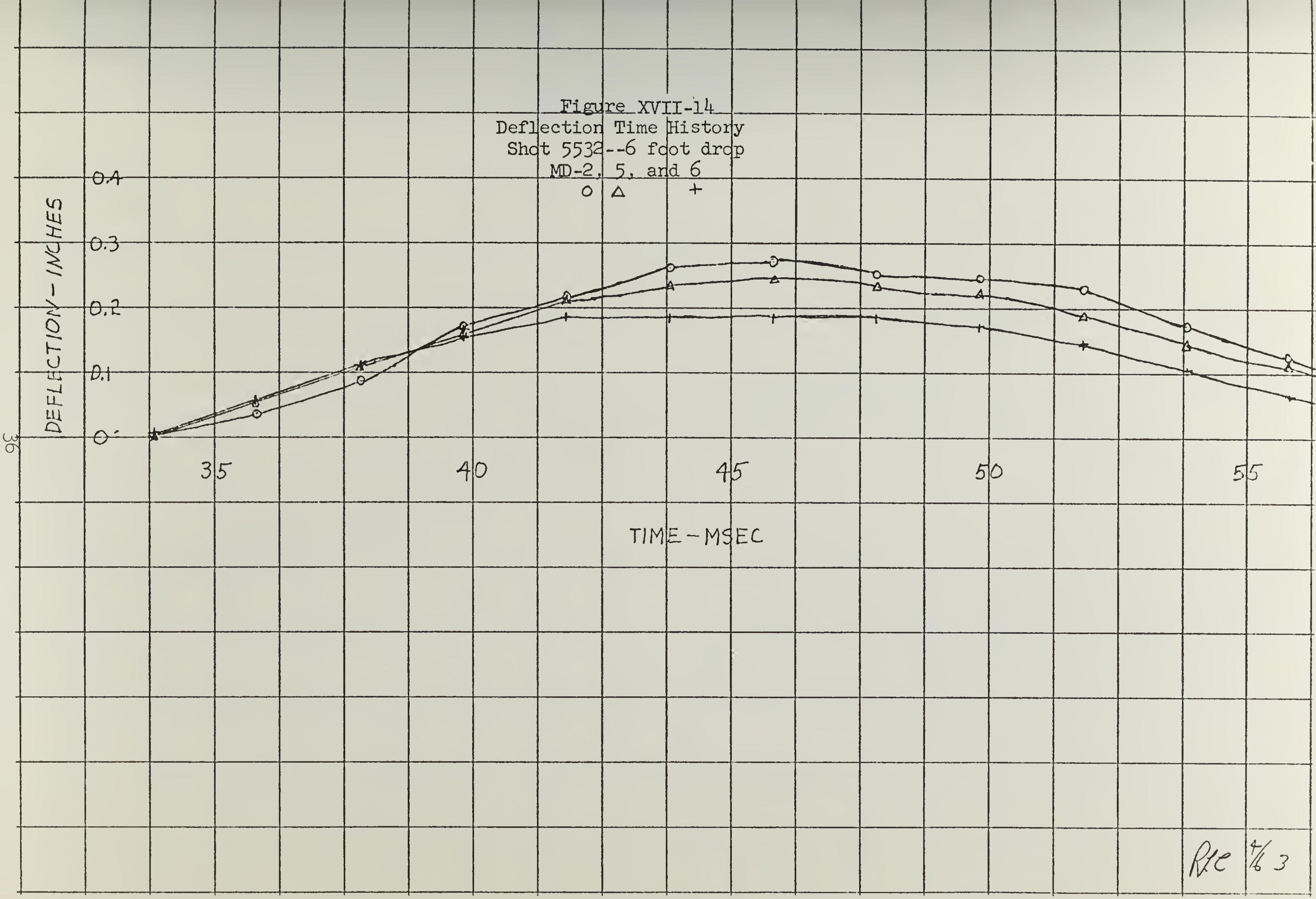

Figure XVII-14
Deflection Time History
Shot 5532--6 foot drop
MD-2, 5, and 6

Rte 4/6 3

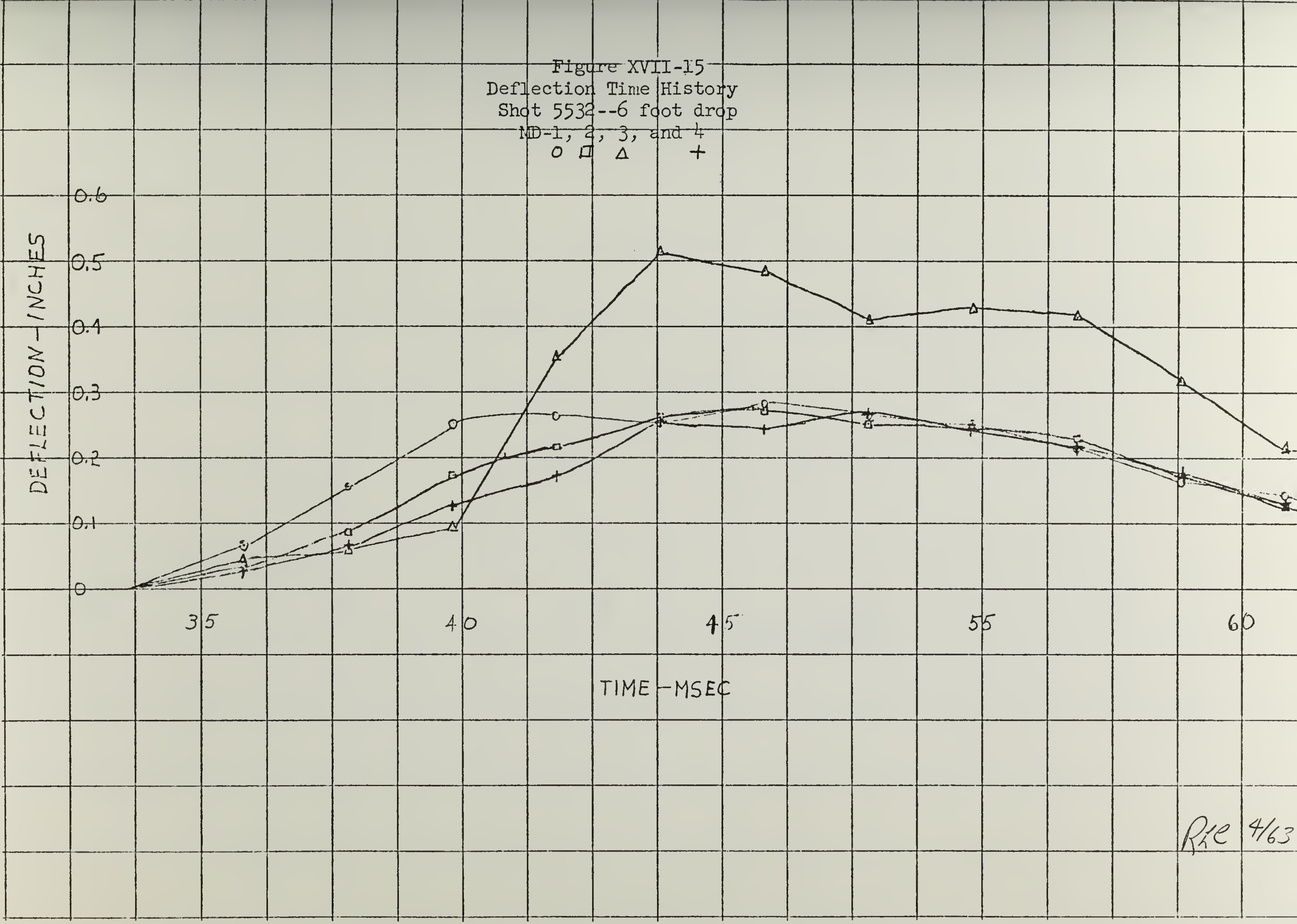

Figure XVII-15
Deflection Time History
Shot 5532--6 foot drop
MD-1, 2, 3, and 4
○ □ △ +

RLC 4/63

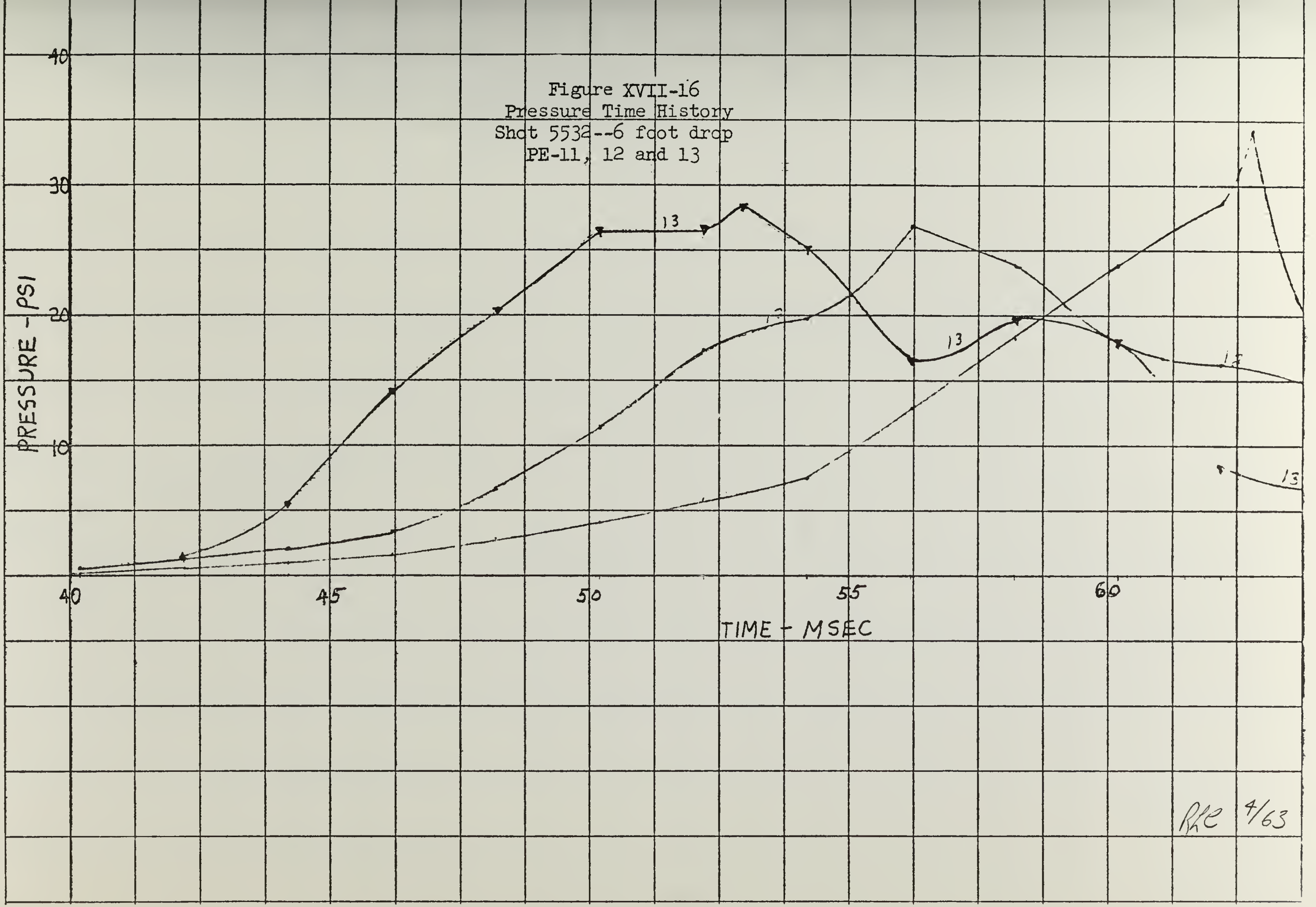

Figure XVII-16
Pressure Time History
Shot 5532--6 foot drop
PE-11, 12 and 13

RLC 4/63

Figure XVII-17
Pressure Time History
Shot 5532--6 foot drop
PE-16, 17 and 18

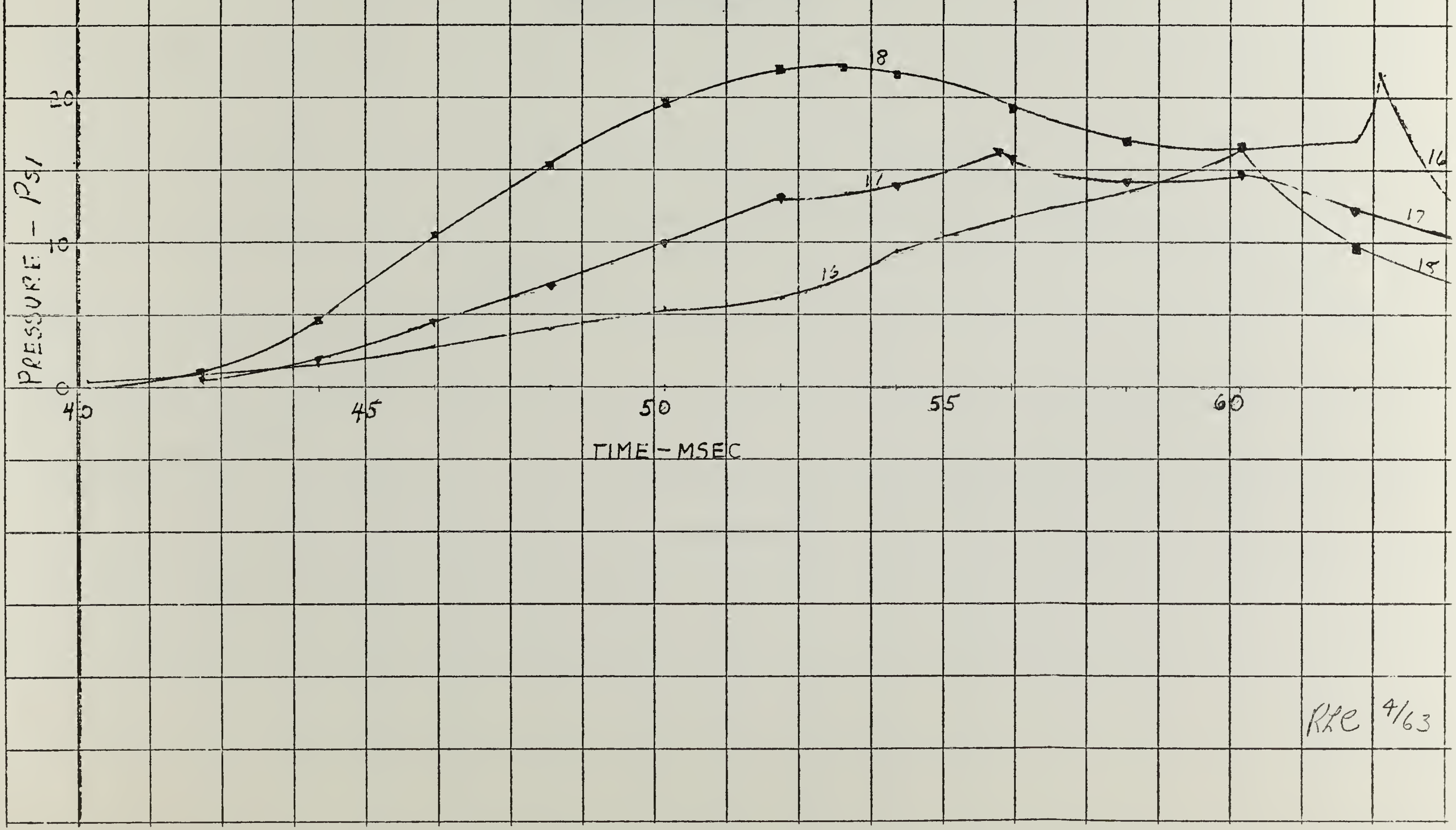

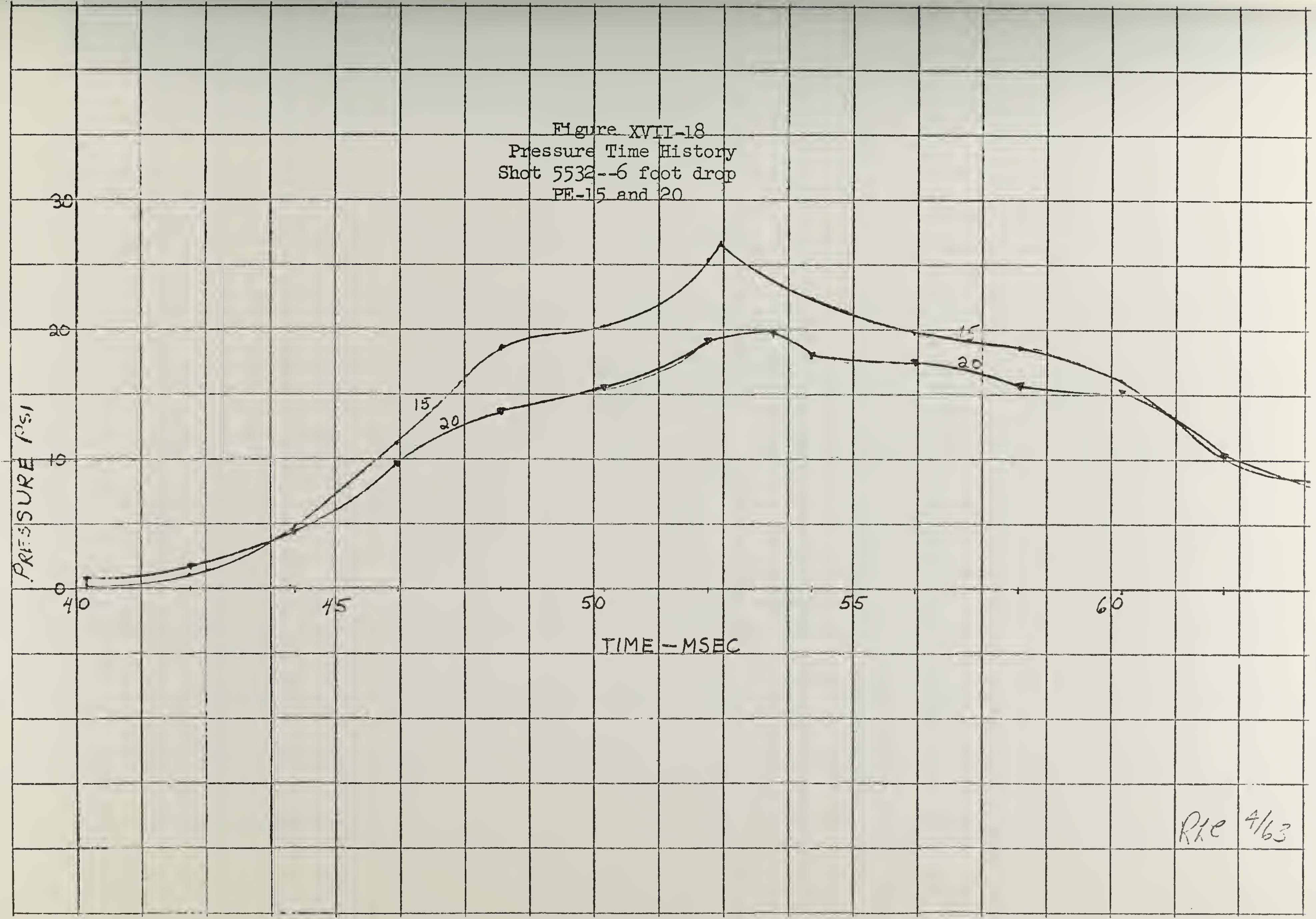

Figure XVII-18
Pressure Time History
Shot 5532--6 foot drop
PE-15 and 20

RKe 4/63

Figure XVIII-1
Pressure Time History
Shot 5533--8-foot drop
PE-3

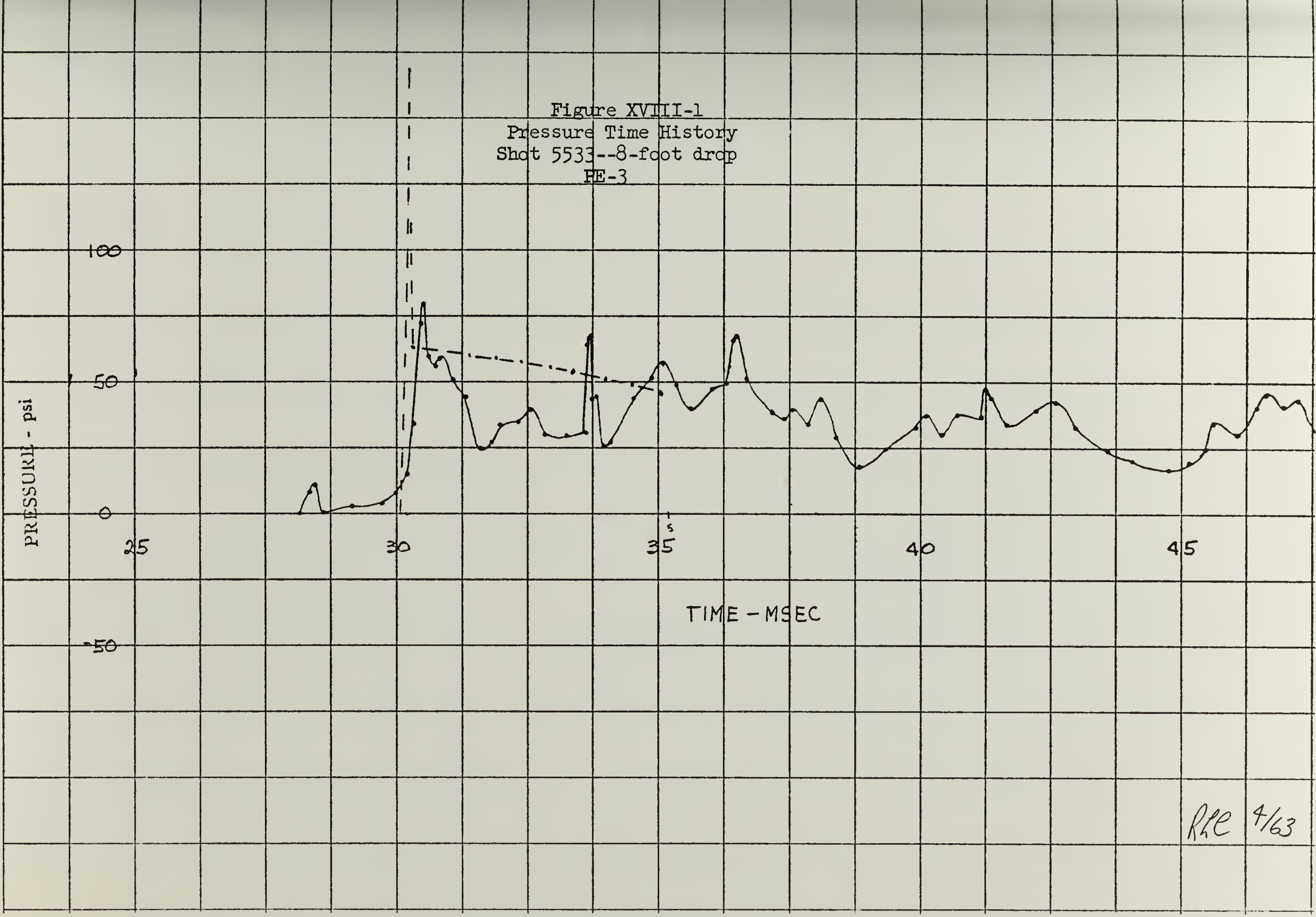

RLC 4/63

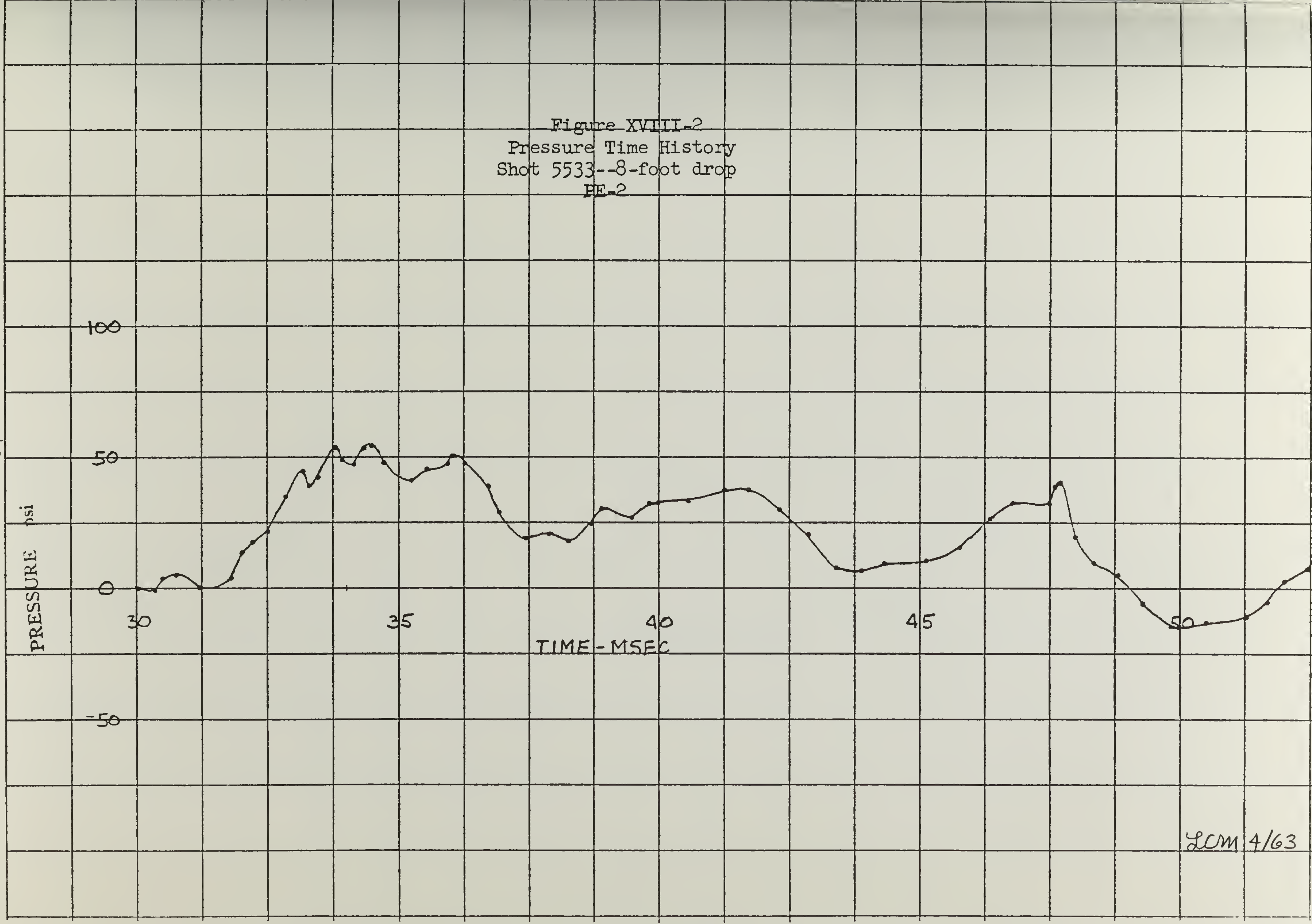

Figure XVIII-2
Pressure Time History
Shot 5533--8-foot drop
PE-2

LCM 4/63

Figure XVIII-3
Pressure Time History
Shot 5533--8-foot drop
PE-1

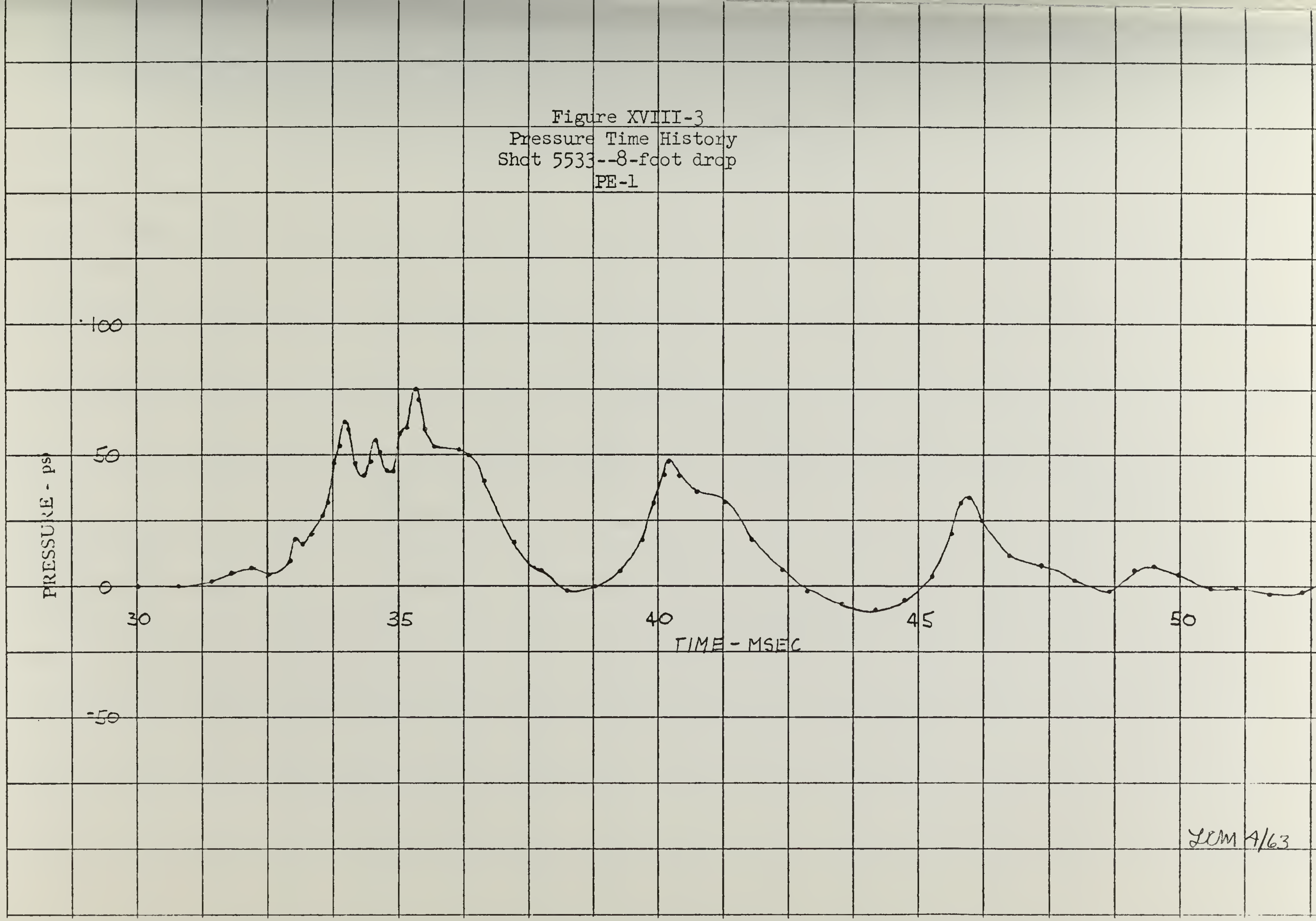

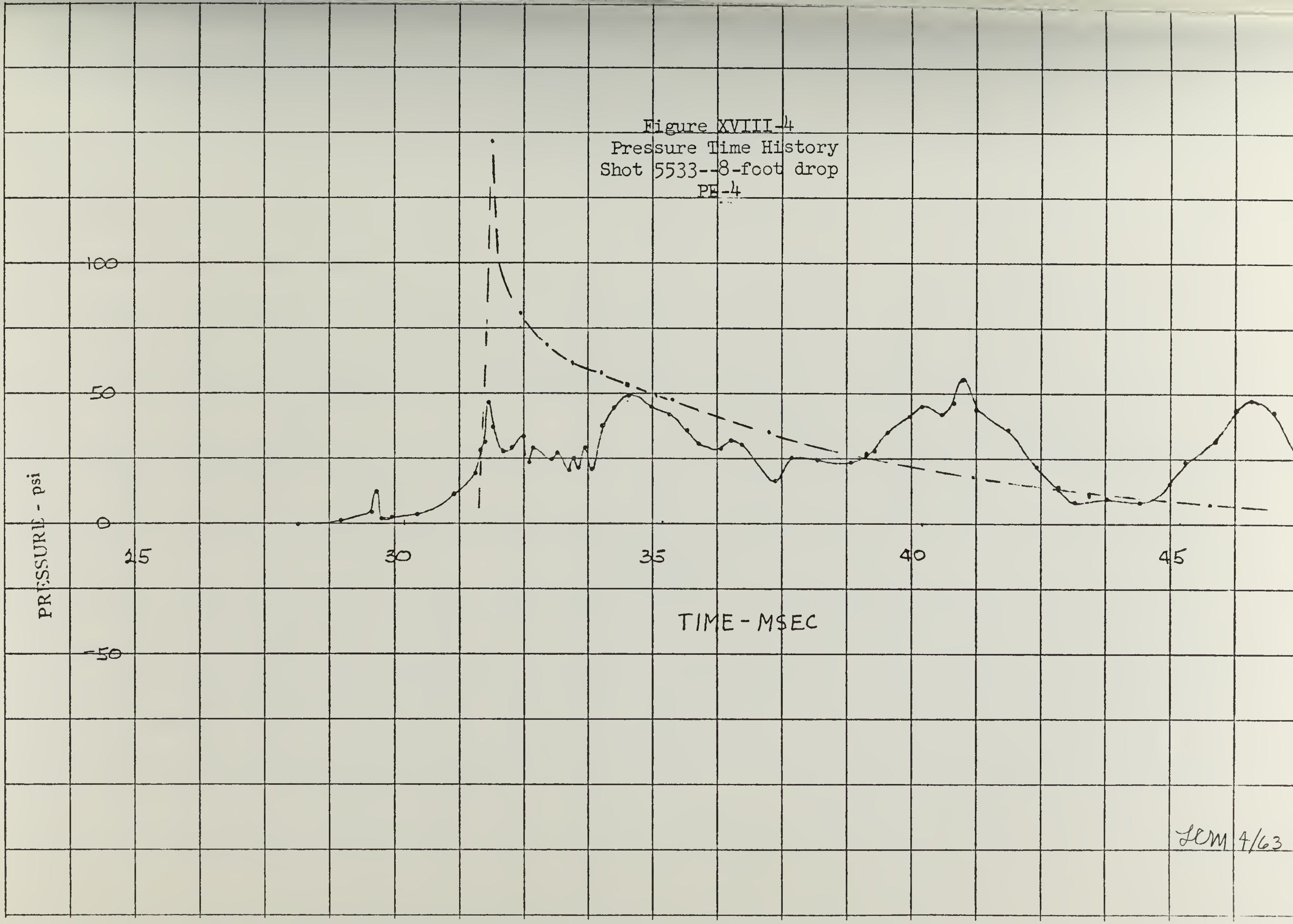

Figure XVIII-4
Pressure Time History
Shot 5533--8-foot drop
PE-4

LCM 4/63

Figure XVIII-5
Pressure Time History
Shot 5533--8-foot drop
PE-5

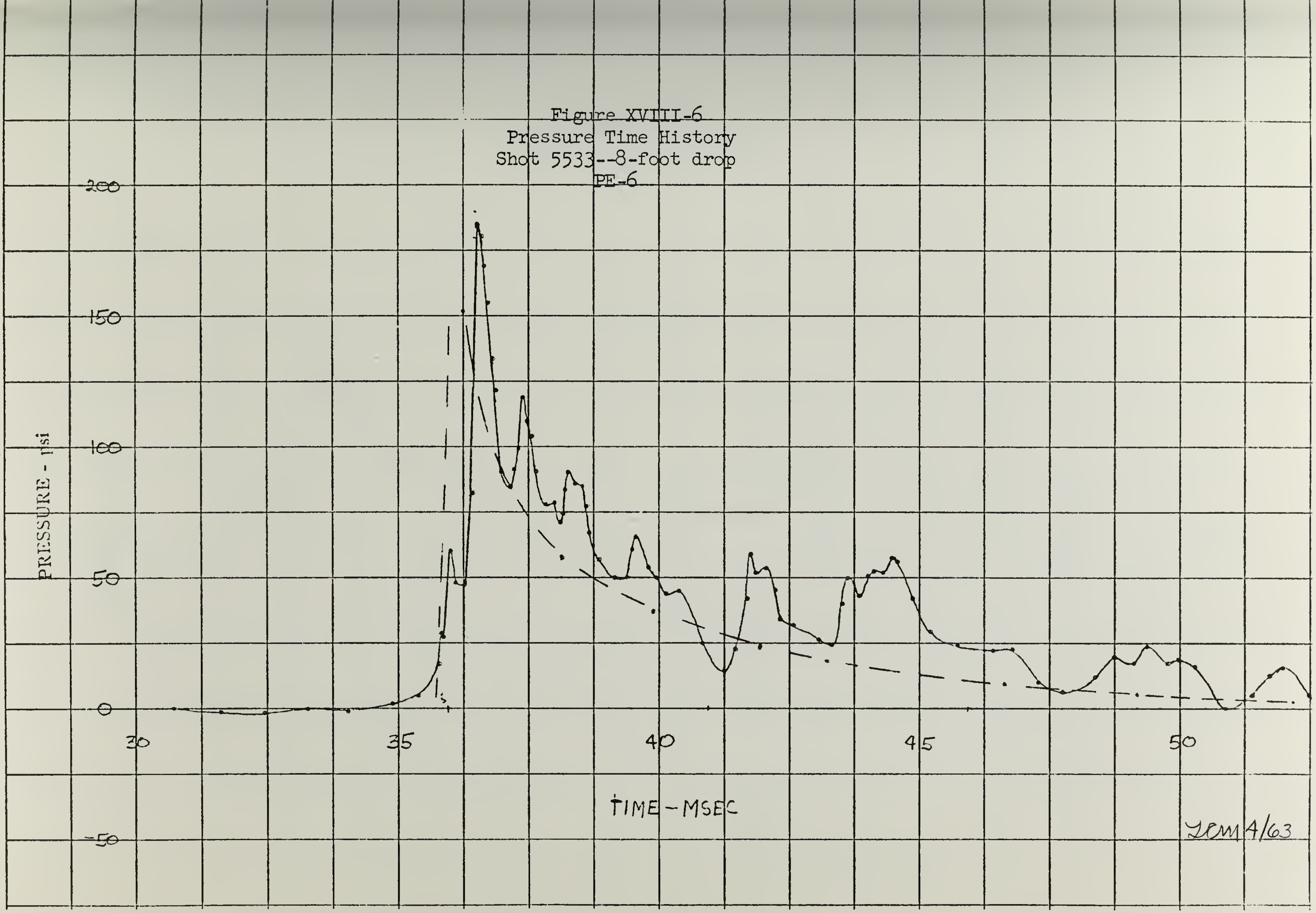

Figure XVIII-6
Pressure Time History
Shot 5533--8-foot drop
PE-6

Figure XVIII-7
Pressure Time History
Shot 5533--8-foot drop
PE-9

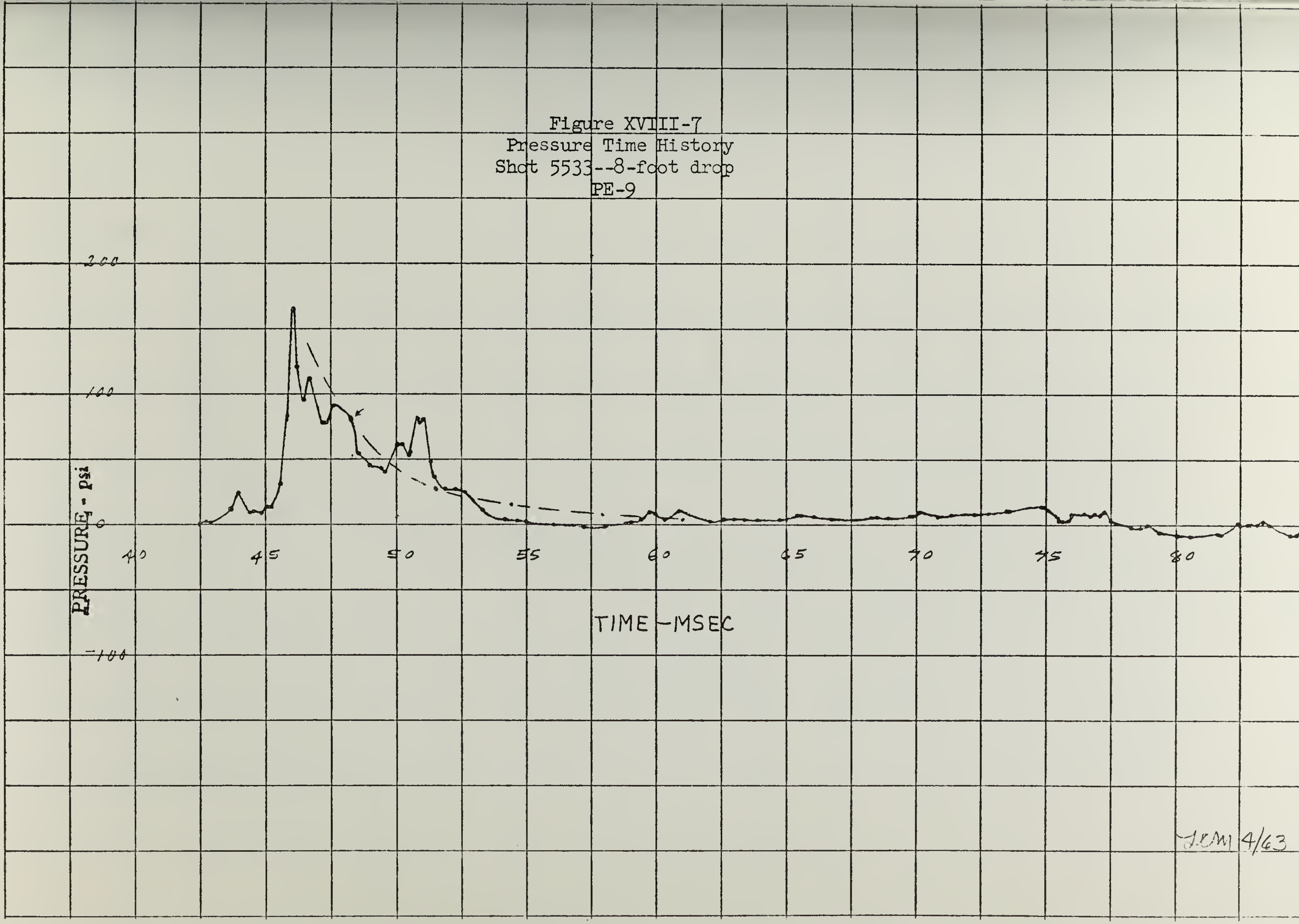

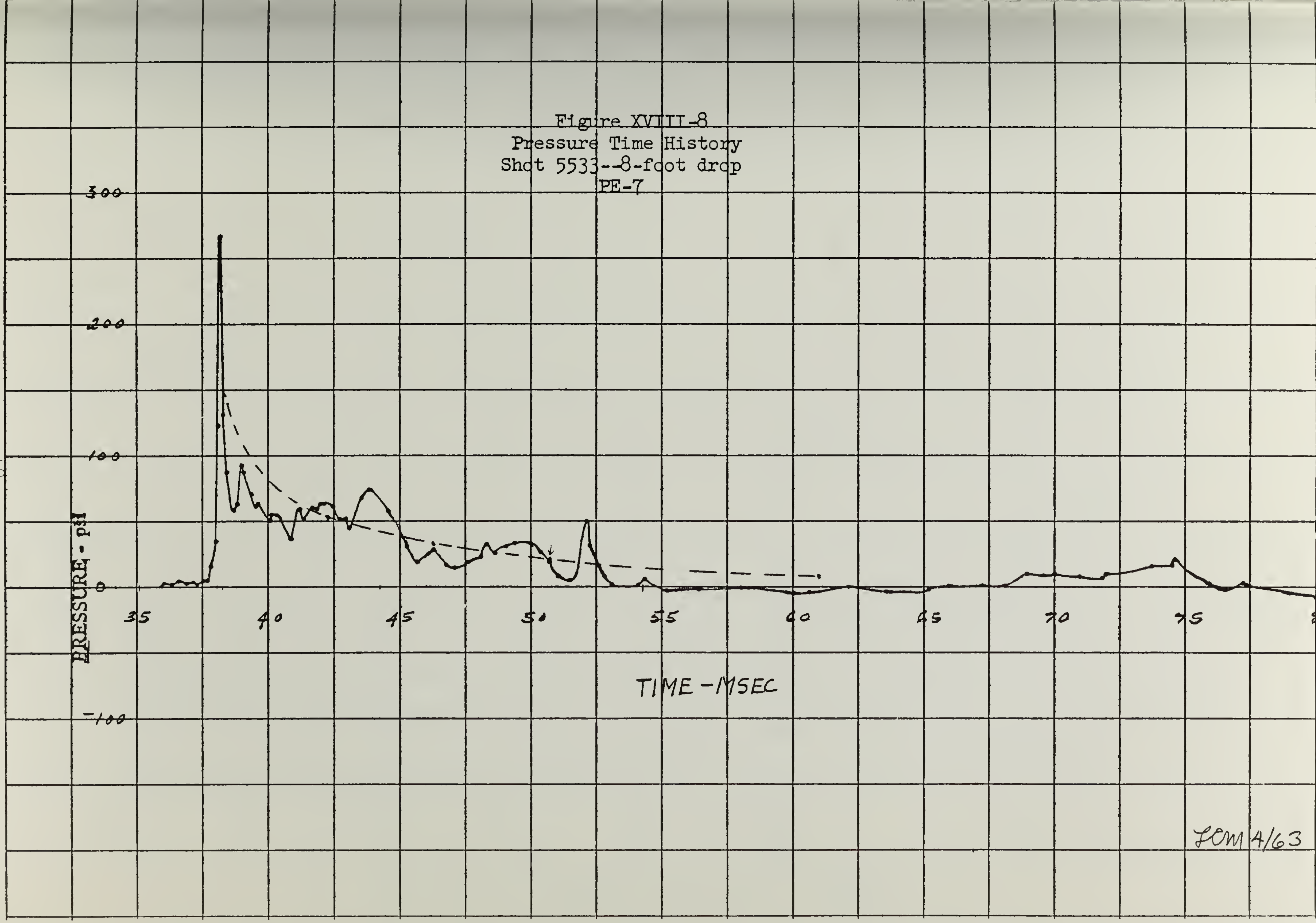

Figure XVIII-8
Pressure Time History
Shot 5533--8-foot drop
PE-7

Figure XVIII-9
Theoretical Girthwise Pressure Distribution
Shot 5533--8-foot drop
At discrete times

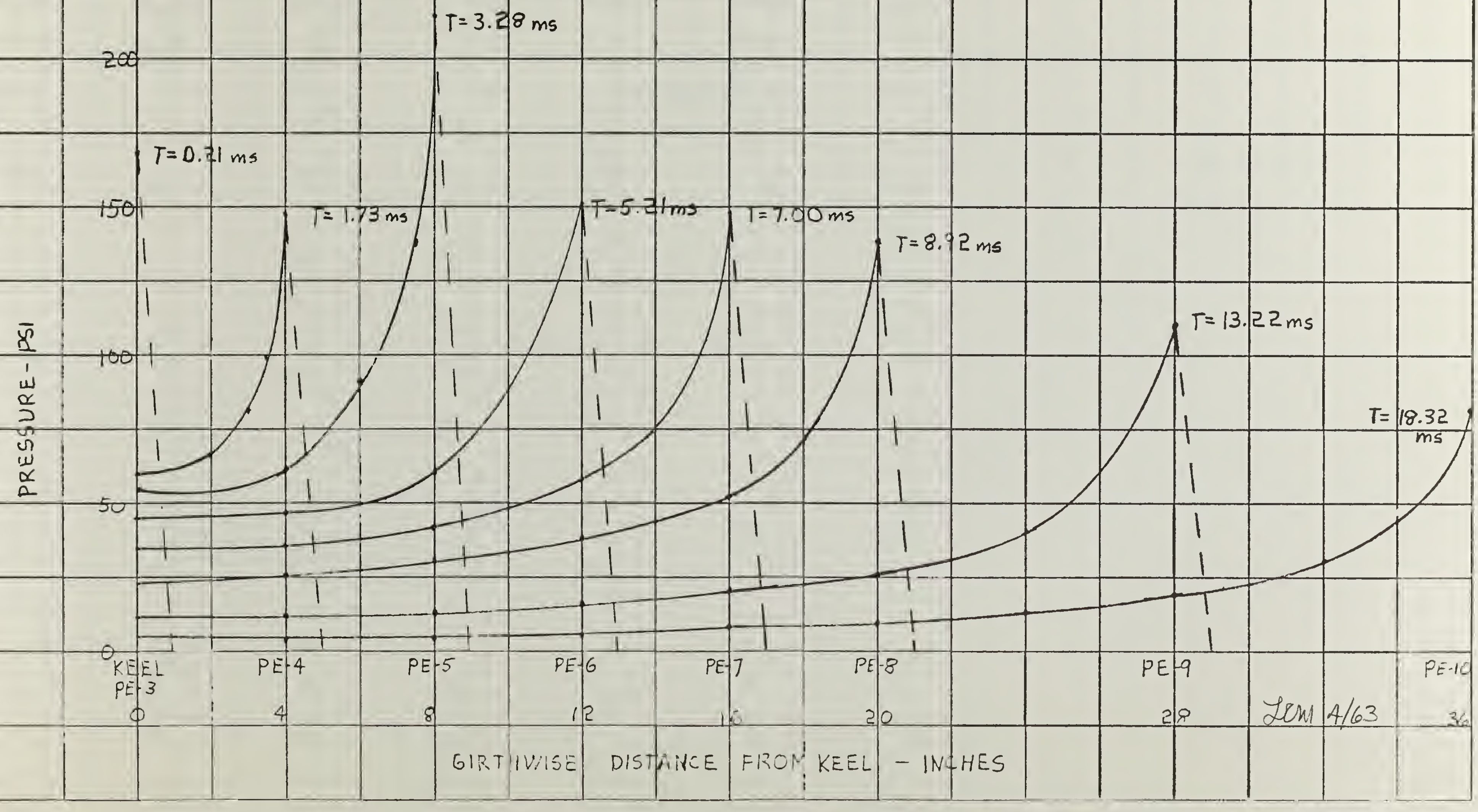

LCM 4/63

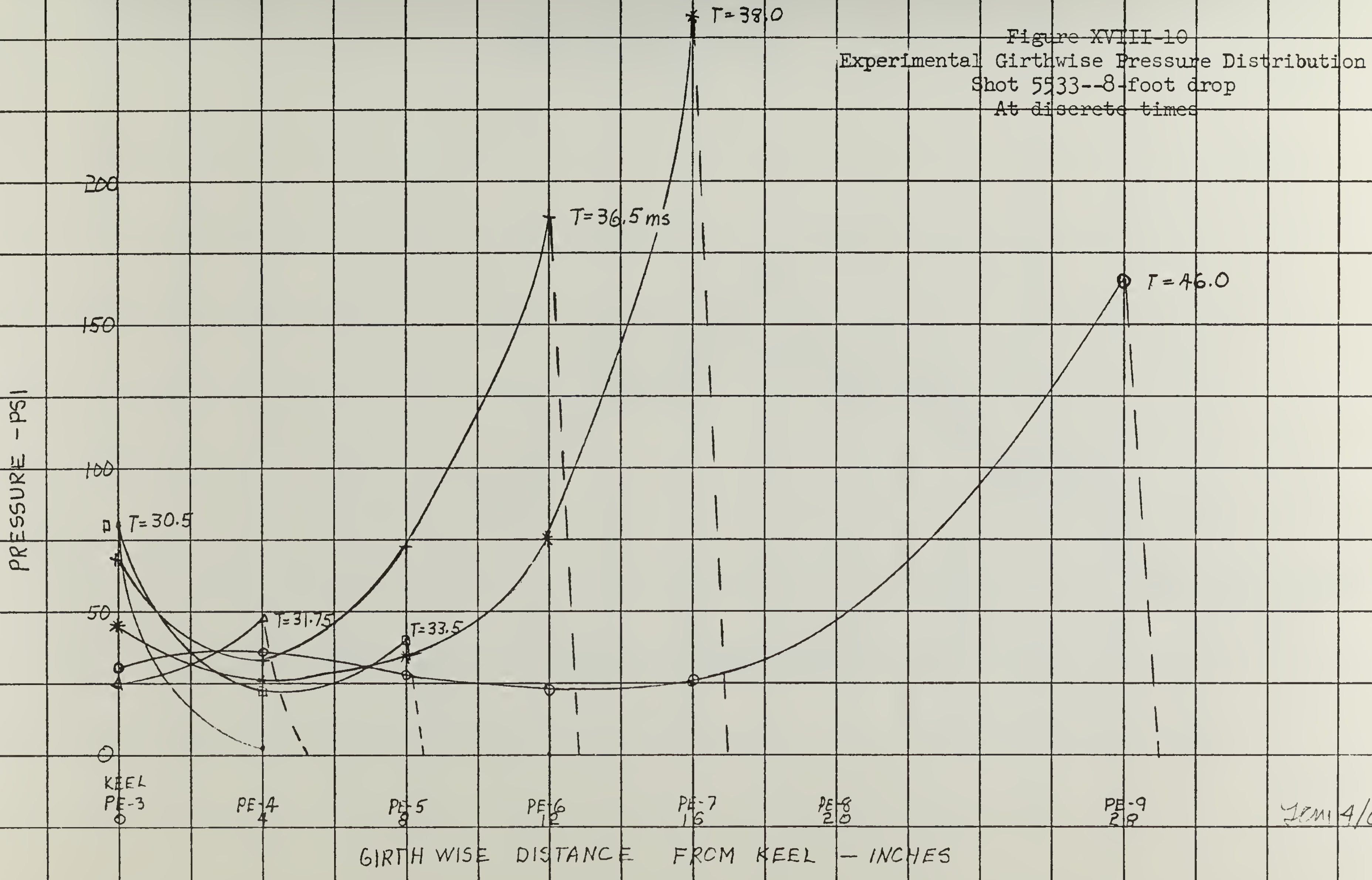

Figure XVIII-10
Experimental Girthwise Pressure Distribution
Shot 5533--8-foot drop
At discrete times

4/63

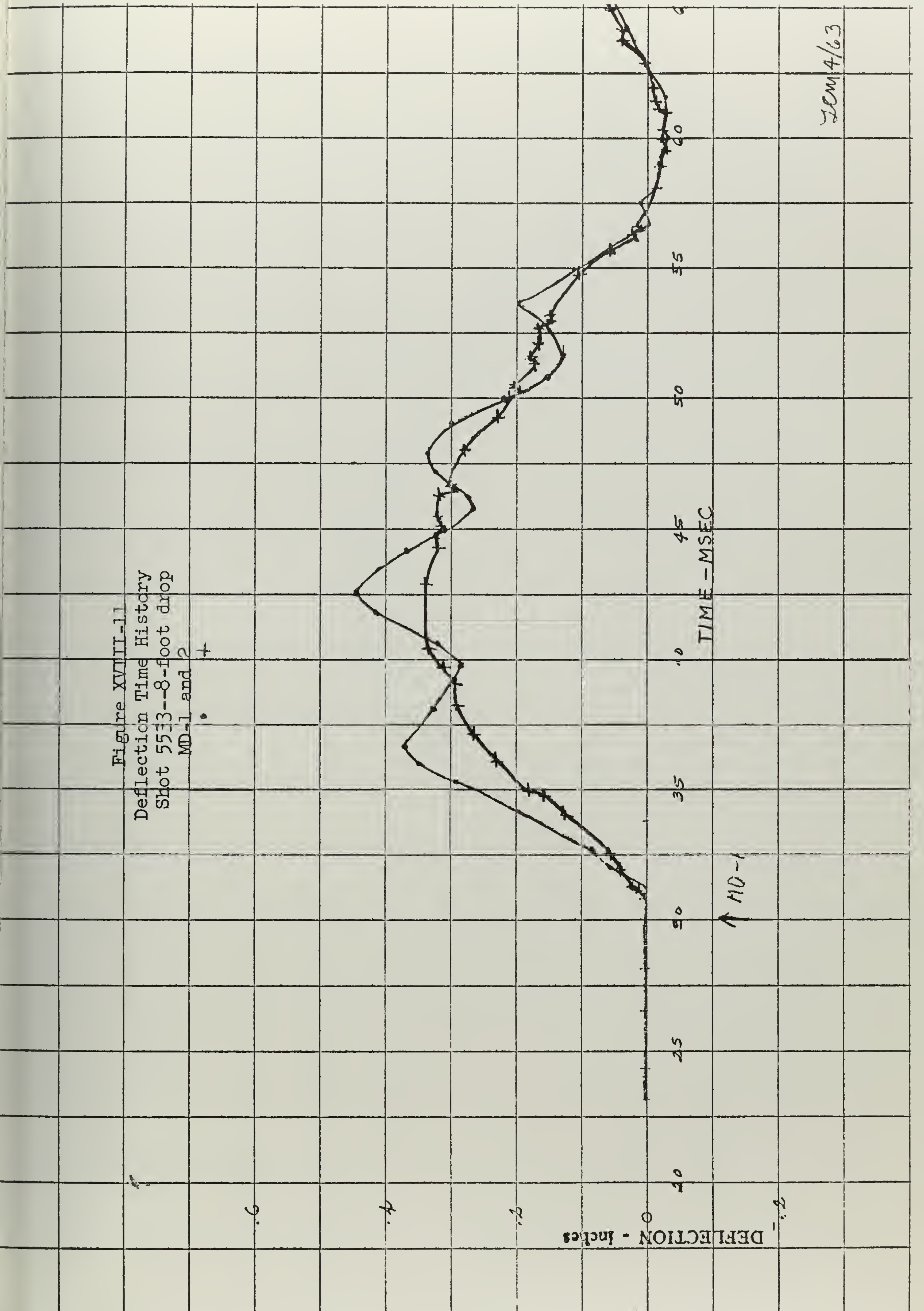

Figure XVIII-11
Deflection Time History
Shot 5533--8-foot drop
MD-1 and 2
• +

Figure XVIII--12
Deflection Time History
Shot 5533--8-foot drop
MD-2 and 4

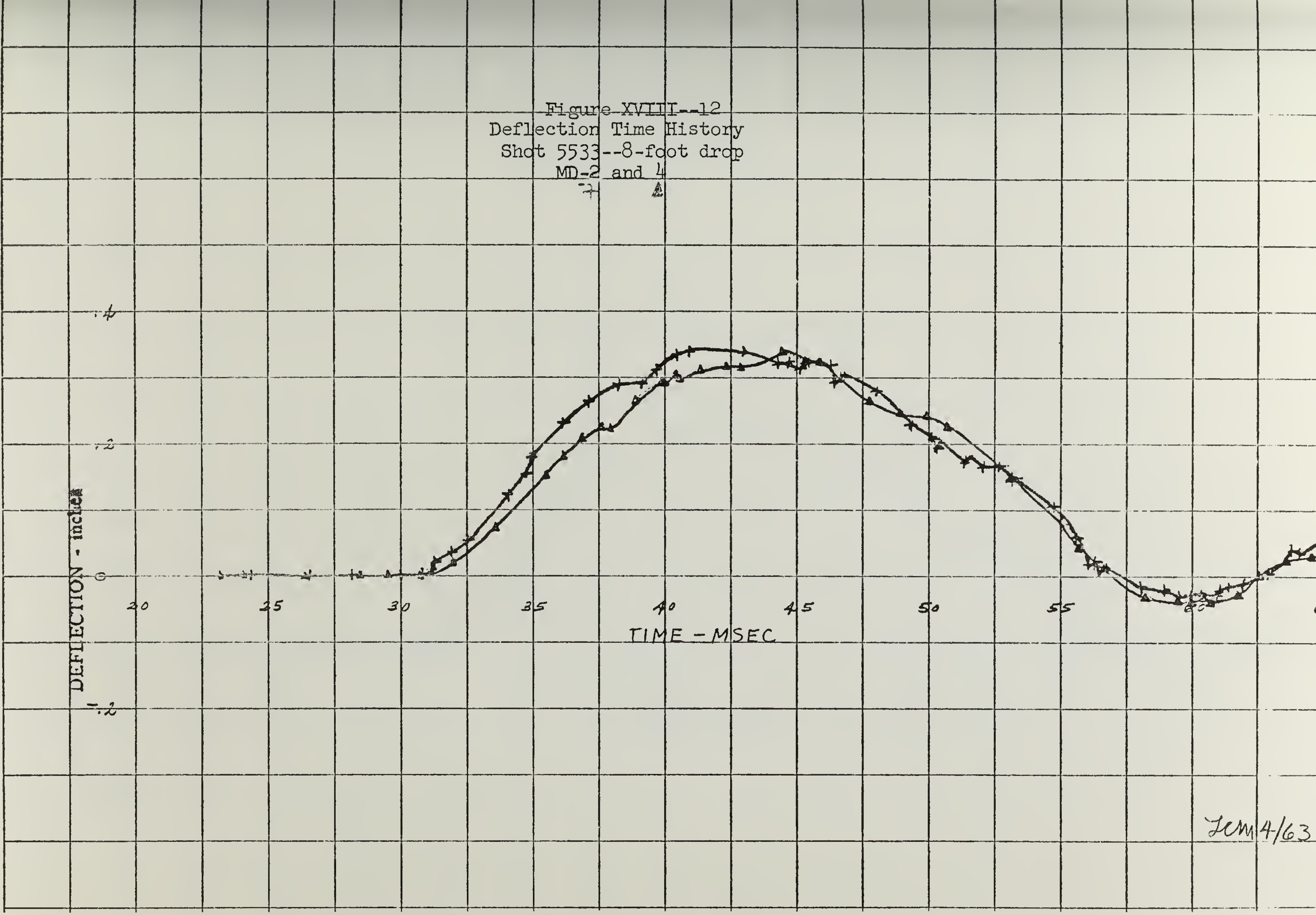

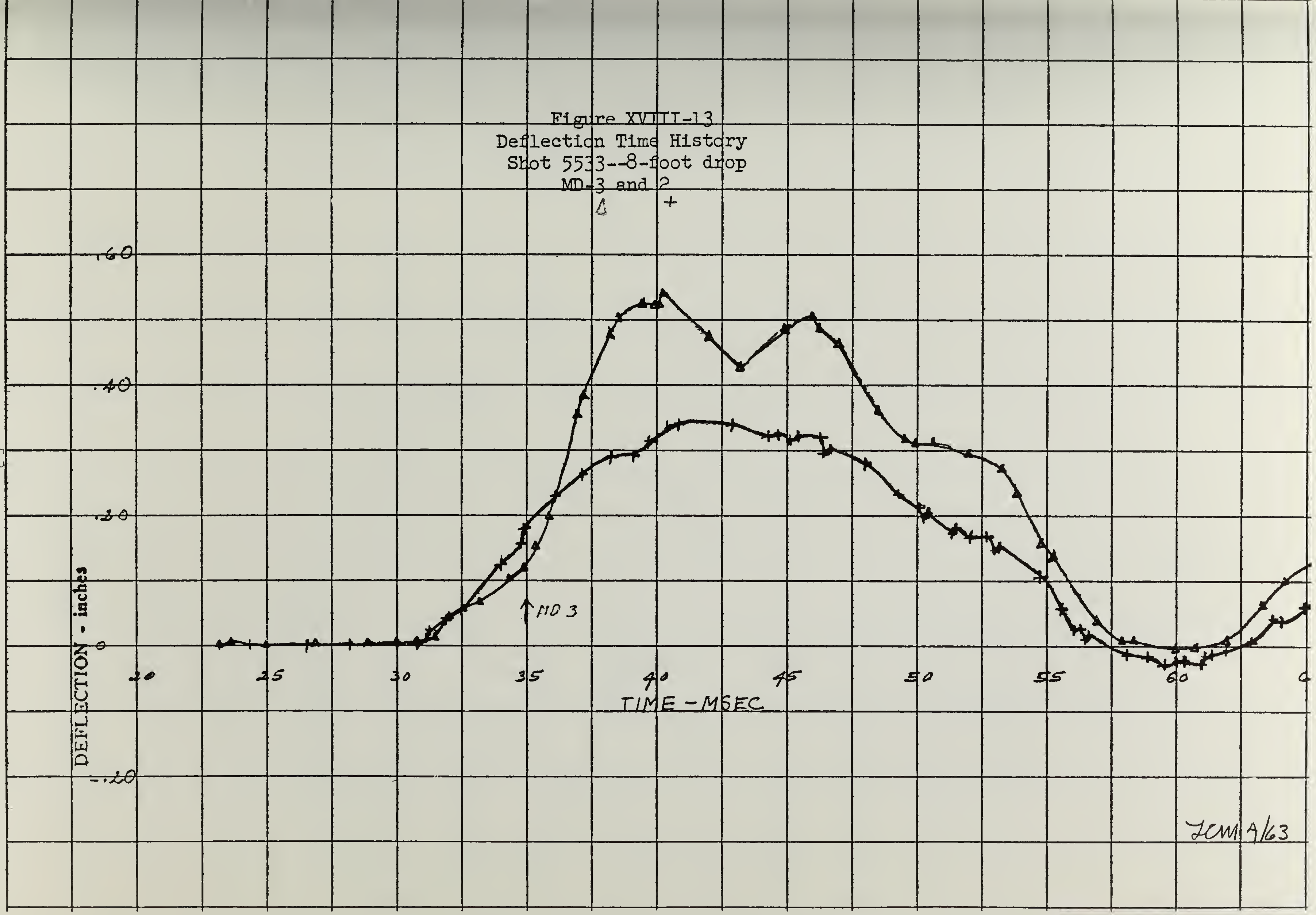

Figure XVIII-13
Deflection Time History
Shot 5533--8-foot drop
MD-3 and 2

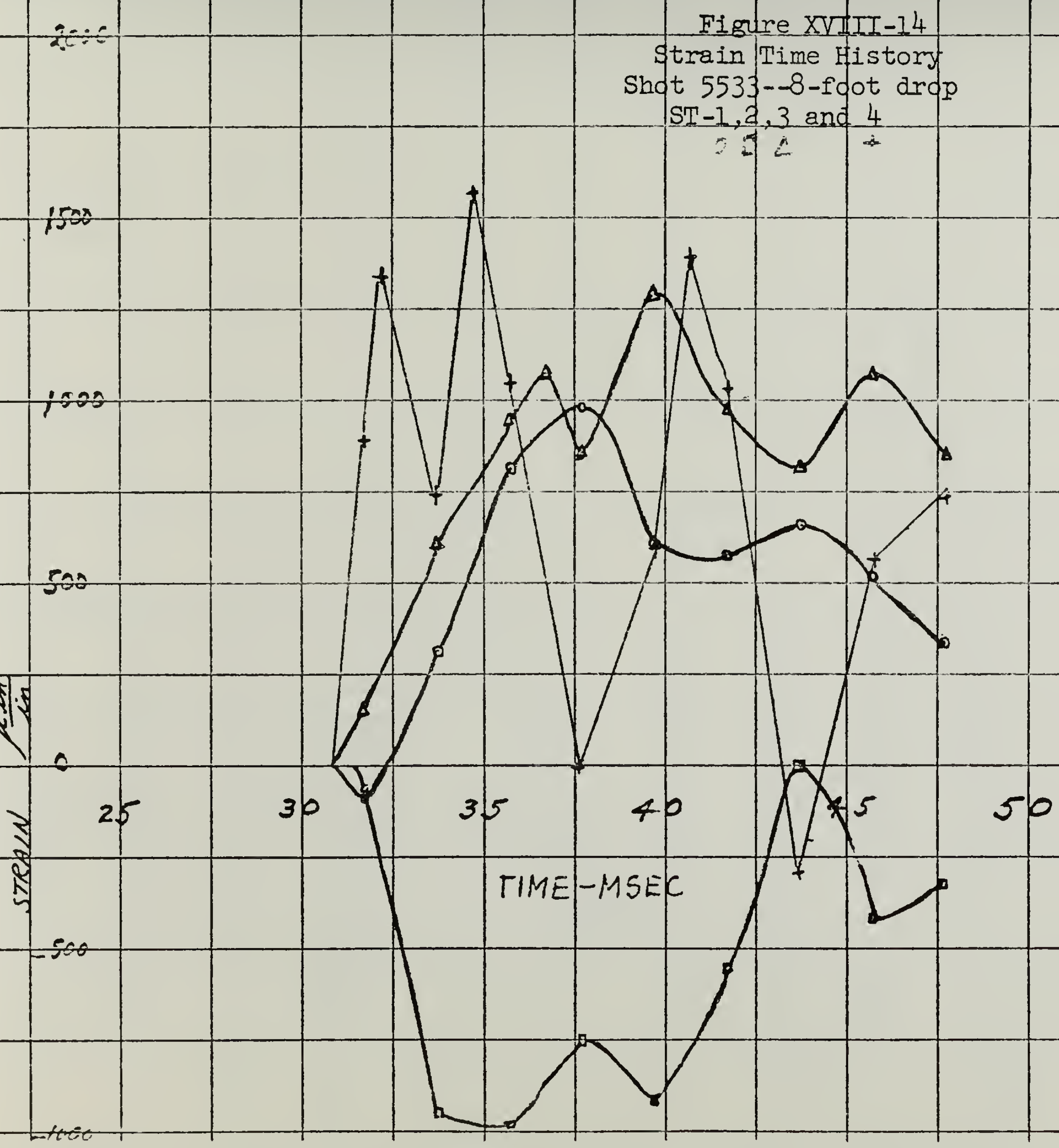

Figure XVIII-14
Strain Time History
Shot 5533--8-foot drop
ST-1,2,3 and 4

JCM 4/63

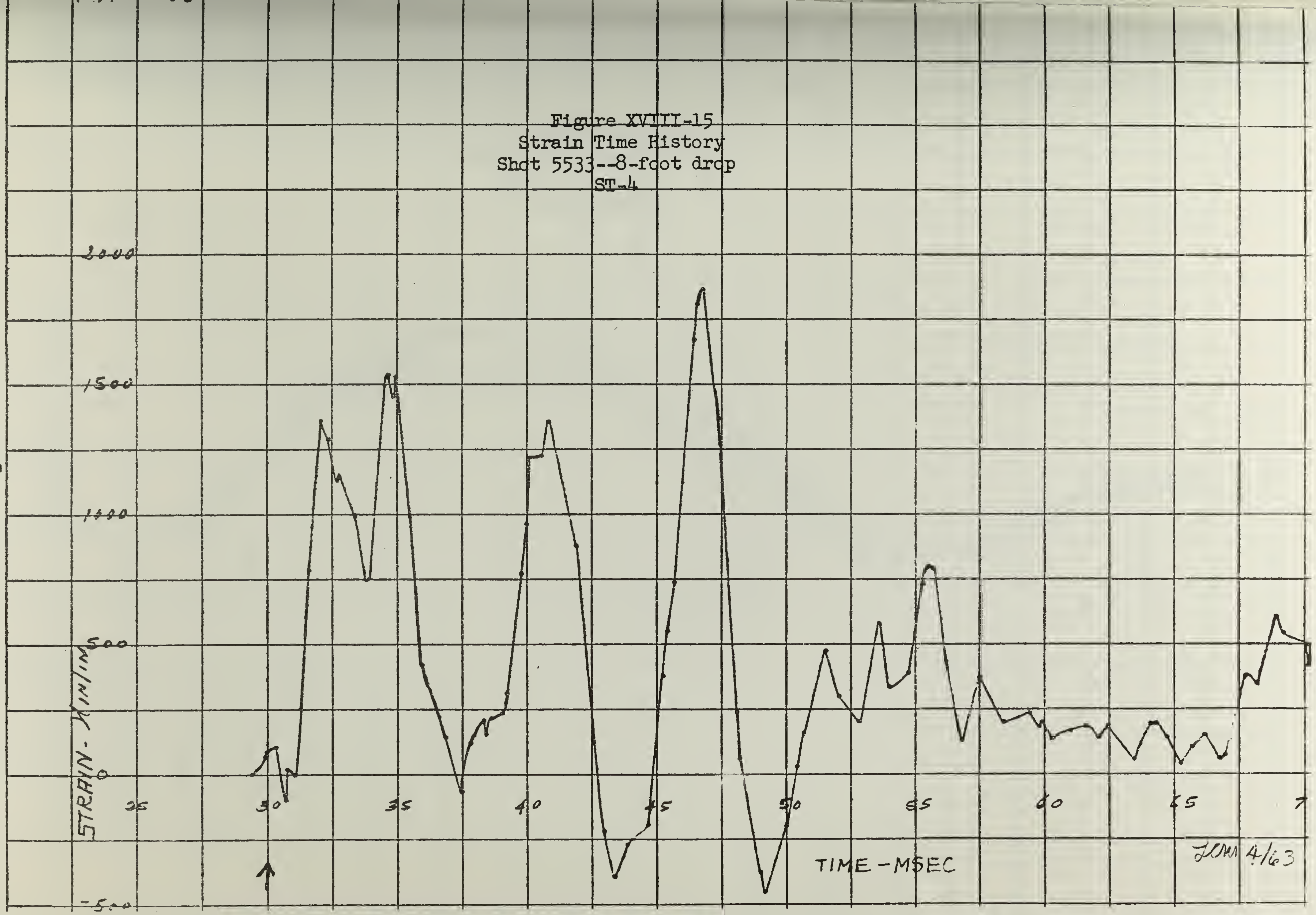
Figure XVIII-15
Strain Time History
Shot 5533--8-foot drop
ST-4

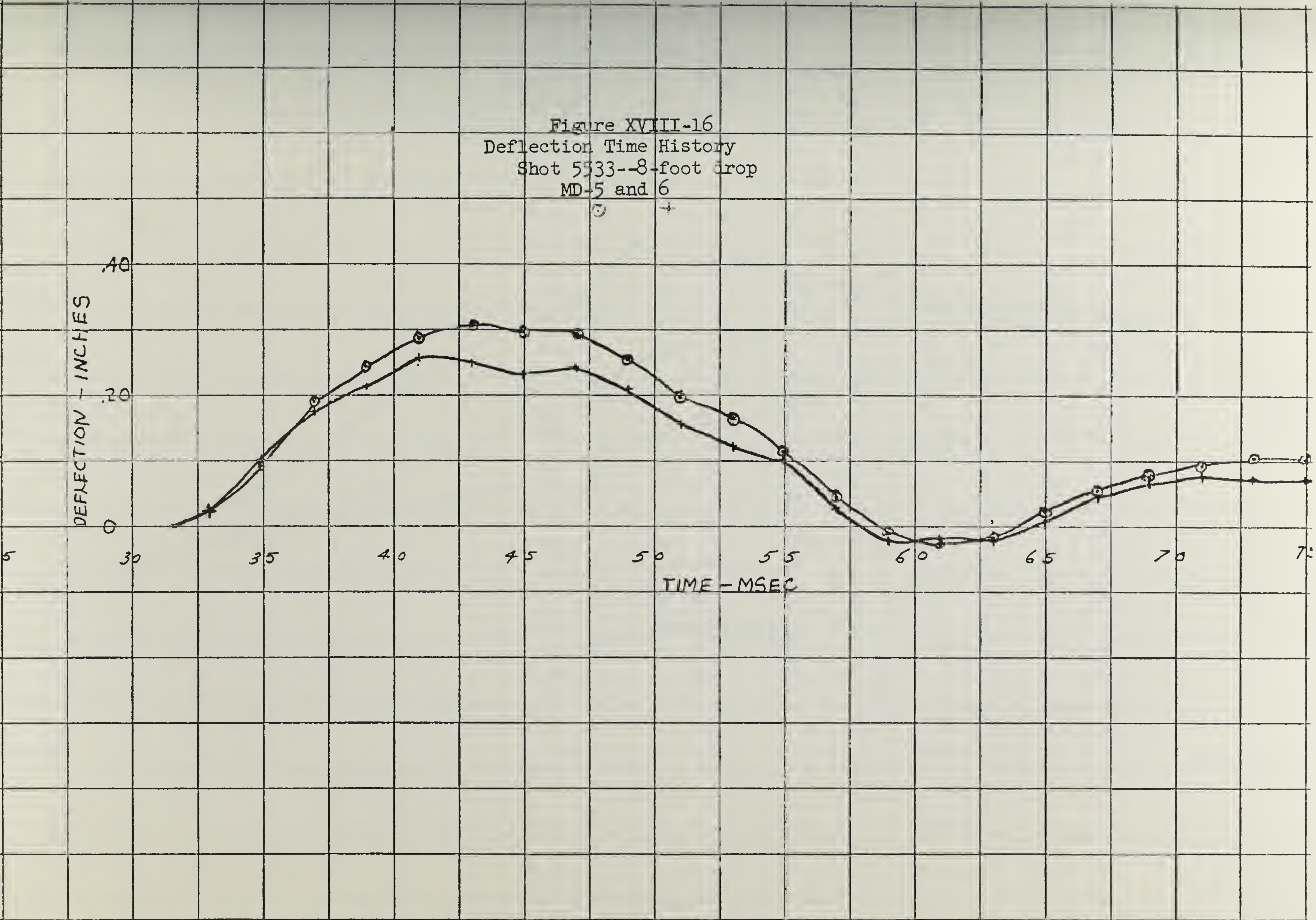

Figure XVIII-16
Deflection Time History
Shot 5533--8-foot drop
MD-5 and 6
⊙ +

Figure XVIII-17
Pressure Time History
Shot 5533--8-foot drop
PE-16, 17 and 18

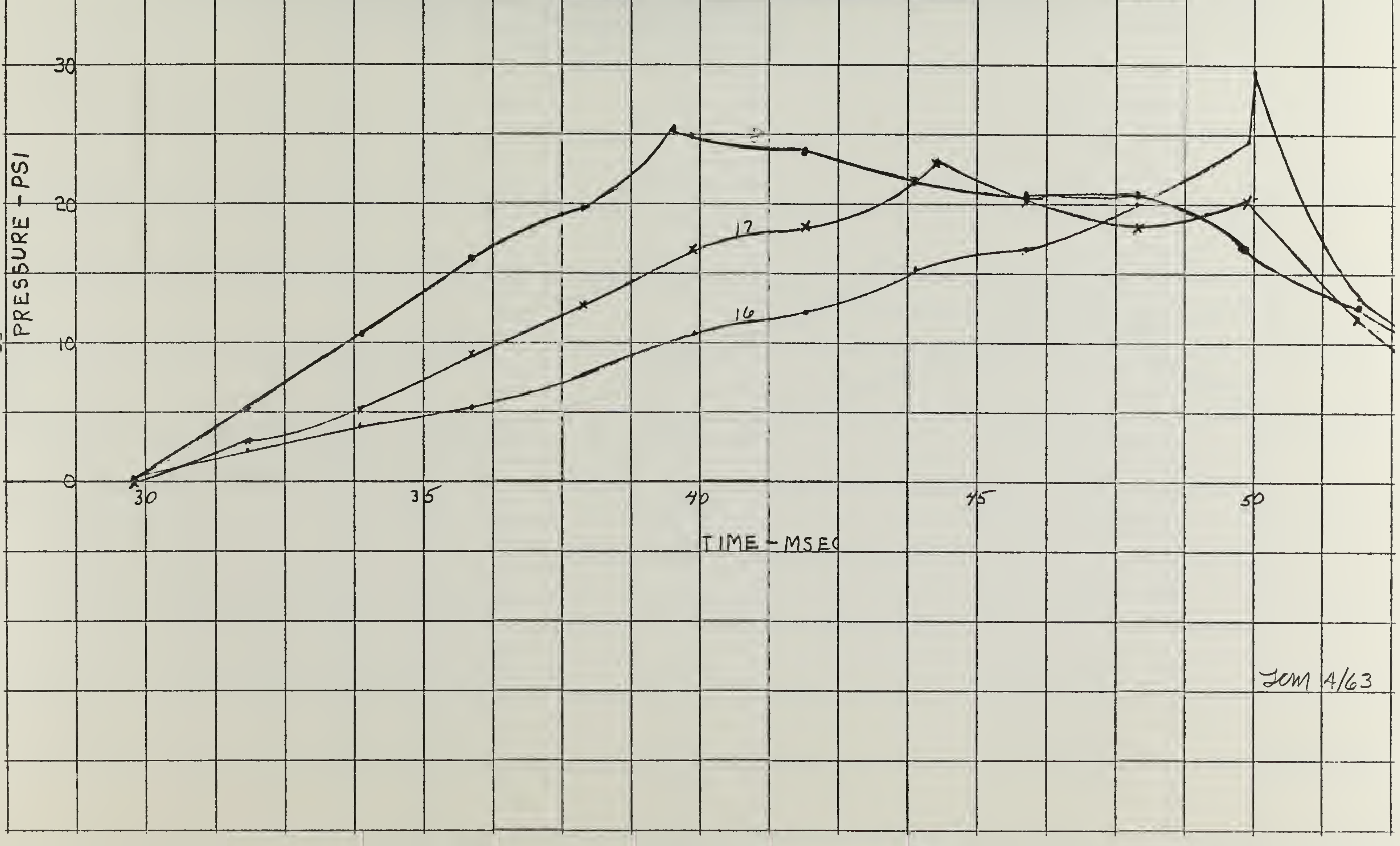

JCM 4/63

Figure XVIII-18
Pressure Time History
Shot 5533--8-foot drop
PE-11, 12 and 13

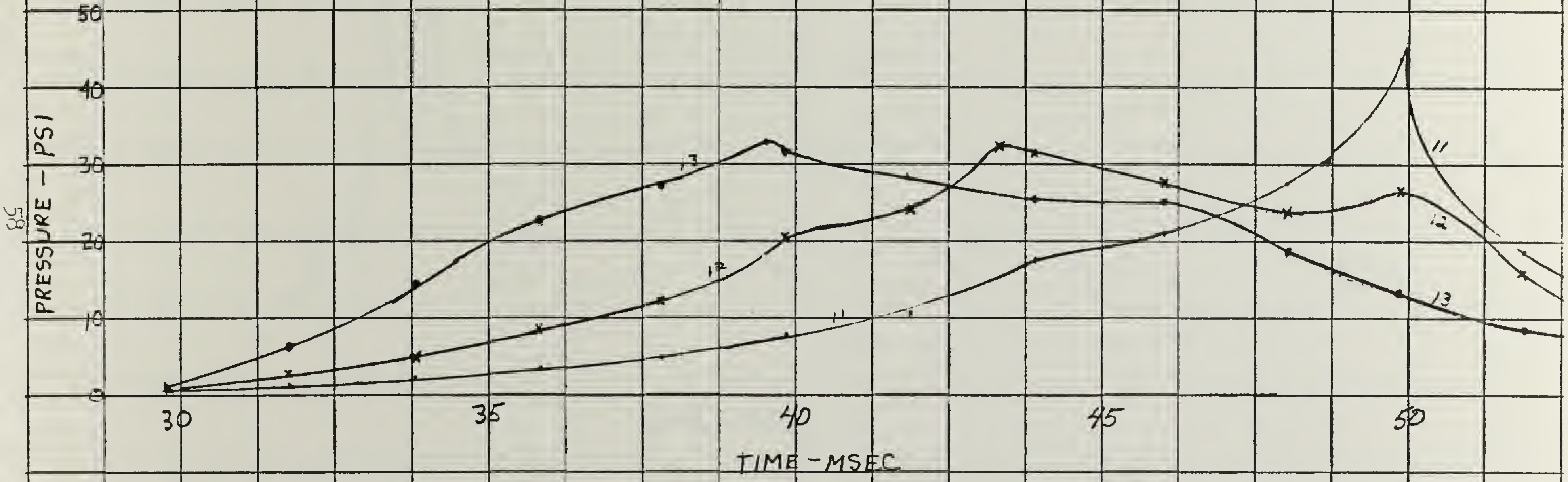

Jem 4/63

Figure XIX-1
Pressure Time History
Shot 5534--25-foot drop
PE-1

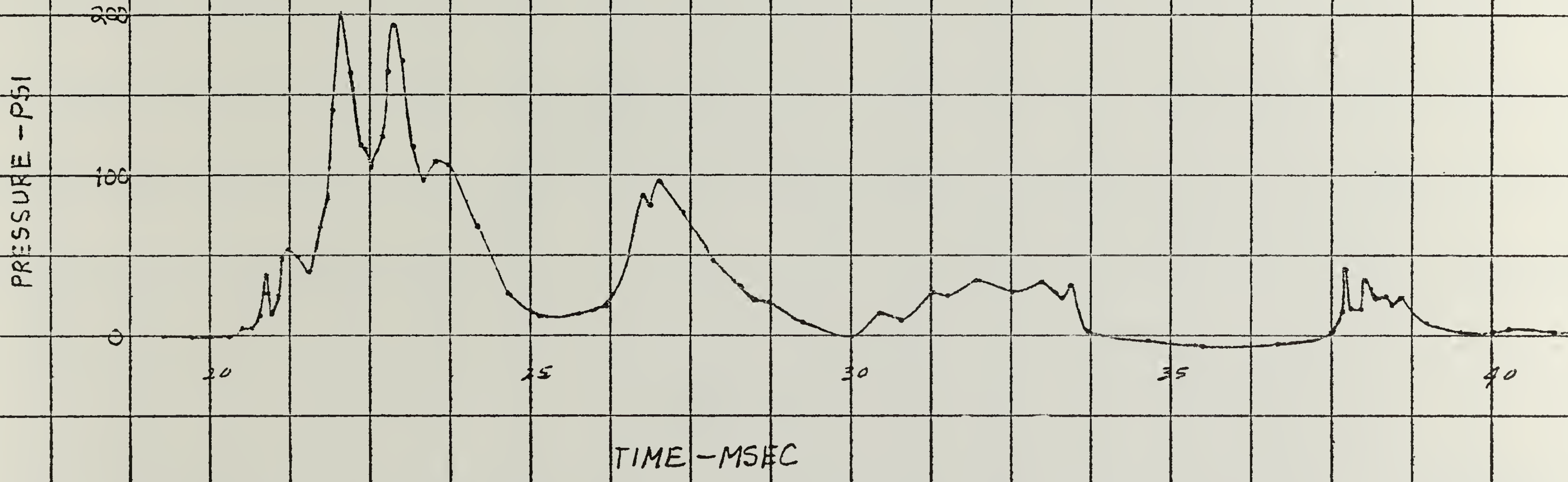

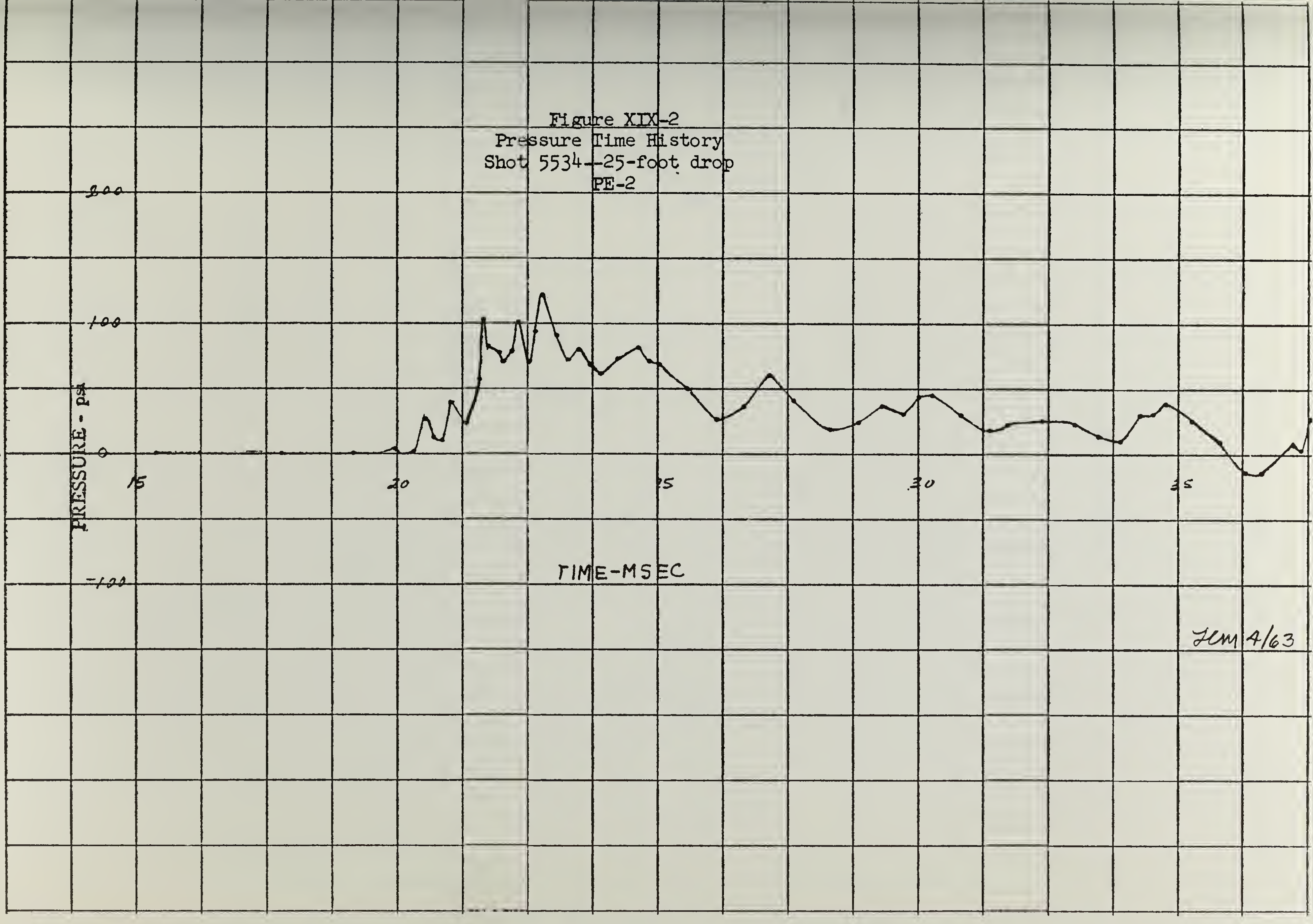

Figure XIX-2
Pressure Time History
Shot 5534--25-foot drop
PE-2

JLM 4/63

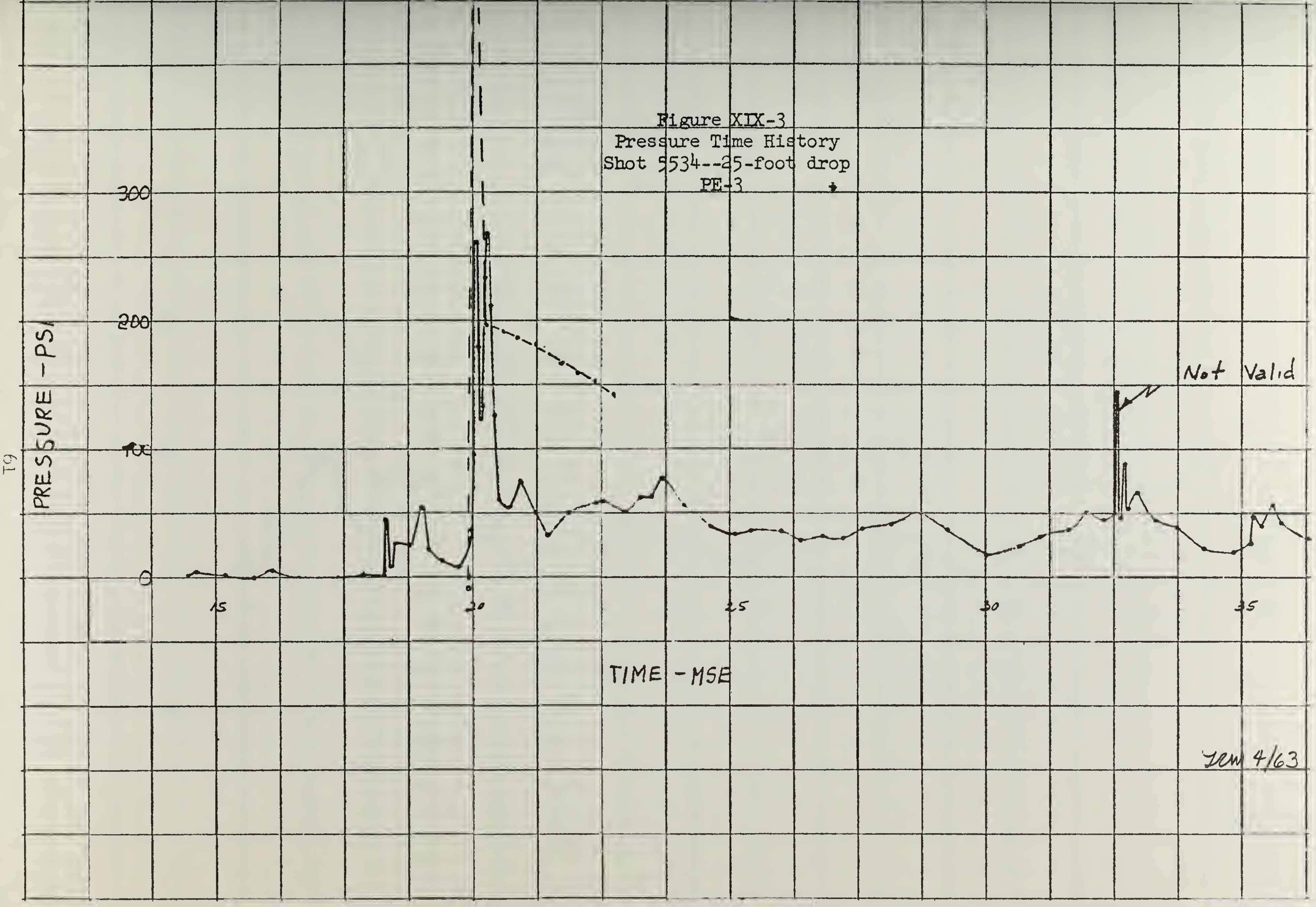

Figure XIX-3
Pressure Time History
Shot 5534--25-foot drop
PE-3

Figure XIX-4
Pressure Time History
Shot 5534--25-foot drop
PE-4

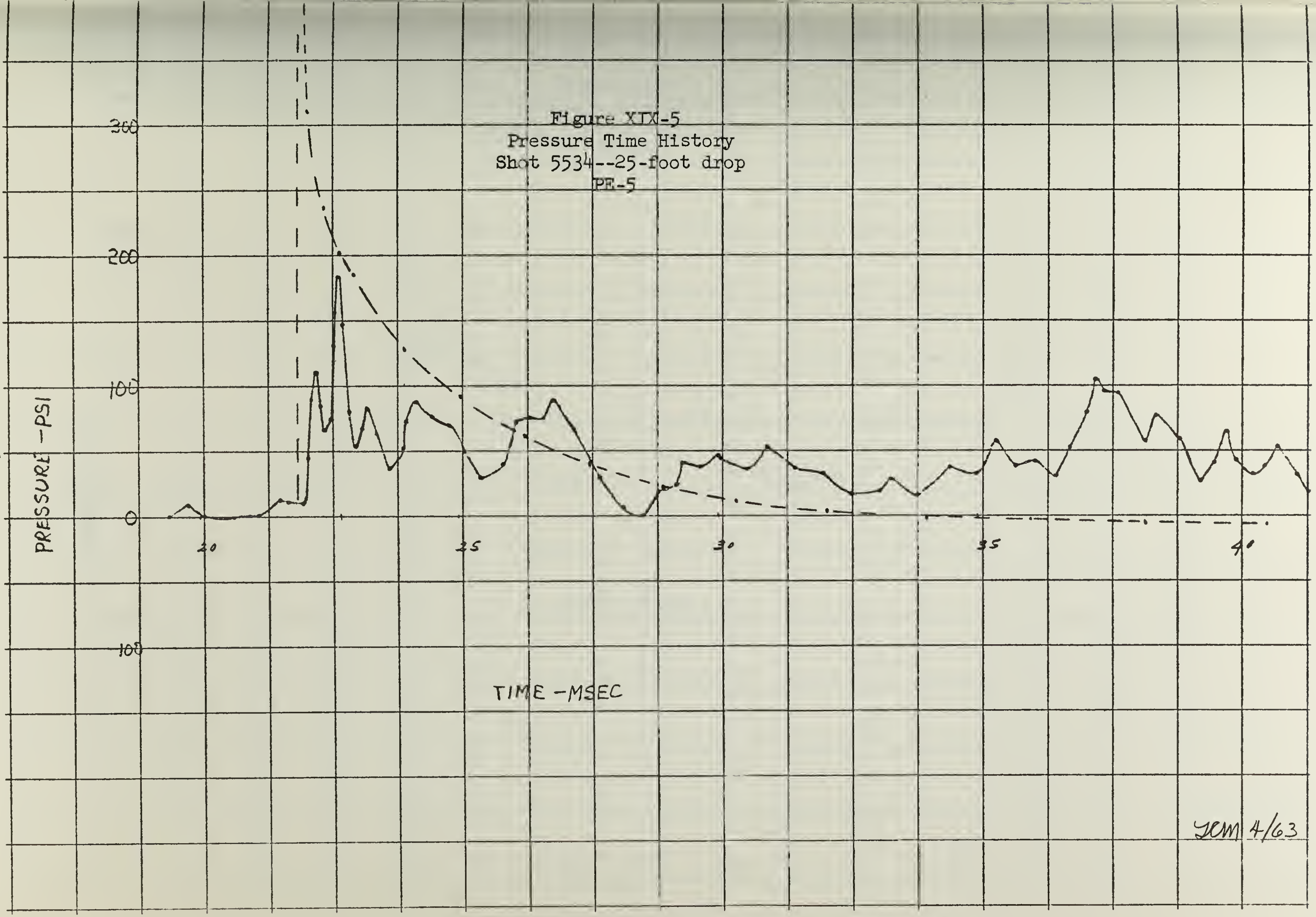

Figure XIX-5
Pressure Time History
Shot 5534--25-foot drop
PE-5

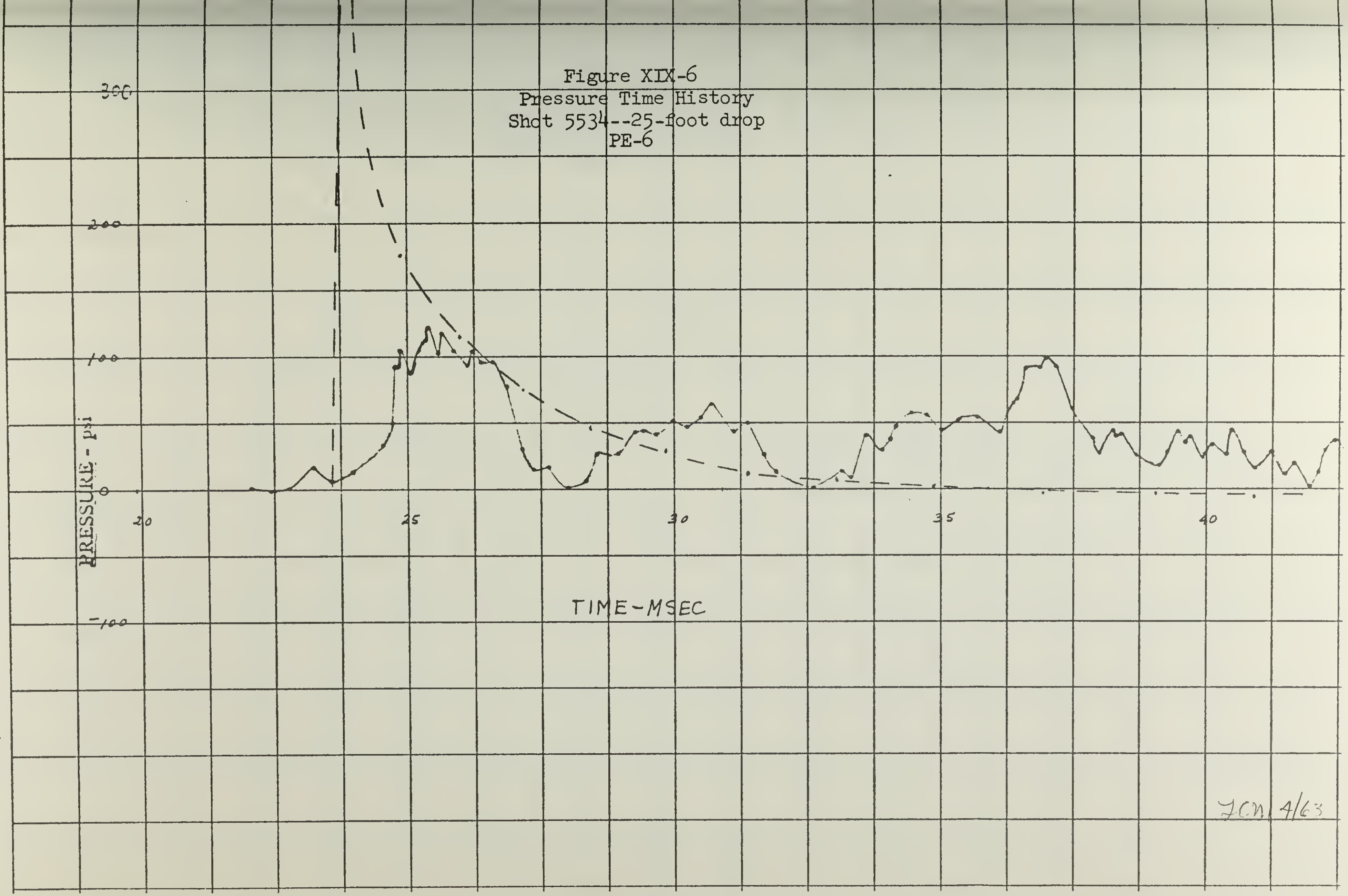

Figure XIX-6
Pressure Time History
Shot 5534--25-foot drop
PE-6

Figure XIX-7
Pressure Time History
Shot 5534--25-foot drop
PE-8

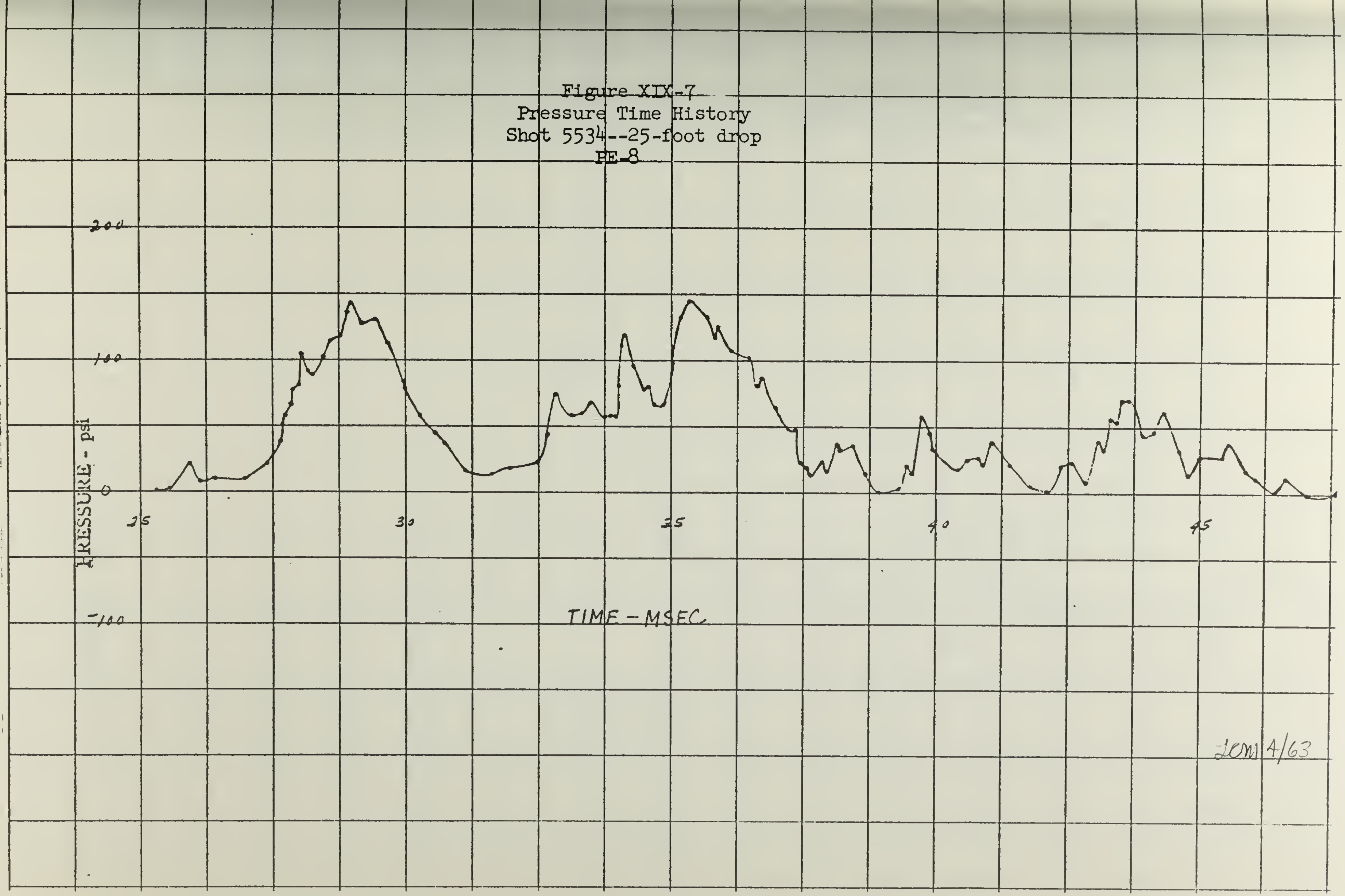

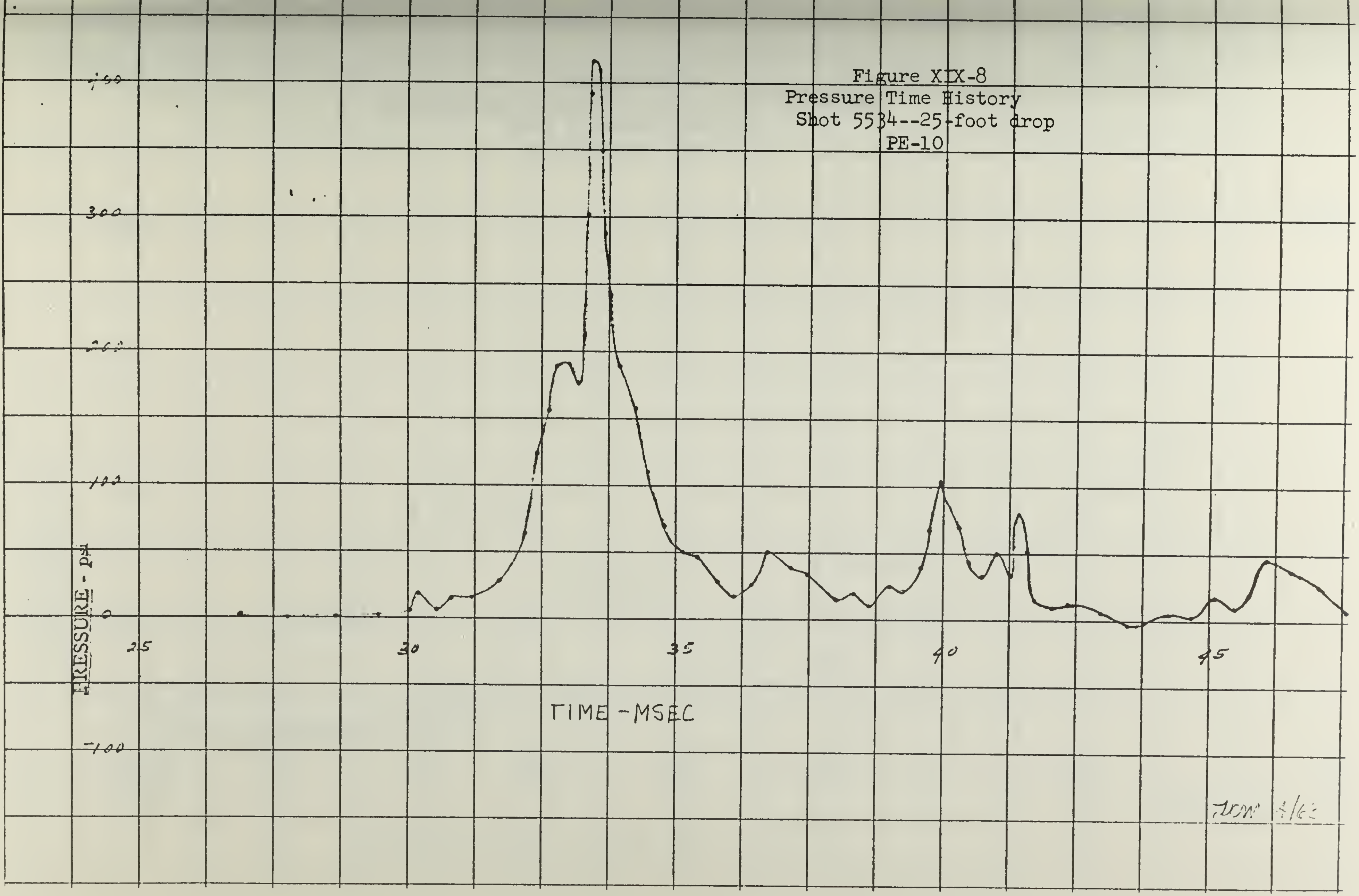

Figure XIX-8
Pressure Time History
Shot 5534--25-foot drop
PE-10

Figure XIX-9
Experimental Girthwise Pressure Distribution
Shot 5534--25-foot drop
At discrete times

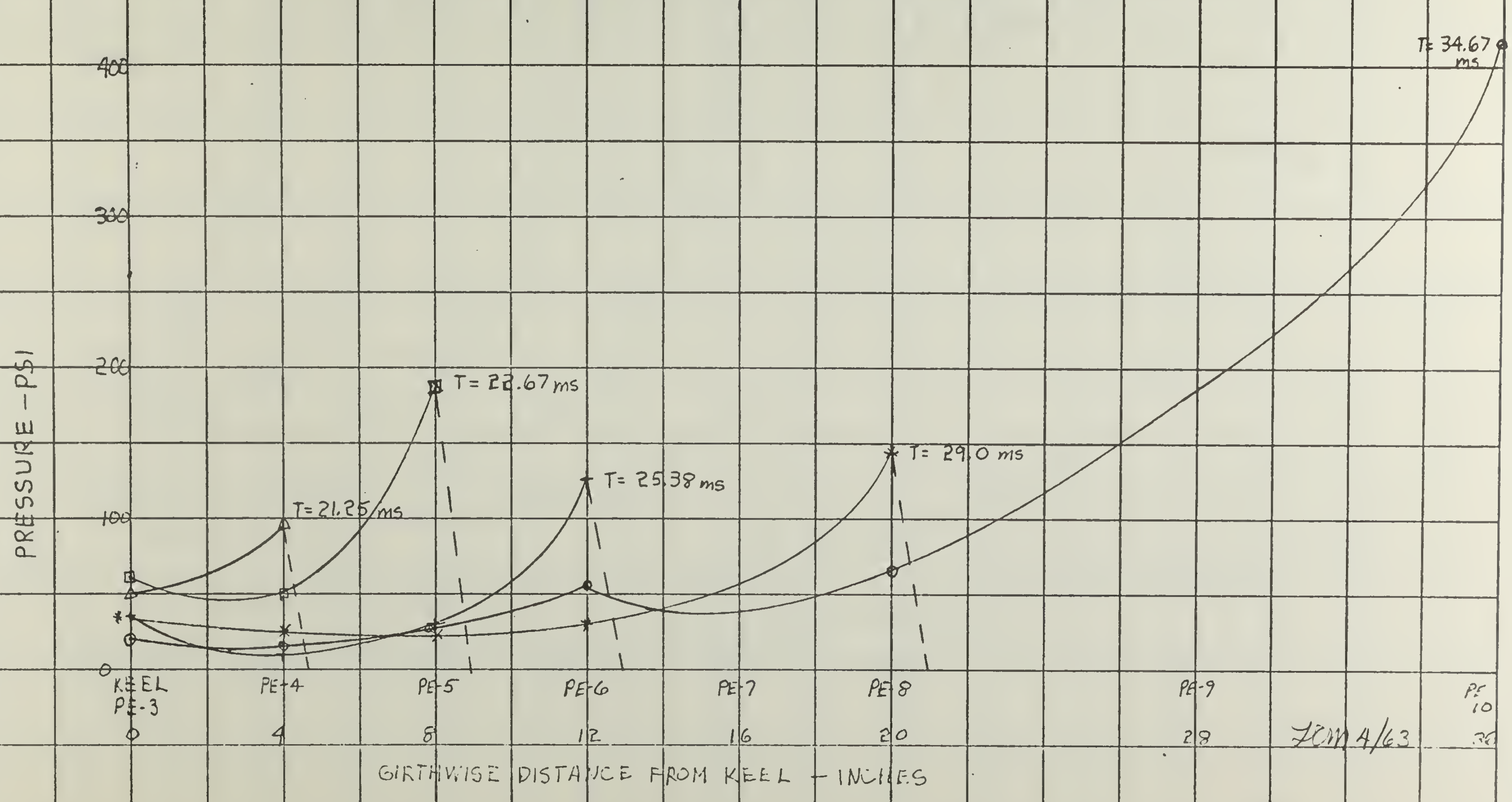

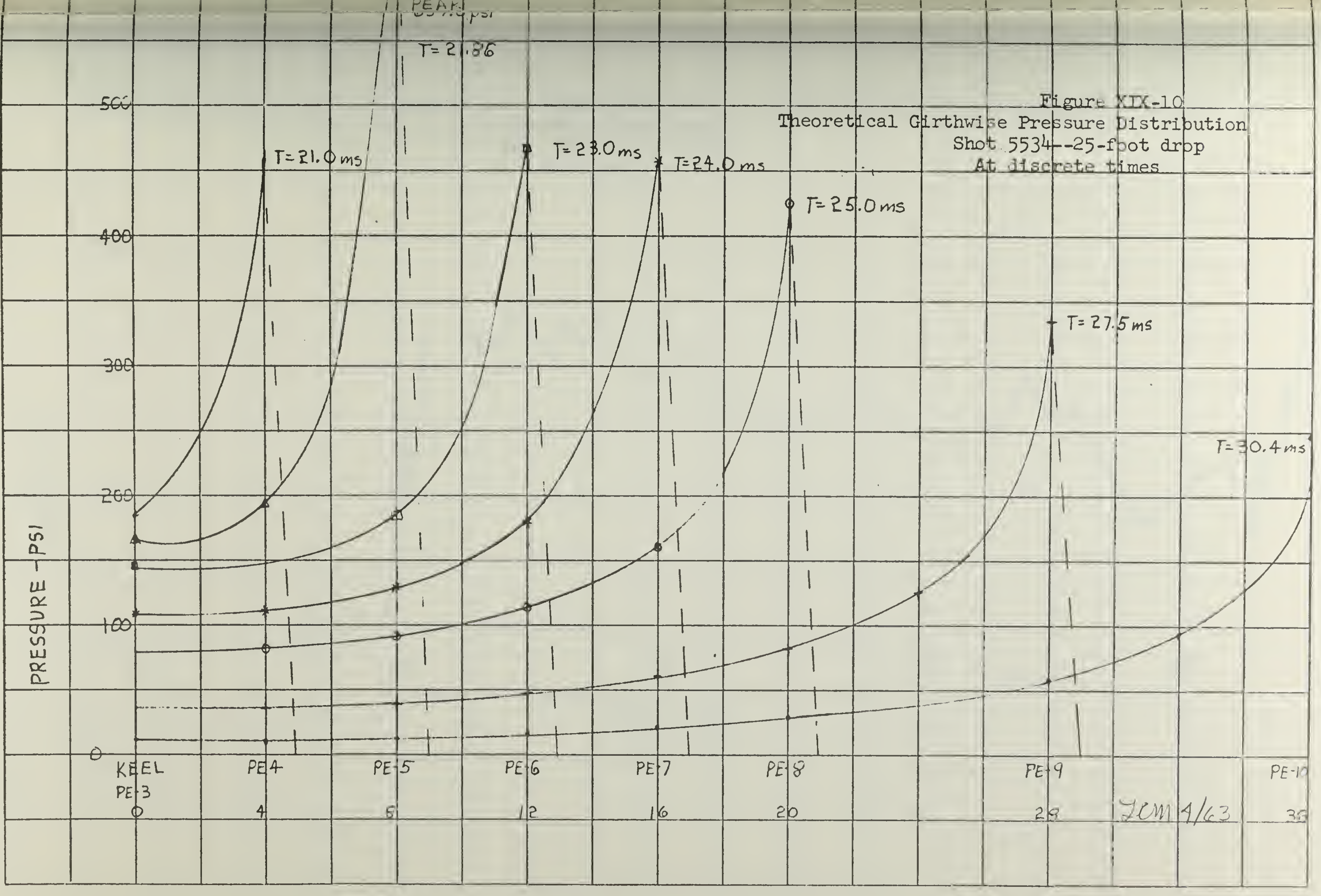

Figure XIX-10
Theoretical Girthwise Pressure Distribution
Shot 5534--25-foot drop
At discrete times

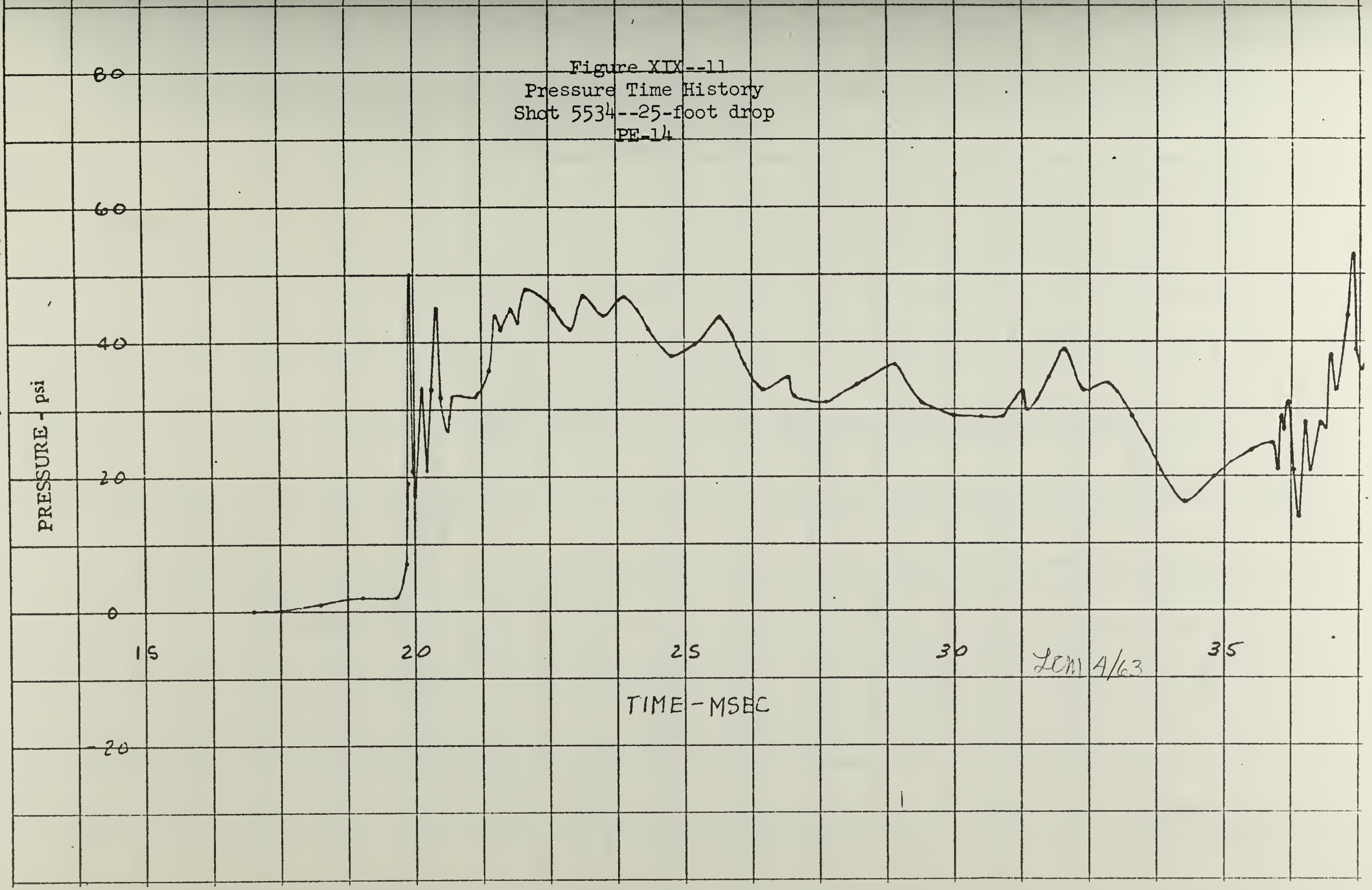

Figure XIX--11
Pressure Time History
Shot 5534--25-foot drop
PE-14

Figure XIX-12
Pressure Time History
Shot 5534--25-foot drop
PE-19

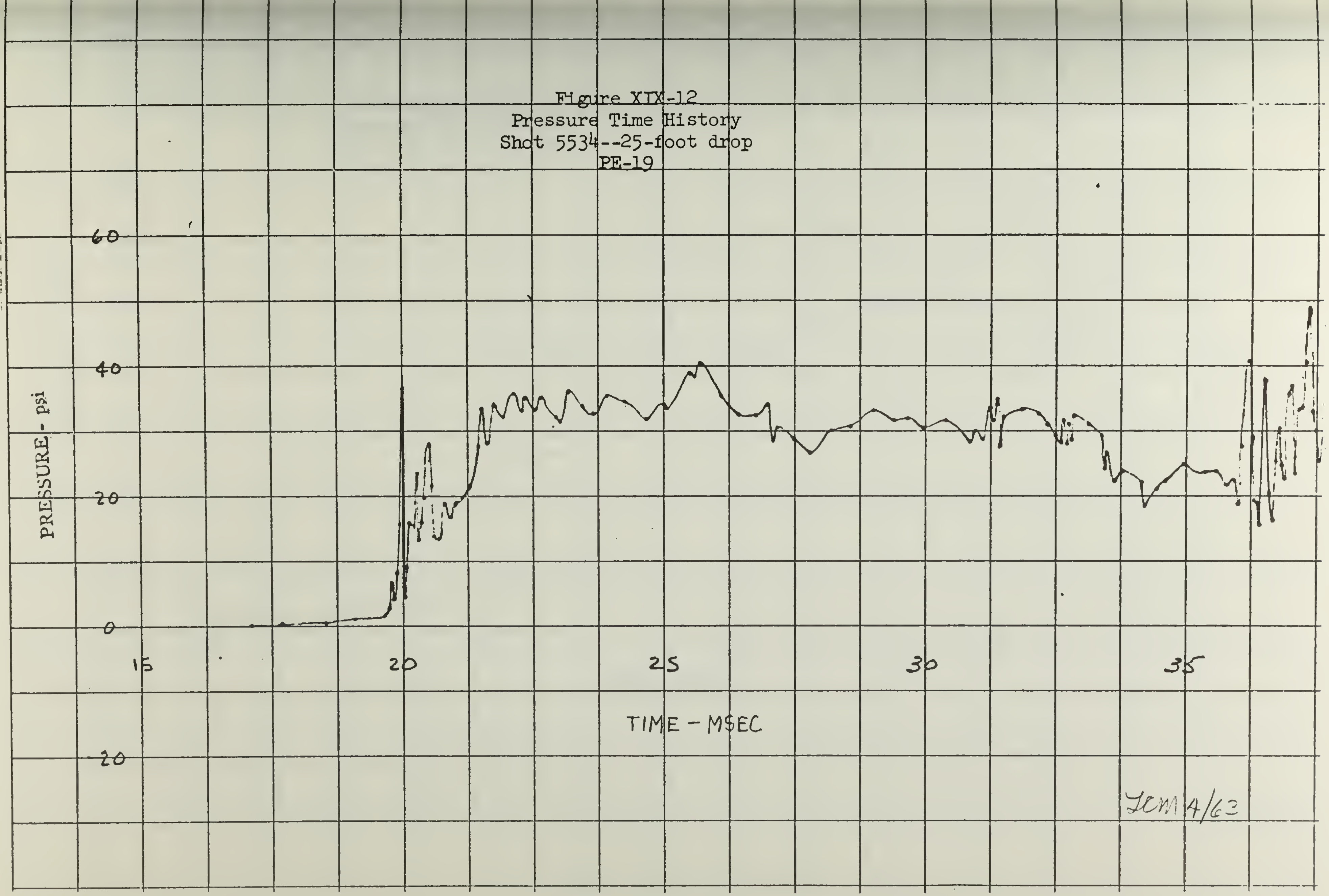

JCM 4/63

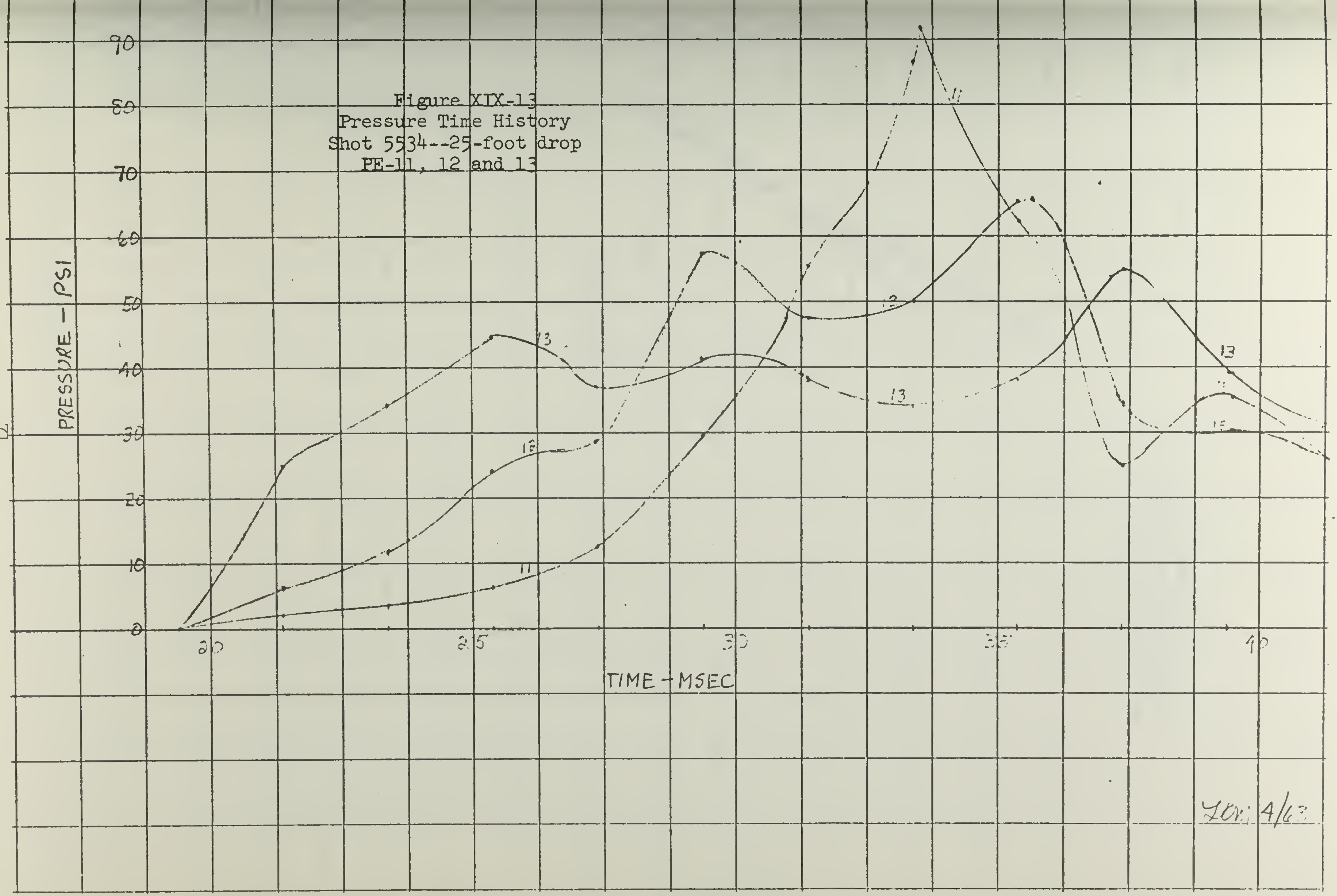

Figure XIX-13
Pressure Time History
Shot 5534--25-foot drop
PE-11, 12 and 13

Figure XIX-14
Deflection Time History
Shot 5534--25-foot drop
MD 2, 5, and 6
· o Δ

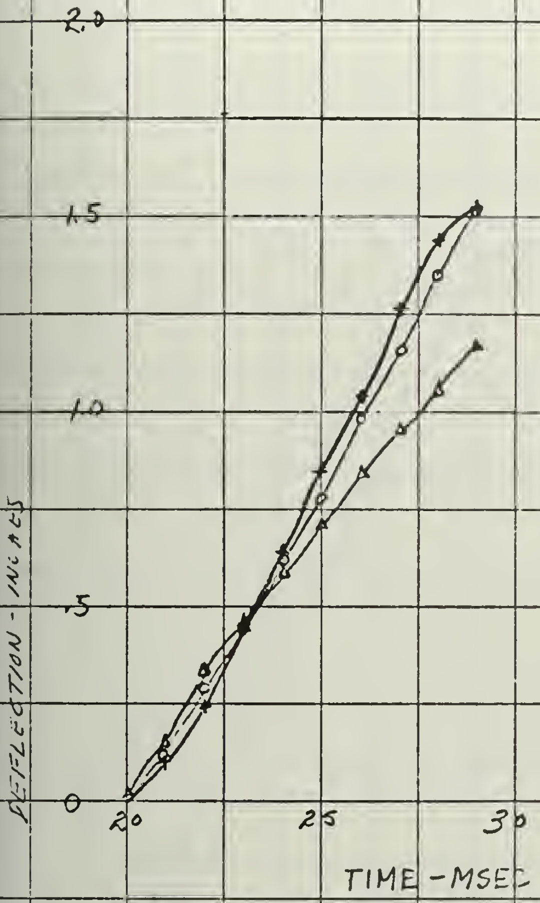

ZERO TIME - TRIGGER

Pf 4/6

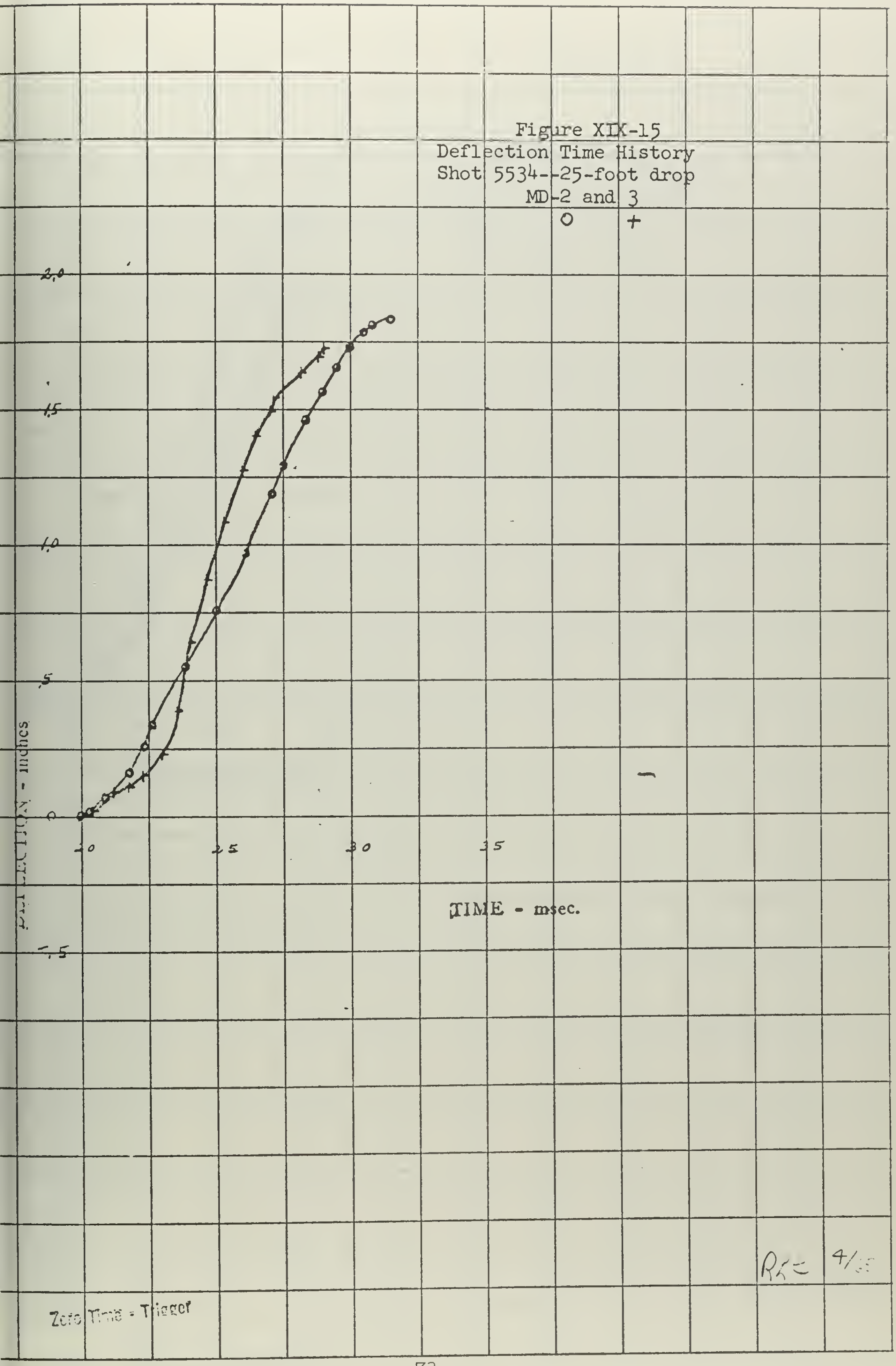

Figure XIX-15
Deflection Time History
Shot 5534--25-foot drop
MD-2 and 3

RK= 4/55

Figure XIX-16
Deflection Time History
Shot 5534--25-foot drop

MD-1, 2, 3 and 4
o + Δ □

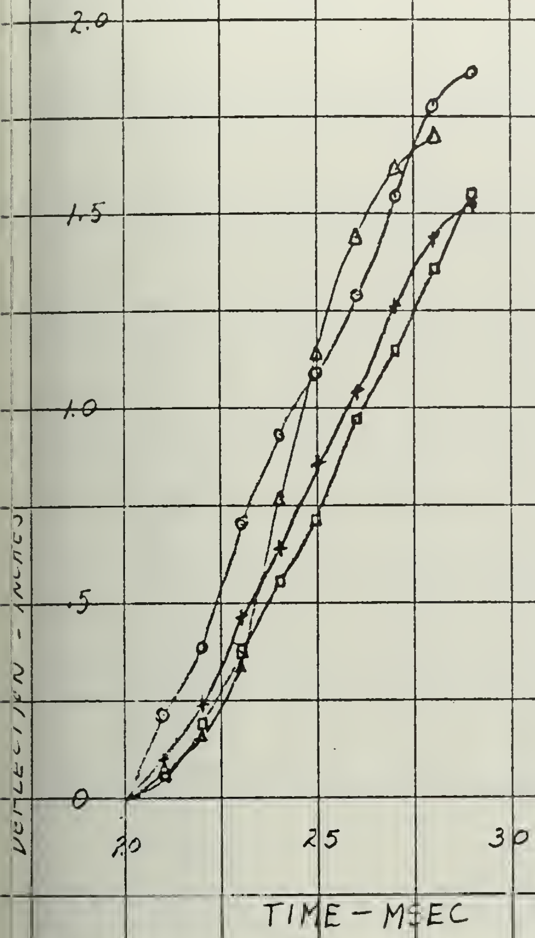

ZERO TIME - TRIGGER

4/63

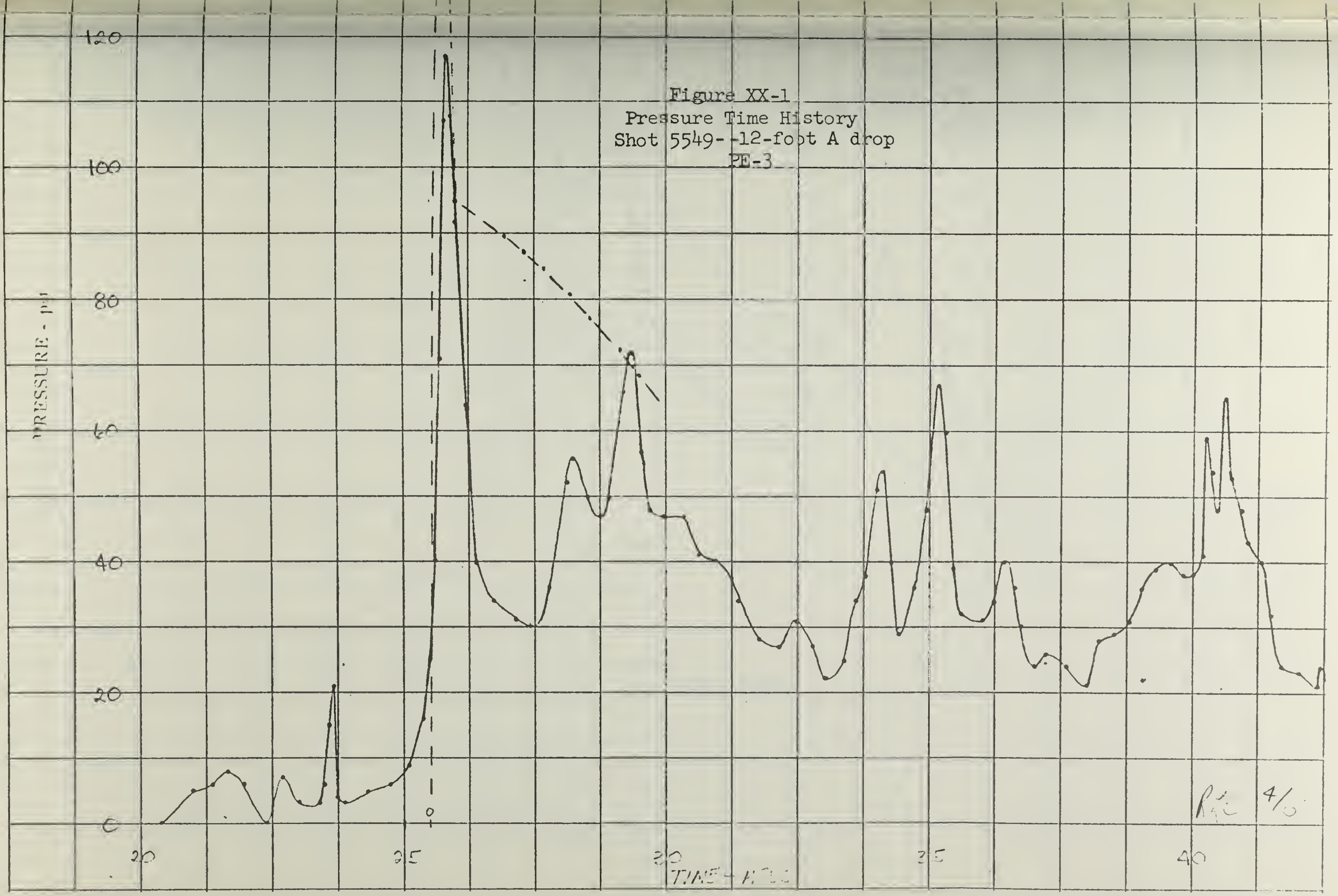

Figure XX-1
Pressure Time History
Shot 5549--12-foot A drop
PE-3

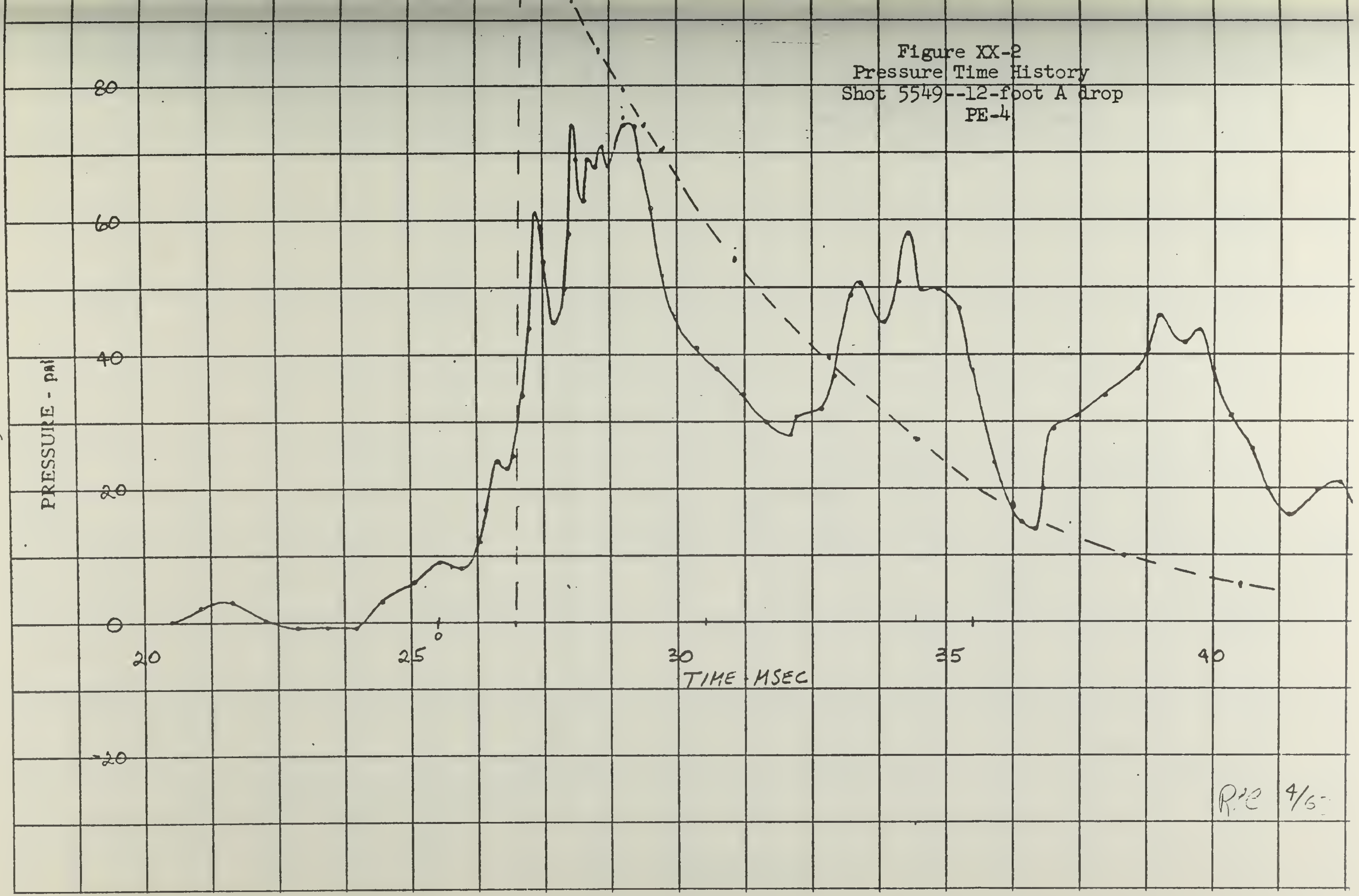

Figure XX-2
Pressure Time History
Shot 5549--12-foot A drop
PE-4

R.C 4/6

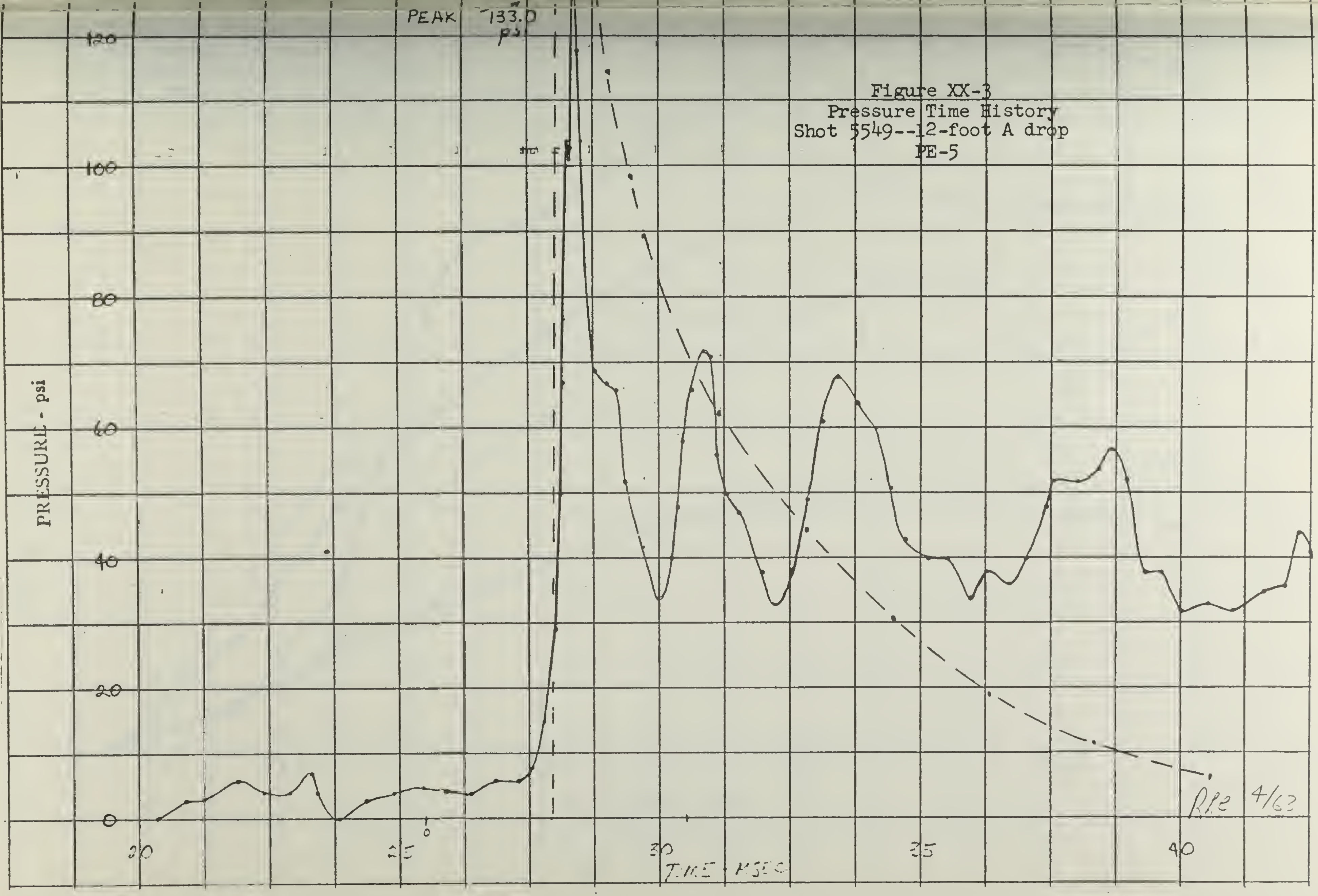

Figure XX-3
Pressure Time History
Shot 5549--12-foot A drop
PE-5

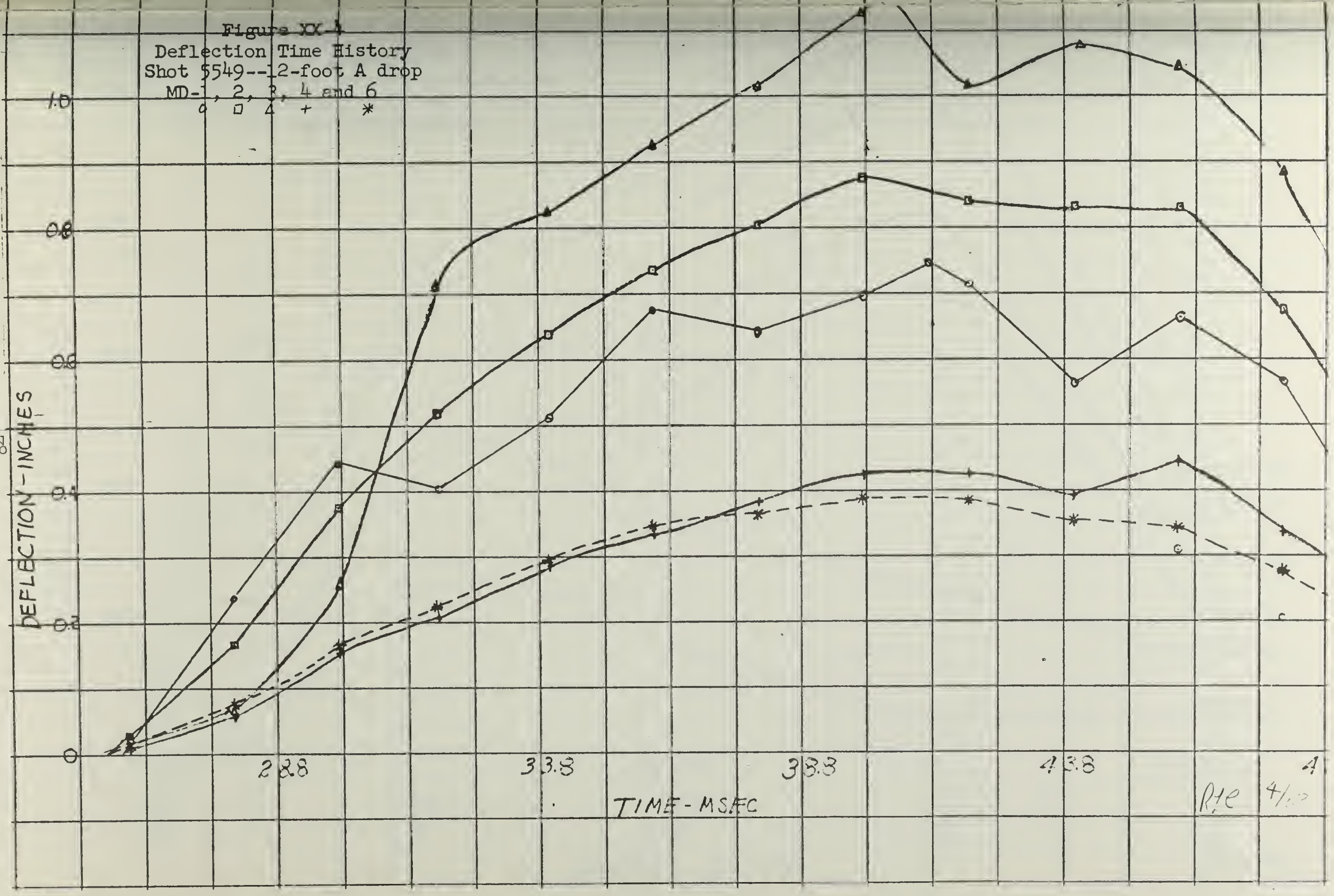
Figure XX-1
Deflection Time History
Shot 5549--12-foot A drop
MD-1, 2, 3, 4 and 6
o □ Δ + *

Figure XX-5
Girthwise Deflection Histories
Shot 5549--12-foot A drop
At discrete times

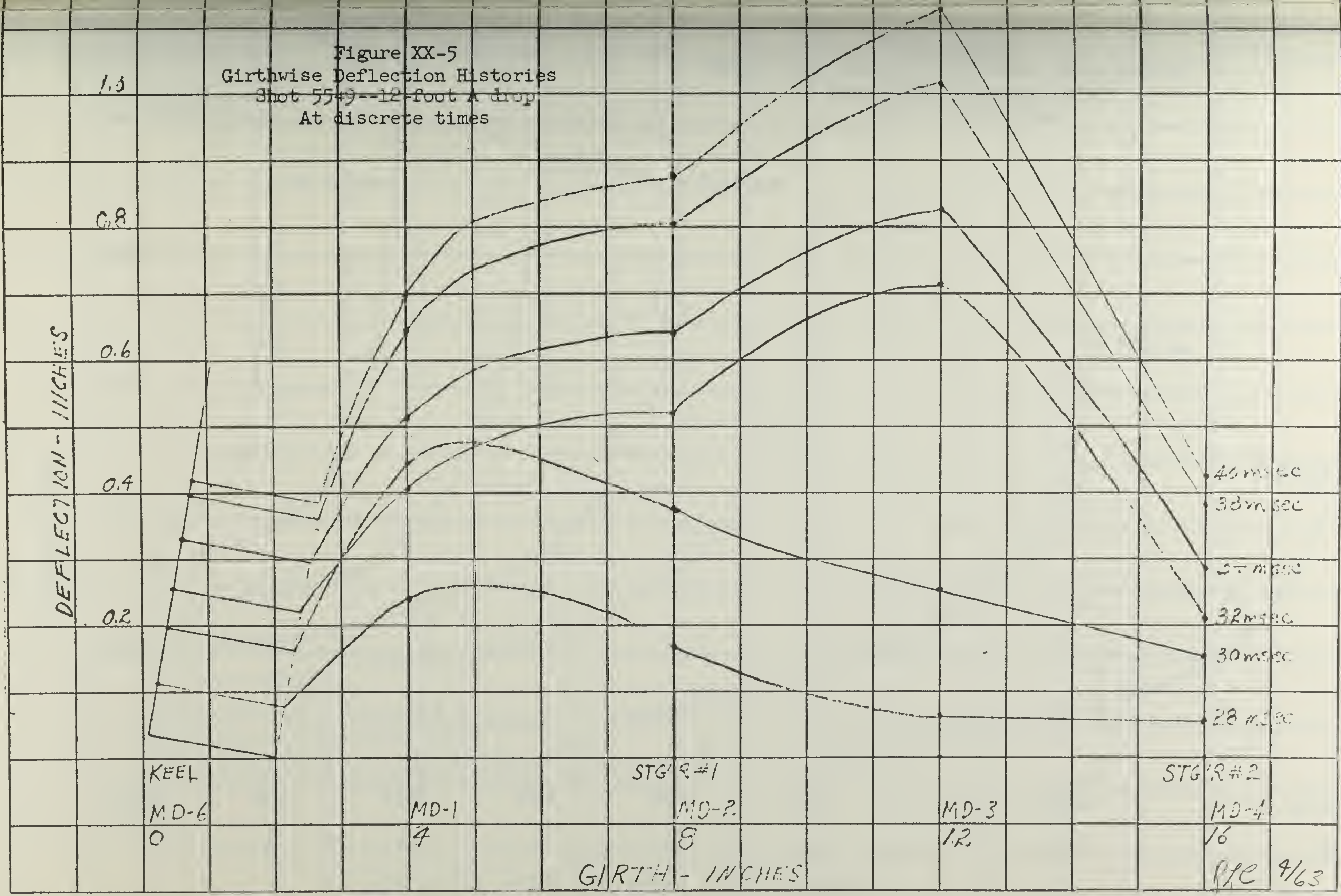

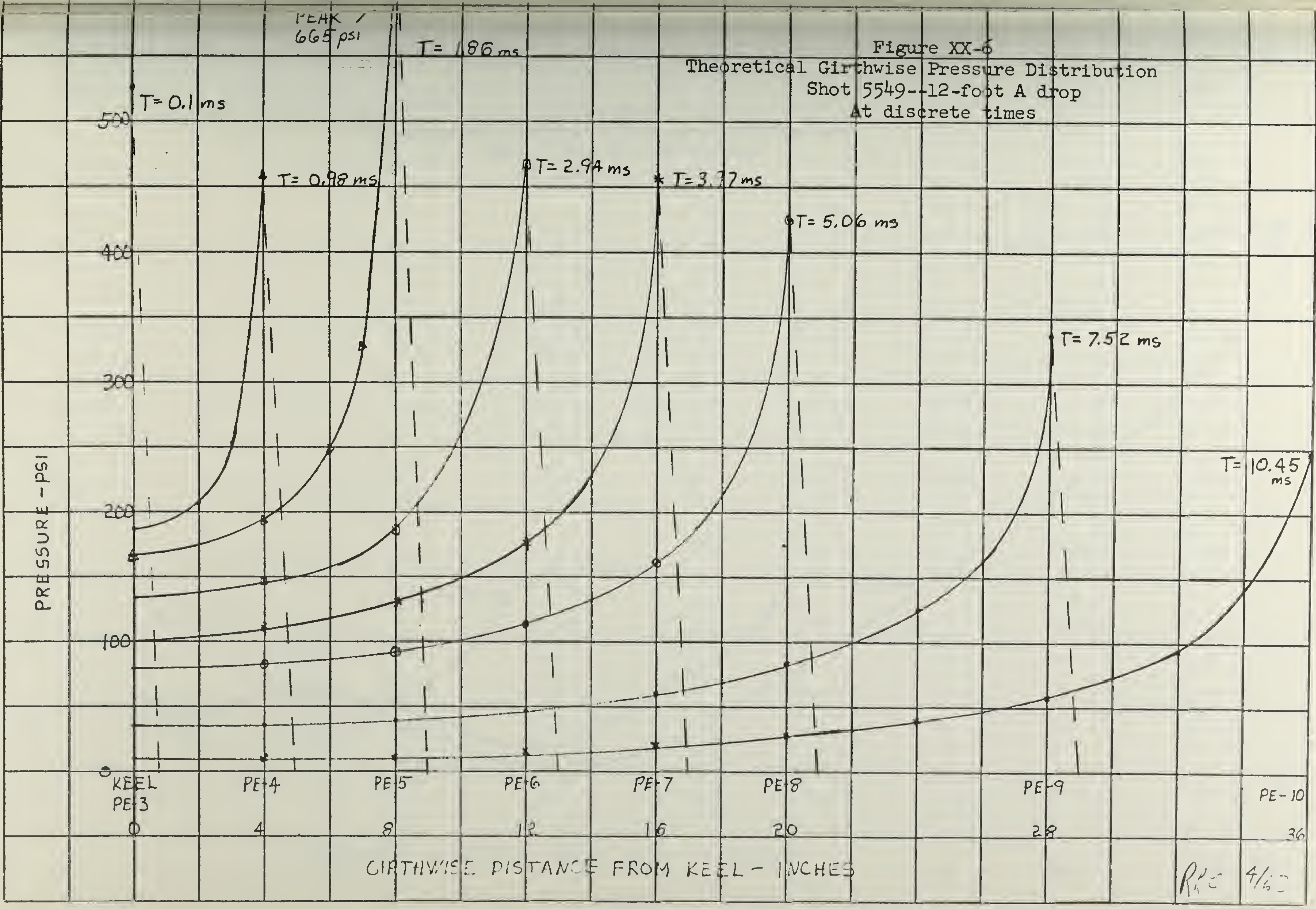

Figure XX-6
Theoretical Girthwise Pressure Distribution
Shot 5549--12-foot A drop
At discrete times

Figure XX-7
Experimental Girthwise Pressure Distribution
Shot 5549--12-foot A drop
At discrete times

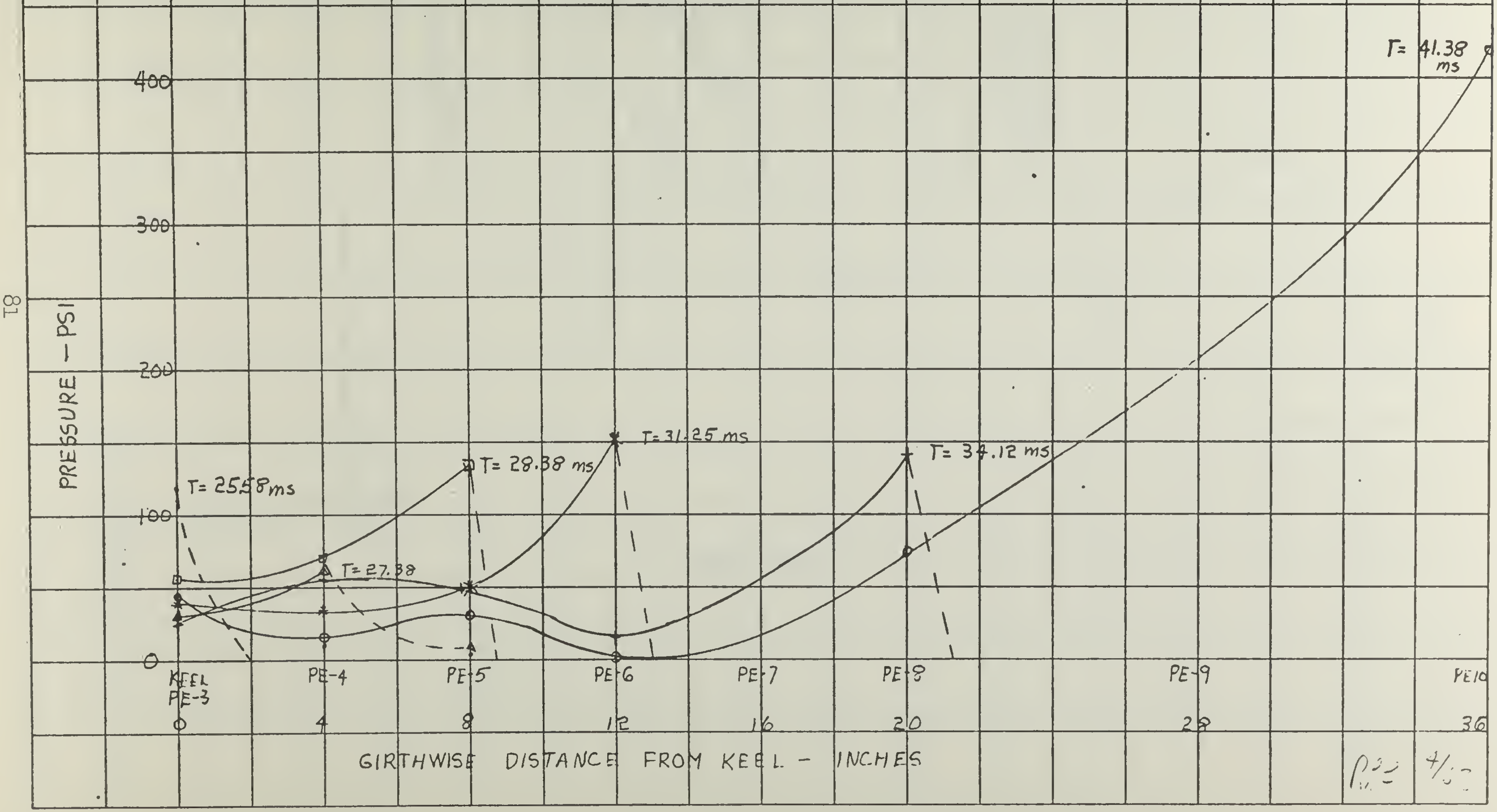

Figure XXI-1
Pressure Time History
Shot 5550--12-foot B drop
PE-3

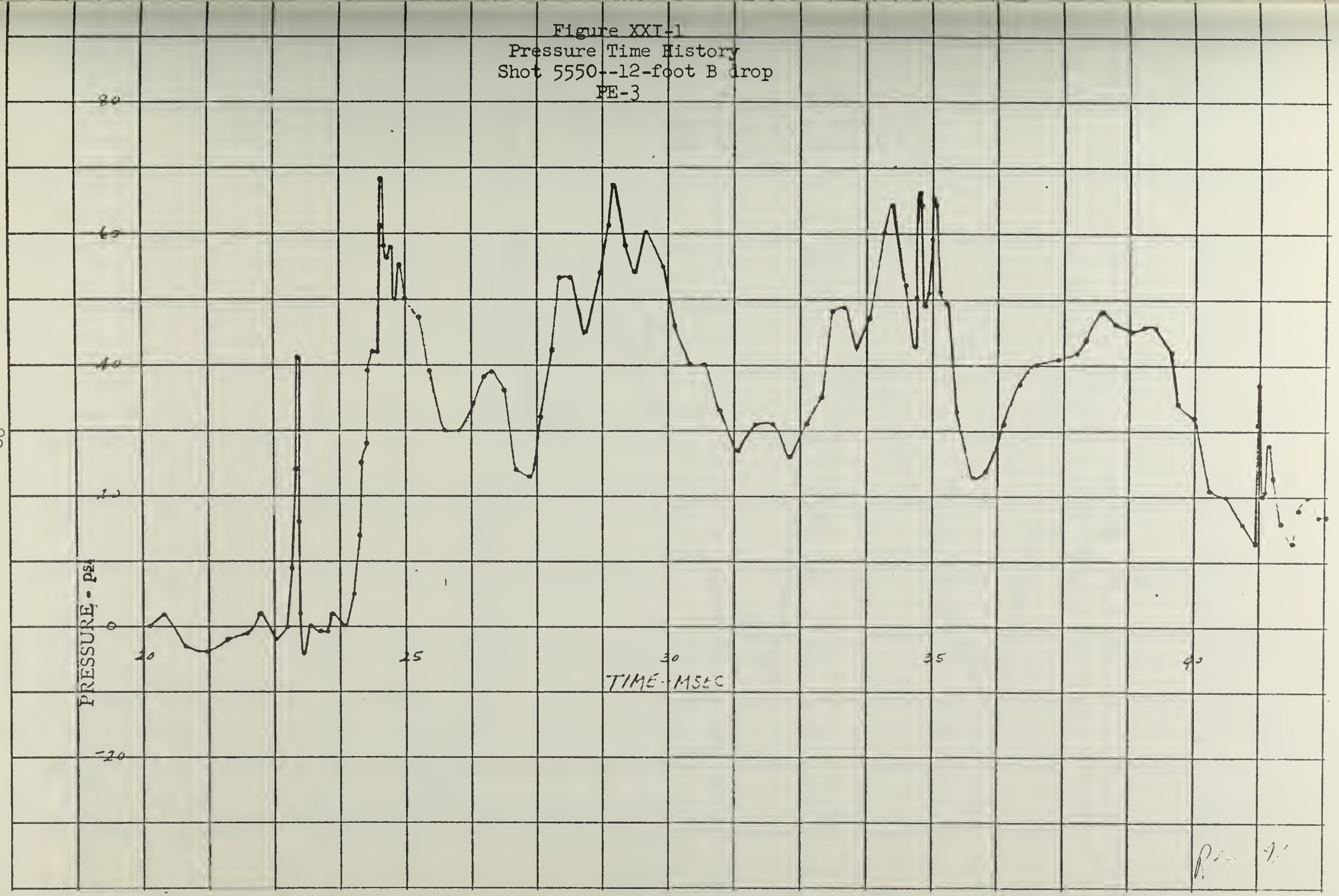

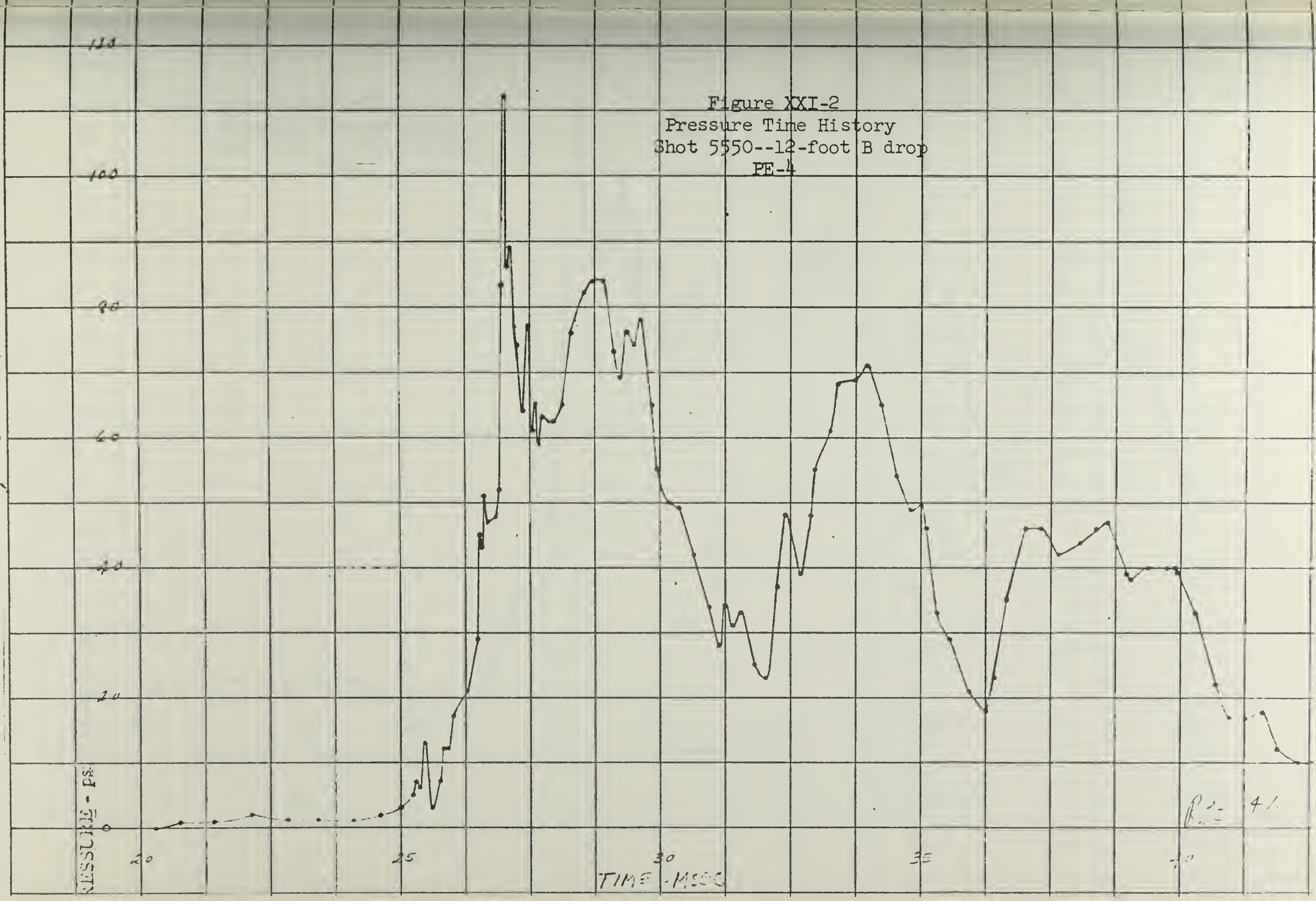

Figure XXI-2
Pressure Time History
Shot 5550--12-foot B drop
PE-4

Figure XXI-3.
Pressure Time History
Shot 5550--12-foot B drop
PE-5

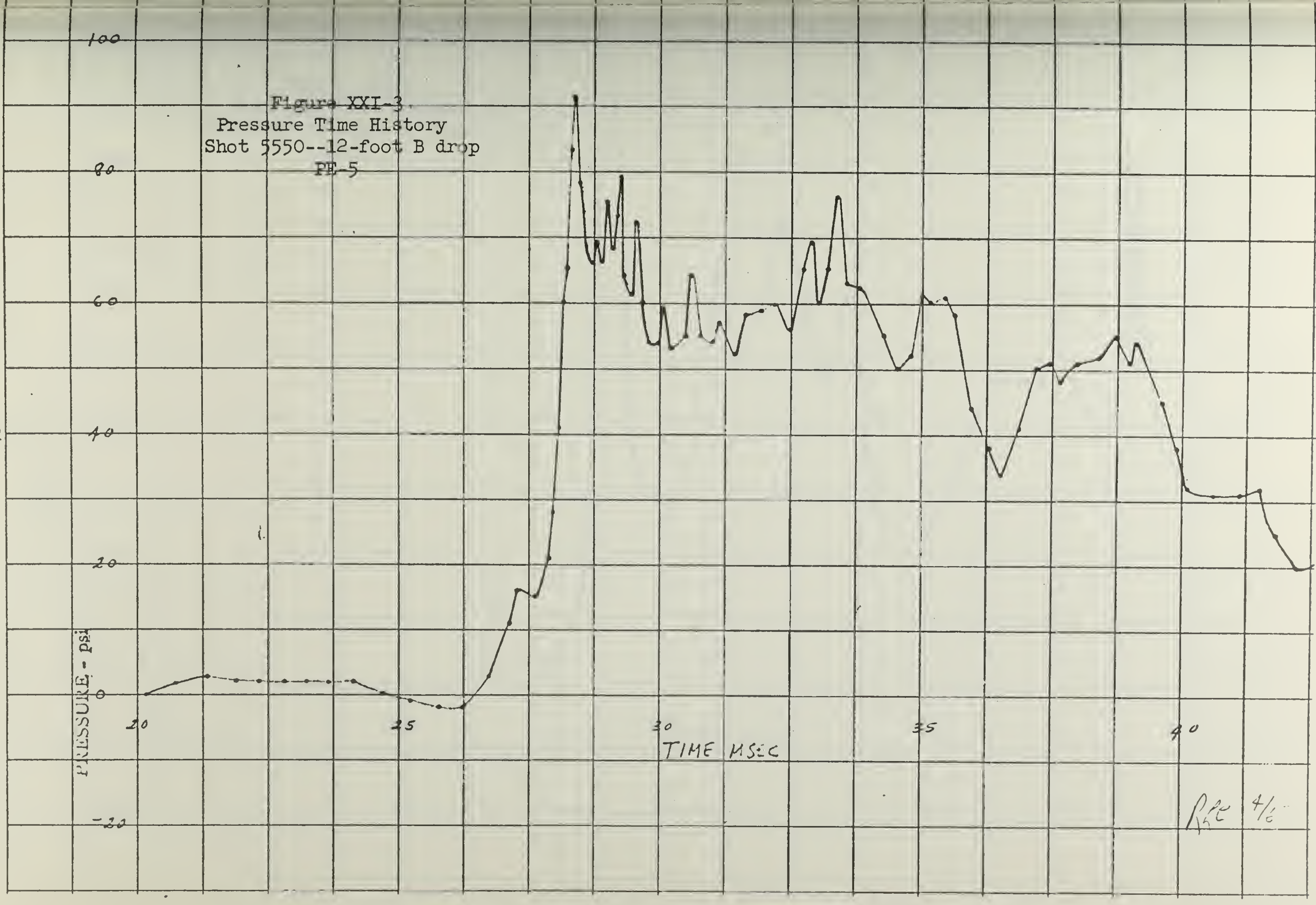

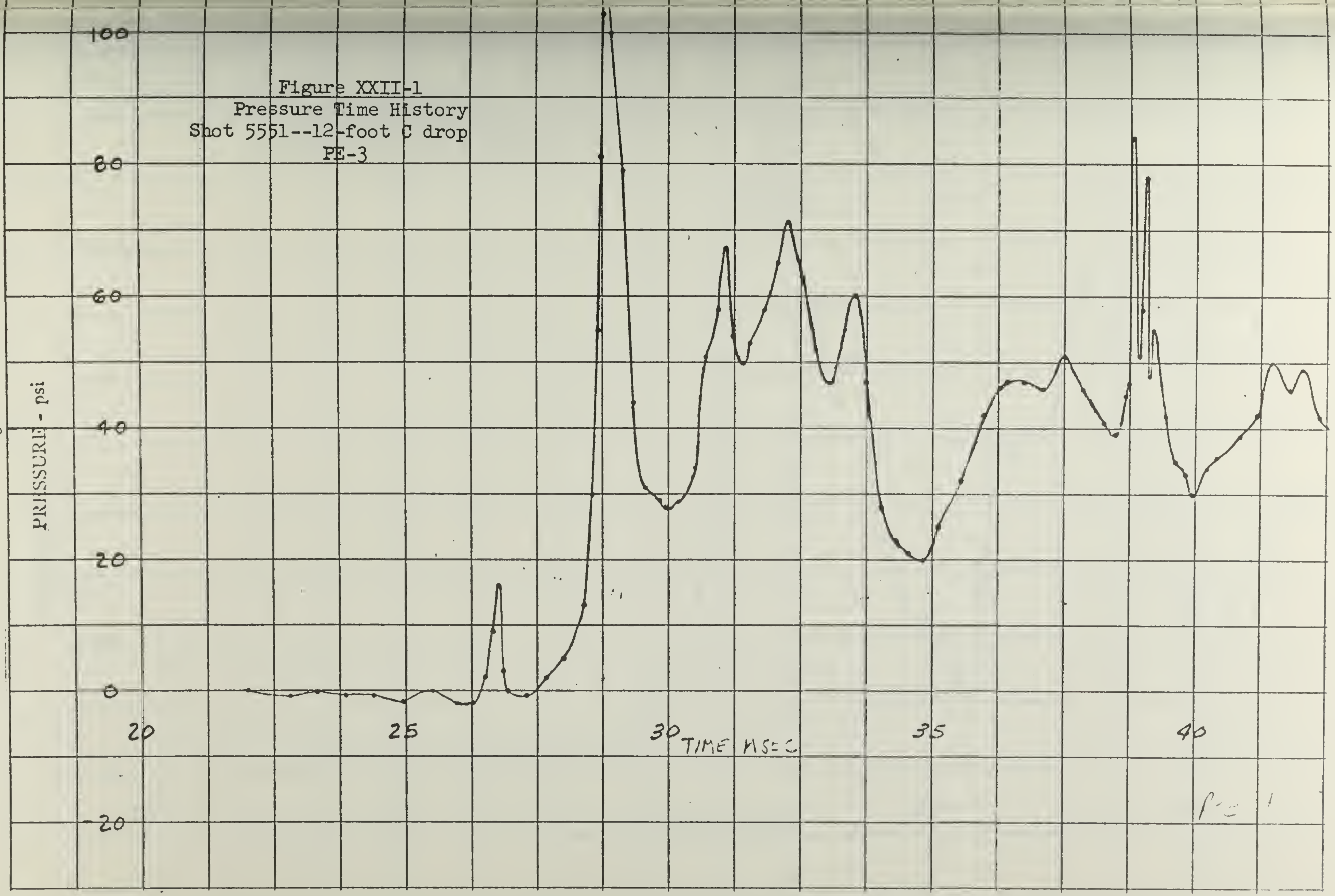

Figure XXII-1
Pressure Time History
Shot 5551--12-foot C drop
PE-3

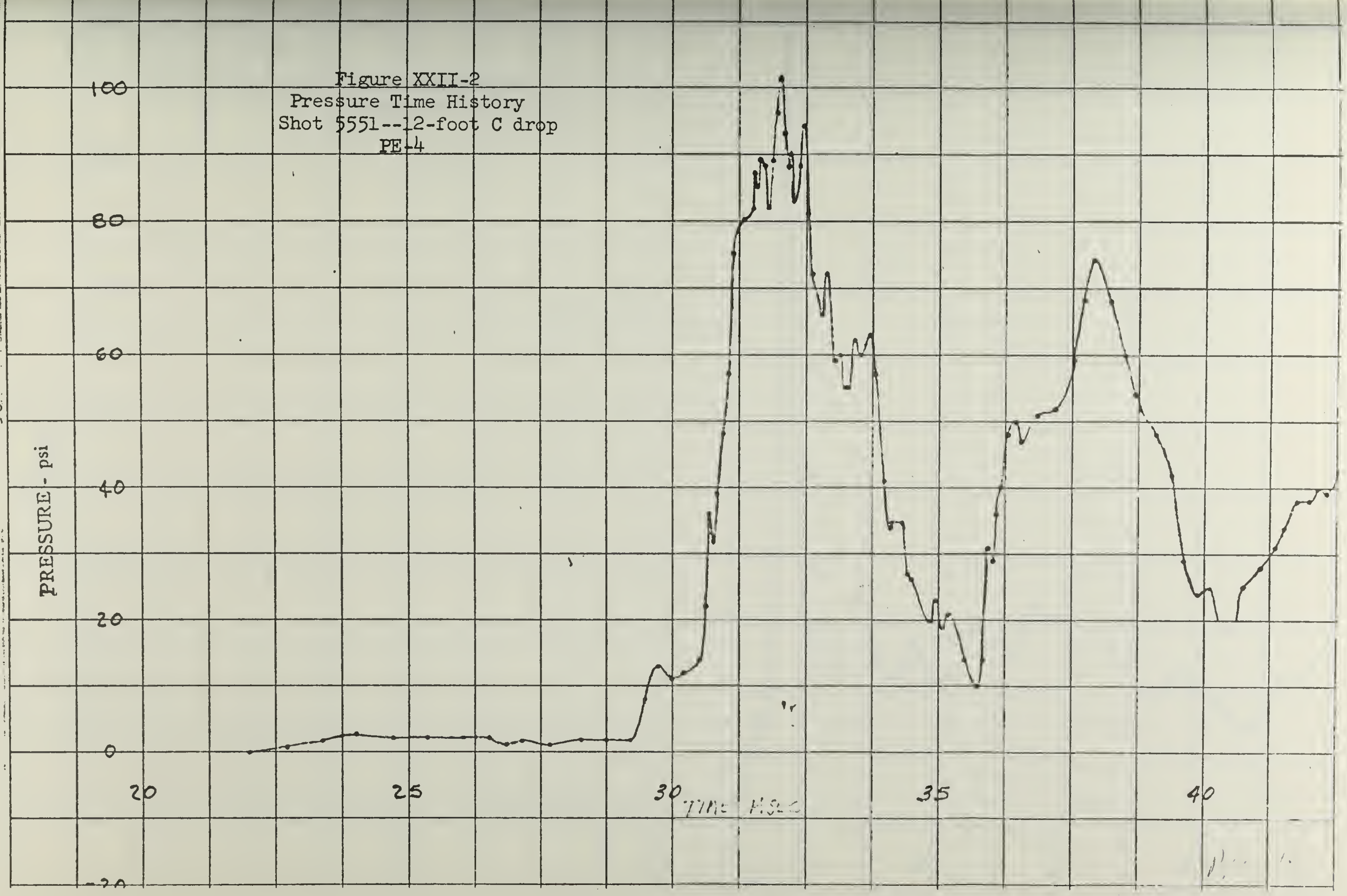

Figure XXII-2
Pressure Time History
Shot 5551--12-foot C drop
PE-4

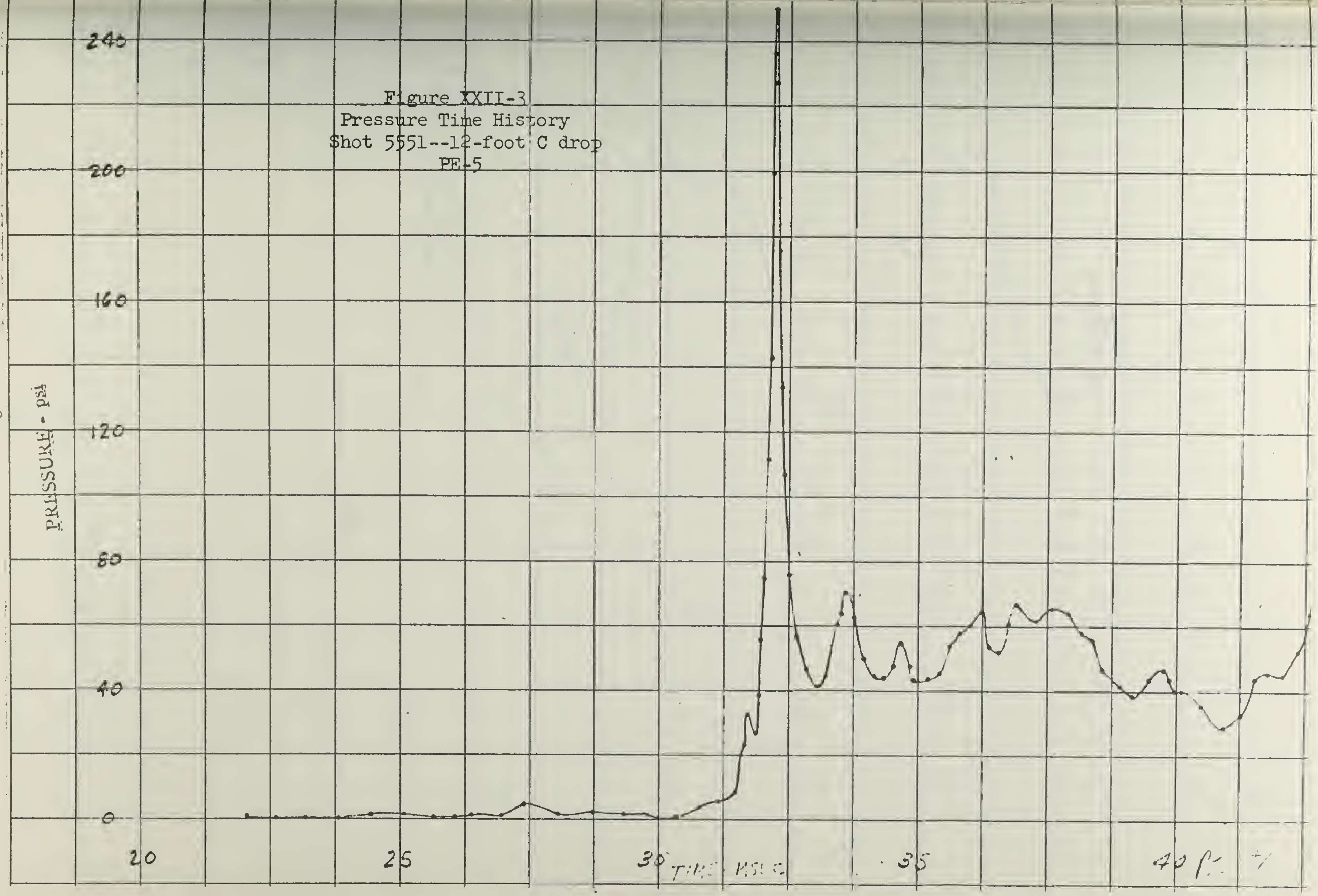

Figure XXII-3
Pressure Time History
Shot 5551--12-foot C drop
PE-5

Figure XXIII-1
Pressure Time History
Shot 5553--12-foot D drop

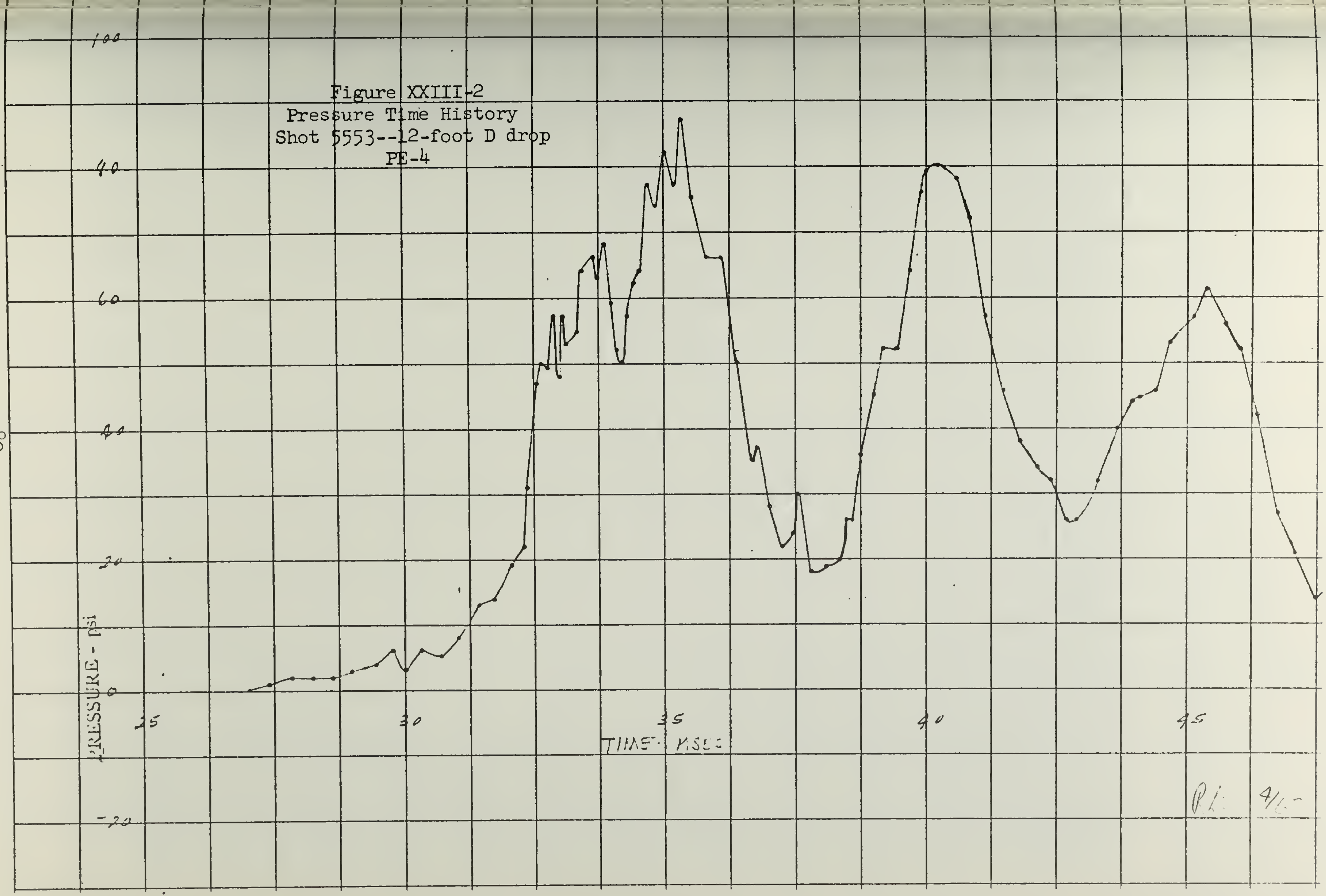
Figure XXIII-2
Pressure Time History
Shot 5553--12-foot D drop
PE-4

Figure XXIII-3
Pressure Time History
Shot 5553--12-foot D drop
PR-5

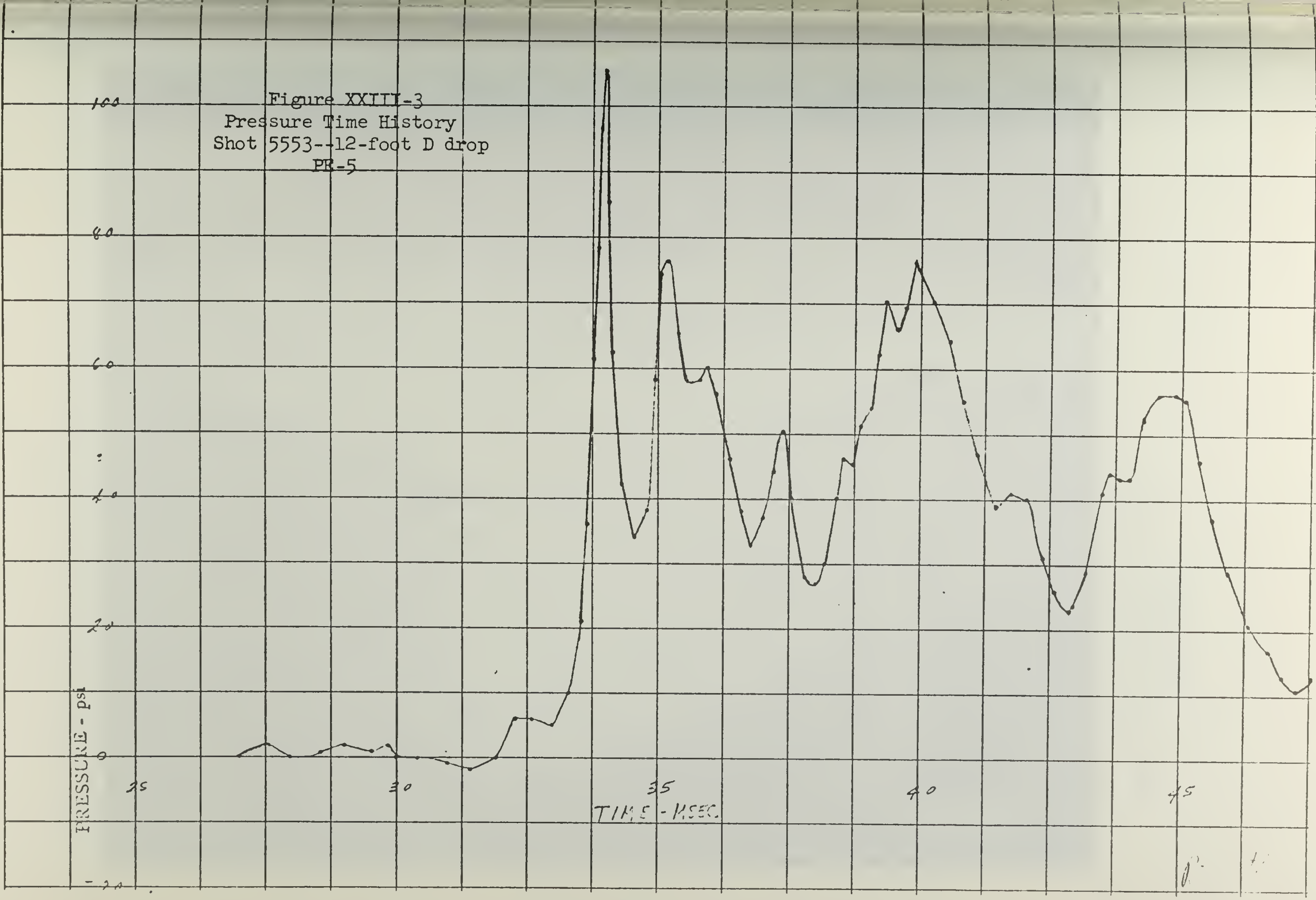

Figure XXIV
Structural Damage, 25-foot drop

Figure XXV
Structural Damage, 25-foot drop

Figure XXVI
Structural Damage, 25-foot drop

Figure XXVII
Structural Damage, 12-foot drop

Figure XXVIII
Structural Damage, 12-foot drop

Figure XXIX
Structural Damage, 12-foot drop

Figure XXX
Structural Damage, 12-foot drop

Figure XXXI-1
Experimental Velocity Time Histories
Shot 5530--2-foot drop
Shot 5531--4-foot drop
Shot 5532--6-foot drop
Shot 5533--8-foot drop
Shot 5549--12-foot drop
VM-1

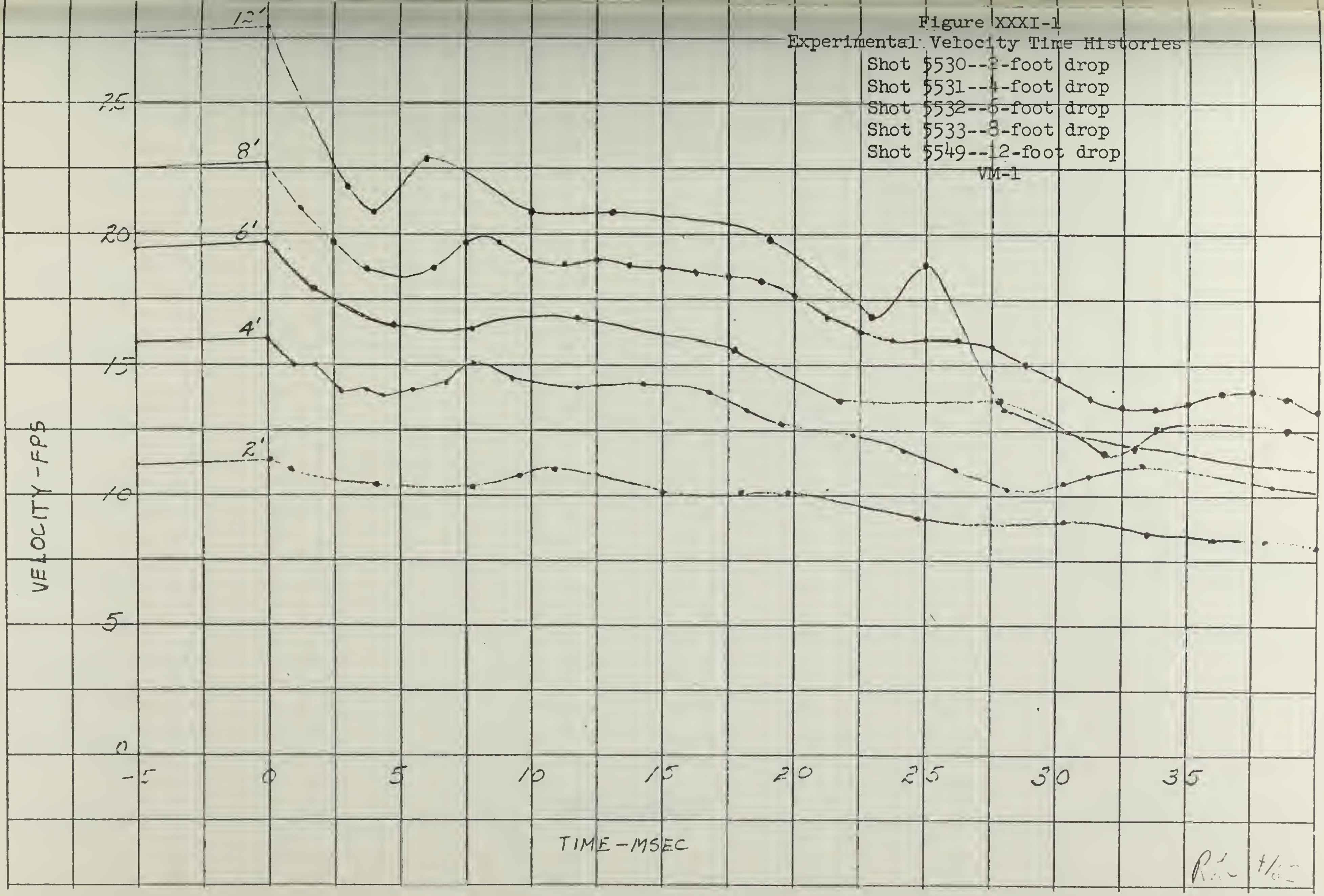

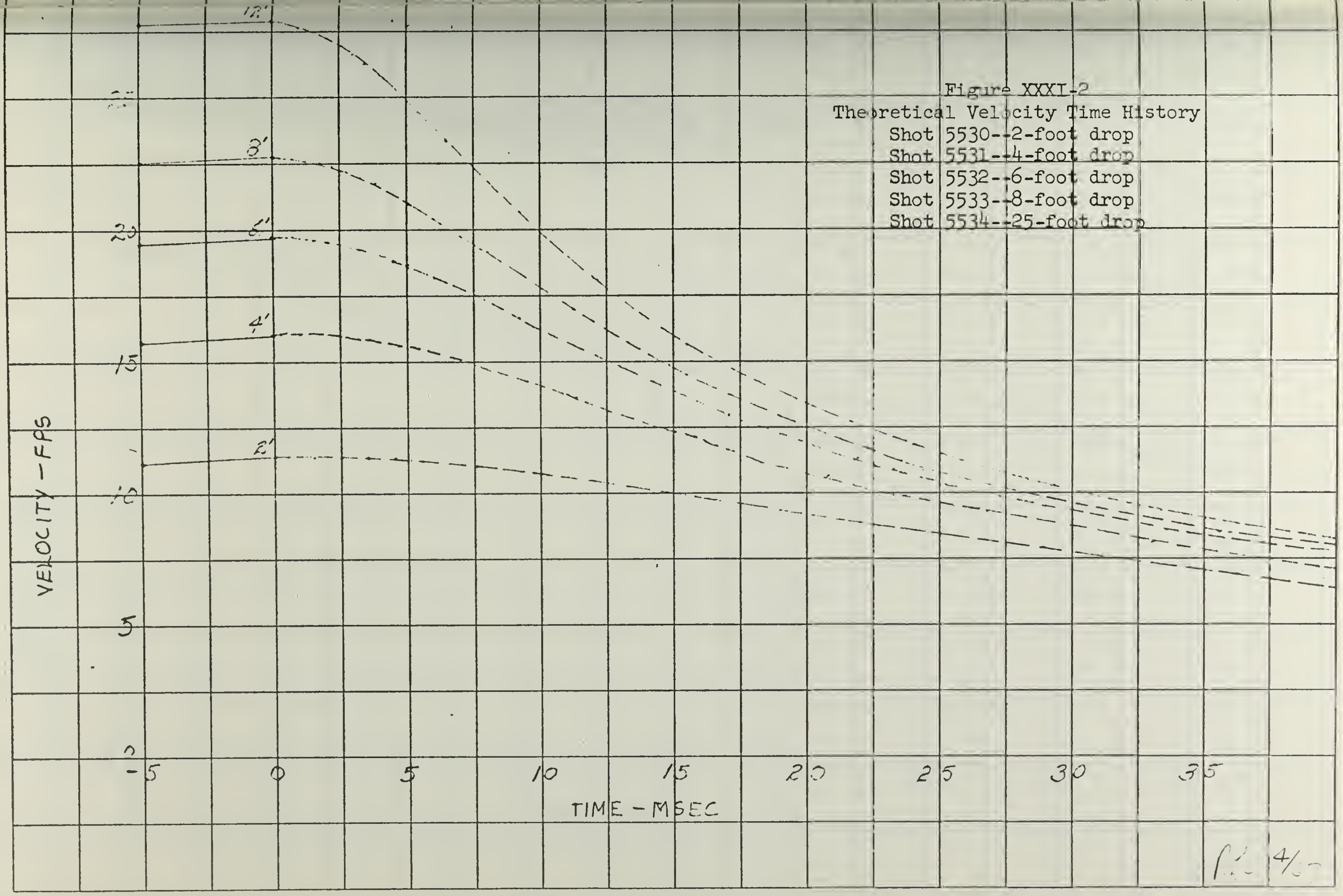

Figure XXXI-2
Theoretical Velocity Time History
Shot 5530--2-foot drop
Shot 5531--4-foot drop
Shot 5532--6-foot drop
Shot 5533--8-foot drop
Shot 5534--25-foot drop

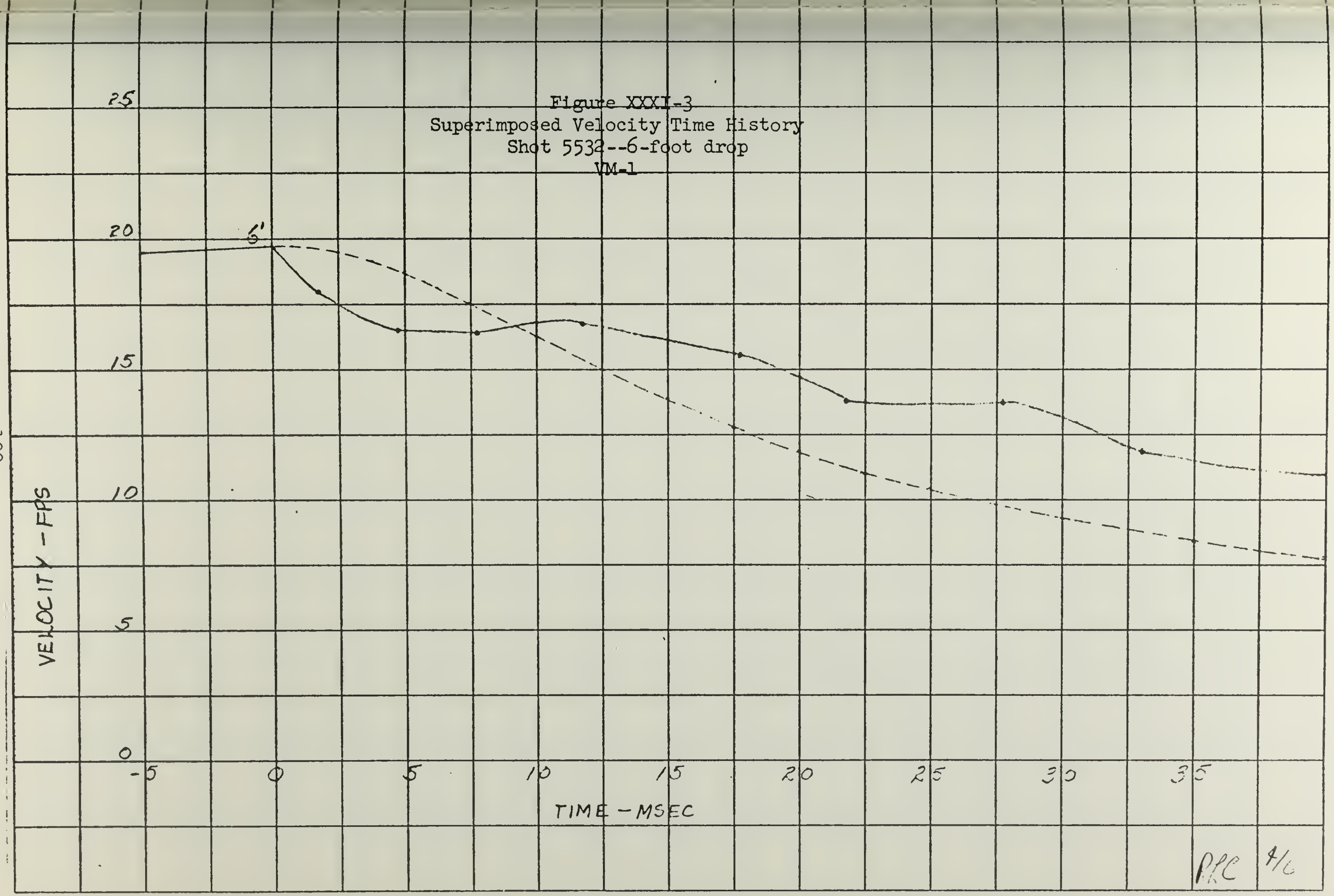

Figure XXXI-3
Superimposed Velocity Time History
Shot 5532--6-foot drop
VM-1

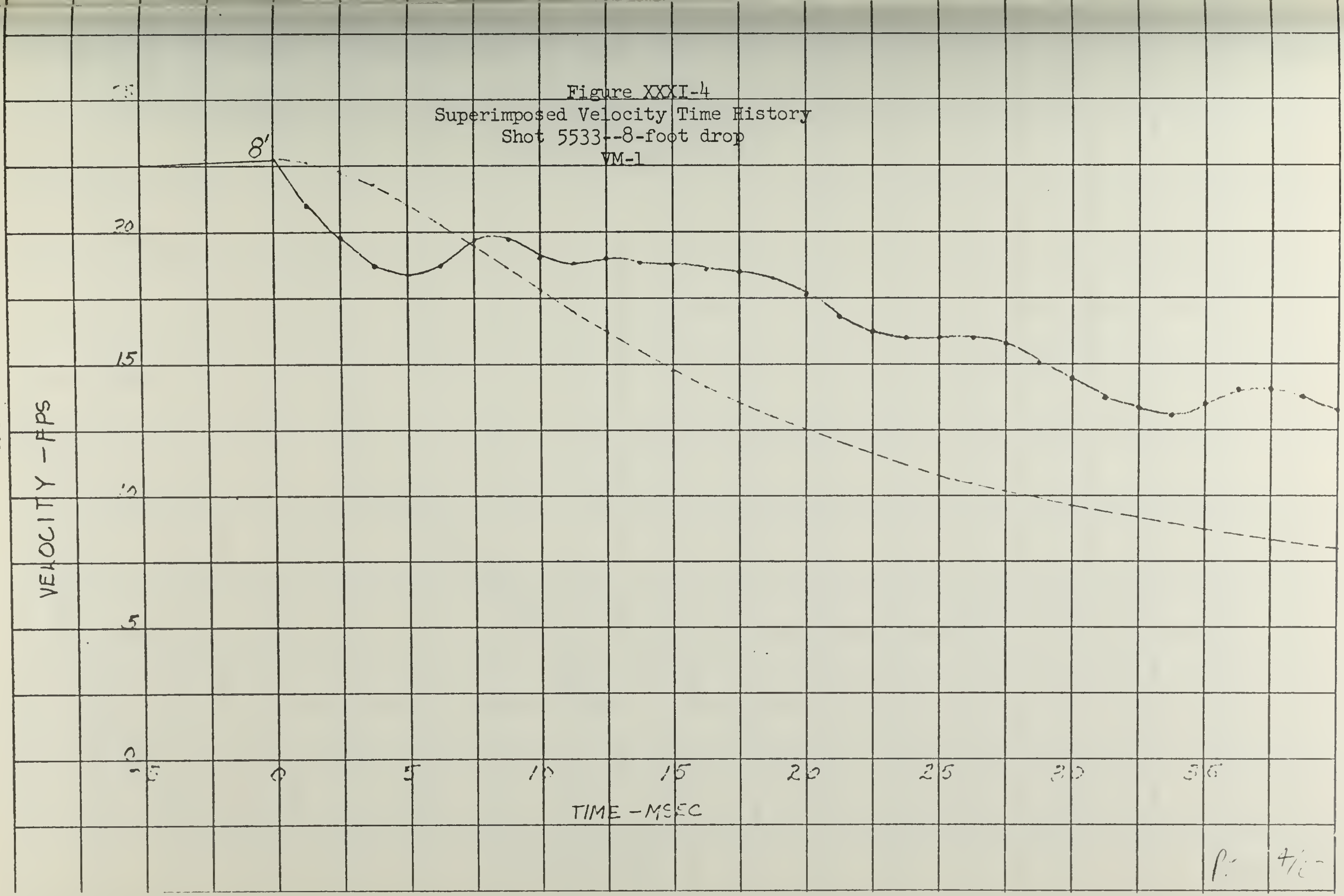

Figure XXXI-4
Superimposed Velocity Time History
Shot 5533--8-foot drop
VM-1

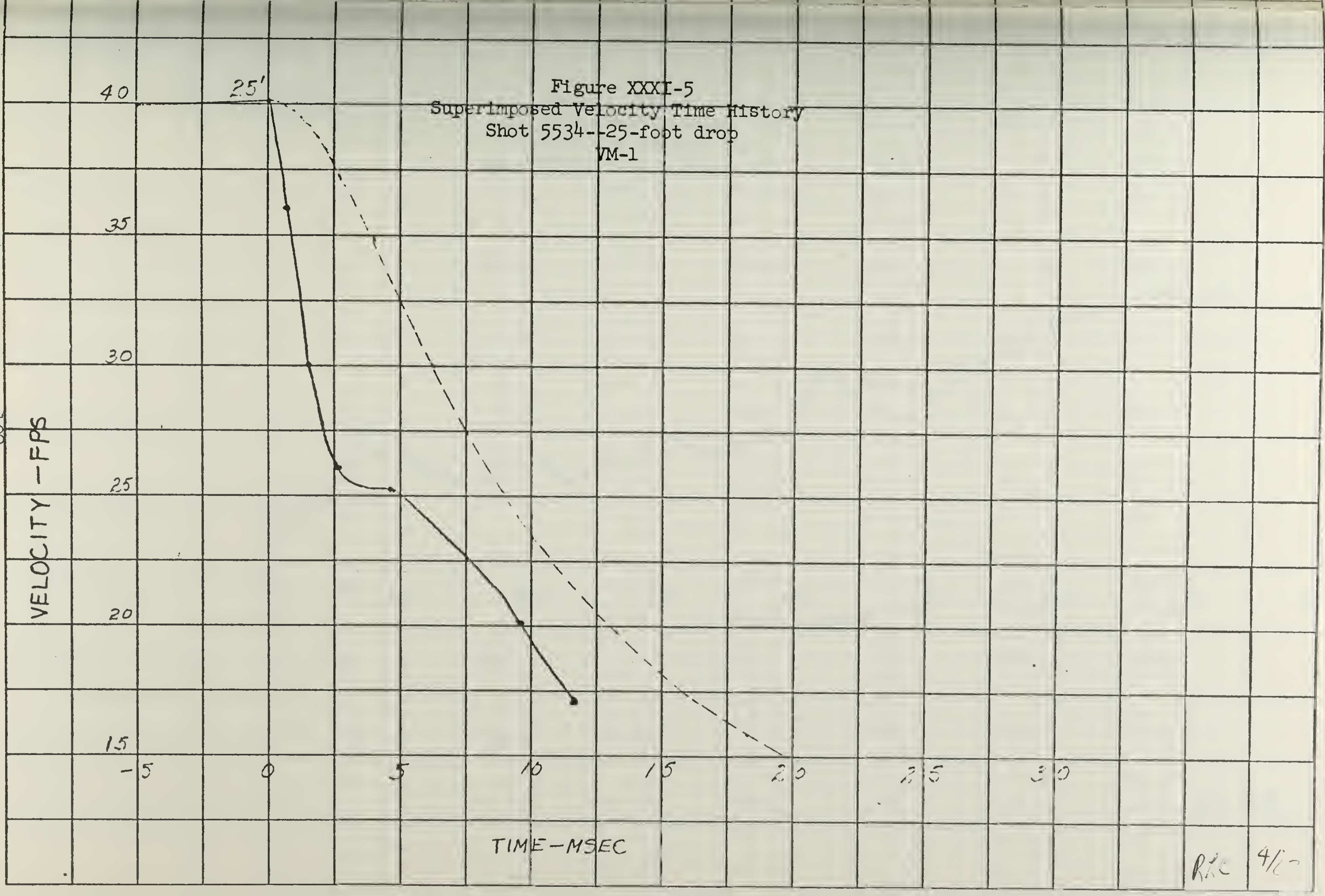

Figure XXXI-5
Superimposed Velocity Time History
Shot 5534--25-foot drop
VM-1

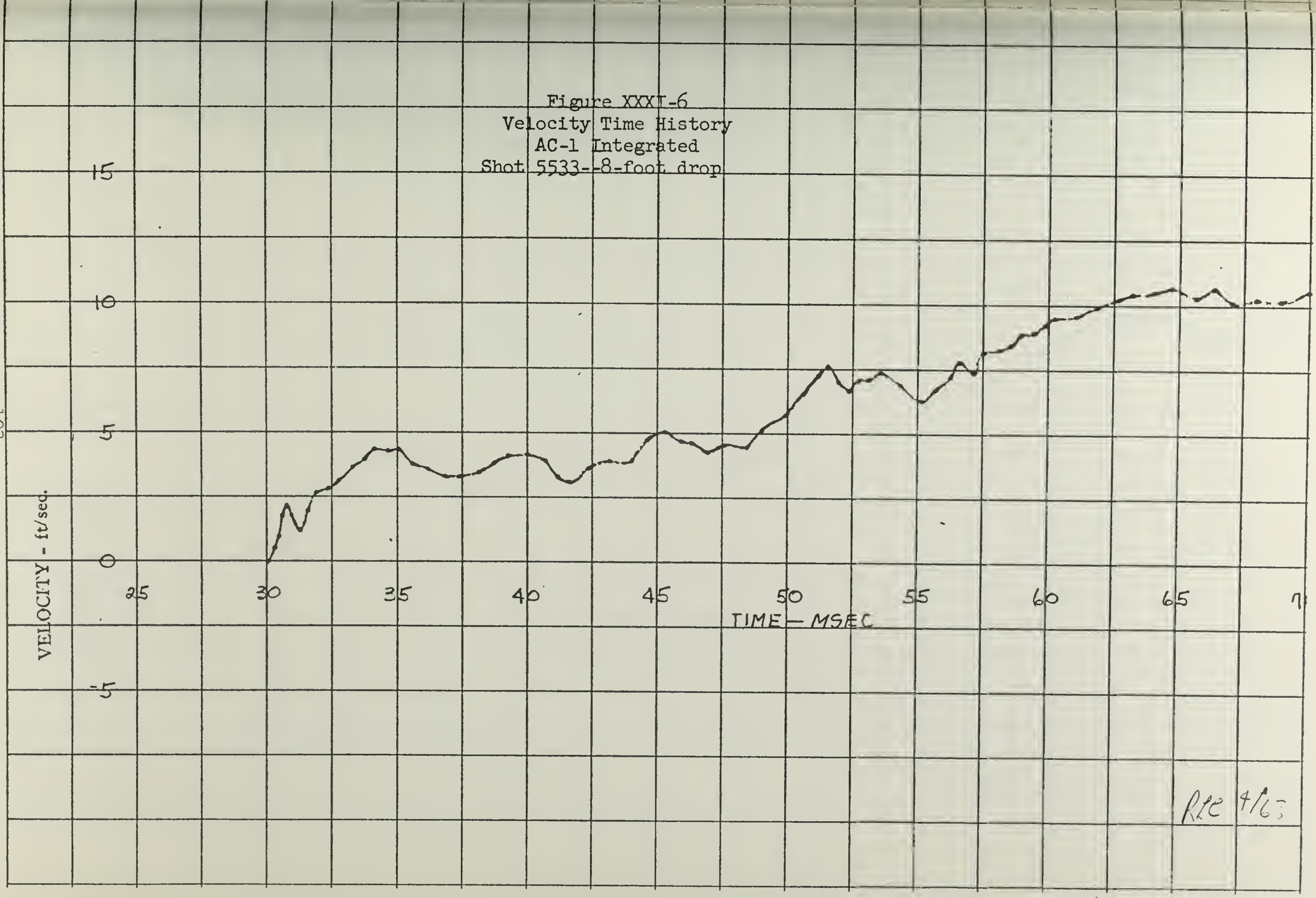

Figure XXXI-6
Velocity Time History
AC-1 Integrated
Shot 5533--8-foot drop

Rlc 4/63

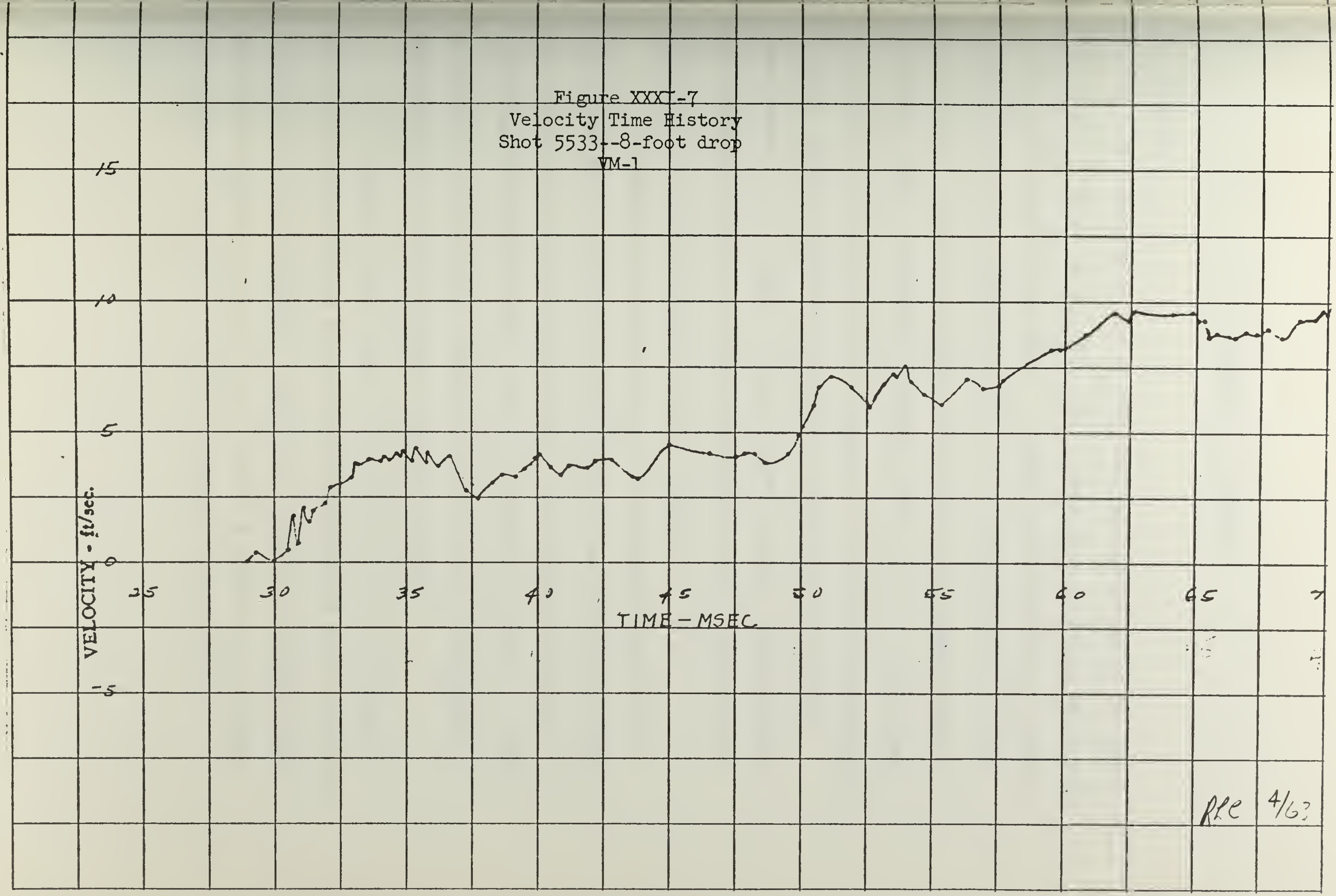

Figure XXXI-7
Velocity Time History
Shot 5533--8-foot drop
VM-1

Rlc 4/63

IV. DISCUSSION OF RESULTS

A. General

The results of the experimental data generated by the model test are considered to be excellent. Checks made on the terminal velocity of each model confirm that $v = (2gh)^{\frac{1}{2}}$ within 2% error. Pressure records of the taped Piezo Electric gages on the bottom of the model show the gage entering the water and then the high pressure spike of the model. Lack of very high frequency wobbles indicates these gages do not move and have faithfully recorded. The deflection measurements from the Magnetic Deflection gages were checked against physical measurements, i.e., damage offsets, and are accurate within 2% also. The integrated velocity from the Accelerometer (AC-1) and Velocity Meter (VM-1) from drop 5534 are almost identical.

Comparison of the records for the repeated 4-foot and 6-foot drops offers proof that changing the model and dropping from the same height gives similar plots for all experimental recordings. The predominant frequencies show up the same and peak pressures are within 3-5 psi in most cases. Repeated drops at 12 feet (see Figures XXVII--XXX) show similar pressure patterns and peaks.

Conditions which affect the reliability of the results are the roll of the model and the water surface. Model A shows a definite tendency to list to starboard (right side of Figure VI, page 6a) and Model B a tendency to list to port. This is a maximum of 1/2 degree per model and results in a 1 degree difference between models.

Water conditions were difficult to control and on some runs a slight swell in the harbor caused some minor variance in drops. The UEB-1 was a very stable platform.

Construction and mounting of the models were considered very good. Checks made by personal inspection of the welds and trueness of the plating established that the models were fair and exceeded any shipbuilding practices. Connections to the carriage were good for the first model and fair for the second. Failure of the keel on Model A shows the end conditions held until the extreme conditions of the 25-foot drop occurred. On Model B the failure of the end support (Figure XXVII) of the keel after the third 12-foot drop (5551) shows the weakness at the end condition which allowed the ends to form a hinge prematurely and rotate. Views of the damage are very much like bottom damage observed in practice.

B. Pressure

Comparison of the experimental and theoretical results reveals that the two-dimensional theory does not accurately predict the peak pressures and the shape of the peaks. While the model is essentially elastic in response (2--8-foot drops) theory predicts the mean pressures after immersion of the point in question with good accuracy. Since the theory is based on the assumptions of incompressibility of water, potential flow and apparent mass, this is expected. The initial phases of contact violate these three assumptions; whereas, after the model is immersed, the flow is established, and the theoretical conditions are approached. Distribution of the added mass is cyclindrical as shown in plots of the underwater pressure gages. See Figures XVII-17, 18 and

XVIII-17, 18.)

As to the accuracy of recording the peaks, Schauer [24] found that the frequency response of the PE gages and the amplifier to be flat up to 100 kc. and rounding of the peaks was an insignificant amount of distortion for the large duration peaks. The impact on the keel (not the plate) falls into the region where cutoff due to frequency response and gage size effect the output. An overall response of 60 kc would be necessary for a flat keel of four inches, but the models, due to construction, had only two inches of flat area. For this reason peaks on the 8-foot, 12-foot and 25-foot drops are assumed to be in a cutoff region.

For the lower drops, up to 8 feet, the peak pressure at the keel is less than ρcv, but bears a constant relationship to $p = K\rho cv$, where K is some constant.

Noting that PE's 4, 6 and 8 are in the center of the plates and PE's 5 and 7 are on the stringers, a definite trend is seen. The pressure is definitely relieved and reinforced at the plate centers by the plate motion. This may amount to twice as much pressure as predicted by theory. Motion of the overall bottom and the sides also affects pressures as shown by the 23 msec period prevalent on so many recordings. A definite change in pressure response is noted starting at the 8-foot drop and continuing to the 12-foot and 25-foot drops. The model acceleration and the interface acceleration begin to diverge. The bottom structure is slowed much faster and the structure begins to behave plastically. Real evidence of damage to the plates begins on the 8-foot drop. A change in response of peak underwater pressure also occurs.

Up to the 8-foot drop, peak pressure in the water varies as KV^2, but above this it varies as $K\rho cV$.

Another distinguishing feature of the pressure histories is the close resemblance they bear to shock waves and modified shock waves, Figures XIII and XVI. The pressures of PE's 3, 5 and 7 have sharp initial rises while the pressures of PE's 4, 6 and 8 have a finite rise time. All have an effective positive time which is large when compared to the natural periods of all structural elements except the overall bottom and the sides. Even for these latter elements the ratio, t_1/T, is about one, which yields a dynamic load factor greater than one. In the case of PE's 4, 6 and 8 which are on the panel centers, a finite rise time, t_o, is noted to be about 3 or 4 msec. The calculated undamped natural period of the panels is 2.2 msec; therefore the ratio, t_o/T, is less than one and the dynamic load factor is about 1.5. A look at the strain gage and deflection gage records show that a period of about 6 msec is very prevelant. Assuming a decreased modulus and an increased mass due to entrained water caused the natural period of the panel to be increased to this value, the resulting dynamic load factor is about 1. These results are based on the assumption that the plate is fully clamped at the edges. If the plate were simply supported, the natural period of vibration would be 4.4 msec for the small panels. This leads to the conclusion that the peak pressure should be used as a uniform pressure for the design of the plating subject to slamming in typical naval design applications.

In the case of the stiffeners, the results are quite different, in that the pressure history is a shock wave with the effective time, t_1, equal to 23 to 28 msec. The natural periods of the keel, stringers, and web frames, with their effective plating of 60h, are 5.6, 0.9 and 0.9 msec respectively. Figure XIV shown that the dynamic load factors for these elements are 1.8, 2.0 and 2.0 respectively. This indicates that twice the slamming pressure should be used for design of the stiffeners on this prototype and similar naval designs.

The resemblance of the pressure histories to shock waves is also observed in the decay. PE's 14 and 15 indicate that the pressure decays to less than 0.1 P_o in a time of 0.1 msec (the time to travel nine inches in water). Another difference found between the theoretical and experimental data is the location of the peak pressure. Theoretically it is right next to the keel, but experimentally it moves. At the lower drops it is close to the keel and as the model deforms it moves outward until at the 12-foot and 25-foot drops it is at the edges of the model. This is mostly due to the change in angle of the water model interface as damage is done. With large damage the outboard edge of the model has an angle much less than the 10 degrees found at the keel. This suggests that bottom sections should be designed with a convex form extending from the keel girthwise and never should be a flat section. This will keep the peak pressures in the region of the thickest plates near the keel. See Figures XVIII-9, 10; XX-6, 7; and XIX-9, 10.

C. Deflections and Strains

Deflections were found to be elastic up to the 6-foot drop where random permanent set was noted in less than 10% of the panels. After the 8-foot drop, all panels showed a small plastic set. After the 12 and 25-foot drops, the individual panels were dished in a roof-top deformation with $\delta_c \geq 0.5$ inches $= 4h$. The keel deformed with hinges at the ends and in the middle. The stringers deformed parabolically between the bulkheads. The web frames formed shear hinges at the sides and keel, which coupled with the stringer deformation allowed the side panels, bounded by the bulkheads, side and keel, to deform as a unit with a maximum deflection of 0.3 inch for the 12-foot A drop and 1.3 inches for the 25-foot drop. By using the offsets given in Appendix C, Figures XXXVI and XXXVII, the plastic deformation energy was calculated as per equation (24) for the fifty panels, the two side panels and the overall bottom for the 12-foot and 25-foot drops. As in the calculation of natural periods, equivalent plating thicknesses were used. An average of eight offsets at the edges of each panel was used as a reference to find each individual δ_c.

The plot of girthwise deflections, Figure XX-5, shows that the whole bottom and the side panels begin to deflect at the instant of impact. In plotting this data, the lower flange of the keel was assumed to be infinitely stiff in relation to the bottom plating, thus making the panels next to the keel only six inches wide.

A comparison of pressure, deflection and strain histories at the same location, Figures XVII-10. 11 and 12, also shows that initial

deflection and stress occur before the free surface of the piled up water, Figure XI, reaches the location. The initial strains are seen to be negative for ST-1, 3 and 4, Figure XVII-13. These normally would be expected to be positive, but are originally put into compression when the keel initially deflects inward on impact.

D. Velocity and Acceleration

The velocity histories, Figure XXXI, show the basic difference between an elastic model and a rigid model. The initial acceleration, hence change of velocity, is very different from that predicted by theory at the water model interface, where the overall model velocity and acceleration are very close to the theoretical as shown by viewing the movies. This would explain partially why equation (23) does not predict the peaks properly. This also confirms Szebehely [2] who believes that acceleration is important.

V. CONCLUSIONS AND RECOMMENDATIONS

A. Conclusions

1. The two-dimensional theory used to predict the pressure distributions gave results which agreed well with the experimental data in the region 4-25 msec after impact.

2. The peak pressures and the shape of the pulse were not predicted by the theory and can be described as blast pulses or modified blast pulses.

3. Plates once in vibration reinforce and reduce the pressure as much as twice the mean predicted value.

4. The peak pressure due to slamming is linear with ρcV.

5. Repeated drops deform the framing system on each drop, but plate damage is confined essentially to the 12-foot A drop.

6. The plate and structure damage are the direct result of the blast-type impulse pressures found on impact. Dynamic load factors indicate that P_o should be used in the design of plating and 2 P_o in design of the stiffeners.

7. As the structure yields or becomes plastic, the pressure peaks away from the keel are modified from sharp rise time to finite rise times.

8. The repeated 12-foot drops were not completely successful because the end conditions on the keel differed from those anticipated in the ship.

9. The fact that the large interface acceleration is different from that of the carriage gives credence to the effect of acceleration on the pressure at impact.

B. Recommendations

1. One of the remaining models should be instrumented as before and dropped repeatedly from 8 feet, making sure the end condition at the keel remains fixed, to recheck the effects of repeated impacts.

2. The second remaining model should be used to study the effects of different model weights as suggested in the original test schedule.

3. The instrumentation on the model should be changed to give more information on the motion of the section. PE's 16--20 should be removed and those channels used to measure acceleration and velocity of the carriage.

4. Future ship designs should use the peak pressure expected (from ship motion studies) to size the plates and twice the peak pressure for design of the framing as a design criteria.

5. The end conditions of the remaining models should be stiffened before more testing proceeds and the connections at the keel (welds especially) should be checked carefully to insure near fixed conditions.

6. Future 1/4 scale model tests should be made using 0° dead-rise models, keeping the other parameters the same. Also, tests should be conducted, independently varying other parameters, such as, plating size, stiffener size and panel dimensions.

7. Pressure measurements, made on ships at sea, should be taken on the stiffeners to record the important pressure peaks due to ρcV.

8. As Research and Development funds are limited, every attempt should be made to optimize the testing recommended to gain the most information from the least number of models.

VI. APPENDIX

Appendix A

Proposed Test Schedule

Test	Drop No.	Model	Mass	Aux. Mass	Range	Height	Remarks
1	1(5530)*	A	1.5	0.0	elastic	2'	
	2	A	1.5	0.0	elastic	2'	rippled water
	3(5531)	A	1.5	0.0	elastic	4'	
	4	A	1.5	0.0	elastic	4'	rippled water
	5(5532)	A	1.5	0.0	elastic	6'	
	6	A	1.5	0.0	elastic	6'	rippled water
	7(5533)	A	1.5	0.0	plastic	8'	**
2	1(5534)	A	1.5	0.0	max. plastic	25'	
3	1(5549)	B	1.5	0.0	med. plastic	12'	
	2(5550)	B	1.5	0.0	med. plastic	12'	repeated drops into med. plastic range to study damage
	3(5551)	B	1.5	0.0	med. plastic	12'	
	4(5553)	B	1.5	0.0	med. plastic	12'	
4	1	C	1.0	0.0	med. plastic	25'	repeated drops into med. plastic range to study damage
	2	C	1.1	0.0	med. plastic	25'	
	3	C	1.2	0.0	med. plastic	25'	
	4	C	same until sufficient damage done				
5	1	D	***	0.0	***	height from 3-1	
	2	D	****	2.0	***	height from 3-1, 5-1	

---

* Numbers in parentheses are the UERD shot numbers

** Extend height until small plastic set.

*** Medium plastic range to study aux. mass effect.

**** Drop two with roll to port, drop one with roll to stbd. - mass from 3-1, 4-1.

As testing proceeded, the proposed test schedule was modified. In Test 1, Drop Numbers 2, 4 and 6 were eliminated. In Test 3, drops from two feet, four feet and six feet were made with Model B before making the four repeated 12-foot drops. These drops were identified by UERD shot numbers 5544, 5545 and 5546, respectively. Tests 4 and 5 will be accomplished later this year.

Appendix B

Block Diagram of Recording Apparatus

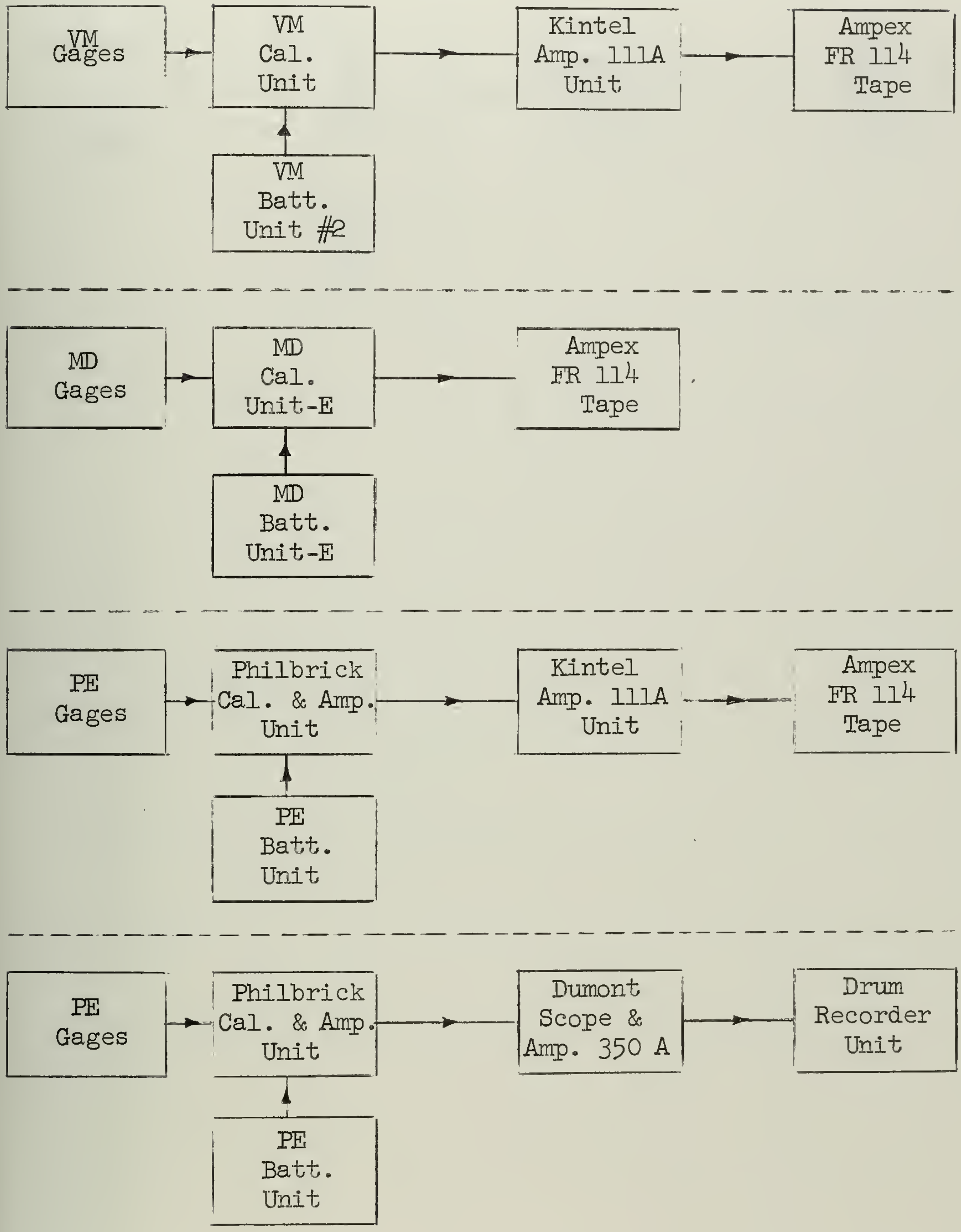

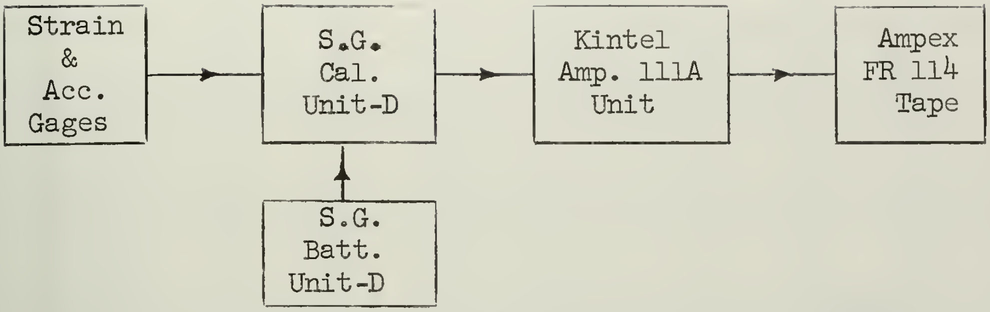
Strain & Acc. Gages
S.G. Cal. Unit-D
Kintel Amp. 111A Unit
Ampex FR 114 Tape
S.G. Batt. Unit-D

Appendix C

Supplementary Data

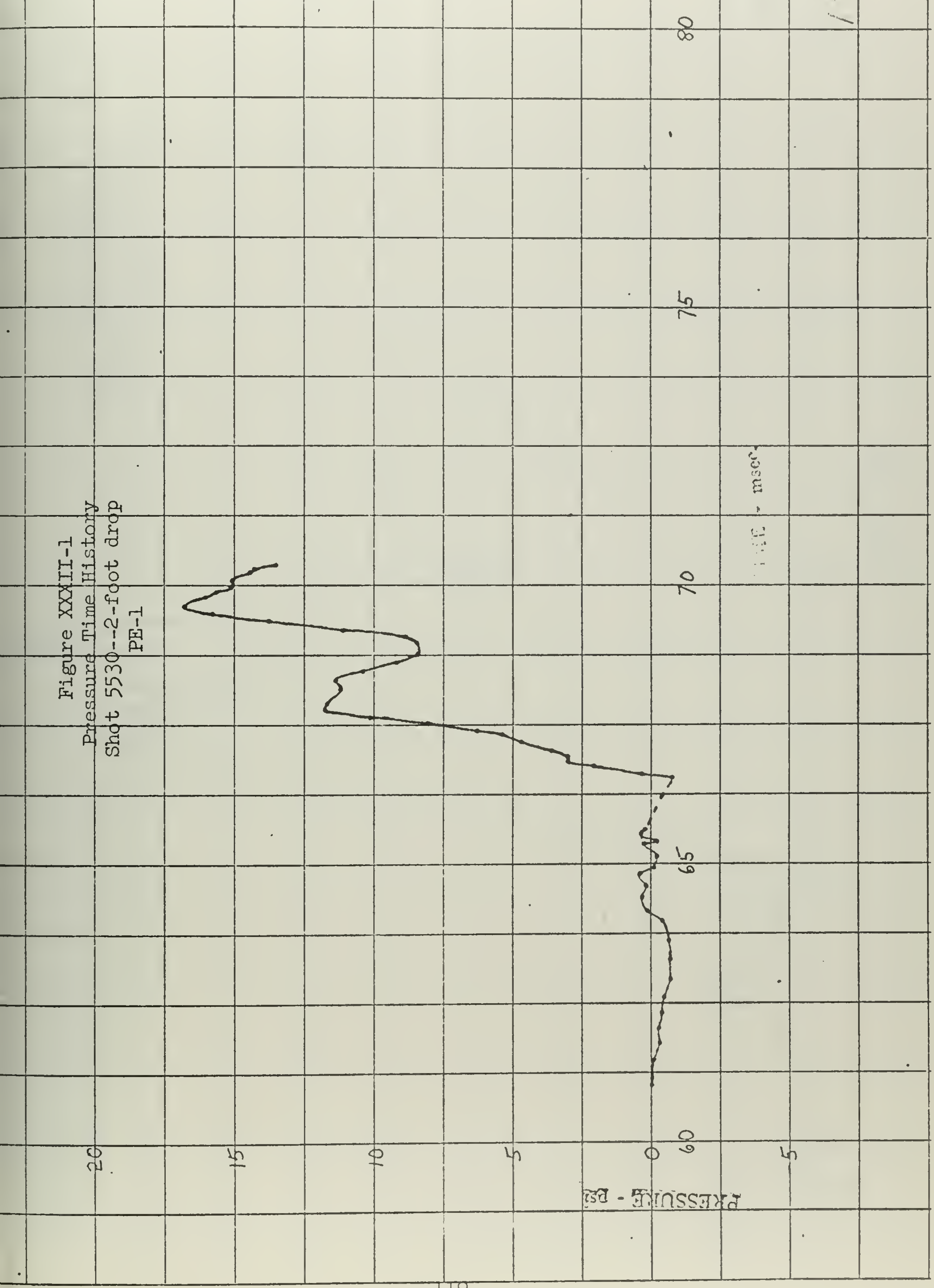

Figure XXXII-1
Pressure Time History
Shot 5530--2-foot drop
PE-1

Figure XXXII-2
Pressure Time History
Shot 5530--2-foot drop
PE-2

4/63

Figure XXXII-3
Pressure Time History
Shot 5530--2-foot drop
PE-3

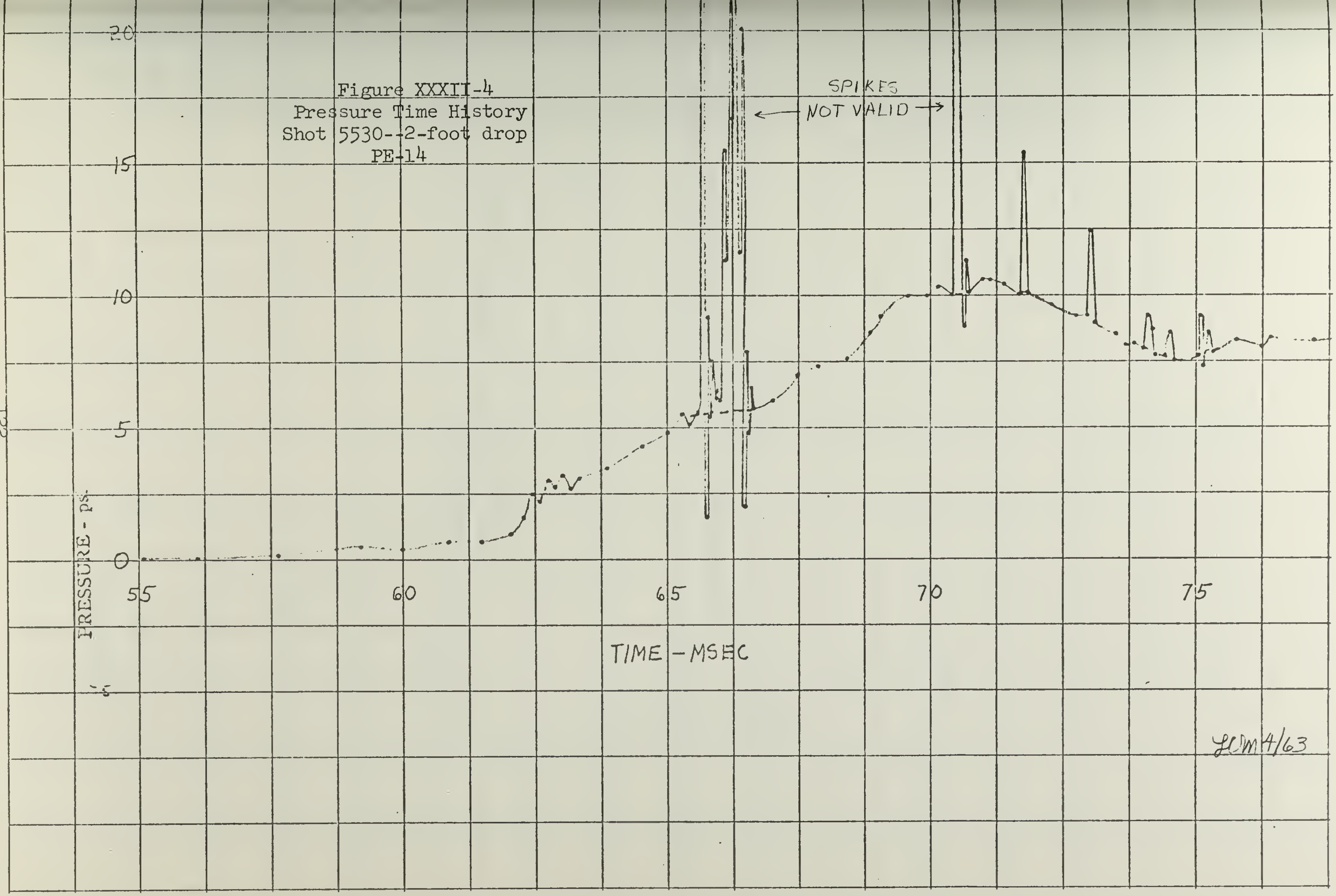

Figure XXXII-4
Pressure Time History
Shot 5530--2-foot drop
PE-14

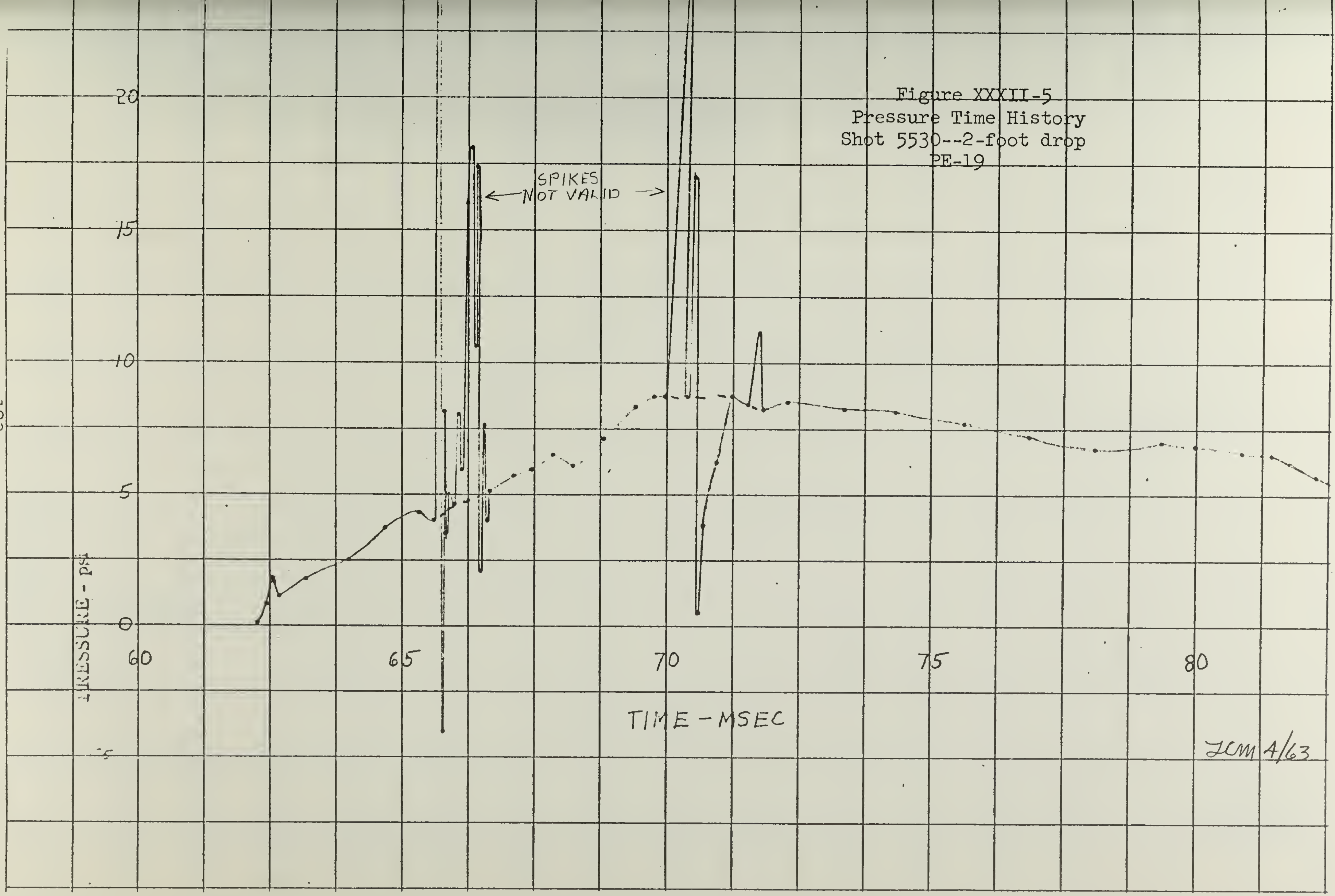

Figure XXXII-5
Pressure Time History
Shot 5530--2-foot drop
PE-19

Figure XXXII-6
Pressure Time History
Shot 5530--2-foot drop
PE-11, 12, 13 and 14

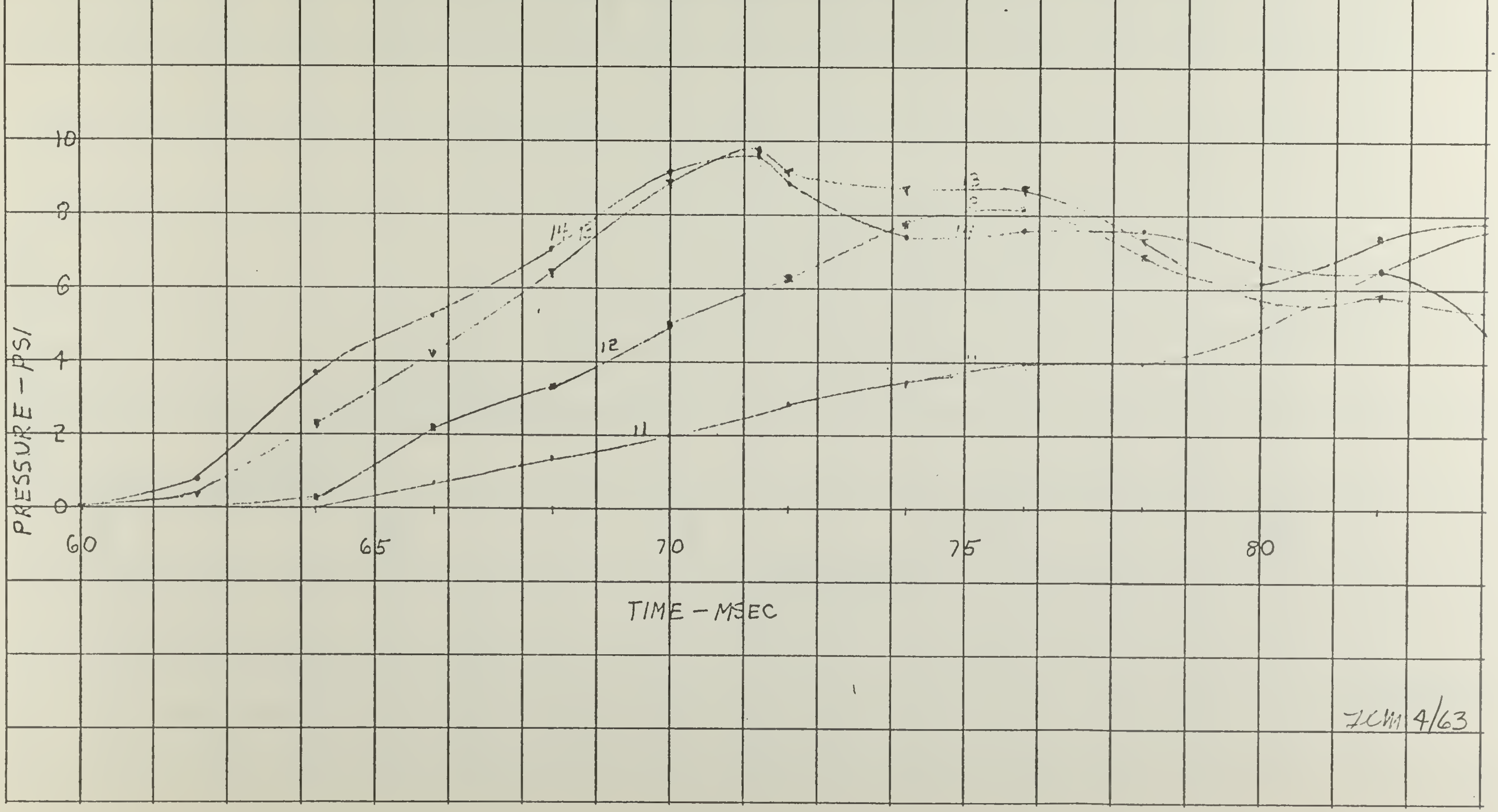

JCM 4/63

Figure XXXII-7
Pressure Time History
Shot 5530--2-foot drop
PE-16, 17, 18 and 19

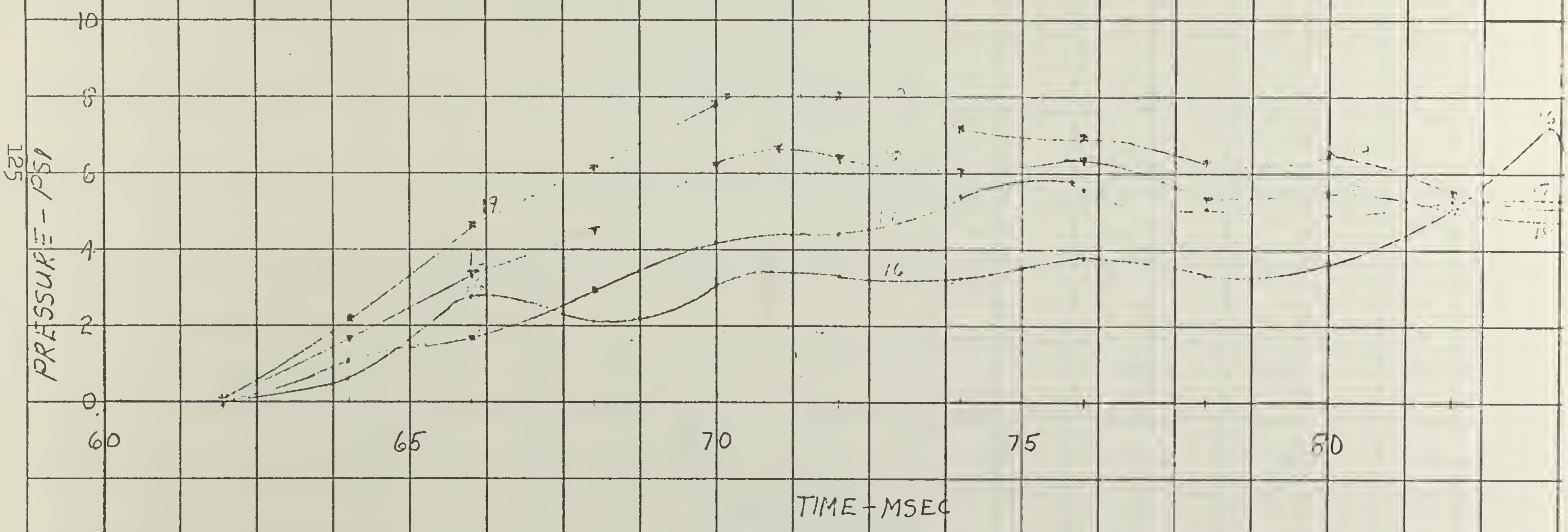

Lem 4/63

Figure XXXII-8

Pressure Time History
Shot 5530--2-foot drop
PE-15 and 20

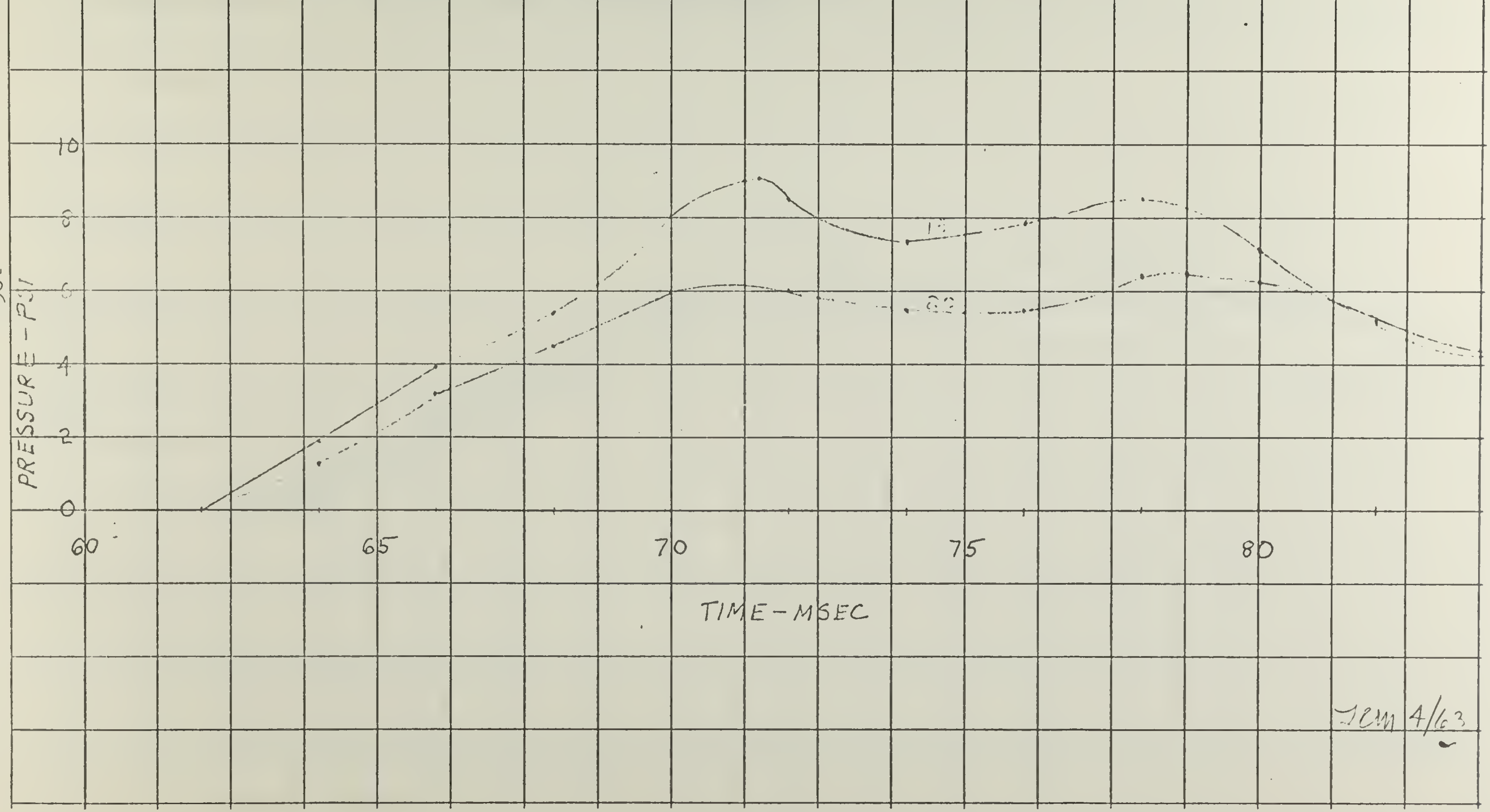

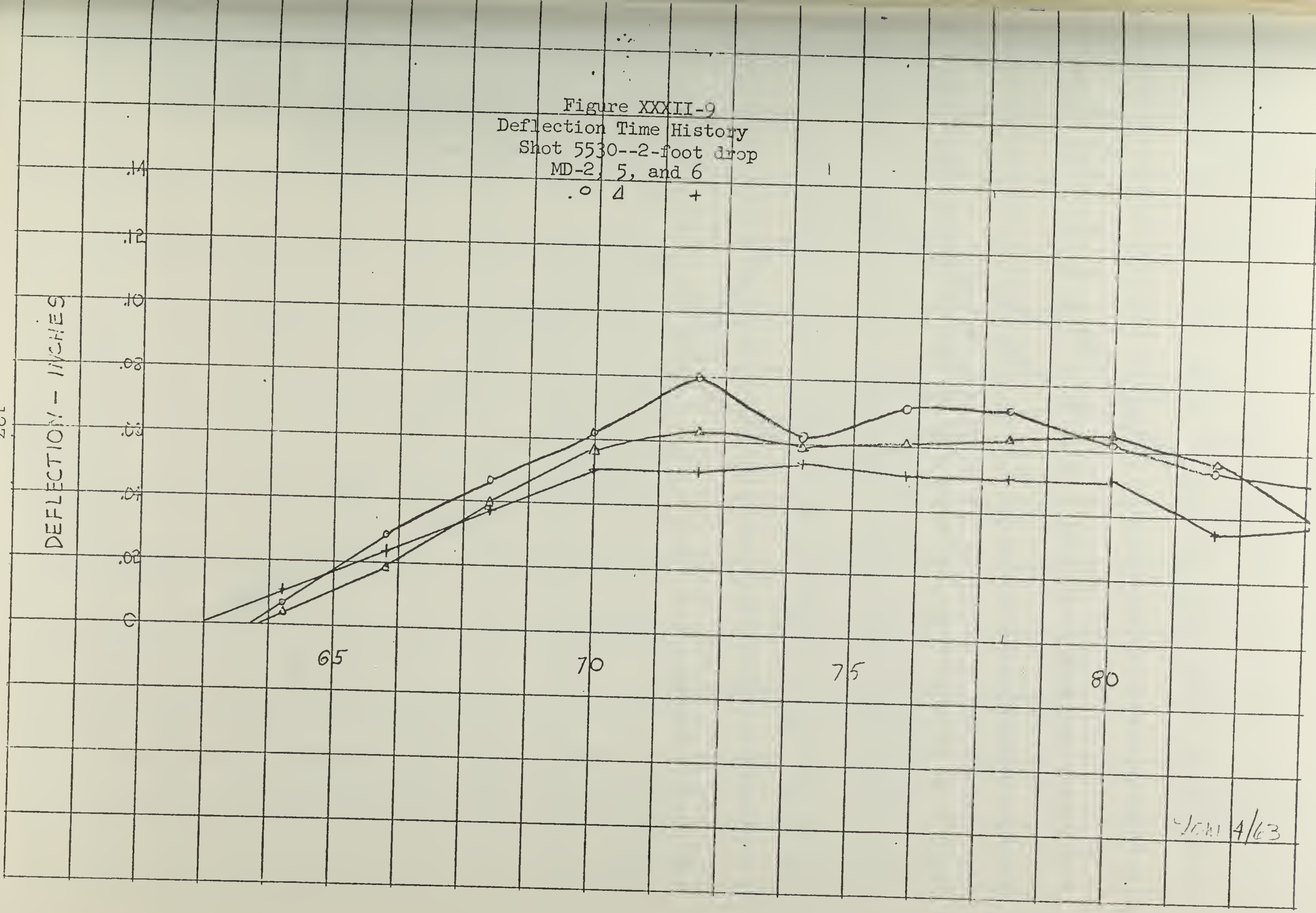

Figure XXXII-9
Deflection Time History
Shot 5530--2-foot drop
MD-2, 5, and 6
○ △ +

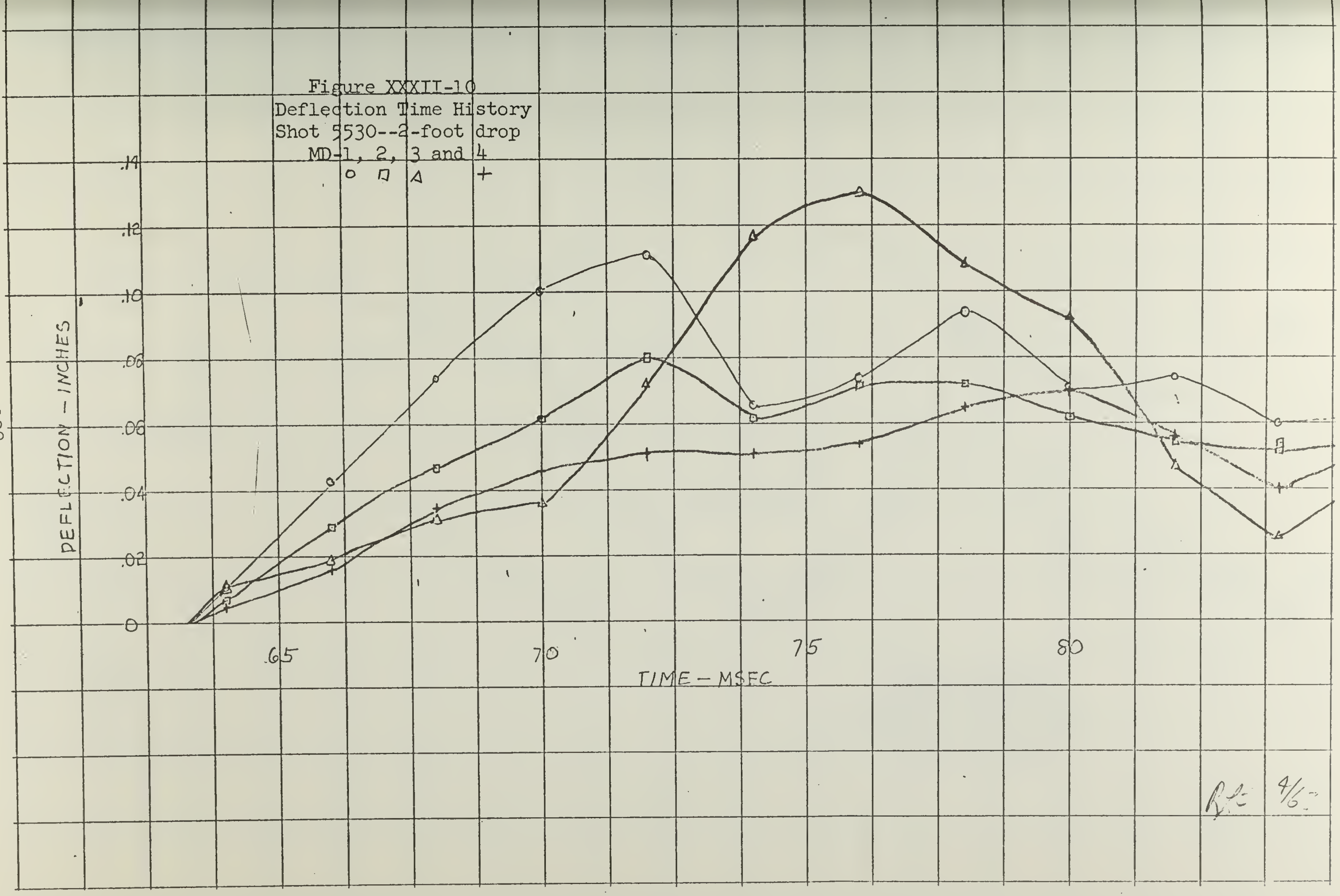

Figure XXXII-10
Deflection Time History
Shot 5530--2-foot drop
MD-1, 2, 3 and 4

4/6

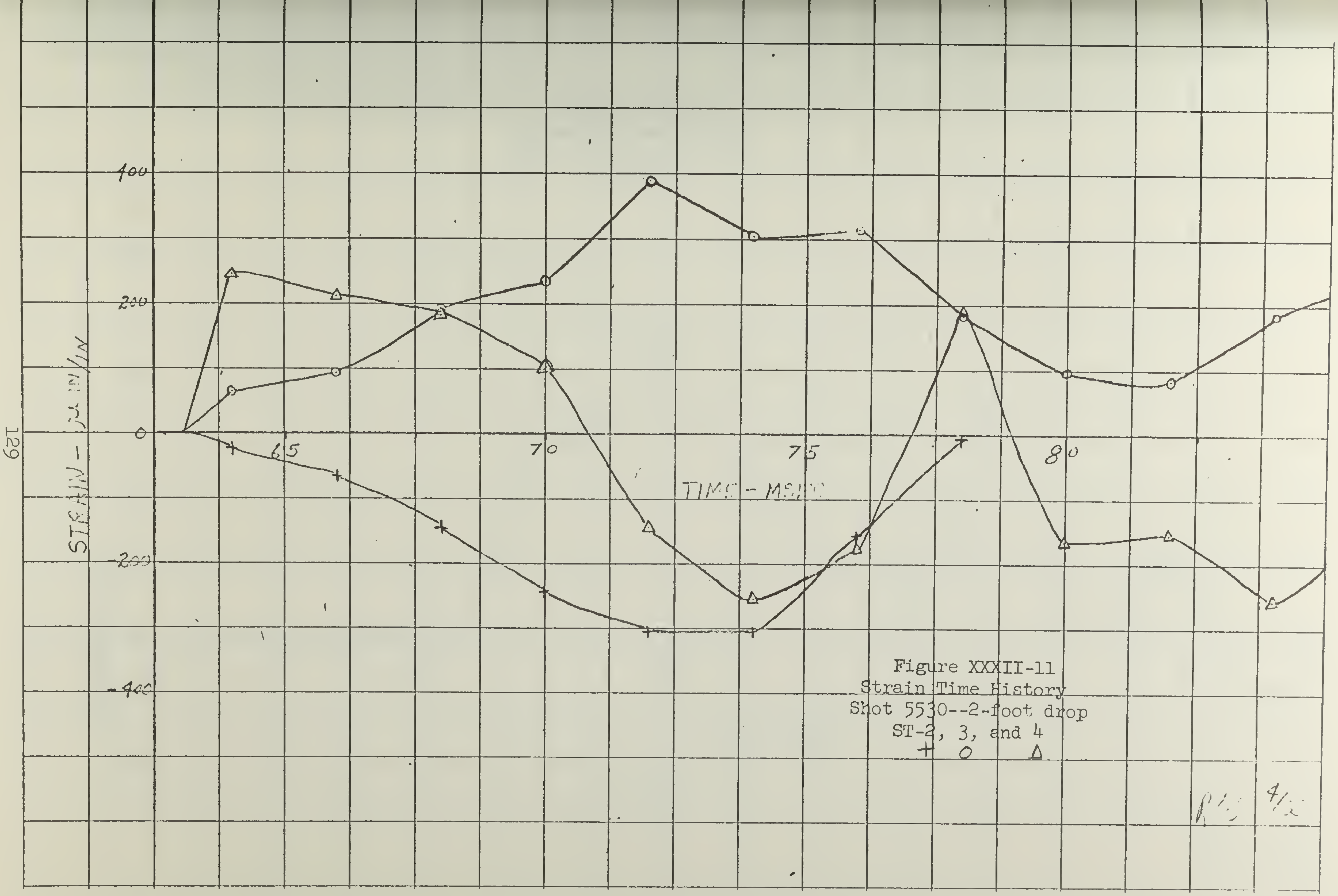

Figure XXXII-11
Strain Time History
Shot 5530--2-foot drop
ST-2, 3, and 4
+ O Δ

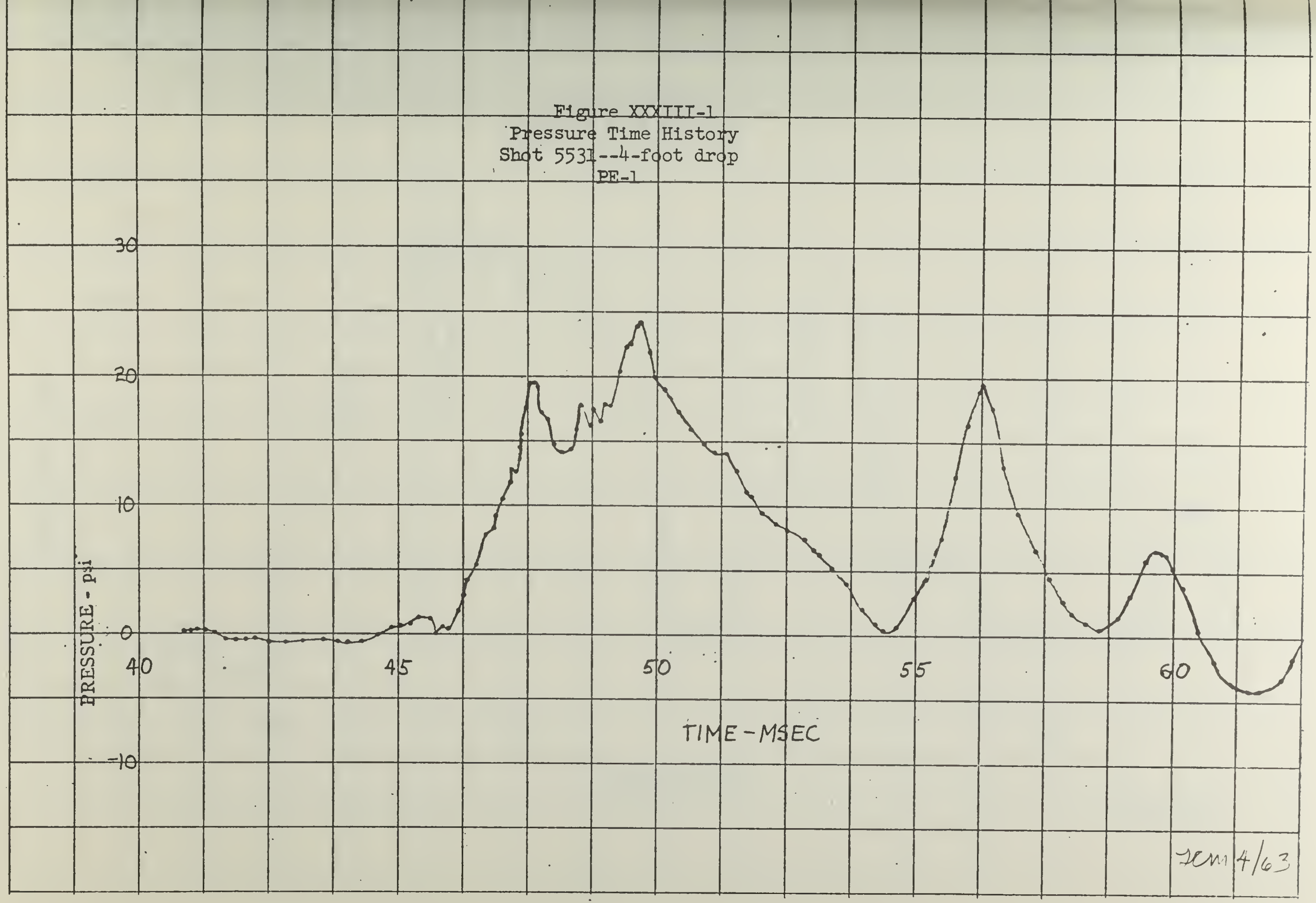

Figure XXXIII-1
Pressure Time History
Shot 5531--4-foot drop
PE-1

Figure XXXIII-2
Pressure Time History
Shot 5531--4-foot drop
PE-2

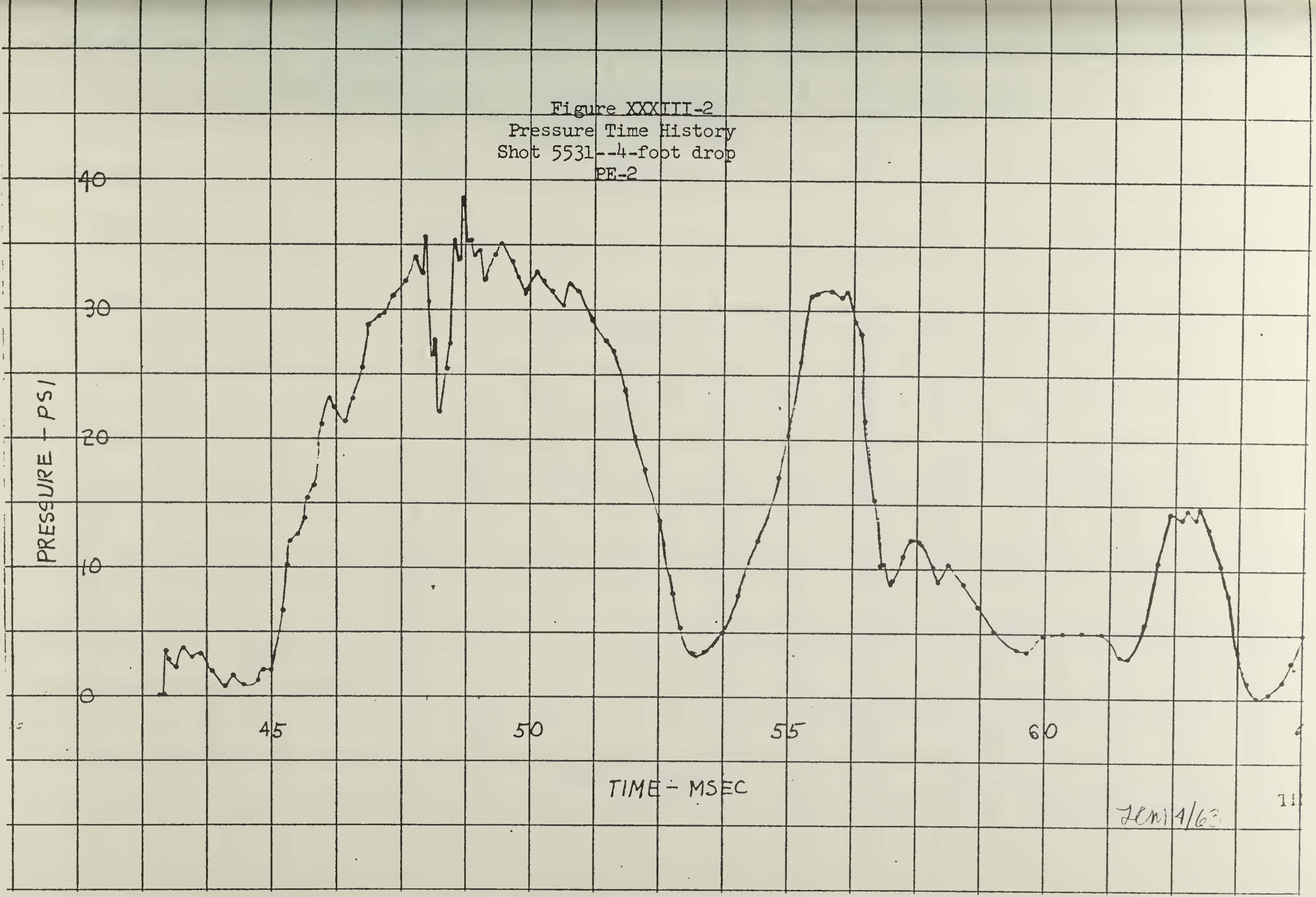

Figure XXXIII-3
Pressure Time History
Shot 5531--4-foot drop
PE-3

Figure XXXIII-4
Pressure Time History
Shot 5531--4-foot drop
PE-4

Figure XXXIII-5
Pressure Time History
Shot 5531--4-foot drop
PE-5

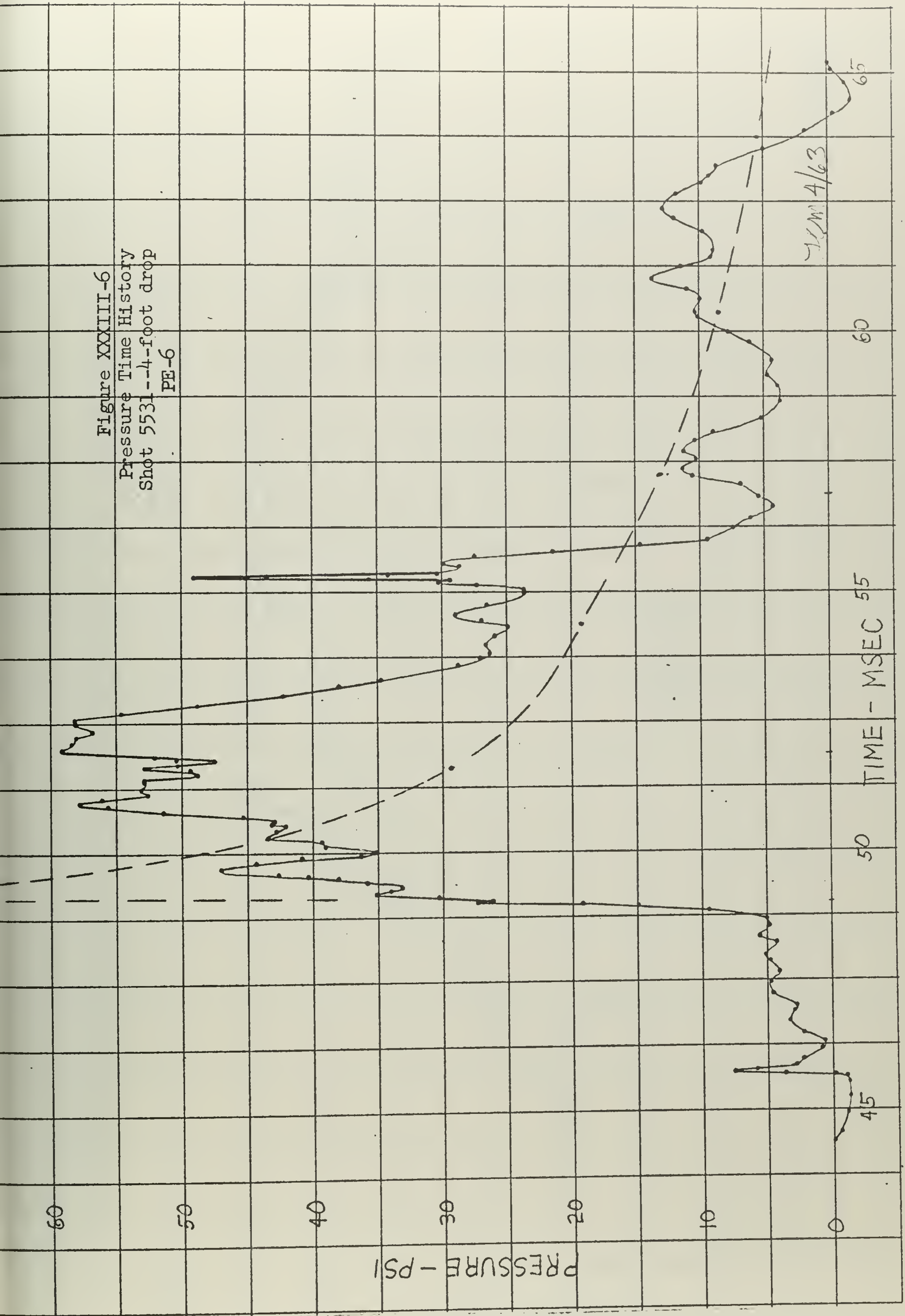

Figure XXXIII-6
Pressure Time History
Shot 5531--4-foot drop
PE-6

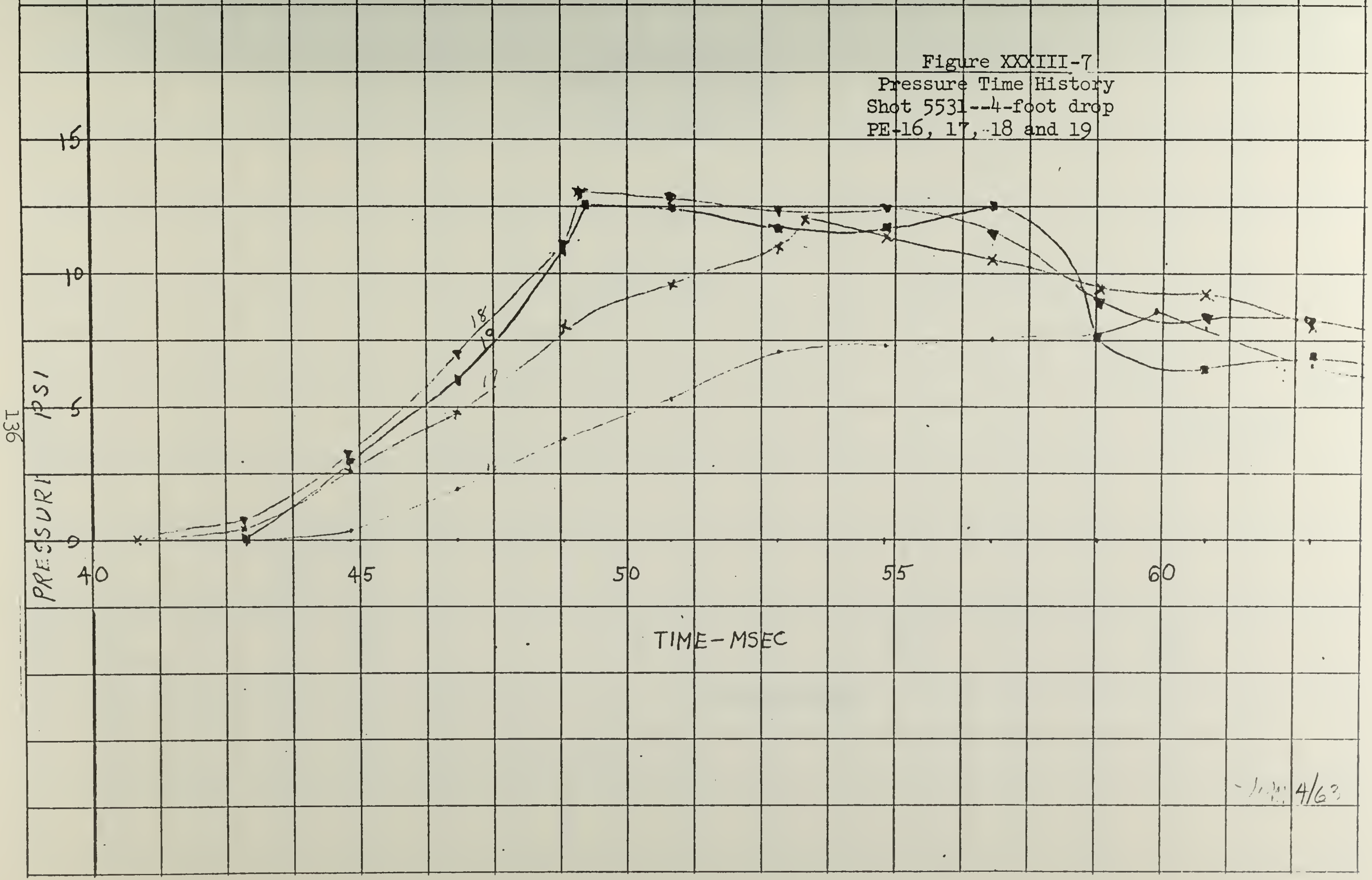

Figure XXXIII-7
Pressure Time History
Shot 5531--4-foot drop
PE-16, 17, 18 and 19

4/63

Figure XXXIII-8
Pressure Time History
Shot 5531--4-foot drop
PE-15 and 20

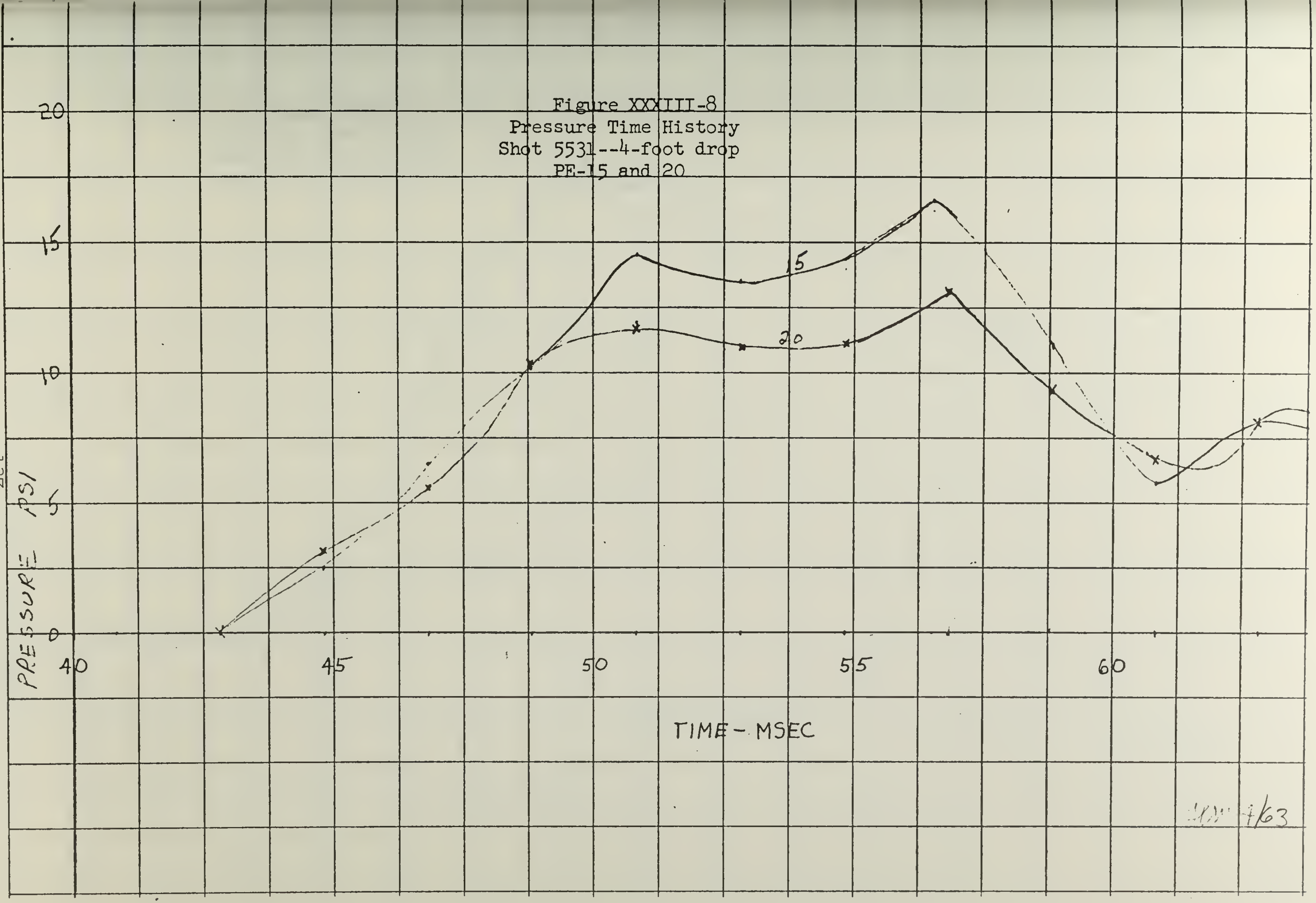

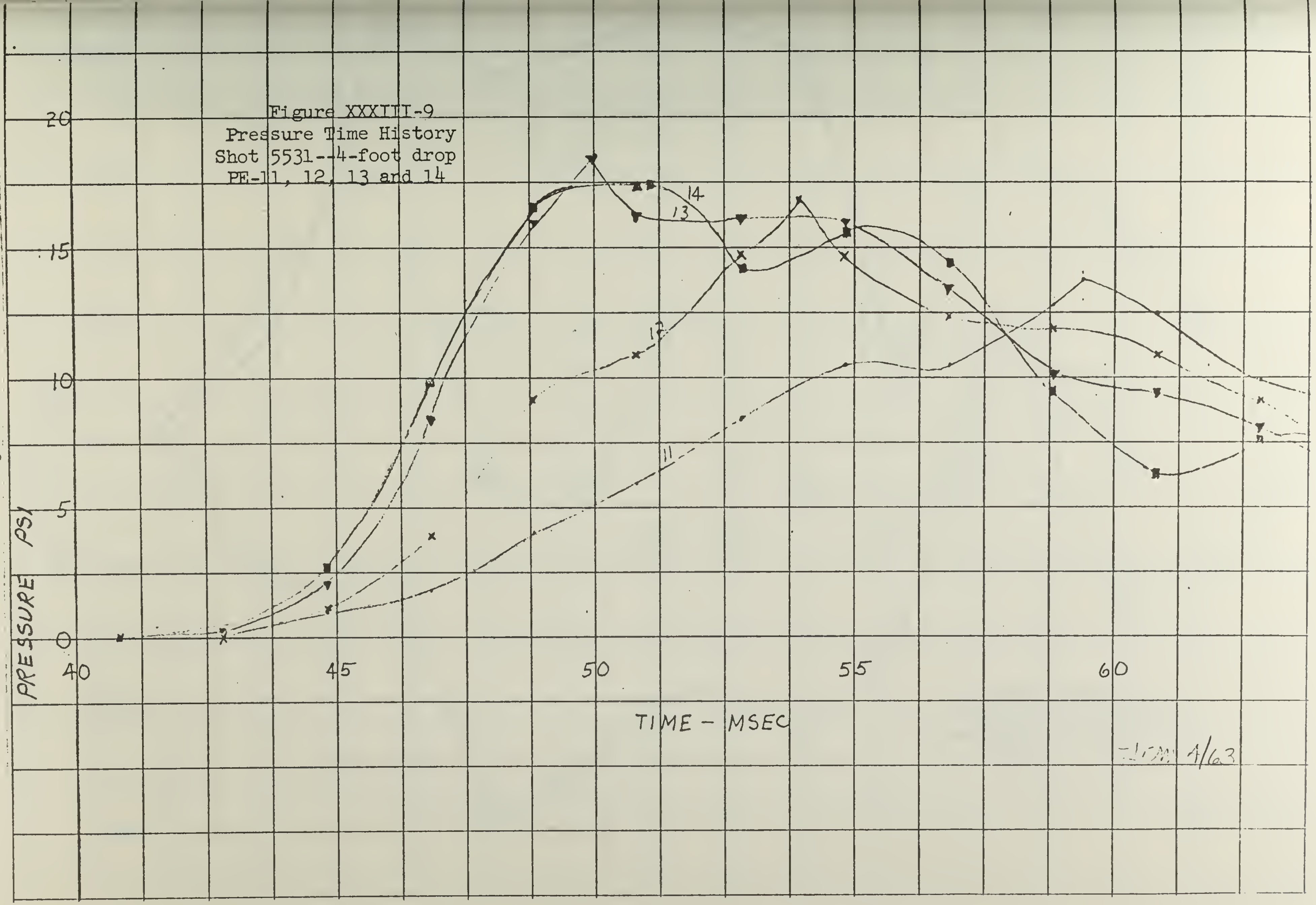

Figure XXXIII-9
Pressure Time History
Shot 5531--4-foot drop
PE-11, 12, 13 and 14

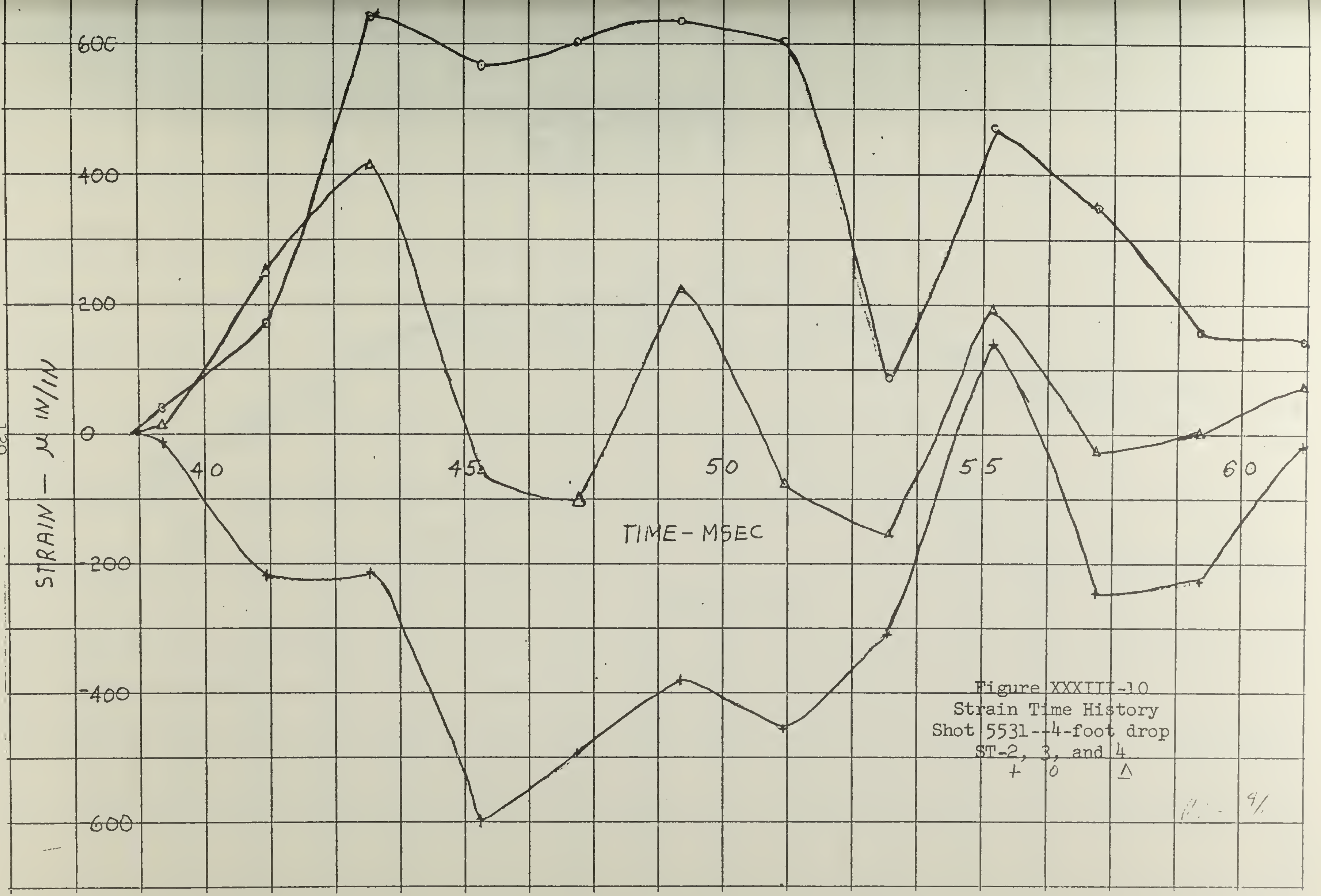

Figure XXXIII-10
Strain Time History
Shot 5531--4-foot drop
ST-2, 3, and 4
+ o Δ

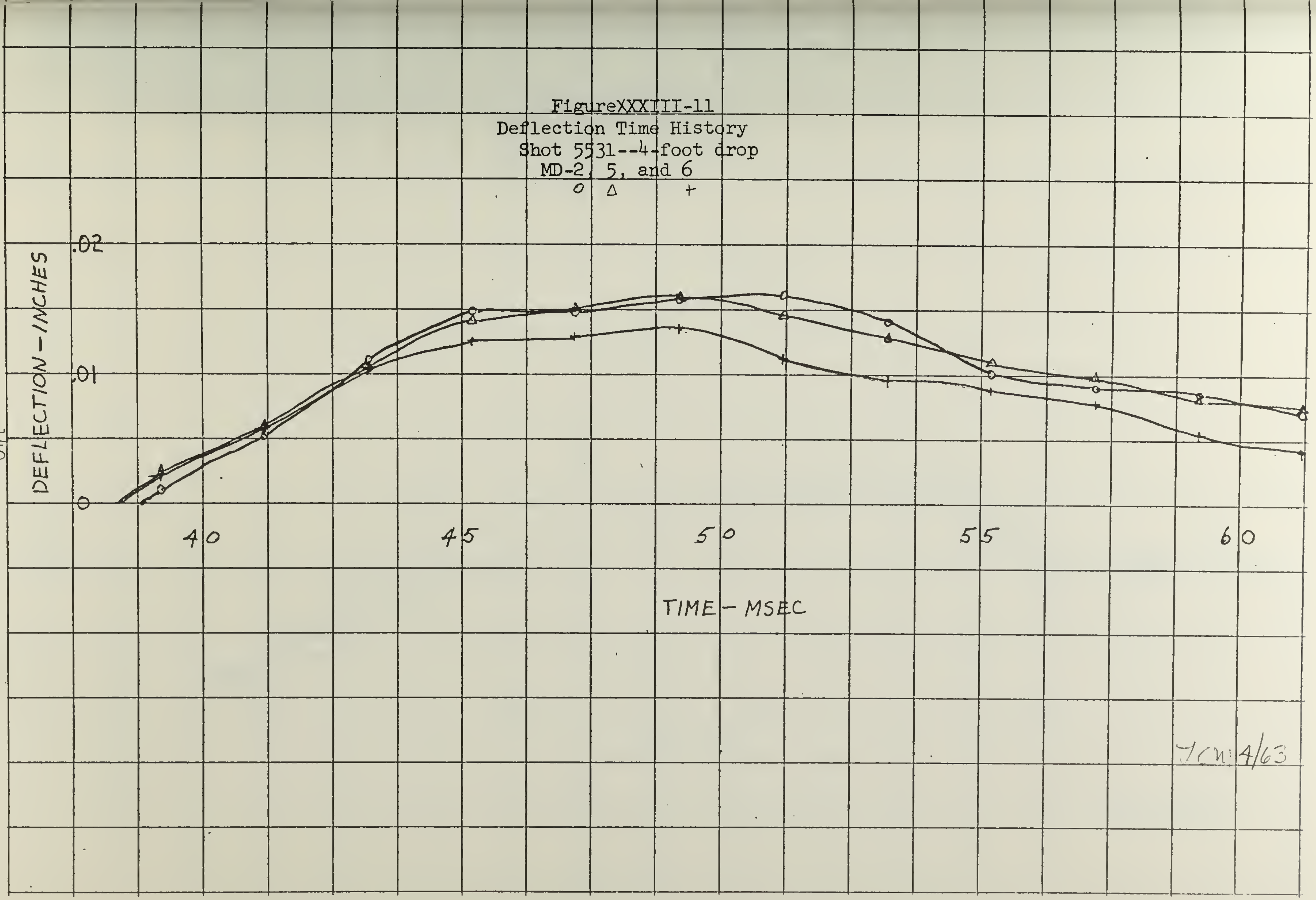

FigureXXXIII-11
Deflection Time History
Shot 5531--4-foot drop
MD-2, 5, and 6

JCN 4/63

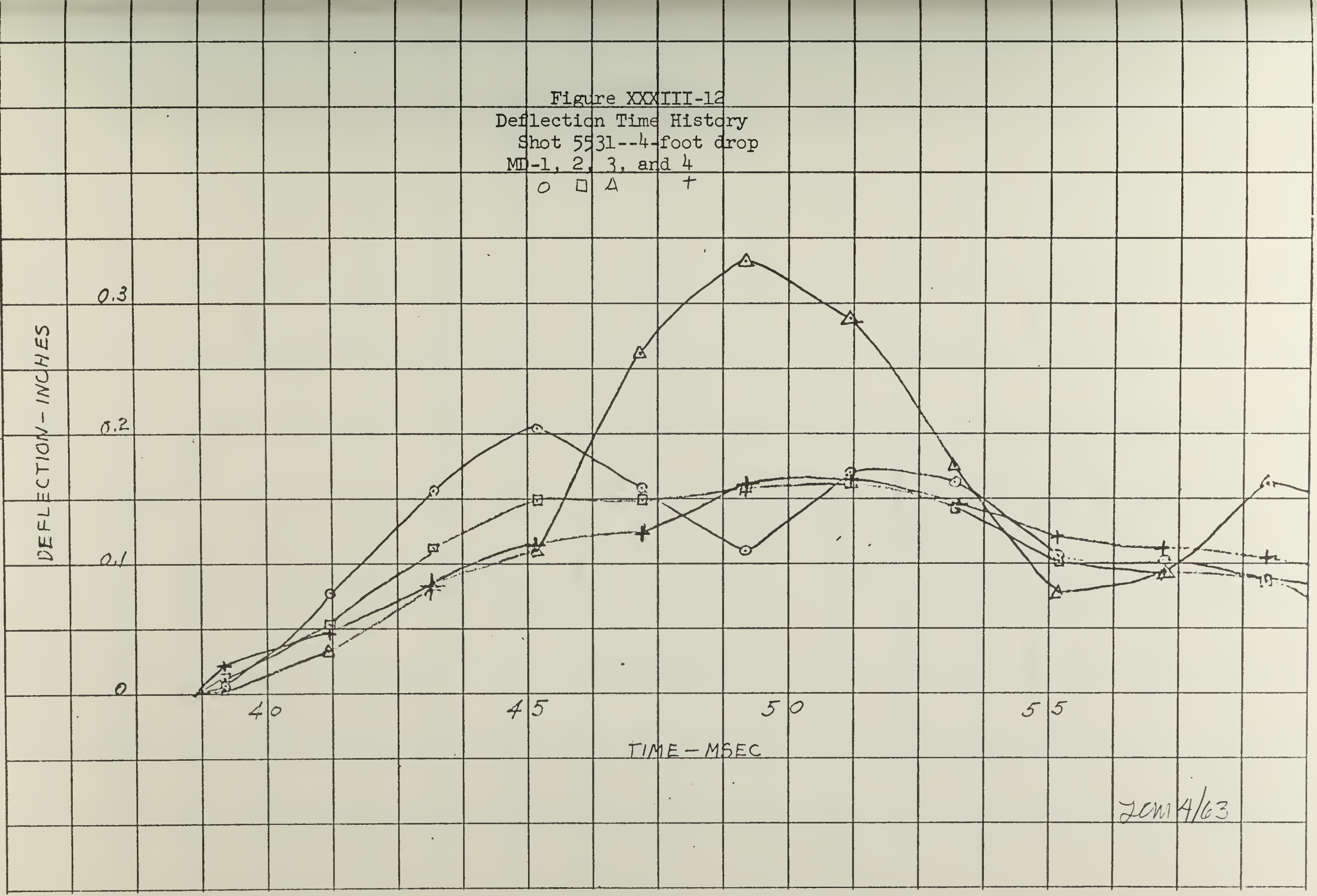

Figure XXXIII-12
Deflection Time History
Shot 5531--4-foot drop
MD-1, 2, 3, and 4

JCM 4/63


Figure XXXIV-1
Pressure Time History
Shot 5545-No. 2 at 4 feet
PE-1

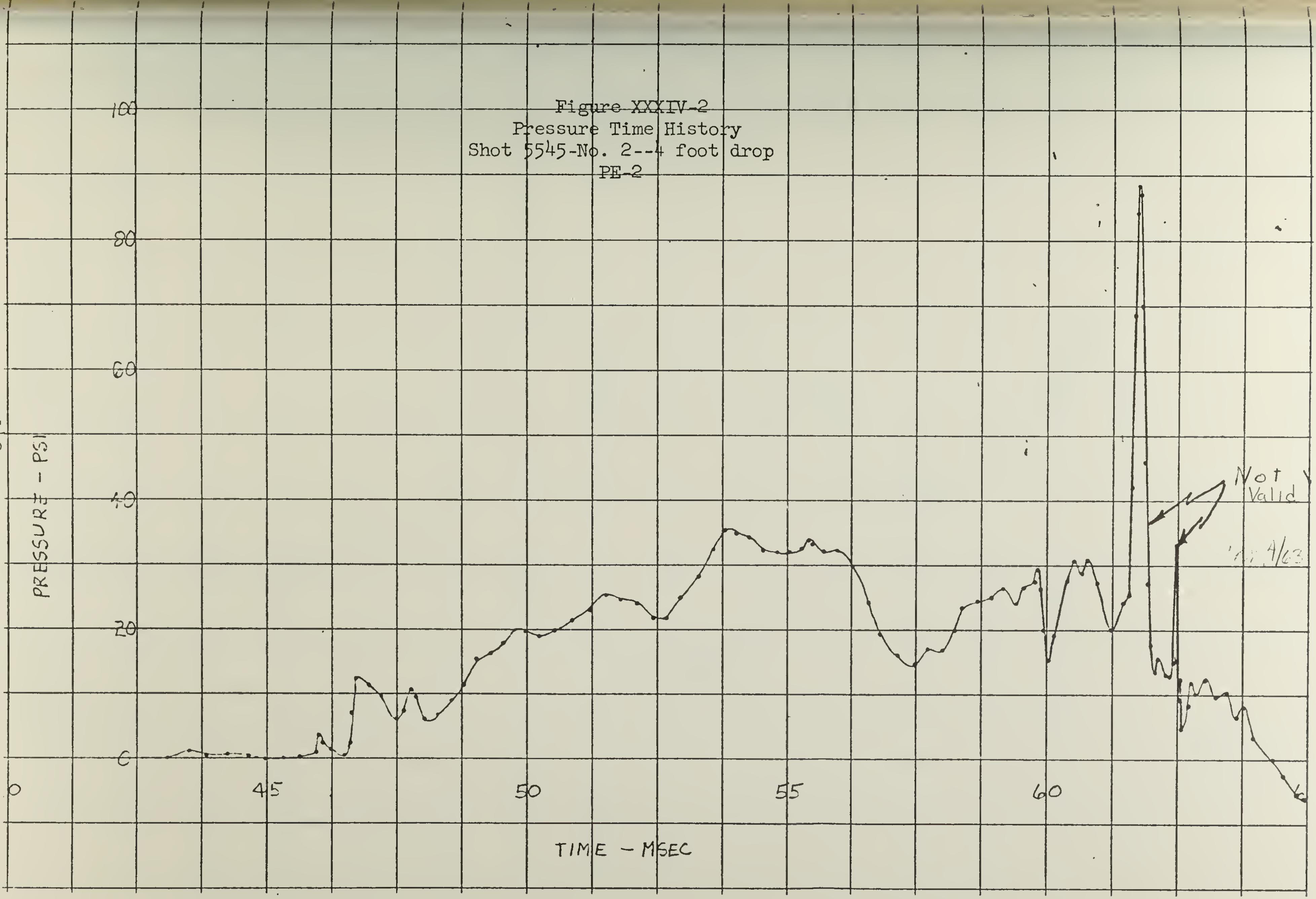

Figure XXXIV-2
Pressure Time History
Shot 5545-No. 2--4 foot drop
PE-2

Figure XXXIV-3
Pressure Time History
Shot 5545-No. 2--4-foot drop
PE-3

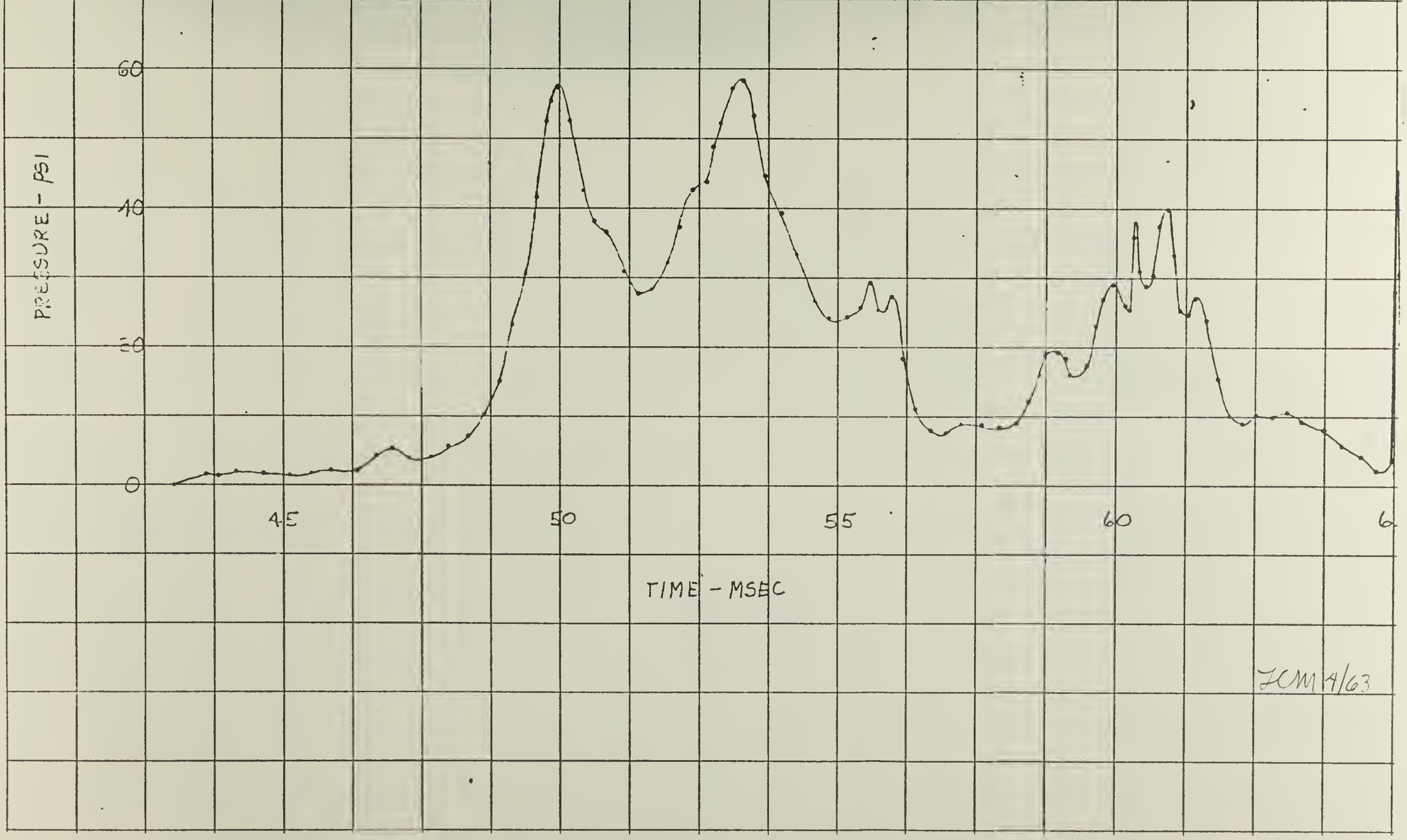

Figure XXXIV-4

Pressure Time History
Shot 5545-No. 2--4-foot drop
PE-4

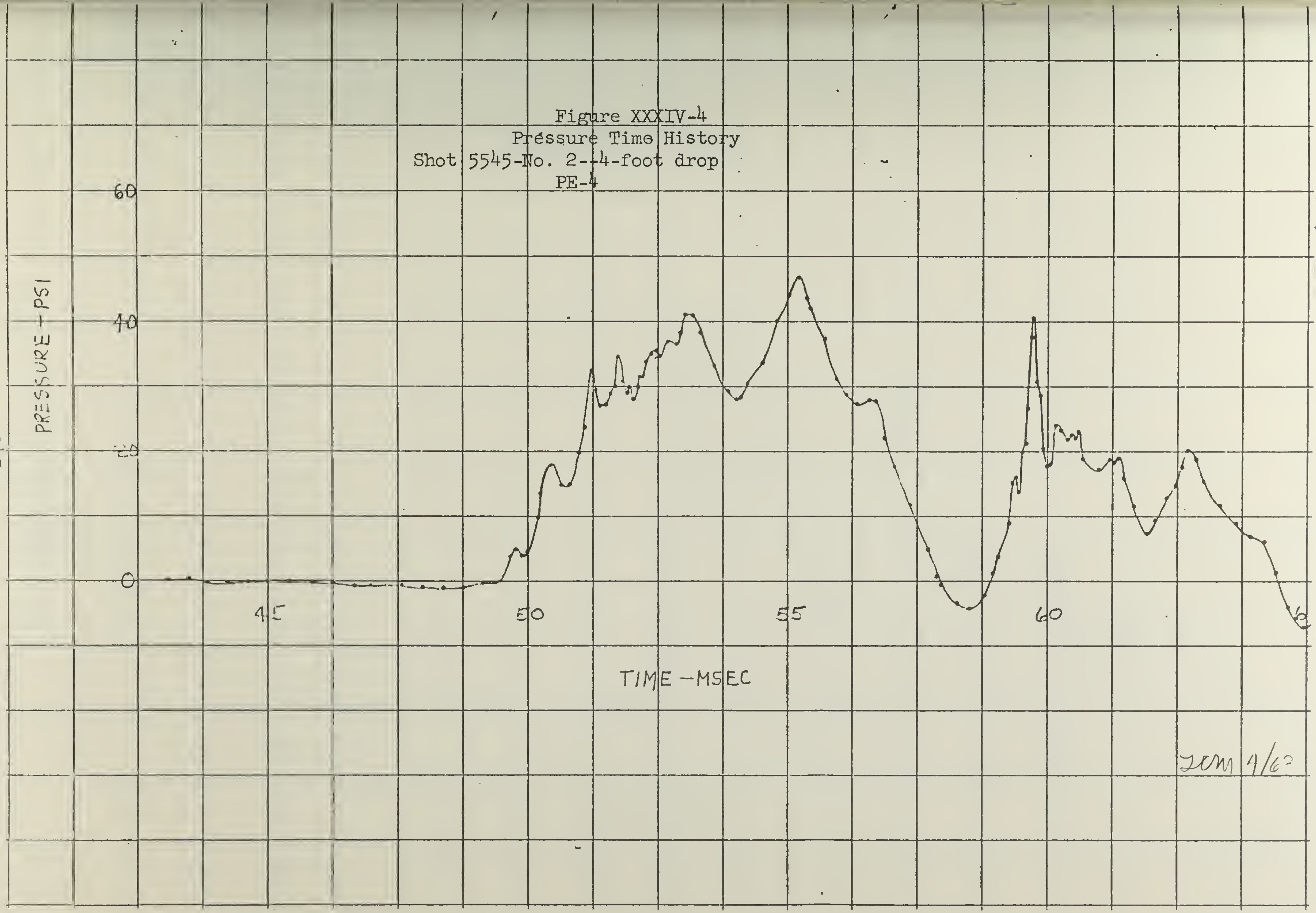

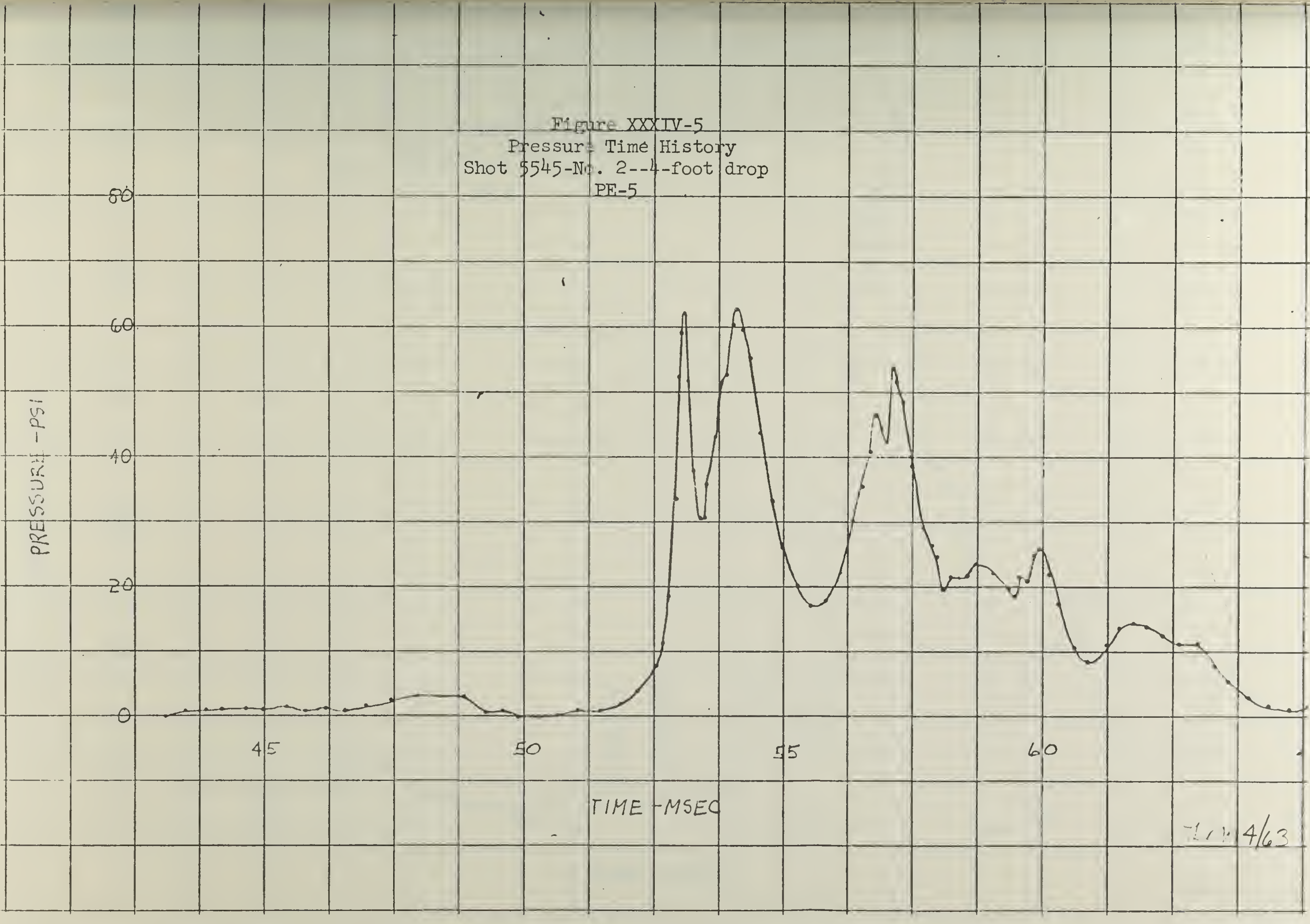

Figure XXXIV-5
Pressure Time History
Shot 5545-No. 2--4-foot drop
PE-5

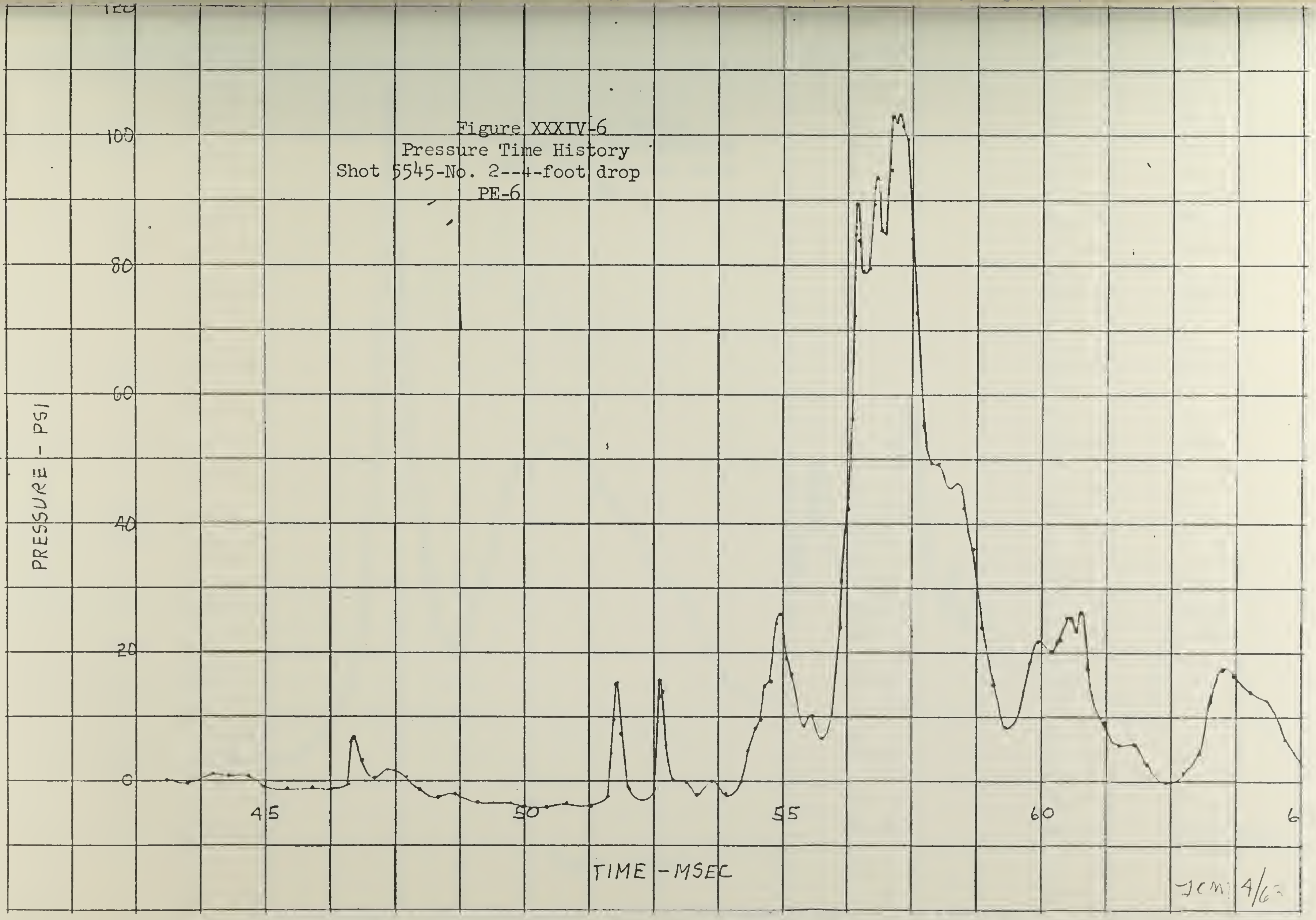

Figure XXXIV-6
Pressure Time History
Shot 5545-No. 2--4-foot drop
PE-6

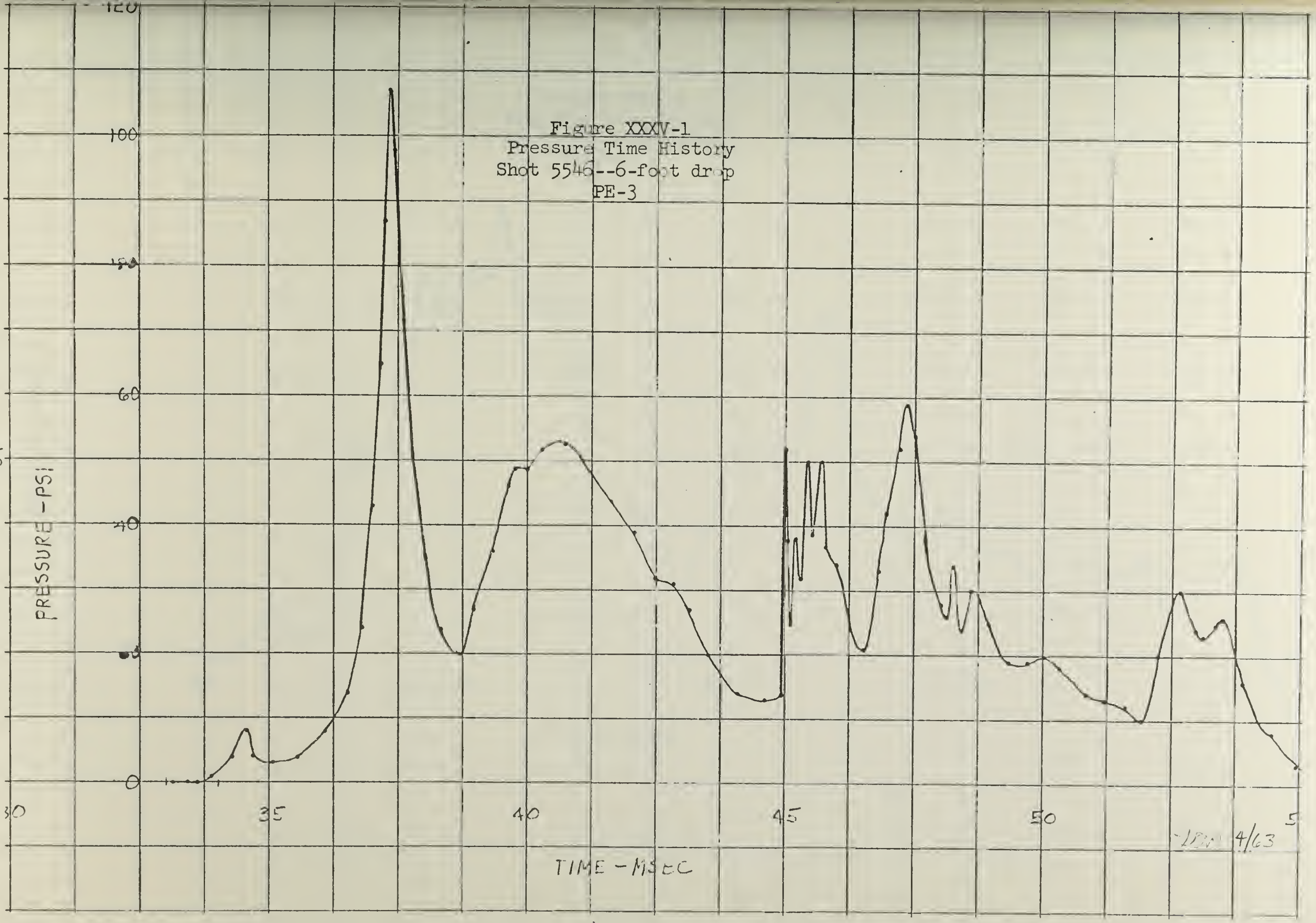

Figure XXXV-1
Pressure Time History
Shot 5546--6-foot drop
PE-3

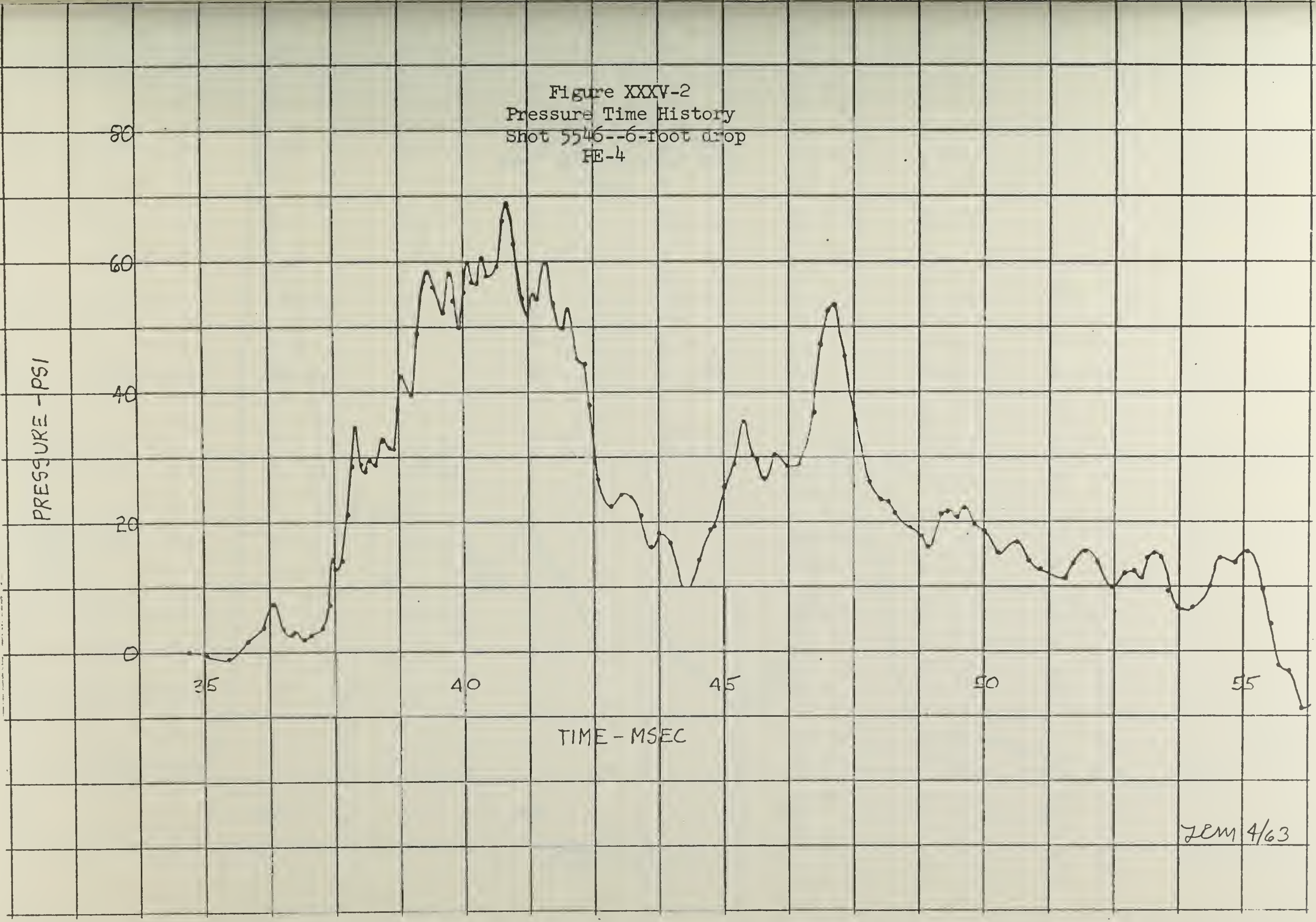

Figure XXXV-2
Pressure Time History
Shot 5546--6-foot drop
PE-4

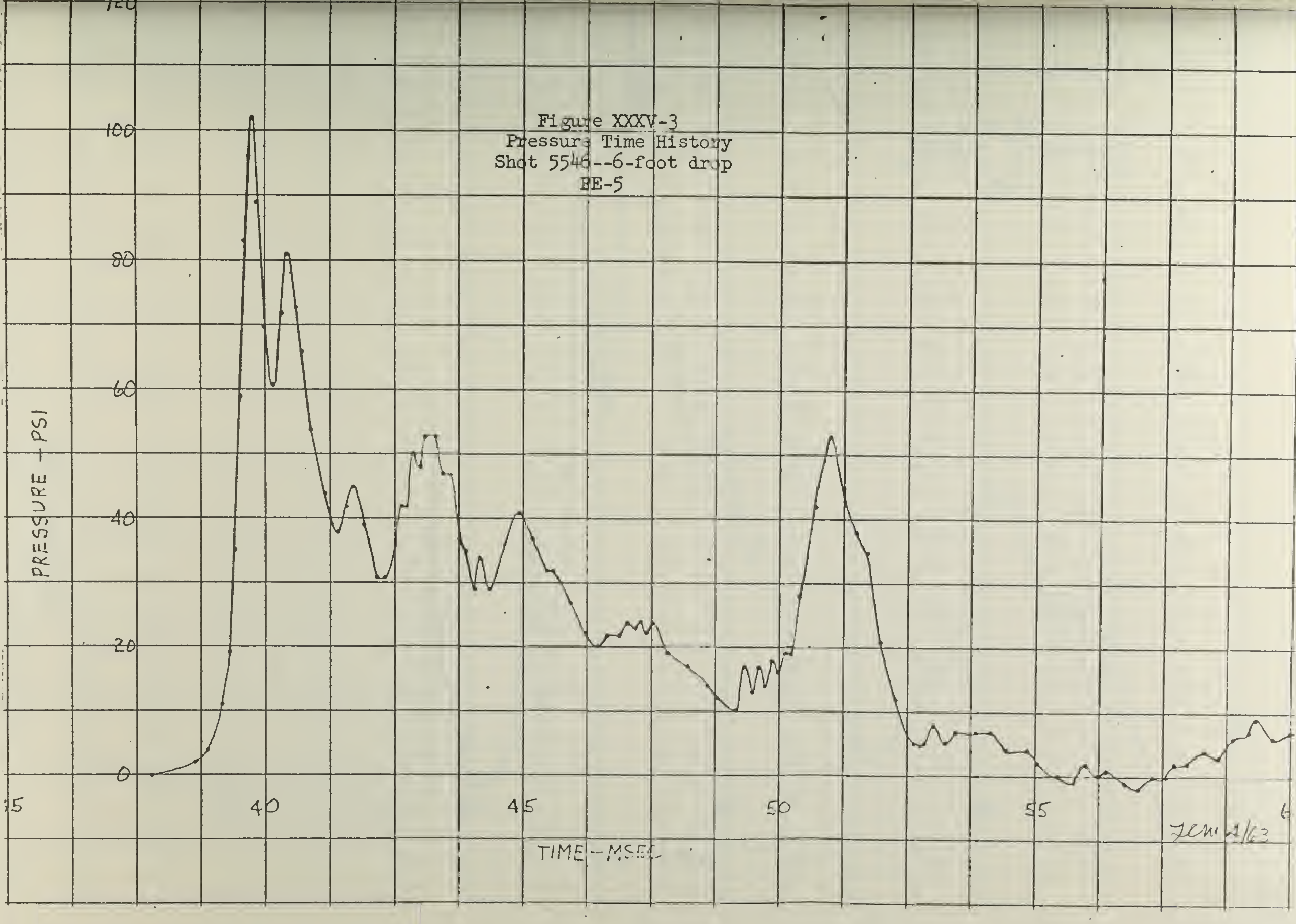

Figure XXXV-3
Pressure Time History
Shot 5546--6-foot drop
BE-5

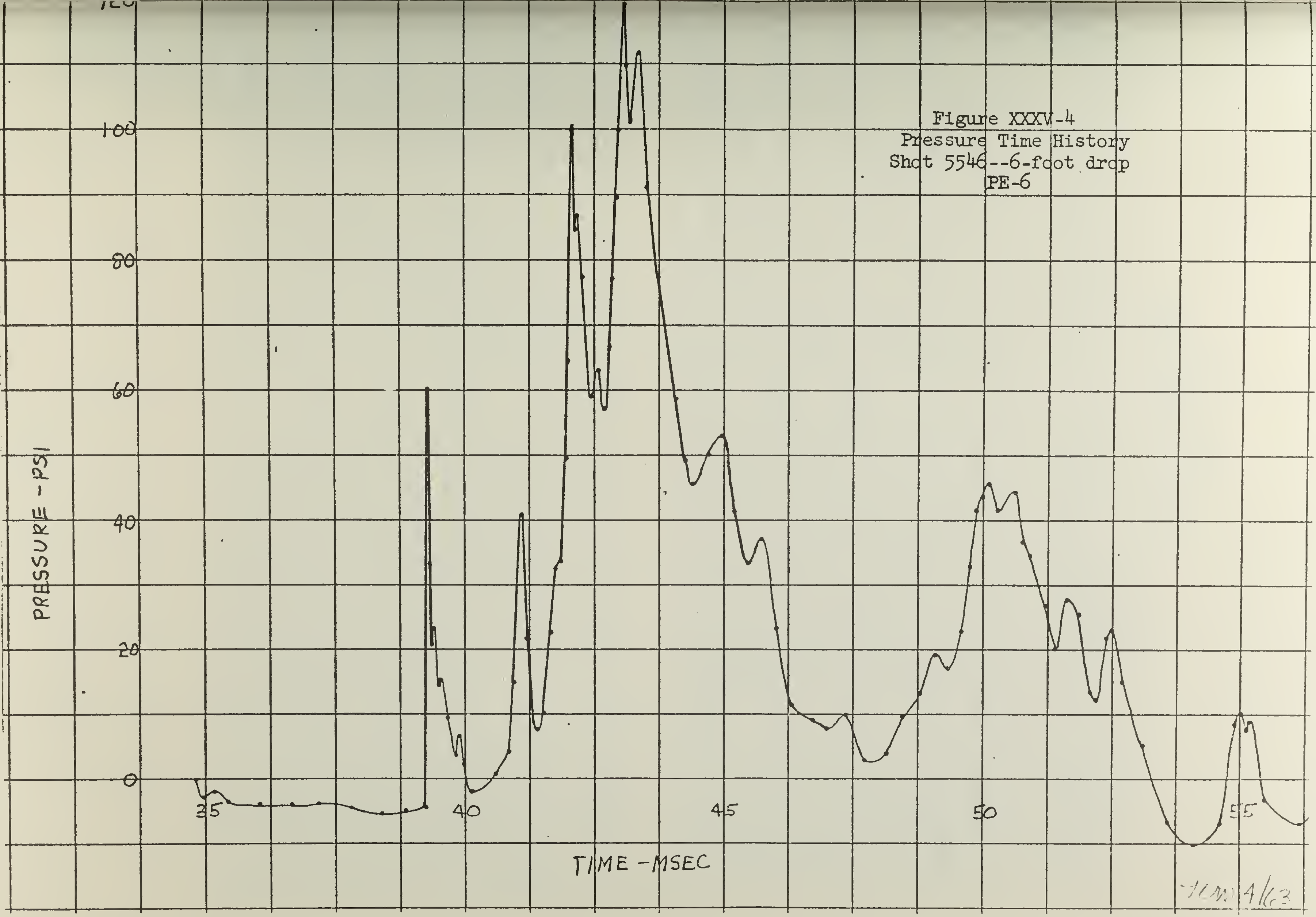

Figure XXXV-4
Pressure Time History
Shot 5546--6-foot drop
PE-6

Figure XXXVI--1

Damage Offsets, Model A

	4½ PORT			4 PORT		3½ PORT			3 PORT		2½ PORT		
HOT#	—	5533	5534	5533	5534	—	5533	5534	5533	5534	—	5533	5534
H(ft)	0	8	25	8	25	0	8	25	8	25	0	8	25
A	0	0	0	0	0	0	0	0	0	0	0	0	0
B	0	0.026	0.245	0.013	0.248	-.031	0.008	0.568	0.024	0.326	0.016	0.083	0.713
C	0	0.058	0.410	0.059	0.406	0	0.049	0.686	0.051	0.742	0	0.095	0.856
D	0	0.095	0.525	0.089	1.254	0	0.156	1.704	0.127	1.478	0.047	0.242	2.039
E	0	0.108	0.960	0.170	1.822	0	0.171	2.002	0.228	2.094	0	0.238	2.252
F	0.016	0.137	1.455	0.207	2.070	0.188	0.300	2.540	0.242	2.640	0.156	0.405	3.095
G	0	0.116	1.220	0.203	1.838	0	0.239	2.028	0.256	2.206	0	0.271	2.358
H	0.031	0.125	1.175	0.217	1.386	0.063	0.261	2.184	0.208	2.072	0.094	0.275	2.141
J	0	0.085	1.380	0.089	0.494	0	0.089	0.694	0.104	0.868	0	0.107	0.984
K	0.047	0.101	0.395	0.053	0.192	0.047	0.063	0.732	0.061	0.454	0.016	0.120	0.817
L	0	0	0	0	0	0	0	0	0	0	0	0	0
	4½ STBD			4 STBD		3½ STBD			3 STBD		2½ STBD		
A	0	0	0	0	0	0	0	0	0	0	0	0	0
B	-.016	0.006	0.163	0.080	0.215	0	0.063	0.632	0.046	0.319	0.016	0.101	0.705
C	0	0.067	0.116	0.031	0.380	0	0.054	0.744	0.076	0.712	0	0.089	0.850
D	0	0.083	0.339	0.059	1.165	0.047	0.179	2.456	0.178	1.438	0.063	0.235	2.045
E	0	0.102	0.422	0.078	1.560	0	0.220	1.828	0.224	2.034	0	0.246	2.200
F	0.031	0.112	0.375	0.133	1.875	0.047	0.309	2.480	0.321	2.660	0.125	0.373	3.035
G	0	0.122	0.398	0.123	1.740	0	0.197	2.962	0.229	2.176	0	0.216	2.390
H	0.031	0.069	0.322	0.064	1.305	0.047	0.194	1.794	0.143	1.542	0.078	0.235	2.155
J	0	0.039	0.104	0.028	0.500	0	0.070	1.116	0.062	0.798	0	0.055	0.930
K	-.031	0.214	0.187	0.026	0.265	0	0.025	1.528	0.042	0.374	0.016	0.075	0.765
L	0	0	0	0	0	0	0	0	0	0	0	0	0

Figure XXXVI--2

Damage Offsets, Model A

	2 PORT		1½ PORT			1 PORT		½ PORT			KEEL
SHOT#	5533	5534	—	5533	5534	5533	5534	—	5533	5534	5534
H(ft)	8	25	0	8	25	8	25	0	8	25	25
A	0	0	0	0	0	0	0	0	0	0	0
B	0.074	0.493	0	0.061	0.713	0.058	0.688	0	0.075	0.798	0.600
C	0.146	0.966	0	0.114	1.016	0.132	1.050	0	0.120	1.016	1.200
D	0.181	1.759	0.047	0.271	2.039	0.173	1.793	-.078	0.210	1.814	1.750
E	0.295	2.342	0	0.260	2.272	0.261	2.275	0	0.234	2.172	2.120
F	0.332	2.955	0.156	0.419	3.365	0.288	2.938	0.156	0.245	3.040	2.600
G	0.332	1.998	0	0.267	2.558	0.288	2.400	0	0.235	2.308	2.460
H	0.271	1.981	0.094	0.318	2.291	0.217	1.863	0.078	0.201	1.946	1.880
J	0.148	0.974	0	0.094	1.084	0.110	1.155	0	0.120	1.134	1.240
K	0.106	0.607	0.031	0.082	0.867	0.073	0.568	0.016	0.099	0.862	0.630
L	0	0	0	0	0	0	0	0	0	0	0
	2 STBD		1½ STBD			1 STBD		½ STBD			
A	0	0	0	0	0	0	0	0	0	0	0
B	0.044	0.435	0.060	0.095	0.391	0.084	0.792	0.047	0.080	0.592	
C	0.109	0.980	0	0.099	0.871	0.120	1.024	0	0.125	1.002	
D	0.156	1.705	0.109	0.264	1.549	0.147	1.666	0.109	0.218	1.936	
E	0.235	2.310	0	0.214	2.071	0.241	2.328	0	0.228	2.188	
F	0.261	2.955	0.156	0.391	2.694	0.272	2.930	0.156	0.247	3.190	
G	0.231	2.510	0	0.230	2.279	0.253	2.052	0	0.216	2.402	
H	0.131	1.895	0.094	0.294	1.764	0.189	1.984	0.109	0.231	2.194	
J	0.075	1.030	0	0.052	0.955	0.113	1.126	0	0.113	1.126	
K	0.037	0.505	0.016	-.030	0.468	0.110	0.508	0.016	0.049	1.088	
L	0	0	0	0	0	0	0	0	0	0	0

Figure XXXVII-1

Damage Offsets, Model B

	4½ PORT						4 PORT					
SHOT #	—	5546	5549	5550	5551	5553	—	5546	5549	5550	5551	5553
H (ft)	0	6	12-A	12-B	12-C	12-D	0	6	12-A	12-B	12-C	12-D
A	0	0	0	0	0	0	0	0	0	0	0	0
B	0.125	0.100	0.125	0.150	0.175	0.200	0.040	0.010	0.060	0.100	0.100	0.100
C	0.050	0.050	0.175	0.100	0.100	0.110	0.050	0.040	0.125	0.150	0.200	0.200
D	0.140	0.140	0.240	0.325	0.350	0.490	0.050	0.055	0.240	0.400	0.500	0.700
E	0.140	0.050	0.175	0.240	0.340	0.500	0.050	0.060	0.340	0.525	0.750	1.000
F	0.100	0.100	0.260	0.325	0.425	0.620	0.050	0.100	0.400	0.625	0.950	1.200
G	0.070	0.060	0.175	0.255	0.360	0.450	0.050	0.050	0.325	0.525	0.800	1.075
H	0.100	0.100	0.200	0.300	0.360	0.400	0.050	0.050	0.275	0.425	0.575	0.740
J	0.040	0.040	0.100	0.175	0.100	0.100	0.050	0.050	0.140	0.125	0.175	0.200
K	0.100	0.100	0.150	0.175	0.200	0.175	0.050	0.050	0.075	0.125	0.150	0.125
L	0	0	0	0	0	0	0	0	0	0	0	0
	4½ STBD						4 STBD					
A	0	0	0	0	0	0	0	0	0	0	0	0
B	0.140	0.110	0.125	0.125	0.150	0.150	0.050	0.075	0.050	0.060	0.075	0.050
C	0.090	0.100	0.175	0.100	0.125	0.100	0.010	0.075	0.050	0.100	0.100	0.100
D	0.100	0.110	0.150	0.200	0.300	0.300	0.025	0.075	0.250	0.425	0.600	0.650
E	0.010	0.050	0.125	0.200	0.300	0.300	-.025	0	0.325	0.600	0.825	0.900
F	-.010	0	0.125	0.240	0.300	0.350	-.100	-.040	0.350	0.725	1.000	1.050
G	0	0.025	0.150	0.250	0.250	0.300	-.040	0	0.325	0.650	0.900	0.975
H	0.025	0.025	0.125	0.200	0.250	0.300	0	0.010	0.210	0.450	0.650	0.700
J	0.025	0.010	0.050	0.075	0.050	0.100	0	0	0.050	0.125	0.125	0.125
K	0.090	0.075	0.100	0.125	0.100	0.100	0.050	0.030	0.060	0.140	0.100	0.100
L	0	0	0	0	0	0	0	0	0	0	0	0

Figure XXXVII--2

Damage Offsets, Model B

	3½ PORT						3 PORT					
SHOT#	—	5546	5549	5550	5551	5553	—	5546	5549	5550	5551	5553
H(ft)	0	6	12-A	12-B	12-C	12-D	0	6	12-A	12-B	12-C	12-D
A	0	0	0	0	0	0	0	0	0	0	0	0
B	0	0	0.200	0.275	0.250	0.375	-.025	0	0.050	0.100	0.160	0.100
C	0	0	0.075	0.150	0.150	0.225	0	0	0.100	0.150	0.200	0.200
D	0	0.075	0.440	0.600	0.750	0.975	0	0.040	0.275	0.390	0.500	0.700
E	0	0.050	0.310	0.550	0.750	1.025	0	0.040	0.360	0.575	0.800	1.050
F	0	0.075	0.525	0.825	1.100	1.425	0	0.025	0.425	0.690	1.000	1.250
G	0	0.015	0.300	0.560	0.750	1.000	-.025	0.025	0.350	0.600	0.750	1.000
H	-.025	0	0.410	0.600	0.750	0.925	-.025	0	0.225	0.350	0.490	0.600
J	0	0	0.100	0.150	0.150	0.200	0.025	0.025	0.125	0.175	0.200	0.250
K	0.025	0.050	0.200	0.275	0.275	0.350	0.025	0.025	0.075	0.100	0.100	0.100
L	0	0	0	0	0	0	0	0	0	0	0	0
	3½ STBD						3 STBD					
A	0	0	0	0	0	0	0	0	0	0	0	0
B	0	0.050	0.075	0.100	0.125	0.125	0	0.050	0.050	0.075	0.100	0.100
C	-.010	0.025	0.050	0.100	0.150	0.125	0	0.025	0.075	0.125	0.175	0.150
D	0	0.025	0.375	0.550	0.725	0.775	-.050	0	0.200	0.350	0.490	0.525
E	-.085	-.010	0.300	0.550	0.800	0.900	-.100	-.060	0.250	0.500	0.750	0.825
F	-.170	-.075	0.500	0.840	1.125	1.225	-.100	-.060	0.340	0.760	1.025	1.125
G	-.100	-.020	0.300	0.575	0.850	0.925	-.090	-.040	0.275	0.550	0.800	0.900
H	-.070	0	0.350	0.575	0.750	0.800	-.100	-.050	0.175	0.325	0.500	0.525
J	-.010	0.010	0.075	0.150	0.200	0.200	-.100	0	0.100	0.140	0.200	0.200
K	-.025	0	0.125	0.225	0.300	0.300	0.030	0.050	0.100	0.140	0.150	0.150
L	0	0	0	0	0	0	0	0	0	0	0	0

Figure XXXVII--3

Damage Offsets, Model B

	2½ PORT						2 PORT					
SHOT #	—	5546	5549	5550	5551	5553	—	5546	5549	5550	5551	5553
H (ft)	0	6	12-A	12-B	12-C	12-D	0	6	12-A	12-B	12-C	12-D
A	0	0	0	0	0	0	0	0	0	0	0	0
B	-.025	0	0.200	0.225	0.300	0.350	-.025	0	0	0.025	0	0.100
C	-.050	-.050	0.075	0.100	0.150	0.250	-.075	-.075	0	0.100	0.050	0.250
D	-.025	-.010	0.475	0.600	0.750	0.950	-.075	-.050	0.140	0.325	0.175	1.000
E	-.050	-.025	0.300	0.475	0.700	1.000	-.100	-.040	0.200	0.525	0.600	1.000
F	-.050	0.060	0.550	0.800	1.150	1.450	-.100	-.070	0.260	0.600	0.700	1.250
G	-.090	-.050	0.300	0.450	0.700	0.950	-.100	-.025	0.260	0.425	0.525	0.900
H	-.050	-.060	0.425	0.600	0.700	0.875	-.100	-.100	0.125	0.300	0.325	0.600
J	[illegible]	0.050	0.125	0.125	0.150	0.250	-.005	-.050	0.075	0.100	0.170	0.300
K	0.025	0	0.225	0.325	0.300	0.350	-.100	-.020	0.075	0.100	0.075	0.100
L	0	0	0	0	0	0	0	0	0	0	0	0
	2½ STBD						2 STBD					
A	0	0	0	0	0	0	0	0	0	0	0	0
B	0	0.025	0	0.150	0.200	0.225	0	0.010	0	0.050	0.075	0.075
C	-.050	0	0.025	0.100	0.125	0.150	-.050	-.060	0	0.075	0.125	0.125
D	-.025	0.025	0.300	0.500	0.650	0.700	-.050	-.050	0.125	0.275	0.400	0.450
E	-.100	-.075	0.200	0.450	0.650	0.775	-.100	-.090	0.200	0.425	0.600	0.700
F	-.040	-.070	0.425	0.800	1.100	1.225	-.110	-.160	0.175	0.525	0.825	0.975
G	-.100	-.075	0.240	0.500	0.725	0.850	-.115	-.075	0.200	0.460	0.700	0.775
H	-.100	0.025	0.375	0.560	0.700	0.775	-.090	-.060	0.150	0.300	0.400	0.500
J	-.010	0	0.050	0.140	0.175	0.200	-.050	-.050	0.050	0.125	0.125	0.150
K	0.050	0.050	0.225	0.300	0.300	0.300	-.025	-.025	0	0.060	0.025	0.050
L	0	0	0	0	0	0	0	0	0	0	0	0

Figure XXXVII--4

Damage Offsets, Model B

	1½ PORT						1 PORT					
SHOT#	—	5546	5549	5550	5551	5553	—	5546	5549	5550	5551	5553
H(ft)	0	6	12-A	12-B	12-C	12-D	0	6	12-A	12-B	12-C	12-D
A	0	0	0	0	0	0	0	0	0	0	0	0
B	0	0.025	0.075	0.140	0.200	0.200	0	0	0.025	0.075	0.100	0.100
C	-.075	-.060	0.050	0.125	0.150	0.200	-.075	-.075	0.025	0.140	0.175	0.250
D	-.050	0	0.500	0.575	0.800	0.950	-.106	-.090	0.140	0.275	0.375	0.450
E	-.090	-.050	0.300	0.500	0.650	0.725	-.085	-.050	0.225	0.400	0.500	0.625
F	0	0.100	0.700	1.025	1.250	1.475	-.090	-.050	0.260	0.440	0.625	0.725
G	-.100	-.075	0.300	0.500	0.675	0.750	-.100	0	0.200	0.350	0.500	0.600
H	-.070	0.025	0.525	0.700	0.800	0.950	-.100	-.075	0.125	0.275	0.350	0.425
J	0	-.025	0.075	0.150	0.375	0.250	-.010	0	0.125	0.200	0.250	0.275
K	0.050	0.040	0.200	0.250	0.450	0.300	-.010	0	0.025	0.050	0.100	0.100
L	0	0	0	0	0	0	0	0	0	0	0	0
	1½ STBD						1 PORT					
A	0	0	0	0	0	0	0	0	0	0	0	0
B	0	0.025	0.025	0.060	0.075	0.100	0	0	0.025	0.050	0.050	0.100
C	-.090	-.090	0.025	0.060	0.125	0.150	-.050	-.050	0.025	0.100	0.150	0.200
D	-.100	-.050	0.300	0.440	0.600	0.650	-.075	-.100	0.100	0.200	0.300	0.375
E	-.100	-.075	0.150	0.350	0.575	0.700	-.075	-.075	0.200	0.375	0.525	0.650
F	-.125	-.075	0.425	0.675	1.025	1.175	-.150	-.150	0.125	0.350	0.575	0.750
G	-.120	-.125	0.200	0.400	0.650	0.750	-.140	-.140	0.125	0.340	0.525	0.650
H	-.100	-.075	0.250	0.450	0.625	0.700	-.100	-.100	0.100	0.250	0.325	0.425
J	-.090	-.075	0.125	0.050	0.150	0.200	-.075	-.075	0.040	0.125	0.200	0.200
K	0	0	0.050	0.150	0.200	0.200	-.050	-.025	0	0.050	0.050	0.050
L	0	0	0	0	0	0	0	0	0	0	0	0

Figure XXXVII--5

Damage Offsets, Model B

	½ PORT						KEEL					
SHOT#	—	5546	5549	5550	5551	5553	—	5546	5549	5550	5551	5553
H (ft)	0	6	12-A	12-B	12-C	12-D	0	6	12-A	12-B	12-C	12-D
A	0	0	0	0	0	0	0	0	0	0	0	0
B	-.090	-.050	0	0.050	0.050	0.100	0	0.010	0.040	0.100	0.125	0.125
C	-.100	-.100	0	0.100	0.100	0.200	-.025	0	0.100	0.200	0.200	0.250
D	-.090	-.070	0.200	0.400	0.500	0.600	-.025	-.025	0.140	0.250	0.350	0.400
E	-.100	-.100	0.125	0.275	0.400	0.500	0	0.025	0.300	0.440	0.500	0.625
F	-.100	-.050	0.375	0.600	0.800	1.000	0	0.025	0.300	0.450	0.625	0.700
G	-.075	-.050	0.175	0.325	0.500	0.550	0.050	0.030	0.275	0.440	0.575	0.625
H	-.100	-.090	0.225	0.425	0.600	0.675	0.025	0.625	0.200	0.320	0.425	0.450
J	-.070	-.090	0	0.275	0.200	0.225	0.050	0.040	0.175	0.250	0.300	0.325
H	-.100	-.090	0	0.100	0.050	0.125	0.050	0.050	0.125	0.150	0.200	0.200
L	0	0	0	0	0	0	0	0	0	0	0	0
	½ STBD											
A	0	0	0	0	0	0						
B	-.050	-.060	0	0.025	0.050	0.125						
C	-.090	-.090	0.025	0.100	0.125	0.175						
D	-.100	-.125	0.075	0.225	0.300	0.350						
E	-.050	-.050	0.200	0.350	0.450	0.575						
F	-.125	-.125	0.150	0.325	0.550	0.525						
G	-.140	-.140	0.100	0.275	0.400	0.475						
H	-.100	-.150	0.125	0.300	0.400	0.425						
J	-.090	-.075	0	0.125	0.150	0.150						
K	-.100	-.075	0	0.100	0.100	0.050						
L	0	0	0	0	0	0						

Appendix D

Calculations of Natural Periods

General

The natural frequency of a rectangular plate is

$$\omega_n = \alpha \sqrt{\frac{Dg}{\gamma h a^4}}$$

where α = a numerical coefficient which depends on the end conditions, the ratio of $\frac{b}{a}$, and the mode of vibration.

D = flexual rigidity = $\frac{E\,h^3}{12(1 - \nu^2)}$

g = acceleration of gravity

γ = weight density

h = plate thickness

a = plate width

b = plate length

E = modulus of elasticity

ν = Poisson Ratio

For structural steels the values used are:

$E = 30 \times 10^6$ psi

$\nu = 0.3$

$\gamma = 488$ lbs/ft^3

Sample Calculations

For a 1/8" x 8" x 18" fully-clamped plate, the ratio $\frac{b}{a} = 2.25$. From interpolation of values given by Hearmon [32], $\alpha = 23.9$.

$D = 5370$ in lb

Using these values:

$$\omega_n = 23.9 \sqrt{\frac{(5370)(32.2)}{(488)(0.125)(.667)^4}} = 2855 \text{ rad/sec}$$

$$T = \frac{2\pi}{\omega_n} = \frac{2\pi}{2855} = 2.2 \text{ msec}$$

The natural periods for the other possible plate elements were calculated and are given in the procedure.

E. BIBLIOGRAPHY

1. Mayo, Wilbur L., "Analysis and Modification of Theory for Impact of Seaplanes on Water," NACA TN 1008 (1945).

2. Szebehely, V. G., "Hydrodynamics of Slamming of Ships," DTMB Report 823, 1952.

3. Abramson, H. N. and Chu, W. H., "Hydrodynamics of Slamming," Southwest Research Institute, Prog. Report No. 1, Contract No. 2729(00), April 1959.

4. Karman, von. Th., "The Impact on Seaplane Floats During Landing," NACA TN 321, October 1929.

5. Bisplinghoff, R. L. and Doherty, C. S., "Some Studies of the Impact of Vee Wedges on a Water Surface," Journal Franklin Institute, 253, 6 pp. 547-561, June 1952.

6. Borg, S. F., "Initial Wedge Impact on a Compressible Fluid," Journal of Applied Physics, 30, 9, pp. 1432-1436, September, 1959.

7. Korvin-Kroukovsky, B. V., "Pitching and Heaving Motions of a Ship in Regular Waves," Trans. SNAME, 65, pp. 590-632, 1957.

8. Ochi, K., "Model Experiments on Ship Strength and Slamming in Regular Waves," Trans. SNAME, pp. 345-383, 1958

9. Szebehely, V. G. and Todd, M. A., "Ship Slamming in Head Seas," DTMB Report 913, February 1955.

10. Wagner, H., "Landing of Seaplanes," NACA TN 622, May 1931.

11. Bisplinghoff, R. L. and Doherty, C. S., "A Two-Dimensional Study of the Impact of Wedges on a Water Surface," MIT Report 1950.

12. Gliddings, A. J., Jr., "Initially Flat Impact of an Elastic Plate on a Compressible Fluid," University of California 1960.

13. Milwitzky, B., "Generalized Theory for Seaplane Impact," NACA Report 1103, 1952.

14. Markey, M. F., "A Generalized Hydrodynamic-Impact Theory of the Loads and Motions of Deeply Immersed Prismatic Bodies," NASA Memo 2-10-59L.

15. Mayo, W. L., "Hydrodynamic Impact of a System with a Single Elastic Mode," NACA Report 1074.

16. Ochi, K. and Bledsoe, M., "Theoretical Consideration of Impact Pressure During Ship Slamming," DTMB Prel. Report 1321.

17. Leibowitz, R. C., "Comparison of Theory and Experiment for Slamming of a Dutch Destroyer," DTMB Report 1511.

18. Todd, A., "Slamming Due to Pure Pitching Motion," DTMB Report 833, 1955.

19. Szebehely, V. G., "On Slamming," DTMB Report 995, 1956.

20. Keil, A. H., "The Response of Ships to Underwater Explosions," DTMB Report 1576, 1961.

21. Kennard, E. H., "The Effect of a Pressure Wave on a Plate or Diaphragm," DTMB Report 527, 1944.

22. Heller, S. R., Jr., "Structural Similitude for Impact Phenomena," DTMB Report 1071, 1958

23. Chu, H. W. and Abramson, N. H., "Hydrodynamic Theories of Ship Slamming-Review and Extension," Tech. Report No. 1, Contract No. Nonr 2729(00), Southwest Research Institute.

24. Schauer, H. M., "Instruments Employed by the Underwater Explosions Research Division of the Norfolk Naval Shipyard," UERD Report 3-50.

25. Fisher, J. W., Driscoll, G. C. and Beedle, L. S., "Plastic Analysis and Design of Square Rigid Frame Knees," Fritz Lab Reprint 123.

26. Heller, S. R., Jr., and Jasper, N. H., "On the Structural Design of Planing Craft,"

27. Vossers, G., "Fundamentals of the Behavior of Ships in Waves," Publication No. 151a of the N.S.M.B.

28. Sedov, L., "On the Impact of a Solid Body on the Surface of an Incompressible Fluid," Tr. CAHI, 1934, Report 187.

29. Sydow, J., "Uber den Einflusz von Federung und Kielung auf den Landestosz," 1938.

30. Ochi, K. and Bledsoe, M., "Hydrodynamic Impact with Application to Ship Slamming, 1962

31. Franklin, J. M., "Effects of Impact on Simple Elastic Structures," DTMB Report 481, April 1942.

32. Hearmon, R. F. S., "Frequency of Vibration of Rectangular Isotropic Plates," Journal of Applied Mechanics, September, 1952

33. Kerley, J. J., Prod. Eng. Design Digest Issue, Mid-October, 1957 pF 34.

34. Howard, J. L., "The Effect of Hull Shape on Dynamic Loadings of Ships' Bottoms Due to Slamming," M.I.T. THESIS, 1961

35. Rouse, H., "Advanced Mechanics of Fluids," John Wiley and Sons, New York, 1959, pp. 73-74, 177-180.

36. Bledsoe, M. D., Bussemaker, O. and Cummings, W. E., "Seakeeping Trials on Three Dutch Destroyers," Trans. SNAME 68, 1960, pp. 39-137.

37. Ogilvie, T. F., "Ship Slamming and Supersonic Airfoil Flow," ONR, Technical Report ONRL-76-62, 1962.

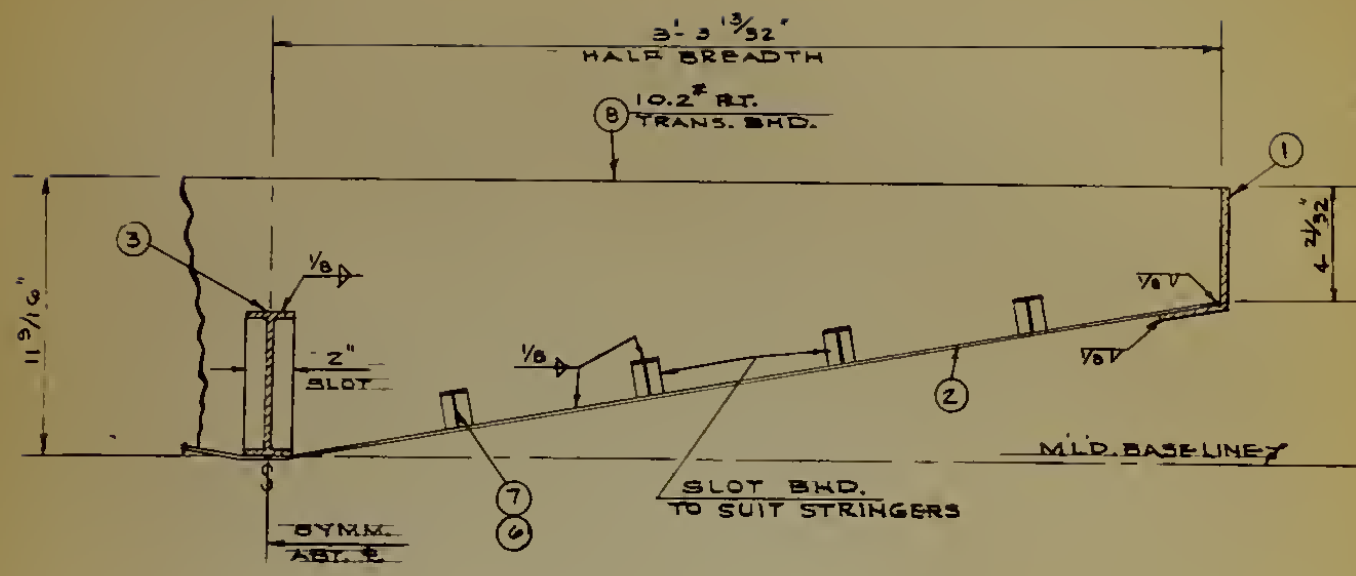

TRANSV. SECTION AT FR. 2 SHOWN
FR. 5 TO BE SIMILAR
FOR DETAILS NOT SHOWN, SEE SECT. AT FR. 3
SCALE ~ 3" = 1'-0"

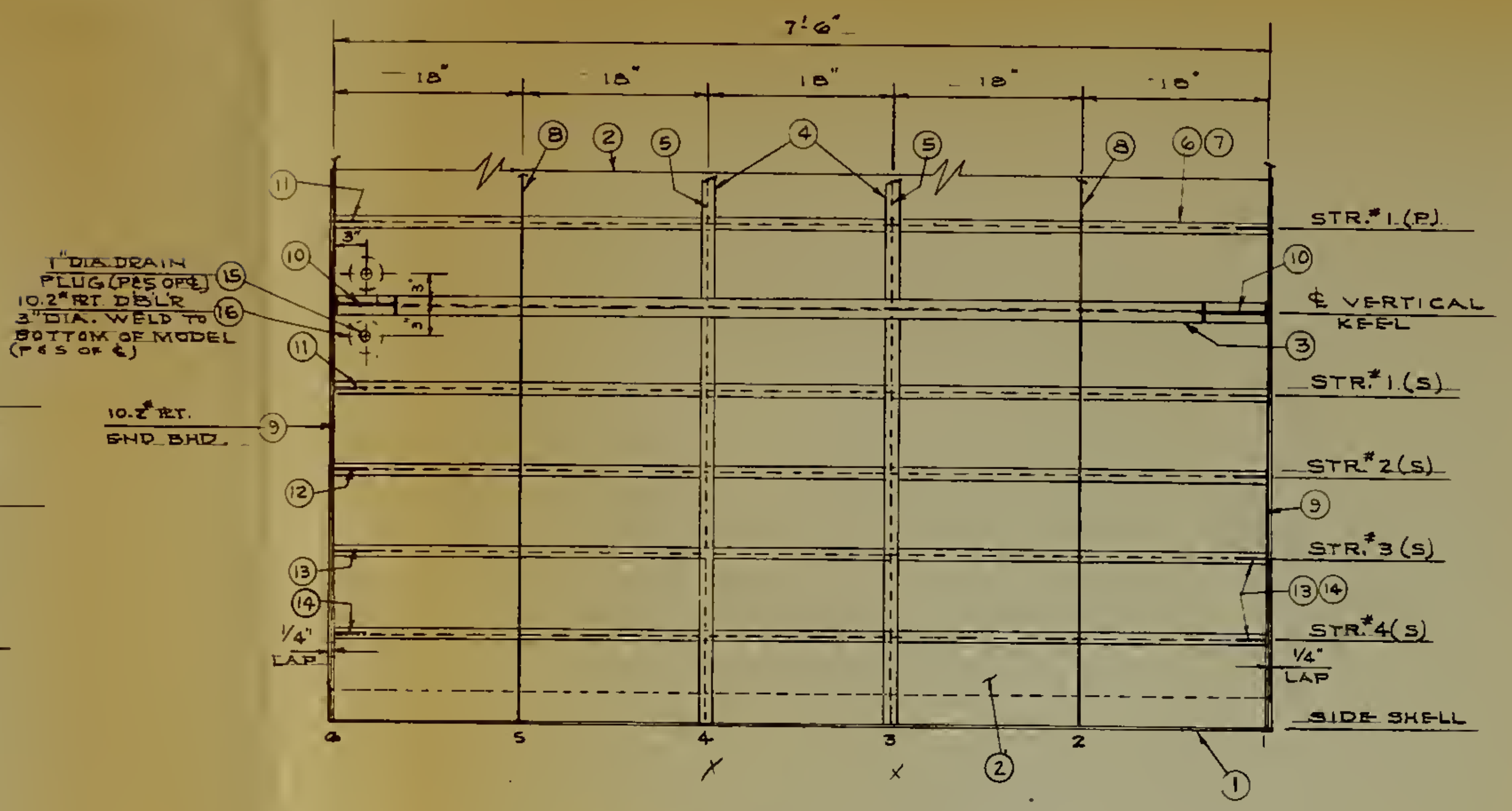

PLAN VIEW OF MODEL
STBD SIDE SHOWN, PORT SIDE SIM. TO OPP. HAND
SCALE ~ 1 1/2" = 1'-0"

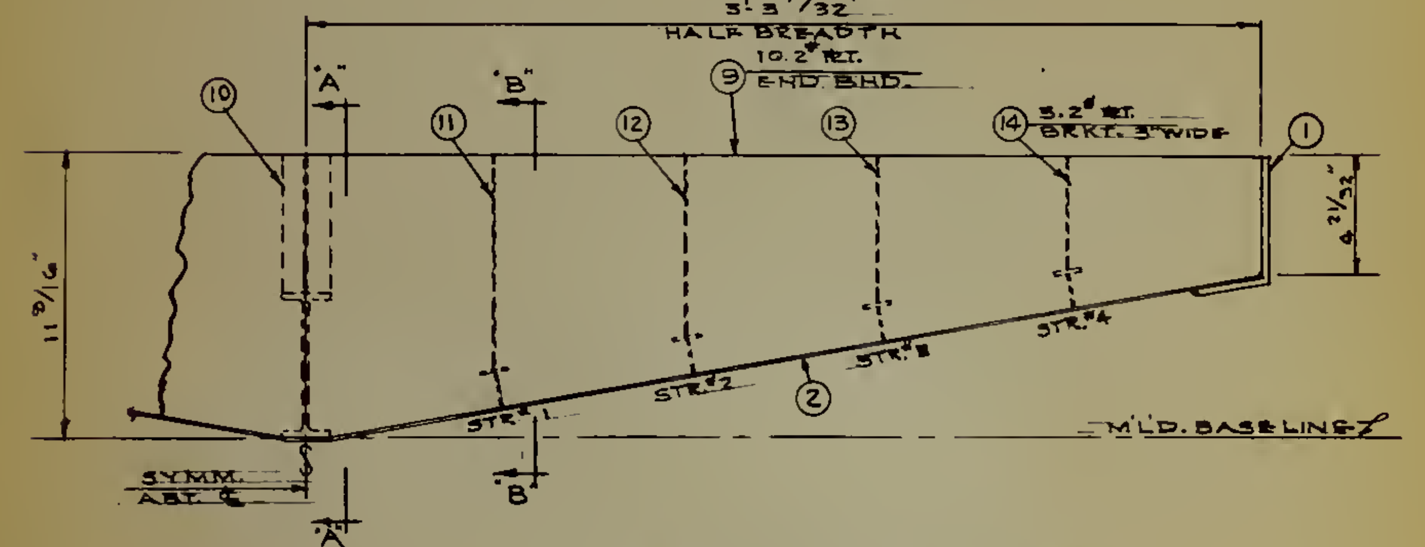

END BULKHEAD AT FR. 6 SHOWN
LOOKING FORD.
FR. 1 TO BE SIMILAR EXCEPT TO OPP. HAND
SCALE ~ 3" = 1'-0"

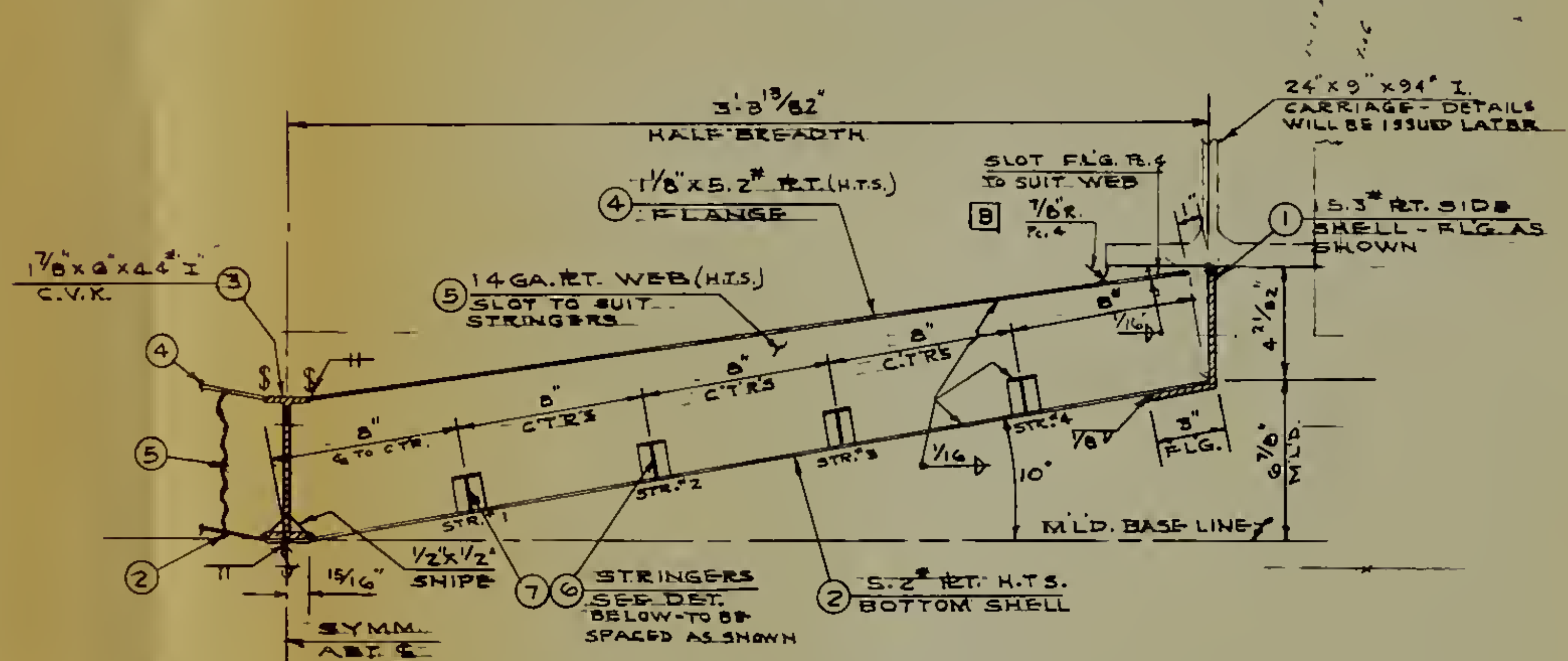

TRANSV. SECTION AT FR. 3 SHOWN
LOOKING FORD.
FR. 4 TO BE SIMILAR
SCALE ~ 3" = 1'-0"

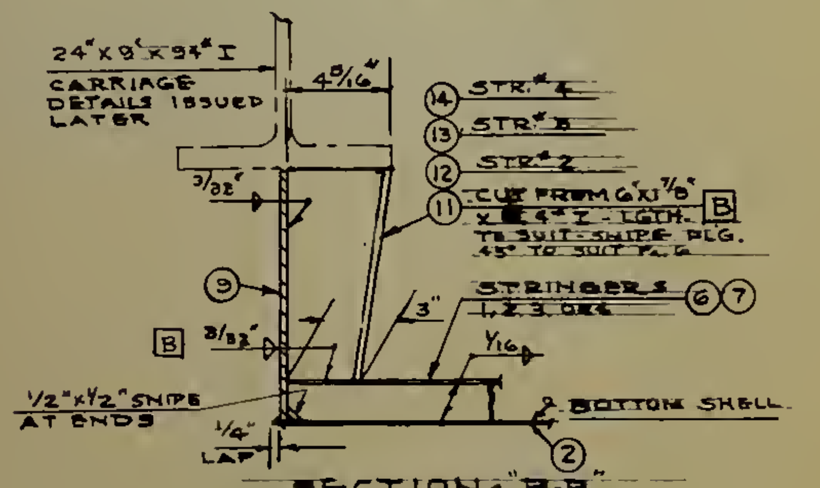

SECTION ~ "B-B"
TYPICAL DETAIL OF END BHD. BRK'TS.
SCALE ~ 3" = 1'-0"

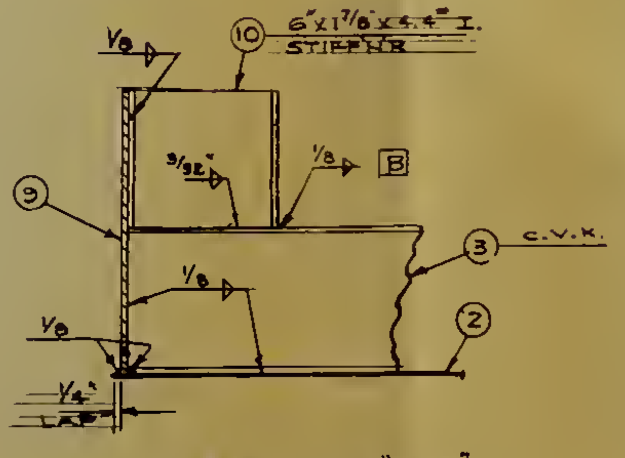

SECTION ~ "A-A"
SCALE ~ 3" = 1'-0"

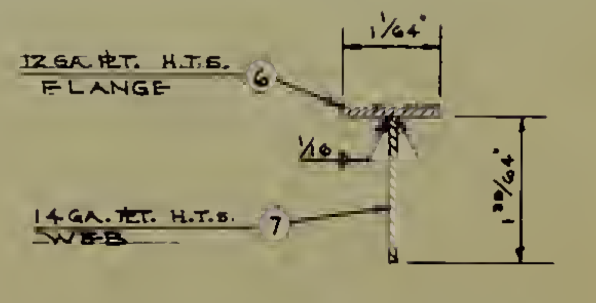

DETAIL OF STRINGERS
FULL SIZE

REVISIONS

REV. NO	ZONE	DESCRIPTION	APPROVED BY	DATE
B 7		GEN. NOTE #4 ALTERED, NOTE #6 ADDED. BOTTOM OF END BHD. STIFFN'RS TO BE WELDED AS NOTED IN SECT'S "AA" & "B-B". BHD STIFF'NR PC. 11-14 INC. CHANGED FROM F.B. RT TO TEE. LIST OF MATL ALTERED. TRANS. WEB PC. 5 ALTERED AS SHOWN TO ALLOW ATTACHMENT TO CARRIAGE.	EE	8/9/—

GENERAL NOTES

1. ALL THICKNESSES GO FORWARD OF THE MOLDED LINE.
2. MODEL TO BE PRIMED AND PAINTED ONE COAT OF HAZE GREY; IDENTIFY STRENGTH MEMBERS AS DIRECTED.
3. ALL MATERIAL TO BE CONSERVED AND UTILIZED (SO FAR AS POSSIBLE) FOR THE MANUFACTURE OF SMALLER STRUCTURAL MEMBERS, AND ALSO FOR ADDITIONAL MODELS, (SEE GEN. NOTE 6).
4. B TEST SPECIMENS (7" x 20") LONG'L. & TRANSV. TO BE CUT FROM EACH (H.T.S.) MOTHER PLATE AND SENT TO MET. LAB. FOR CHEMICAL AND PHYSICAL ANALYSIS. PLATES ARE NOW IDENTIFIED 1 THRU. 20. LAY-OUT SHEETS (FURNISHED BY CODE 783) SHOWS MODEL, & PC. NOS. WHICH MUST BE CUT FROM EACH RT. USED.
5. IMPORTANT:
   EXTREME CARE TO BE EXERCISED IN MAINTAINING FAIRNESS OF STRUCTURE.
6. B BOTTOM SHELL PLATING, PC. NO. 2, & STRINGERS, PC. 6 & 7 TO BE ORIENTED WITH THE ROLLED DIRECTION FORE AND AFT. THE TRANSVERSE WEBS & FLANGES, PC. 4 & 5, ROLLED DIRECTION TO BE ATHWARTSHIPS.
7. SCALE WT. OF MODEL 760 LBS.

11/8/62
LARRY

PRINTS ISSUED

DATE	
11	
17	
23	
28	
31	
38	
41	
51	
55	
58	
64	
67	
68	
71	
72	
74	
124A	
128	
225	
270	
308A	
310	
338	
339	
340	
343	
350	
334	
720	2
7830	4
C.O.V.	
BUSHIPS	
BUORD	
PEARL H.	
LONG B'H	
SAN FRAN.	
MARE IS.	
PUGET S.	
CHASN.	
NYS.	
PHILA.	
BOSTON	
PORTS.	
TOTAL	

PIECE NO.	NAME OF PIECE	NO. REQ.	MAT.	STOCK NUMBER	REMARKS OR SERVICE	ROUTING
16	DBLR. RT.	2	M.S.	SHOP PROVIDE	10.2# RT. 3" DIA.	
15	DRAIN PLUG	2	STL.	SHOP PROVIDE	1" DIA. PIPE PLUG	
14	BHD. BR'KT	4	M.S.		CUT FROM 6" x 1 7/8" x 4.4# I - 4 3/4" LG.	
13	BHD. BR'KT	4	M.S.		" " " - 6" LG.	
12	BHD. BR'K'T	4	M.S.		" " " - 7 1/2" LG.	
11	BHD. BRKT	4	M.S.		CUT FROM 6" x 1 7/8" x 4.4# I - 8 3/4" LG.	
10	BHD. STIFF	2	M.S.	SHOP PROVIDE	1 7/8" x 6" x 4.4# I - 5 9/16" LG.	
9	END BHD.	2	M.S.	SHOP PROVIDE	CUT FROM 12" x 6'-8" x 10.2# RT.	
8	TRANS. BHD.	2	M.S.	SHOP PROVIDE	CUT FROM 12" x 6'-8" x 10.2# RT.	
7	LONG'L. WEB	8	H.T.S.	FURNISH BY U.E.R.D.	1 35/64" x 14 GA. RT. - 7'-6" LG.	
6	LONG'L. FLG	8	H.T.S.	" "	1 1/64" x 12 GA. RT. - 7'-6" LG.	
5	TRANS. WEB	4	H.T.S.	" "	CUT FROM 6" x 3'-4" x 14 GA. RT.	
4	TRANS. FLG	4	H.T.S.	FURNISH BY U.E.R.D.	1 1/8" x 5.2# RT. - 3'-2 3/4" LG.	
3	KEEL	1	M.S.	SHOP PROVIDE	1 7/8" x 6" x 4.4# I - 7'-6" LG.	
2	BOTTOM SHELL	2	H.T.S.	FURNISH BY U.E.R.D.	3'-4" x 7'-6 3/4" x 5.2# RT.	
1	SIDE SHELL	2	M.S.	SHOP PROVIDE	CUT FROM 8" x 7'-6 3/4" x 15.3# RT.	

LIST OF MATERIAL QUANTITIES FOR ONE MODEL

DRAWN BY
TRACED BY CULPEPPER 7/26/62
CHECKED BY W.G. BUTT 7/26/62
DESIGN SUPVR Harrell
ENGINEERING SUPVR E. Elsworth 7/26/62
E.E.
APPROVED

SLAMMING MODEL
(1/4 SCALE OF PROTOTYPE)

U.E.R.D OF STRUCTURAL MECHANICS LAB. D.T.M.B., PORTSMOUTH, VA.

WP-157 R.U. NO. 757 REV. B

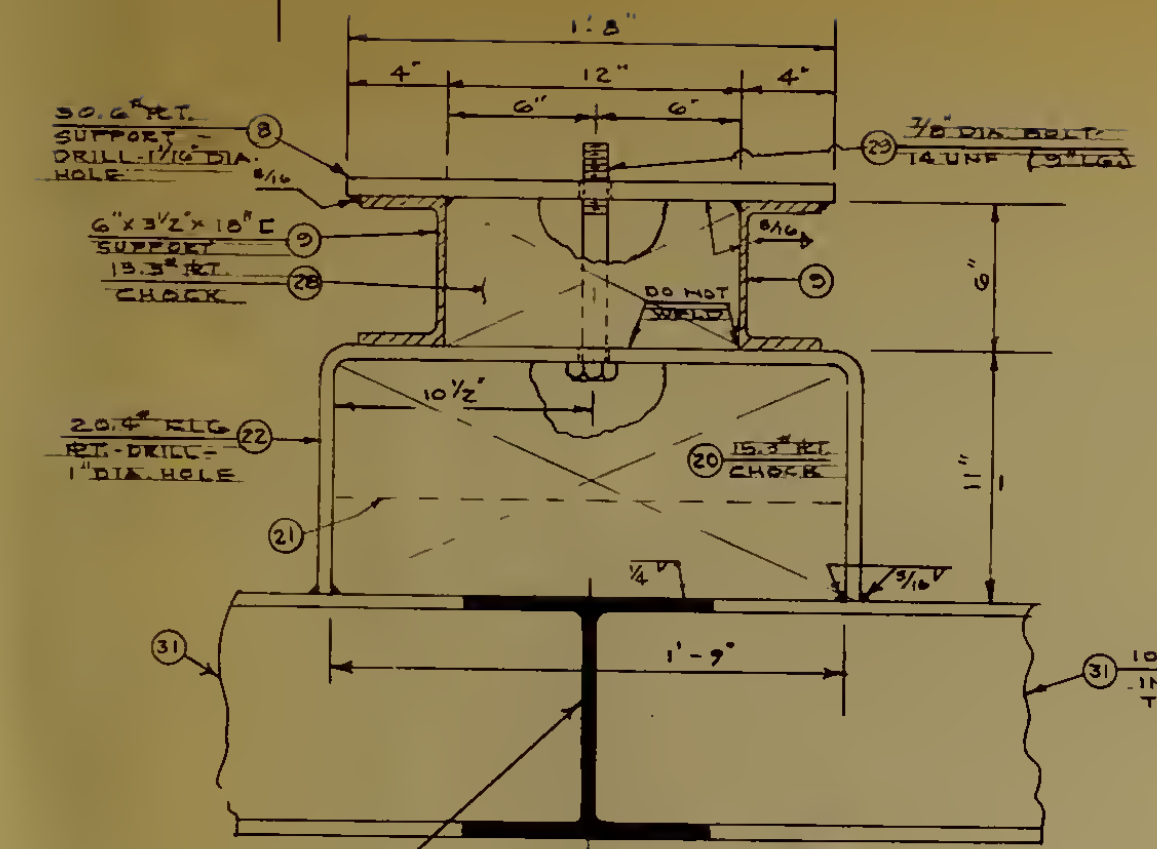

DETAIL~"C"

SCALE~3"=1'-0"

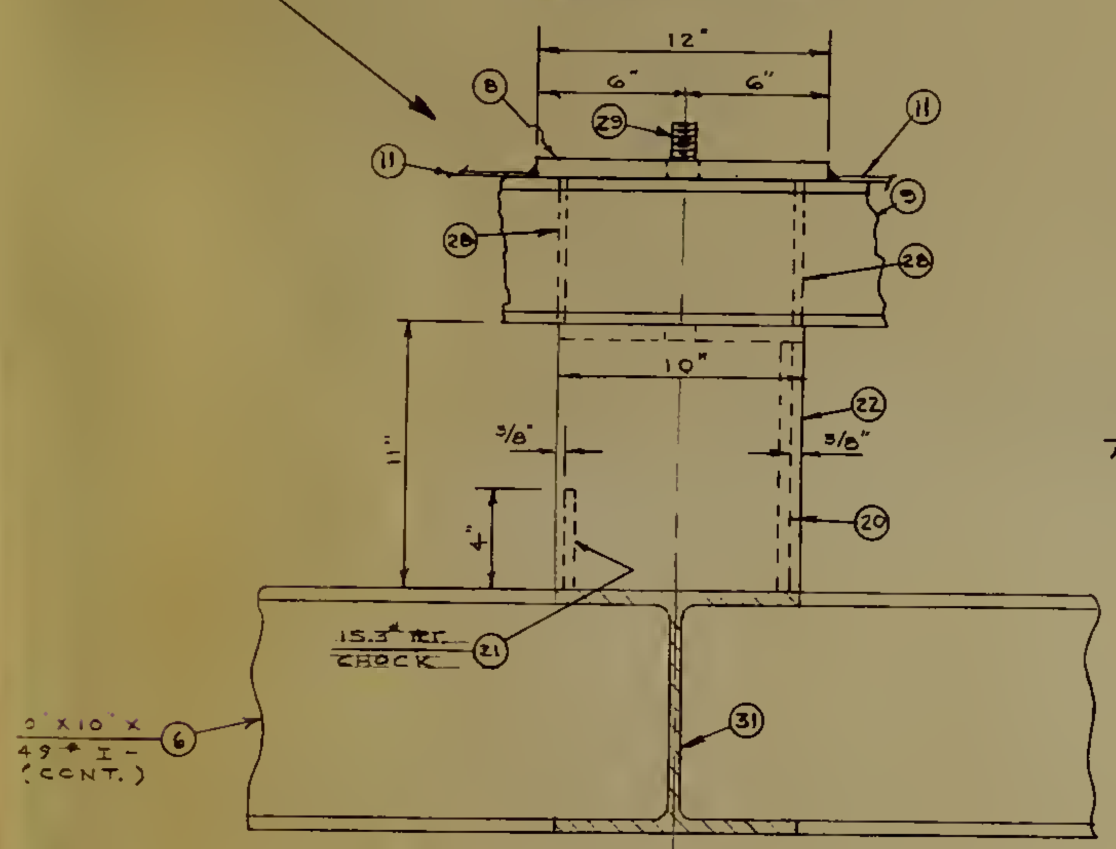

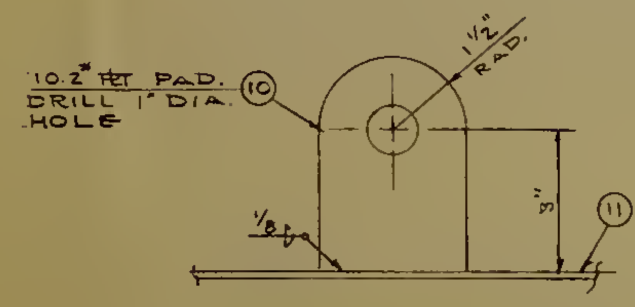

DETAIL~"D"

SCALE- HALF SIZE

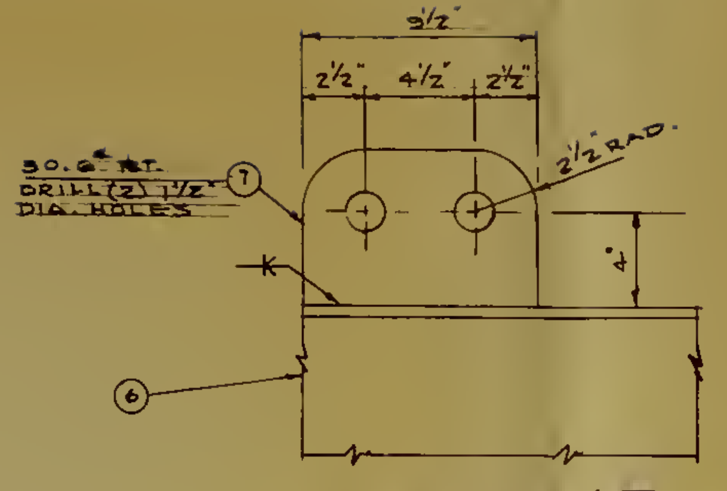

DETAIL~"B"

SCALE~3"=1'-0"

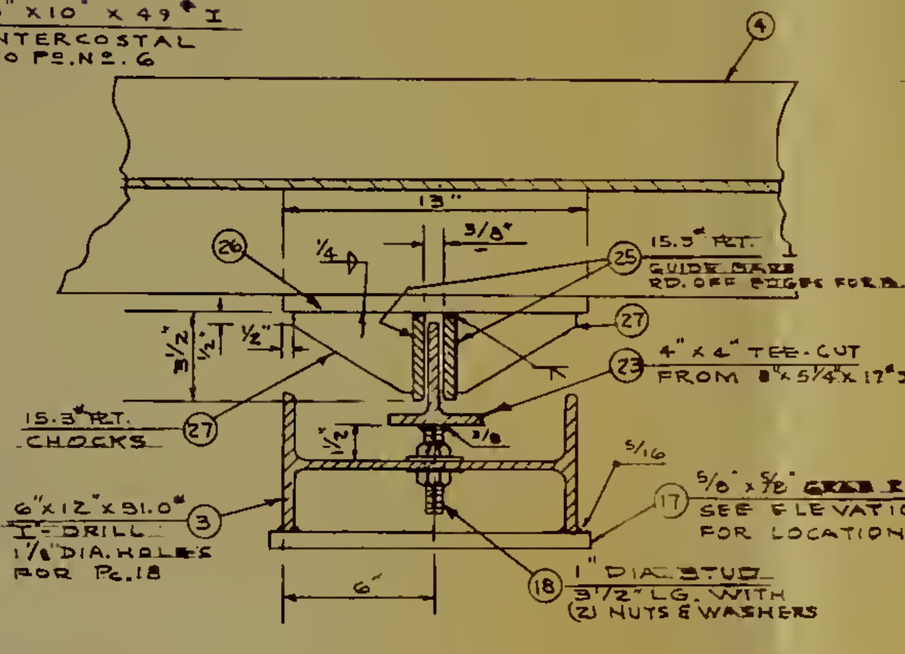

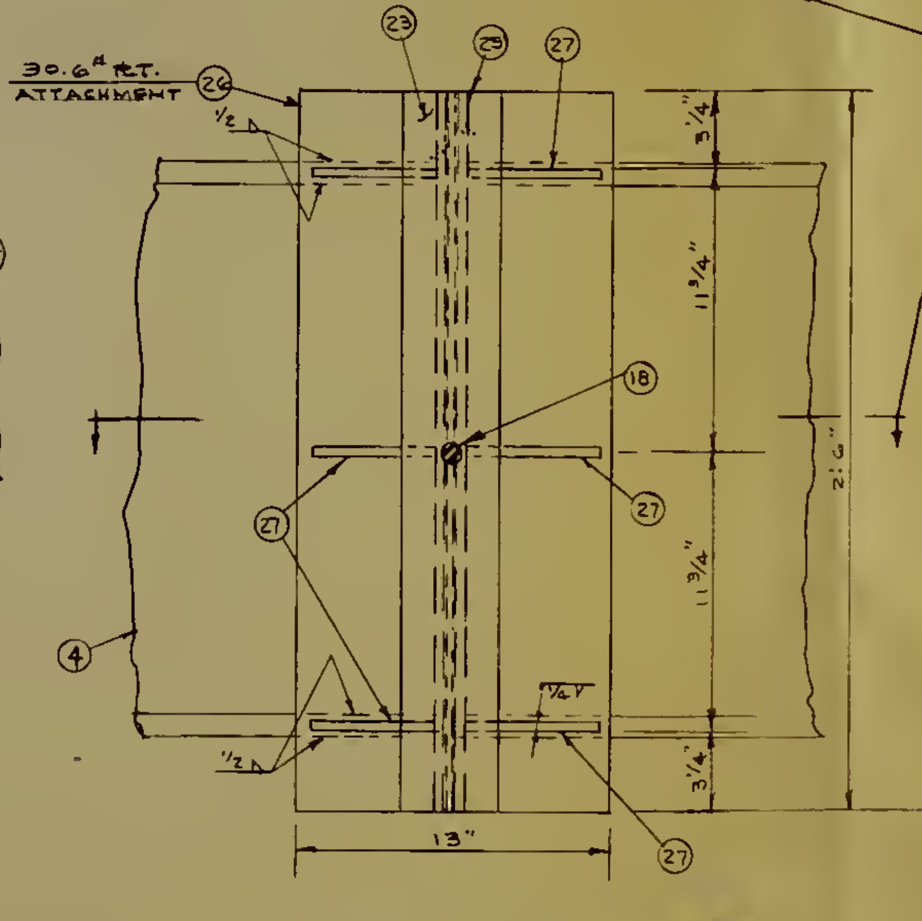

SECTION~"A-A"

SCALE~3"=1'-0"

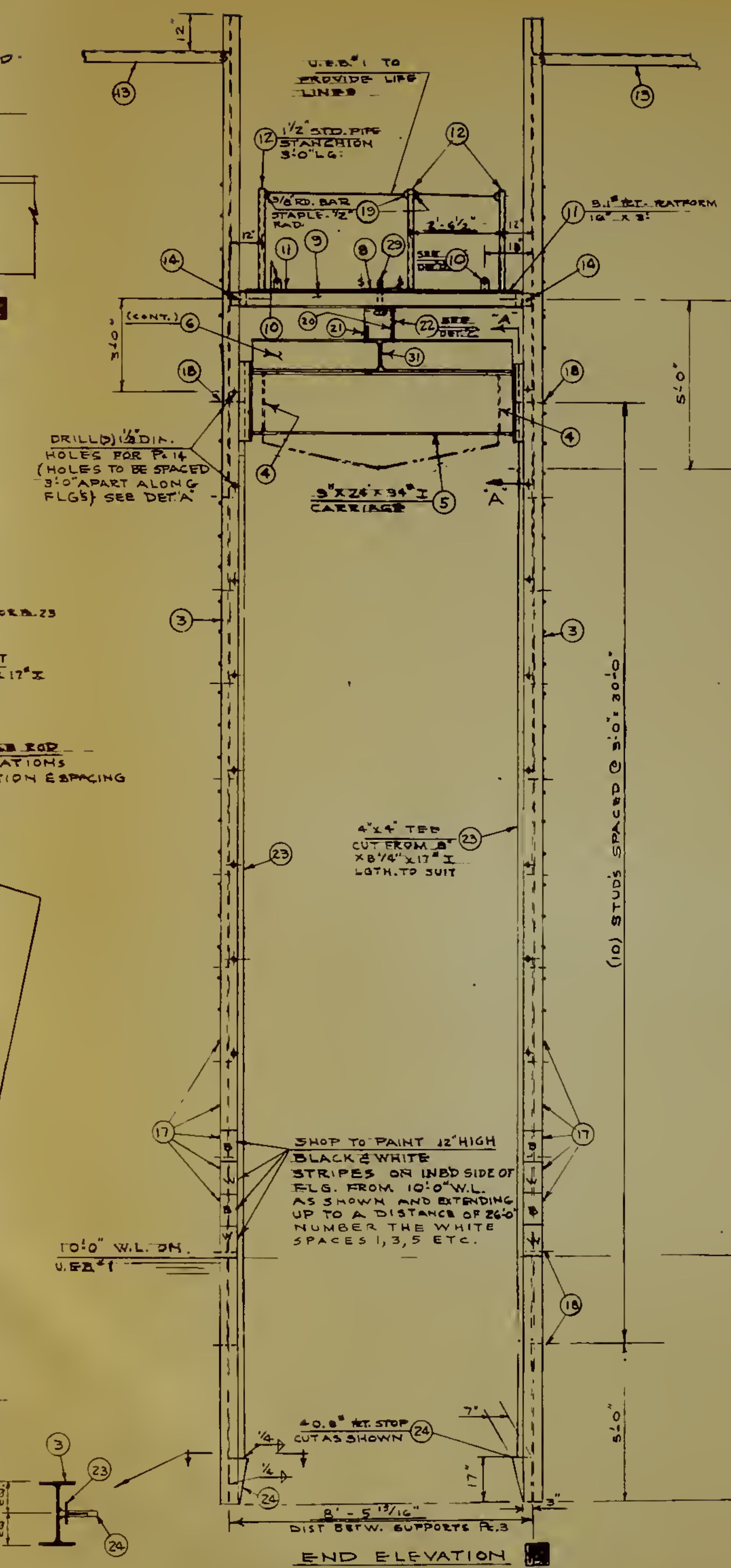

END ELEVATION

LOOKING FORD.

BRKTS. AND PIPE BRACES OMITTED

SCALE~1/2"=1'-0"

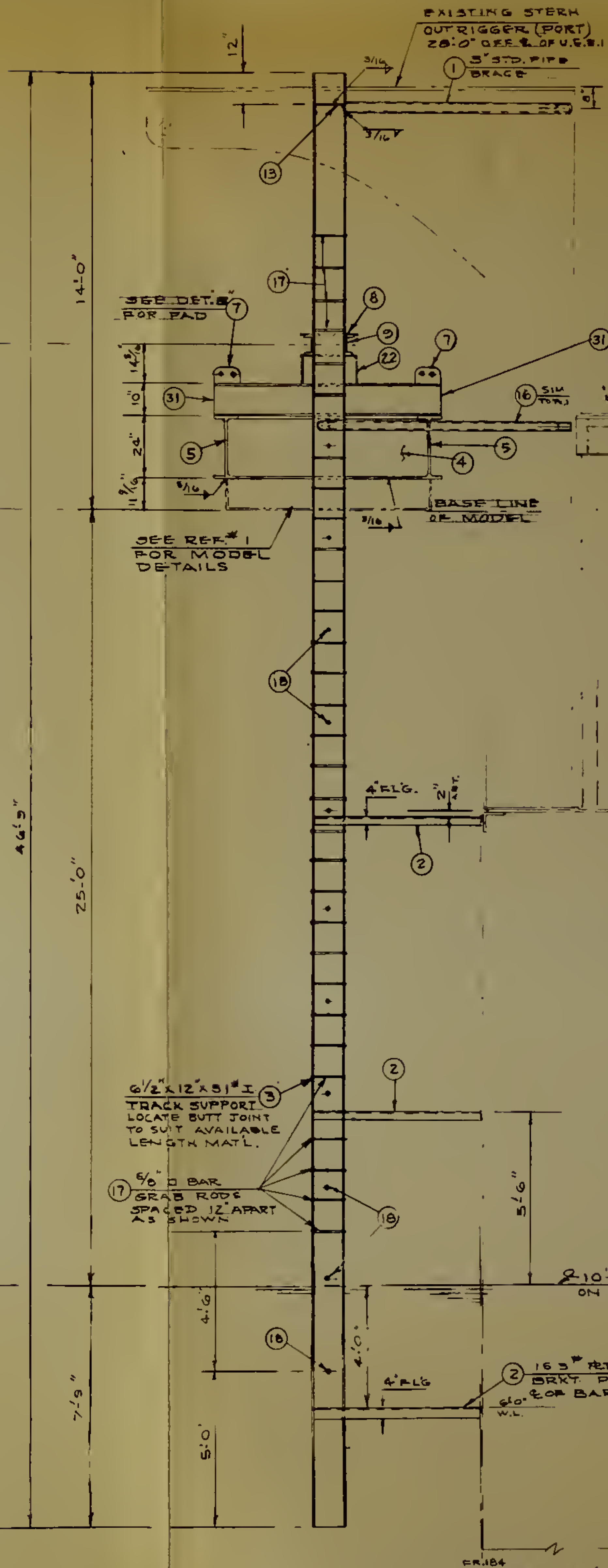

ELEVATION STBD SIDE (LOOKING TO PORT)

SCALE~1/2"=1'-0"

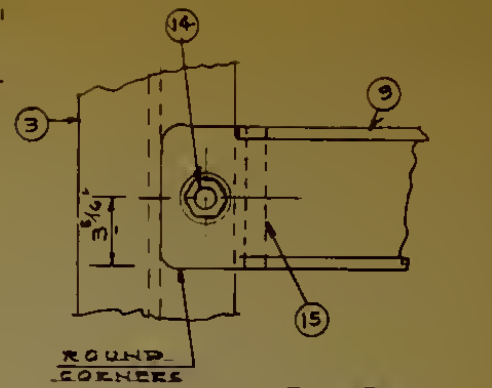

SIDE VIEW

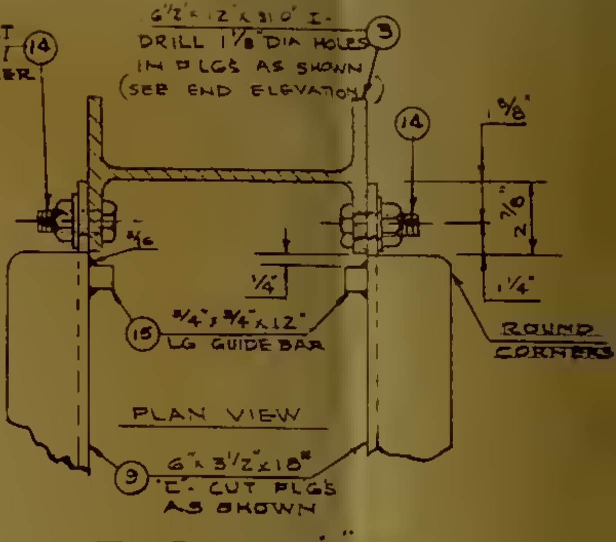

PLAN VIEW

DETAIL~"A"

SCALE~3"=1'-0"

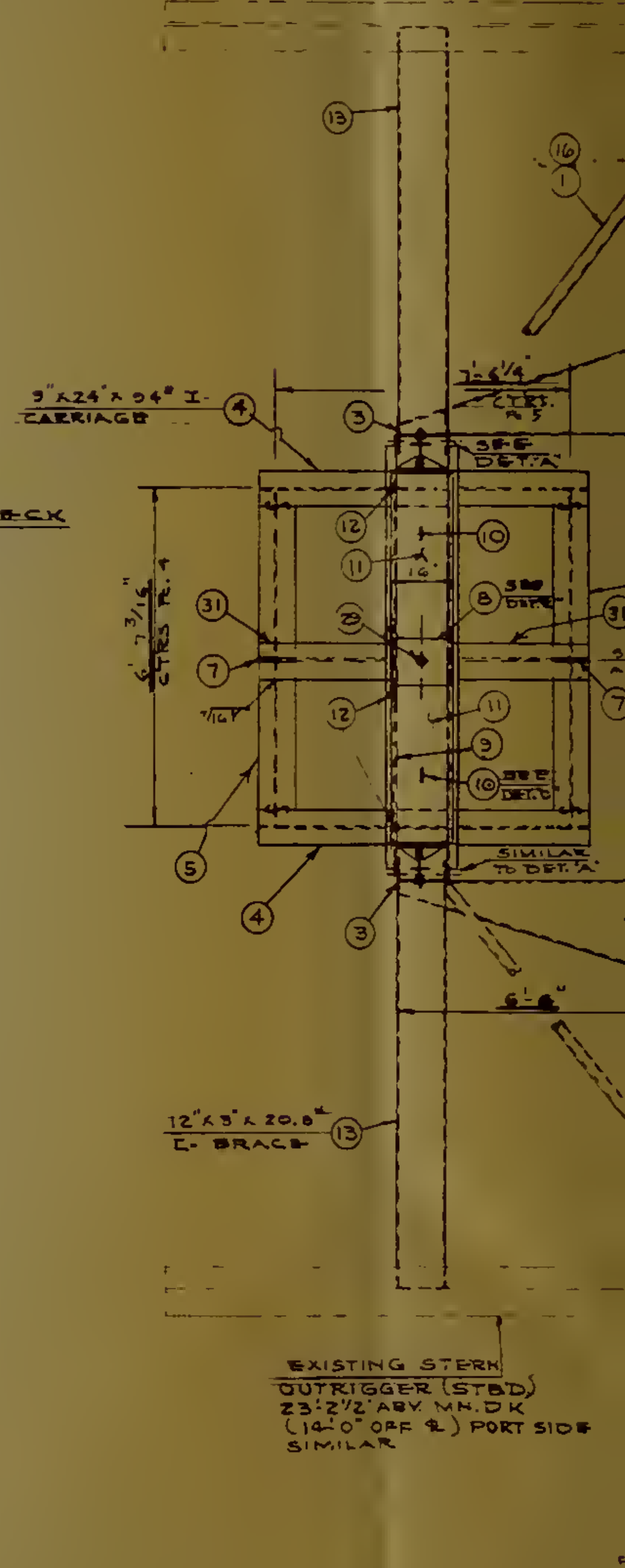

PLAN VI

SHOWING GENERAL ARR'G'T

SCALE-1/

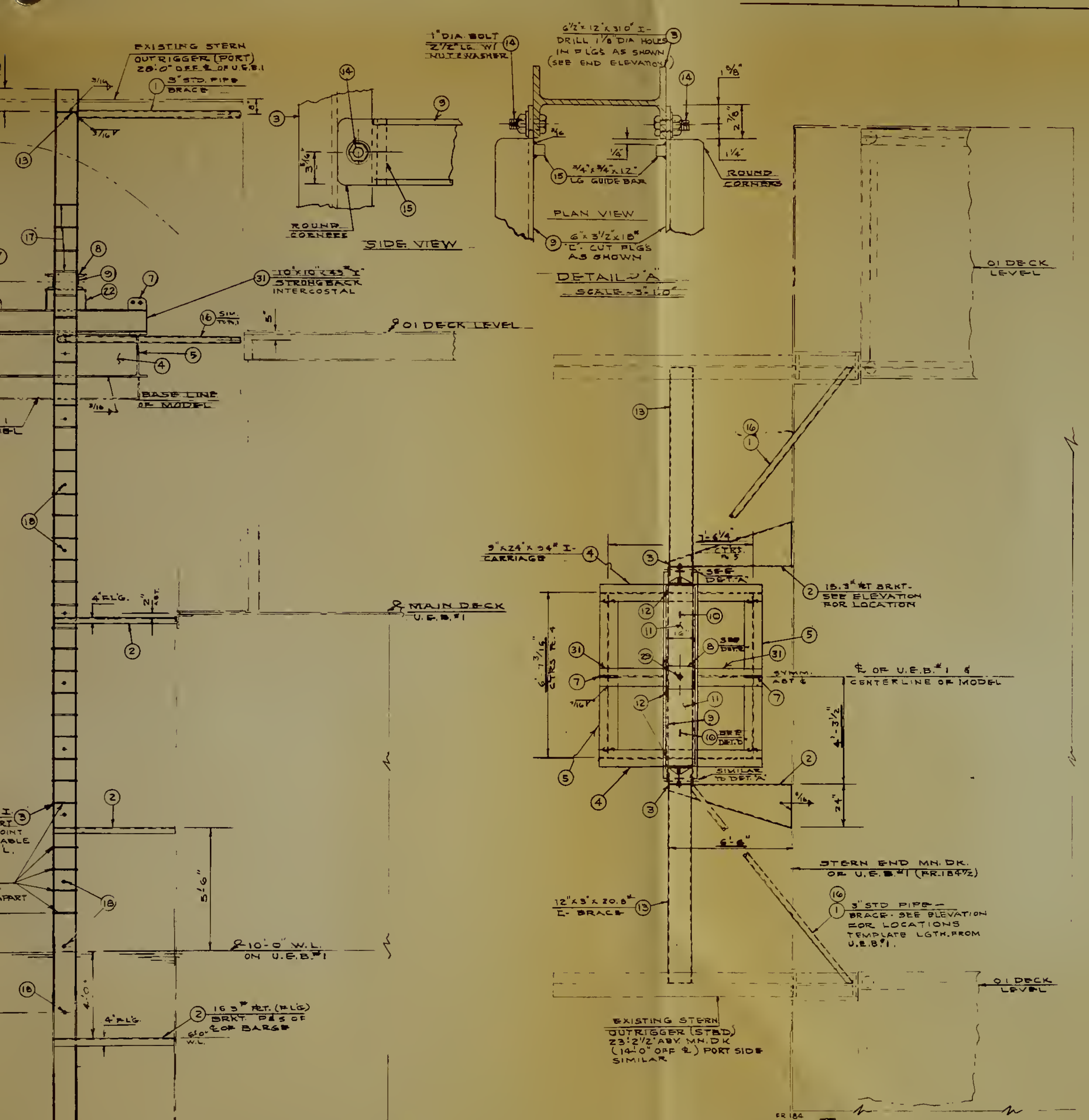

DETAIL "A"
SCALE - 3" = 1'-0"

PLAN VIEW B
SHOWING GENERAL ARR'G'T FOR TESTING SLAMMING MODELS
SCALE - ½" = 1'-0"

ELEVATION STBD SIDE (LOOKING TO PORT) B
SCALE - ½" = 1'-0"

REVISIONS				
REV. NO	ZONE	DESCRIPTION	APPROVED BY	DATE
B		PLAN ALTERED TO SHOW MODEL ROTATED 90°. LIST OF MAT'L. ALTERED TO SUIT. W. C. Bott 12-11-62	Harrell	10/17/62

GENERAL NOTES

1. BEFORE MODEL #1 (SHOWN ON REF. 1), IS INSTALLED ON CARRIAGE, SHOP IS TO INSTALL Pc. 30, A 20.4# ℞. AT BOTTOM OF CARRIAGE Pcs 4 & 5 SO AS TO TEST PROOF OPERATION OF RIG.
2. SHOP TO APPLY A COAT OF GREASE ON WEB OF "TEE" BAR GUIDE Pc. 23
3. EXTRA BOLTS Pc 29 TO BE DELIVERED TO U.E.B. #1.

REFERENCE PLAN

1. SLAMMING MODEL (¼ SCALE OF PROTOTYPE) R.U. No. 757

PIECE NO	NAME OF PIECE	NO REQ	MAT.	STOCK NUMBER	REMARKS OR SERVICE	ROUTING
31	STRONG BACK	2	M.S.	SHOP PROVIDE	10" × 10" × 49# I (ABT. 4'-3" LG.)	
30	TEST ℞	1	M.S.	SEE NOTE 1 SHOP PROVIDE	6'-8" × 7'-7" × 20.4# ℞.	//
29	SUPPORT BOLT	6	M.S.	SHOP PROVIDE	⅞" DIA. 14 UNF. 9" LONG	
28	CHOCK	2	M.S.		CUT FROM 6" × 12" × 15.3# ℞.	
27	CHOCKS	12	M.S.		CUT FROM 9" × 5⅝" × 15.3# ℞	
26	ATTACHMENT ℞.	2	M.S.		13" × 2'-6" × 30.6# ℞.	
25	GUIDE BARS	4	M.S.		3½" × 2'-6" × 15.3# ℞	
24	STOP	2	M.S.		CUT FROM 7" × 17" × 40.8# ℞.	
23	"T" BAR GUIDE	2	M.S.		[illegible]	
22	FLG. ℞.	1	M.S.		10" × 3'-9" × 20.4# ℞ FLG.	
21	CHOCK	1	M.S.		CUT FROM 4" × 1'-9" × 15.3# ℞	
20	CHOCK	1	M.S.		CUT FROM 10½" × 1'-9" × 15.3# ℞	
19	STAPLES	4	M.S.		⅝" DIA. RD. BAR - ½" RAD.	
18	STUD BOLTS	22	M.S.		1" DIA - 3½" LG W/(2) NUTS & WASHERS	
17	GRAB RODS	62	M.S.		⅝" × ⅝" D-BAR - 13" LG	
16	PIPE BRACE	2	M.S.		3" STD. PIPE - ABT. 13'-0" LG.	
15	GUIDE BAR	4	M.S.		¾" × ¾" × 12" - SEE DET. A	
14	BOLT W/NUT	4	M.S.		1" DIA. BOLT - 2½" LG W/WASHER	
13	[BRACE	2	M.S.		12" × 3" × 20.8# [- ABT. 9'-5¼" LG	
12	STANCHION	8	M.S.		1½" STD. PIPE - 3'-0" LG	
11	PLATFORM	2	M.S.		CUT FROM 16" × 3'-3½" × 5.1# ℞.	
10	HANDLING PAD	2	M.S.		CUT FROM 3" × 4½" × 10.2# ℞	
9	SPREADER	2	M.S.		6" × 3½" × 18# [- ABT. 8'-7" LG	
8	SUPPORT ℞.	1	M.S.		CUT FROM 12" × 20" × 30.6# ℞.	
7	LIFTING PAD	2	M.S.		CUT FROM 6½" × 9½" × 34.6# ℞.	
6	STRONGBACK	1	M.S.	SHOP PROVIDE	10" × 10" × 49# I - 7'-6" LG	
5	CARRIAGE	2	M.S.	IN CUSTODY OF X-11	24" × 9" × 94# I. 6'-7" LG	
4	CARRIAGE	2	M.S.	IN CUSTODY OF X-11	24" × 9" × 94# I - 6'-9" LG.	
3	TRACK SUPPORT	2	M.S.	SHOP PROVIDE	12" × 6½" × 31.0# I - ABT. 44'-9" LG	
2	BRACKETS	6	M.S.	"	CUT FROM 28" × 6'-6" × 15.3# ℞.	
1	PIPE BRACE	2	M.S.	SHOP PROVIDE	3" STD. PIPE - ABT. 12'-7" LG	

LIST OF MATERIAL QUANTITIES FOR ONE TESTING RIG

PRINTS ISSUED												
DATE												
11												
17												
23												
26												
31												
36												
41												
51												
55												
58												
64												
67												
68												
71												
72												
74												
124A												
126												
225												
270												
506A												
510												
520												
526												
540												
543												
550												
564												
C.O.V.												
BUSHIPS												
BUORD												
PEARL H.												
LONG B'H												
SAN FRAN.												
MARE IS.												
PUGET S.												
CHASN.												
NYD.												
PHILA.												
BOSTON												
PORTS.												
TOTAL												

DRAWN BY Culpepper
TRACED BY 5/10/62
CHECKED BY Harrell
DESIGN SUPVR Harrell
ENGINEERING SUPVR 9/7/62
9/7/62
APPROVED DIVISION HEAD
E. Chappell 9/7/62 PROJECT OFFICER DATE

CARRIAGE AND GUIDE TRACK
(WP-157)

UERD OF STRUCTURAL MECHANICS LAB. DTMB, PORTSMOUTH, VA.
R.U. NO. 766 REV. B
SCALE: AS NOTED SHEET 1 OF 1